7

RESOLUTION OF COMPOSITE RADIOACTIVE DECAY CURVES BY FOURIER DECAY ANALYSIS

by

ALI JOWZANI-MOGHADDAM

B. S., National University of Iran, 1975

A MASTER'S THESIS

submitted in partial fulfillment of the

requirements for the degree

MASTER OF SCIENCE

Department of Nuclear Engineering

KANSAS STATE UNIVERSITY
Manhattan, Kansas

1978

Approved by:

N. Dean Eckhoff Herman J. Bonnert
Major Professor

TABLE OF CONTENTS

ACRONYMS

ADC	Analog-to-Digital Convertor
DNE	Department of Nuclear Engineering
EC	Electron Capture
eV	Electron Volt
FDA	Fourier Decay Analysis
fWhm	Full Width Half Maximum
Ge(Li)	Lithium-Drifted Germanium Detector
GRA	Graduate Research Assistantship
IBM	International Business Machines
KSU	Kansas State University
LS	Least Squares
NAA	Neutron Activation Analysis
NaI(Tl)	Sodium Iodide Thallium-activated detector
NWT	Number of Points Chosen to Perform a Numerical Integration
RSR	Rotary Specimen Rack
TLS	Transformed Least Squares

NOMENCLATURE

Symbol	Explanation
A	Activity of the product at the end of the irradiation
A_o	Activity at t=0, time of removal from neutron flux
A_1	Defined in Eq. (1.2-4)
A_t	Activity at t=0
a	Fitting parameter, real part of $\Gamma(z)$
a_o	Fitting parameter
a_1	A parameter
a_1, a_2, a_3	Fitting parameters (Appendix F)
a_1^i, a_2^i, a_3^i	Parameters defined in Appendix F
B_m	Bernoulli number
b	Fitting parameter, imaginary part of $\Gamma(z)$
b_0	Fitting parameter
b_1	A parameter
b_1, b_2, b_3	Fitting parameters (Appendix F)
b_1^i, b_2^i, b_3^i	Parameters defined in Appendix F
$b_{i,j}$	Defined in Section 4.3
C	Counts (at time, t)
C_0	Counts (at time, zero)
Ci	Courie

NOMENCLATURE (contd.)

Symbol	Explanation
c	Index for real parts
dy_i	Defined in Section 4
dg(x)	Defined in Appendix A
$\frac{d}{dt}$	Differential operator with respect to t
$\frac{dN}{dt}$	Defined in Eq. (1.2-1)
E	Defined in Eq. (4.1-3)
E_o	Defined in Eq. (1.3-3) and Eq. (4.2-4)
E_1	Defined in Eq. (4.3-2)
E_e	Energy of scattered neutron
E_n	Neutron energy
$E(x_o, \mu)$	Defined in Eq. (2.2-3)
E_γ	Incident gamma-ray energy
E'_γ	The energy of scattered photon
e	Base of natural logarithm (= 2.71828)
e_i	Defined in Eq. (4.1-2)
exp(z)	e^z (exponential function)
F_o	Activity at t = o
F_c	Defined in Eq. (2.3-8)
F_s	Defined in Eq. (2.3-9)
F_t	Activity after time t
$F(\mu)$	Defined in Eq. (2.1-11)

Nomenclature (contd.)

Symbol	Explanation
$F(\psi)$	Defined in Eq. (2.1-10)
$f(b)$	Defined in Section 4
$f(x)$	Defined in Appendix A
$f(t)$	Defined in Eq. (1.6-1)
$f(b_1)$	Defined in Eq. (4.3-9)
$f'(b)$	$\partial f/\partial b$
$f^*(x)$	Defined as $e^x f(e^x)$
$f^*(-x)$	Defined as $e^{-x} f(e^{-x})$
$f_1, \ldots, f_6$	Defined in Appendix F
$G(\mu)$	Defined in Eq. (2.1-15)
$g(x)$	Defined in Eq. (2.1-10)
$g(\lambda)$	Sum of delta functions
$H(\mu)$	Real part of $F(\mu)/K(\mu)$
h	A parameter, Plank's constant
$h\nu$	Energy of photon
$h(\lambda)$	Step function (Eq. (2.1-2))
i	Complex unit number = $\sqrt{-1}$), integer index associated with ith species, integer number
j	Integer index associated with jth species
J	Jacobian
$J(\mu)$	Imaginary part of $F(\mu)/K(\mu)$
K	Name of the first shell in atom
K_c	Real part of $K(\mu)$
K_s	Imaginary part of $K(\mu)$

Nomenclature (contd.)

Symbol	Explanation
$K(\mu)$	Defined in Eq. (2.1-16)
k	A parameter
l	A parameter
lnz	Natural, Naperian logarithm ($\log_e z$)
m	Number of intervals, rest mass of electron, index number, a parameter, minute
m_o	Rest mass of electron
mb	Millibarn
N	Number of product nuclei, neutron number
N_o	Number of original target nuclei
N_i	Activity of t = o due to nuclei of ith specimen
n	Neutron, number of items, an integer number, a parameter
p	Proton, a parameter, defined in Appendix A
R	Defined in Eq. (F-2)
R(z)	Real part of z(=x)
s	Defined as x-y, a parameter, index for imaginary parts, a variable
$T_{1/2}$	Half-life
t	Time, a parameter
t_o	Time defined in Section 2.2
t_1	Time of neutron flux exposure
t_2	Elapsed time from the end of the irradiation
U	Argument of complex function $\Gamma(z)$
V	Modulus of complex function $\Gamma(z)$
w_i	Weighting factor for "data point" i

Nomenclature (contd.)

Symbol	Explanation
w_{oi}	Weighting factor for "data point" i, Section 4.2
X	X-ray
x	A transformed variable (recall $t = e^{x}$), a real part of z
x_o	Limit of integration
x_i	Independent variable (ith)
$x_o, \ldots, x_m$	A set of points
$x'_1, \ldots, x'_n$	A set of points defined in Appendix A
y	A transformed variable (recall $\lambda = e^{-y}$), imaginary part of z, defined in Section 4
y_i	Defined in Section 4
$y_1, \ldots, y_i$	Uncorrelated variables
Z	Atomic number
z	Defined as x + iy, complex number

Greek Symbols

α	Alpha particle, a parameter
β	A parameter
β^+	Positron
$\Gamma(z)$	Gamma function
γ	Gamma photon, Euler's constant
Δ	Defined in Eq. (4.1-14)
$\Delta\mu$	Increment of parameter μ
$\Delta\lambda_i$	Change of parameter in λ_i
ΔN_i	Change of parameter in N_i

Nomenclature (contd.)

Symbol	Explanation
$\delta(x)$	Dirac delta function
θ	The angle between the direction of the primary and scattered photons, polar angle, argument of $\Gamma(z)$
k	Linear pair production attenuation coefficient
λ	Characteristic decay constant of product radioactive nuclei (sec^{-1}), a variable
λ_i	Decay constant of ith specimen
μ	Independent variable
μ_o	Limit of integration
μ_i	Independent variable (ith)
μCi	Microcurie
ν	Frequency
Π	Factorial function
π	3.1415926....
$\sum$	Overall summation
σ	Microscopic cross section for interaction (cm^2/nucleus). standard deviation
σ_z	Standard deviation of the determination of any parameter z
σ^2	Variance
σ_z^2	Defined in Eq. (4.1-18)
σ_i^2	Variance for "data point" i
τ	Photoelectric linear attenuation coefficient

Nomenclature (contd.)

Symbol	Explanation
ϕ	Neutron flux (neutrons/cm^2-sec)
ψ	A variable
$\frac{\partial}{\partial a}$	Partial derivative with respect to a
$\frac{\partial^2}{\partial^2 a}$	Partial derivative with respect to a of second order
$n!$	Factorial of n
$\|z\|$	Absolute value of z
$\|\Gamma(z)\|$	Modulus of function $\Gamma(z)$
(a,b)	Open interval (a,b), nuclear reaction: capture of a and emission of b, as in (n,p)
[a,b]	Closed interval

LIST OF FIGURES

LIST OF FIGURES (contd.)

LIST OF FIGURES (contd.)

LIST OF FIGURES (contd.)

LIST OF TABLES

LIST OF TABLES (contd.)

LIST OF TABLES (contd.)

1.0 INTRODUCTION

1.1 General Discussion

The value of activation analysis as a research tool was recognized almost immediately upon the discovery of artificial radioactivity by the famous husband-and-wife team, Fredric and Irene Curie-Joliot, in 1933. The first activation analysis experiment was carried out in 1936 by the Nobel prize-winning Hungarian, George Hevesy, and Hilde Levi in Copenhagen when they bombarded impure yttrium with neutrons to activate and measure the contaminant, a small quantity of dysprosium (1). Activation analysis has been involved in identificiation and determination of materials, as a sensitive, versatile analytical tool employing nuclear energy. Activation analysis is a powerful tool for determining the elements present in an unknown sample. This particularly valuable technique can identify trace amounts of elements as small as a few parts per million, or in some cases, parts per billion. Effectiveness of neutron activation analysis (NAA) in comparison with other types of analysis, such as spectroscopic, gravimetric, and calorimetric analysis can be shown in Fig. (1.1-1). The bar graph shows that NAA is potentially more sensitive, by an order of magnitude, for those elements with high nuclear cross sections. It shows further that greater sensitivity can be obtained when high-flux reactors are used for irradiating the sample. Other advantages of NAA are its speed and the fact that the sample (or specimen) is usually undamaged. The principles of NAA are discussed, in detail, by many authors (1, 2, 3, 4, 5, 6, 7, 8, 9, 10, 11).

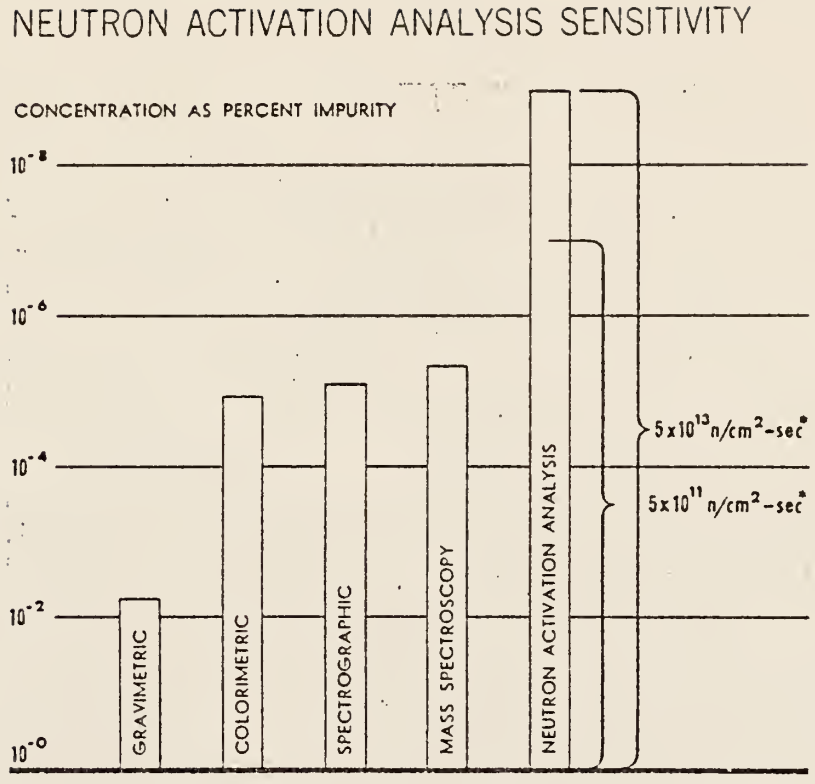

Fig. 1.1-1. Comparison of the sensitivity of neutron activation analysis with other types of analysis (1).

1.2 Basic Principles of Neutron Activation Analysis

The basic principle of NAA is that a given element is activated, i.e., converted into a radioactive nuclide, by a suitable nuclear reaction with neutrons. The radioactive product can then be identified by its radiation, e.g., gamma rays, and by its half life. Using a comparison sample containing a known amount of the particular element and treating it in the exactly the same way as the unknown specimen allows the quantity of element in the sample to be determined. The four nuclear reactions of primary importance to NAA are the (n,γ), (n,p), (n,α), and $(n,2n)$ reactions. These notations represent the absorption of a neutron (^1_0n) by a nucleus and the subsequent emission of a prompt gamma ray, proton, alpha particle, or two neutrons, respectively. The (n,γ) reaction is predominantly produced by thermal neutrons, whereas (n,p), (n,α), and $(n,2n)$ reactions usually require fast neutrons. The majority of NAA work is carried out with thermal neutrons from a reactor, leading to the (n,γ) reaction.

For each nuclear reaction the activity of the product nuclide is directly proportional to the number of atoms of the parent nuclide. Therefore, the activity of the product can be used to calculate the amount of the parent which was originally in the sample being studied. The equation governing the rate of formation of the product nuclide is given by the well known differential equation

$$\frac{dN}{dt} = \sigma N_o \phi - \lambda N, \qquad (1.2\text{-}1)$$

where N = product nuclei,

ϕ = neutron flux, a constant,

N_o = number of original target nuclei,

σ = microscopic cross section for interaction,

λ = decay constant of the product nucleus.

The parameters ϕ and N_o are usually taken as constants, which is reasonable for most nuclear reactor irradiations. However, neutron flux (ϕ) actually is time dependent (12). With ϕ and N_o as constant, the solution of Eq. (1.2-1) is

$$A = N\lambda = N_o\sigma\phi\ (1 - e^{-\lambda t_1}), \qquad (1.2\text{-}2)$$

where t_1 = time of neutron flux exposure,

A = activity of the radioactive product at the end of the irradiation.

After time t_1, the sample is removed from the neutron flux. When the target sample is removed from the reactor the production term, the first term on the right hand side of Eq. (1.2-1) is zero; hence, the number of radioactive atoms begin to decrease according to the characteristic half-life of the nuclide. The mathematical expression (a solution to Eq. (1.2-1) with $\phi = 0$) that describes the process of radioactive decay of a single nuclide is:

$$A_t = A_o e^{-\lambda t}, \qquad (1.2\text{-}3)$$

where A_t = activity after time t,

A_o = activity at t=o, time of removal from neutron flux,

λ = decay constant

So, the radioactivity of the product after an elapsed time t_2 from the end of the irradiation would be,

$$A_1 = N_o \sigma \phi (1-e^{-\lambda t_1})\ e^{-\lambda t_2} \qquad (1.2\text{-}4)$$

The radioactive species formed in the activation generally produces gamma rays, either by direct emission or by annihilation of positrons. The gamma radiation is measured with the aid of a scintillation detector or a lithium drifted germanium semiconductor detector connected to a multichannel analyzer, with as many as several thousand channels, which can display on an oscilloscope the gamma-ray spectrum. In Fig. (1.2-1), a block diagram of the procedure is shown.

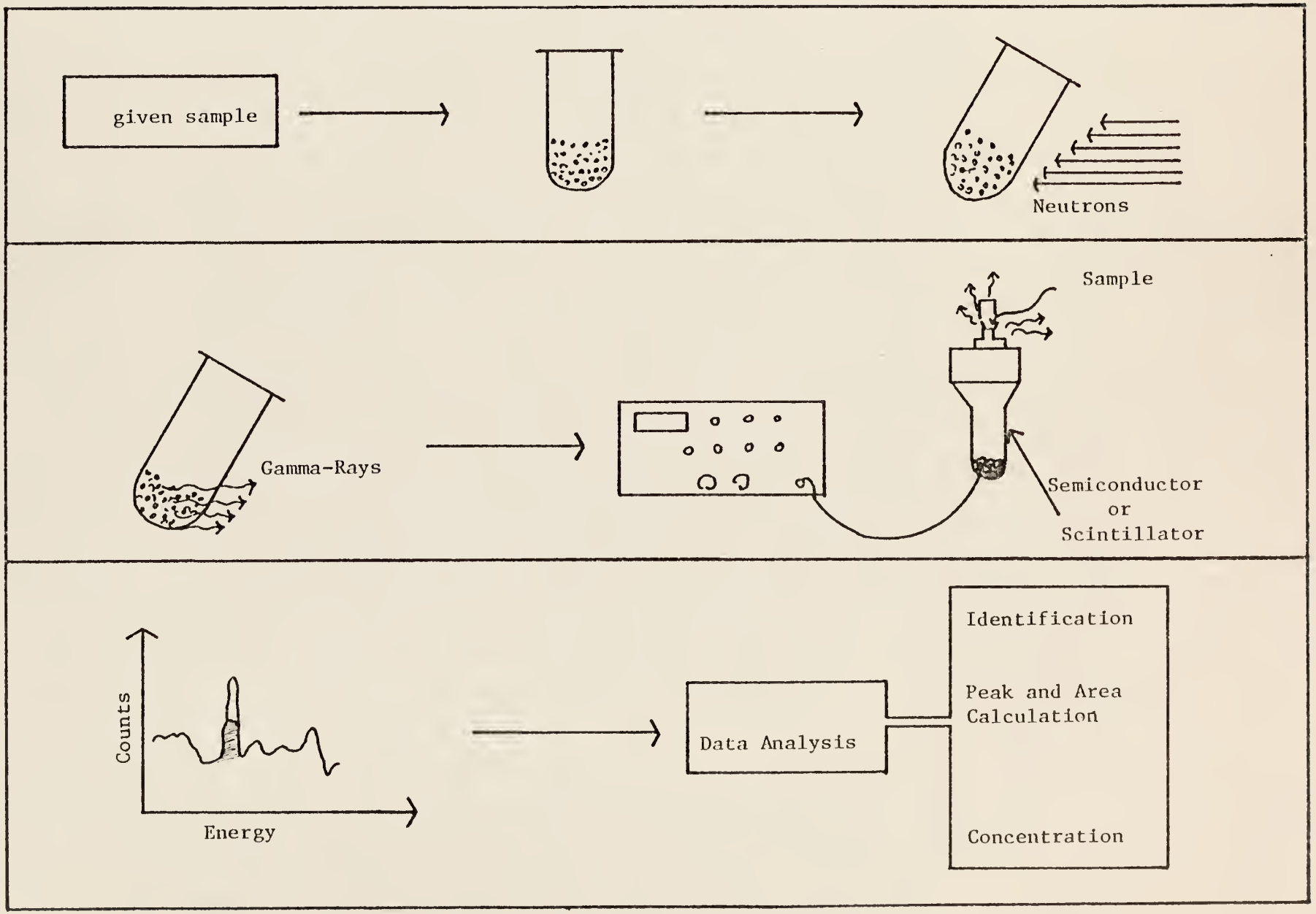

Fig. 1.2-1. A diagram of the neutron activation analysis procedure.

1.3 Interaction of Gamma Rays with Matter (3)

A knowledge of the basic processes by which a photon interacts with matter is essential to an understanding of the NAA procedure. Gamma rays are highly penetrating radiation. Their effective range depends on their energy, but it might require several centimeters of metal to reduce the intensity of gamma radiation to such an extent that it becomes difficult to detect. There are three basic modes of gamma-ray interaction with matter. These modes are designated as the photoelectric, Compton (incoherent) scattering, and the pair production processes. There are several other mechanisms, e.g., coherent scattering, which can be important in special cases; in fact, Fano (13) has catalogued 12 different processes of gamma interaction with matter. Almost all gamma-ray interactions take place with electrons. Normally a gamma ray has only a single interaction with an electron.

For gamma rays of low energy ($\leq$0.1 MeV) the photoelectric process is the most important interaction process. High atomic number absorbers are important for the photoelectric process. When the gamma ray interacts via the photoelectric process the energy of the photon is transferred completely to the electron. In this case electrons are ejected from the atom (or molecule) encountered by the radiation. The energy of the ejected electron is equal to the difference between the energy of the incident photon and the binding energy of the shell from which the electron was ejected. The energy absorbed by recoil of the nucleus of the atom is negligible compared with the energy of the gamma

ray and photoelectron. It is believed that the interaction is with K-shell electrons about 80 percent of the time for those gamma rays with energy greater than the binding energy of the K-shell electrons. As a result of this interaction process the atom is left with a vacancy in the shell from which the electron was ejected; this vacancy is filled by another electron resulting in the emission of X rays or Auger electrons. The importance of the photoelectric process decreases with increasing gamma-ray energy (see Fig. 1.3-1).

Compton scattering plays a major role when the absorber is a material of low atomic number, and the energy of the radiation is neither too high nor too low (>0.1 MeV). Nevertheless, increase of the atomic number of the absorber increases the extent of absorption caused by Compton scattering. This process is an inelastic scattering process between a photon and an individual electron. The energy is shared between the recoil electron and the secondary photon. This secondary (or scattered) photon travels in a direction different from that of the primary photon. In Compton scattering the energy of the scattered photon and electron are given by the following relationship (see Fig. 1.3-1),

$$E_\gamma' = \frac{E_\gamma}{1+E_o(1-\cos\theta)} , \qquad (1.3\text{-}1)$$

$$E_e = E_\gamma - E_\gamma' \qquad (1.3\text{-}2)$$

where E_γ = incident gamma-ray energy,

E'_γ = scattered gamma-ray energy,

E_e = scattered electron energy,

$E_o = E_\gamma/mc^2$, (1.3-3)

θ = the angle between the direction of the primary and scattered photons.

The importance of Compton scattering for gamma-ray absorption decreases with increasing energy of the photon (see Fig. 1.3-1).

At high gamma-ray energies (> 5.0 MeV) and for absorbers of high atomic number, pair production dominates the absorption process. The probability of pair production increases with the square of the atomic number of the absorber. Pair production results in complete absorption of the gamma ray and production of a positron-electron pair. The process requires a minimum energy of 1.022 MeV to create an electron-poistron pair, i.e., the rest mass energy equivalent of a position-electron pair. Any excess energy will be shared as kinetic energy between the positron and electron. Thus, for each interaction between a gamma ray and matter, the result is either the ejection of an electron or the formation of a positron-electron pair carrying a considerable amount of energy. Figures (1.3-1) and (1.3-2), are presented for a more complete illustration of the process. A plot of the gamma-ray cross section vs energy for each process in NaI(Tl) has been presented in Fig. (1.3-1) (14). The plot is similar for Ge(Li) detectors. Figure (1.3-2) illustrates the relative importance of the three major types of gamma-ray interaction. The interaction of gamma rays with matter is discussed in more detail by many authors (2,3,4,7,9,10,11,14).

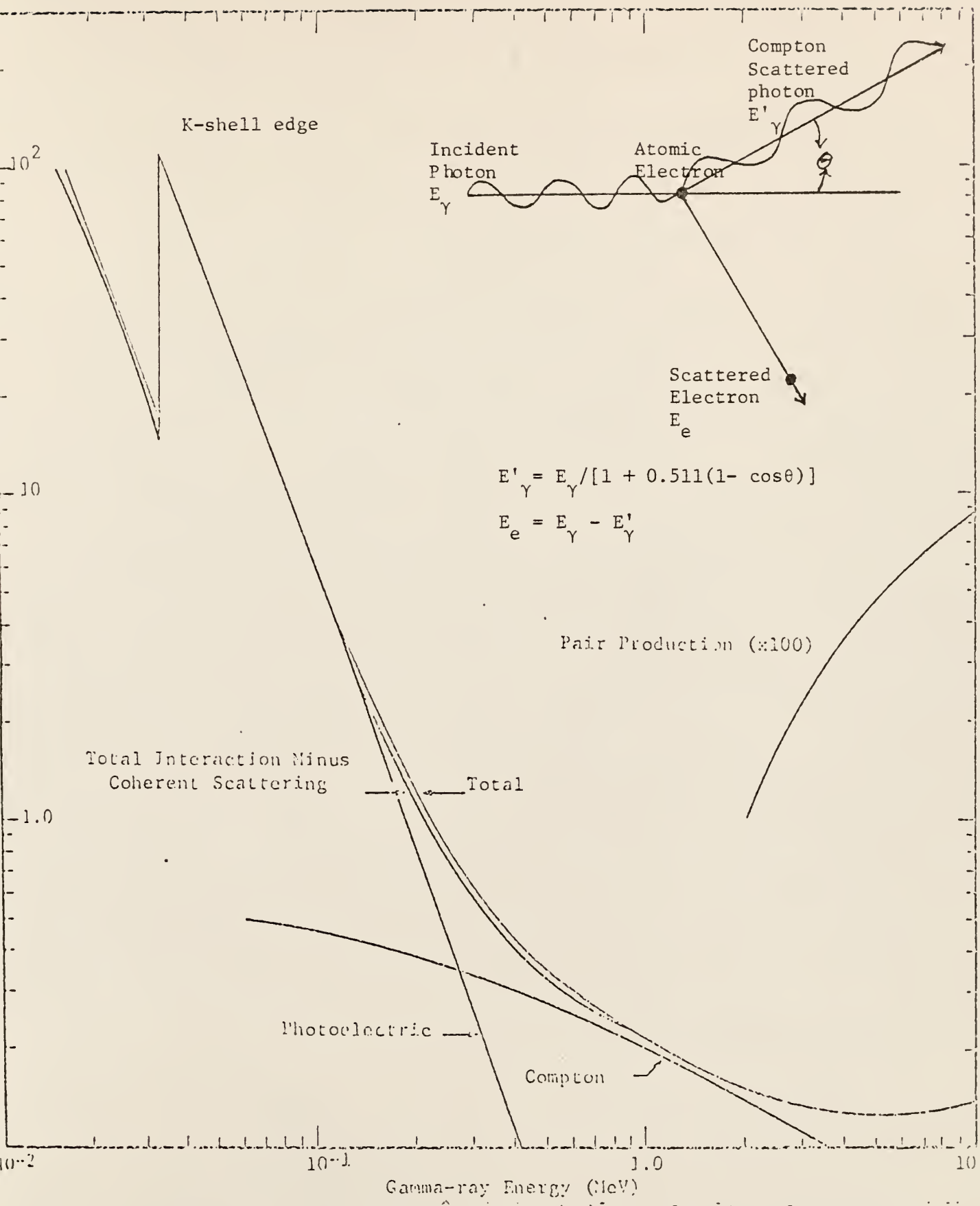

Fig. 1.3-1. Absorption coefficient, $\hat{\pi}$, for NaI(Tl) as a function of gamma-ray energy (14).

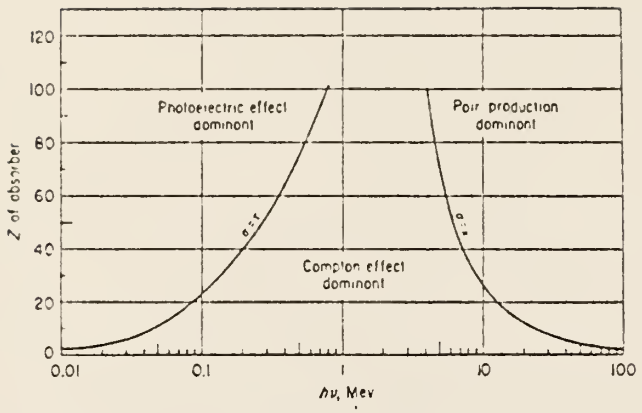

Fig. 1.3-2. Relative importance of the three major types of gamma-ray interaction (4).

1.4 Gamma Ray Spectrometry (9)

The objective of gamma-ray spectrometry is to analyze the gamma-ray spectrum of a sample of unknown composition (an "unknown sample") to determine the gamma rays present in the unknown sample. Gamma-ray spectrometry deals primarily with gamma rays with energy components from about .03 MeV to about 3 MeV. Only a brief discussion of the characteristics necessary for an understanding of the response of an ordinary Ge(Li) detector to gamma rays is discussed here. Gamma-ray spectrometry has been discussed, in detail by many authors (7,9,10, 11,15,16,17,18). The three major interaction processes, photoelectric effect, Compton scattering, and pair production, are discussed briefly below.

The photoelectric process, wherein a gamma-ray deposits all of its energy in a material in a single event, is the most useful of the three processes in gamma-ray spectrometry. In the semiconductor this process is characterized by the Gaussian-shaped peak (photopeak) in the pulse-height analyzer spectrum (see Fig.1.4-1). This spectrum is collected by a Ge(Li) detector and amplification system connected to a multichannel analyzer. The photopeak resulting from total energy loss is the most distinguishing and most important characteristic in all spectra. The position of this peak and its intensity are used to determine the energy and intensity of gamma rays which produce the gamma-ray spectrum. The width (full width at one half the maximum peak height) of this peak is denoted as fwhm and is a measure of the

energy resolution of the detector, i.e., the ability to distinguish between two gamma rays.

The Compton process also contributes to the gamma-ray spectrum, but it doesn't produce significant peaks in a gamma-ray spectrum. As shown in Fig.(1.4-1), the Compton process is characterized by the nearly flat continuum below the four small peaks. The backscatter peak is caused by the Compton process for gamma rays scattering with material outside the detector and corresponds to the photoelectric process for a source gamma ray whose initial direction of travel was away from the detector. The Compton scattered gamma rays can be directed back to the detector; hence, these gamma rays can interact via the photoelectric process, principally, or the Compton process. Because the scattering process occurs for a wide range of angles, the backscatter peak has a larger fwhm than an incident gamma ray with the same energy.

The annihilation peak is the result of pair production and the annihilation of an electron-positron pair in materials outside the detector, e.g., the source material, air, or detector container. The resulting 0.511 MeV can be directed into the detector and will interact by the photoelectric process or Compton scattering.

A pair production event produces an electron-positron pair in the detector material; the positron is quickly annihilated, with another electron yielding two 0.511 MeV gamma-rays, which travel in opposite directions. Thus, 1.022 MeV is the threshold for the pair production process, but in practice the process is not evident below

about 1.5 MeV (7). The energy of the source gamma ray in excess of the rest mass energy of the electron-position pair (1.022 MeV) is transferred to the electron-position pair as kinetic energy and is thus deposited within the detector. If both 0.511 MeV gamma-rays produced in the annihilation of the electron positron pair escape undetected, a peak, called the double-escape peak, will occur at a point equal to the source gamma-ray energy minus 1.022 MeV. If only one of these 0.511 MeV annihilation gamma-rays escape the detector undetected and the other interacts within the detector by the photoelectric process, it leads to the formation of a peak, called the single-escape peak. This peak will appear at an energy corresponding to 0.511 MeV less than the energy of incident photon.

Thus, for a nuclide emitting a single gamma-ray with energy greater than about 1.5 MeV, a unique gamma-ray spectrum will be formed with five identifying peaks.

According to theory the photopeak should be a spike with zero width in the gamma-ray spectrum, however, due to statistical fluctuations in the electron output of the detector the theoretical spike is spread out to form an approximately Gaussian-shaped peak. The Ge(Li) detector is a semiconductor base with the lithium drifted region serving as a depleted region under a reverse bias. The gamma ray traverses this region causing the formation of electron-hole pairs according to band theory (3). This process causes an induced charge in the detector's external circuit. Virtually all components and processes exhibit a

random or stochastic behavior, which effects the resolution (or line width of the gamma-ray photopeak) of the detector. These random processes can be grouped as the electron-hole formation, the detector and amplifier noise, and miscellaneous other effects.

The width or resolution property of the detector is equal to the square root of the sum of the squares of the characteristic width for each of these three random processes. Of major importance is the stochasticity of electron-hole pair with its characteristic width being proportional to the square root of the product of the gamma-ray energy and the average energy required to produce an electron-hole pair. For Ge this average energy was measured as 2.84 eV (3). Ge(Li) enjoys almost a factor of ten better resolution than scintillation detectors (NaI(Tl)), but the resolution varies with energy more slowly for the scintillation detector. Also, the scintillation detector has about a factor of ten better efficiency than the Ge(Li) detectors. However, the resolution gain is of so much value as to make the Ge(Li) more useful for modern NAA.

The benefits of gamma-ray spectrometry notwithstanding, there are problems of resolving two gamma-ray photopeaks (even for the Ge(Li) with its outstanding improvement in resolution), e.g., the photopeaks for ^{56}Mn (0.8467 MeV) and ^{27}Mg (0.8438 MeV) can be difficult to resolve, especially for certain concentration ratios. The most difficult resolution problem is that of determining the concentration of radioactive isotopes which yield annihilation photopeaks. Some isotopes are positron-only emitters yielding only an annihilation photopeak.

However, virtually every other gamma-ray emitting radioactive isotope can also contribute to the annihilation photopeak, as was illustrated above. Thus, the annihilation photopeak consists of contributions from many radioactive isotopes and a time dependent analysis must be performed.

Determining the area under a photopeak makes possible the calculation of the number of nuclei in the sample. This area is directly proportional to activity. The escape peaks are superimposed upon the Compton continuum; therefore, this continuum must be taken into account in calculating their areas. The complicated pulse-height spectrum produced from monoenergetic photons incident upon the detector presents a basic problem in the exact interpretation and analysis of data obtained with a Ge(Li) spectrometer, i.e., the exact area of a photopeak may be very difficult to determine.

As the gamma-ray energy and the number of gamma rays increases, the pulse height distribution becomes more complicated. An activated sample with several nuclides in it could yield a gamma-ray spectrum which contains the superposition of many photopeaks, escape peaks, annihilation, and Compton continua. Because each gamma ray contributing to the full spectrum decays at a rate different from all other gamma rays, the photopeak area calculation is even more difficult.

It is possible to use digital computers for the analysis of the complex spectrum obtained in gamma-ray spectrometry (19,20,21,22,23); satisfactory results are often obtained. One such procedure uses a

large matrix, the elements of which describe the response of the spectrometer to monoenergetic gamma rays. Gamma-ray spectrometry in NAA plays an essential role for resolving the necessary components in a spectrum and in determining the amount of an element in the unknown sample.

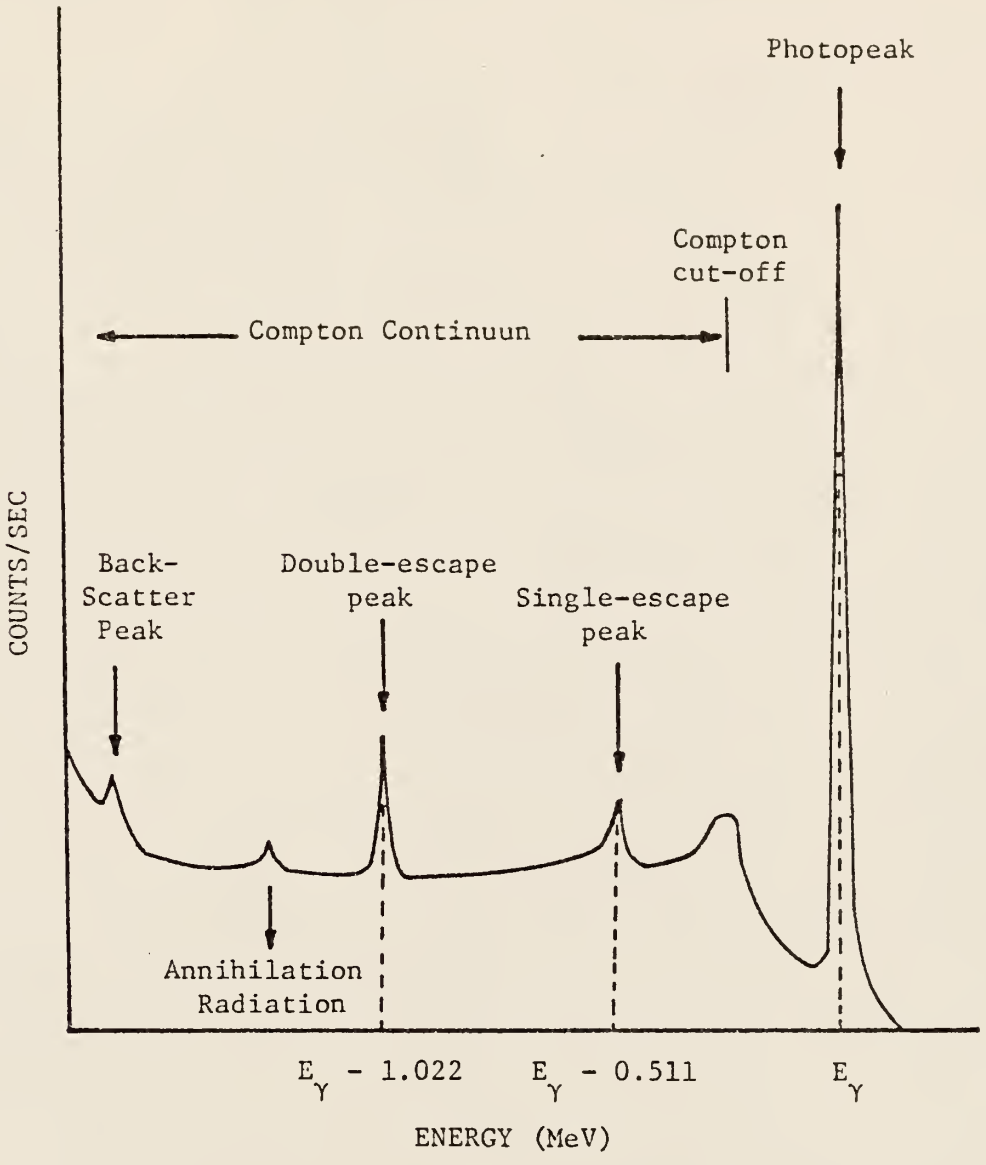

Fig. 1.4-1. A typical spectrum produced by a mono-energetic gamma ray emitter. (E_γ>1.022 MeV)

1.5 Fast Neutron Activation Analysis

Fast neutrons are those with energy more than 0.5 MeV. These neutrons are energetic enough to cause a variety of nuclear reactions which do not occur at lower neutron energies. Fast neutrons have the power of penetration and for many element, the cross sections for nuclear activation are quite adequate; unfortunately the radiation dose associated with a given flux of fast neutrons is many times greater than the corresponding dose for thermal neutrons. Activation analysis with 14 MeV neutrons offers certain attractive features absent in thermal neutron activation work. Depending upon the particular element under consideration, 14 MeV neutron activation offers a choice of nuclear reactions. In general, three predominant reactions can be induced, i.e., (n,p), (n,α), and (n,2n). In the light elements, the appropriate selection of a reaction considerably simplifies their determinations. The elements O, F, N, Al, and Si are in this category. Some reactions involved in wheat irradiation are mentioned here.

Reaction	Half-life of product
$^{14}N(n,2n)^{13}$	9.96 min
$^{31}P(n,\alpha)^{28}Al$	2.3 min
$^{16}O(n,p)^{16}N$	7 sec
$^{19}F(n,2n)^{18}F$	1.87 h
$^{31}P(n,2n)^{30}P$	2.5 min

The disadvantage of fast neutron activation appears primarily from the small cross sections exhibited for a wide range of energies and the rapid loss in neutron energy with penetration into the sample.

The (n,2n) reaction used for our work may occur when the scattered neutron carries enough energy to exceed the binding energy of the neutron in the target nucleus. The result is the removal of one neutron from the target nucleus, for example in the case of ^{14}N (n,2n) ^{13}N. Since all nuclei with the exception of deuterium and beryllium have neutron binding energies in excess of about 6 MeV, only high energy neutrons can be used for such reactions. The resulting nuclide, in most cases, since the N/Z ratio has been reduced to (N-1)/Z, the product nucleus is unstable with respect to positron or electron capture (EC)(2).

The method for activation in this work was 14 MeV neutron activation analysis for nitrogen in NH_4NO_3 and wheat. The reaction used was $^{14}N(n,2n)^{13}N$. Figures (1.5-1) and (1.5-2) give an illustration of the cross section of this reaction. The isotope ^{13}N decays by positron emission with about a 10 minute half life, resulting annihilation gamma rays of energy 0.511 MeV. In Fig. (1.5-3), the decay scheme of ^{13}N to the ground state ^{13}C is illustrated. In the explanation for this decay scheme, it is customary, when distinguishing between positron emission and electron capture, to show a vertical line from the radioactive nuclide that represents an energy drop of 1.022 MeV for positron emission to allow the 0.511 MeV photons that accompany the annihilation of the positron. Thus, ^{13}N which decays by positron emission directly to the

ground state ^{13}C, is measured by the two 0.511 MeV annihilation photons.

The reaction $^{14}N(n,2n)^{13}N$ is not an ideal reaction for our work. Radiation of the energy of 0.511 MeV rises from the reaction $^{31}P(n,2n)^{30}P$. If the reaction is used for quantitative analysis of nitrogen, further problems arise because the impact of fast neutrons on hydrogen present in the specimen releases protons. Protons displaced by neutron bombardment engage in the reaction $^{13}C(p,n)^{13}N$, giving additional counts which are of course, indistinguishible from those attributed to the (n,2n) reaction on ^{14}N.

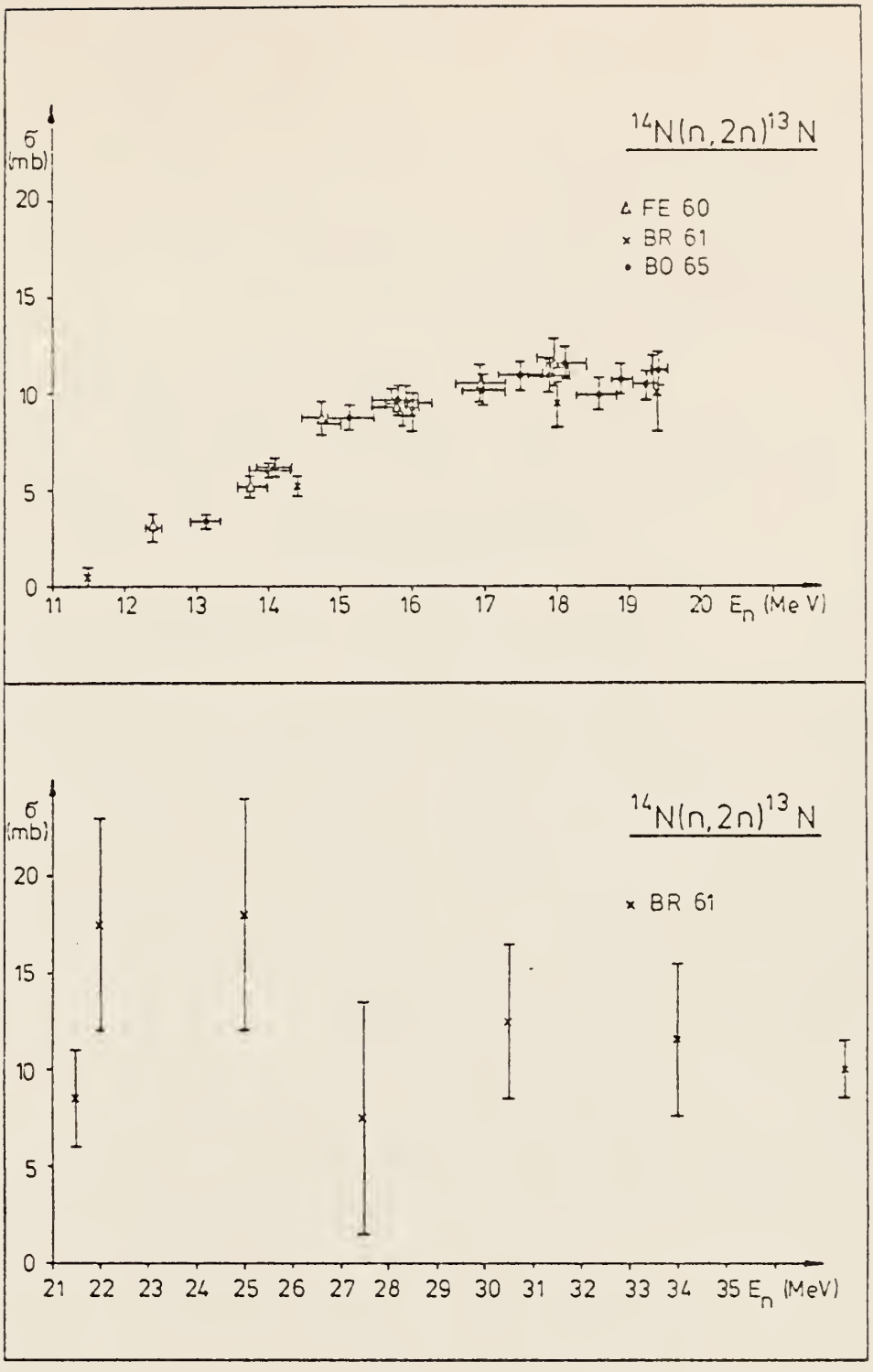

Figure 1.5-1. Graphs of nuclear cross section for $^{14}N(n,2n)^{13}N$. FE60, BR61, BO65 mean the data are obtained from the three reference explained in (66).

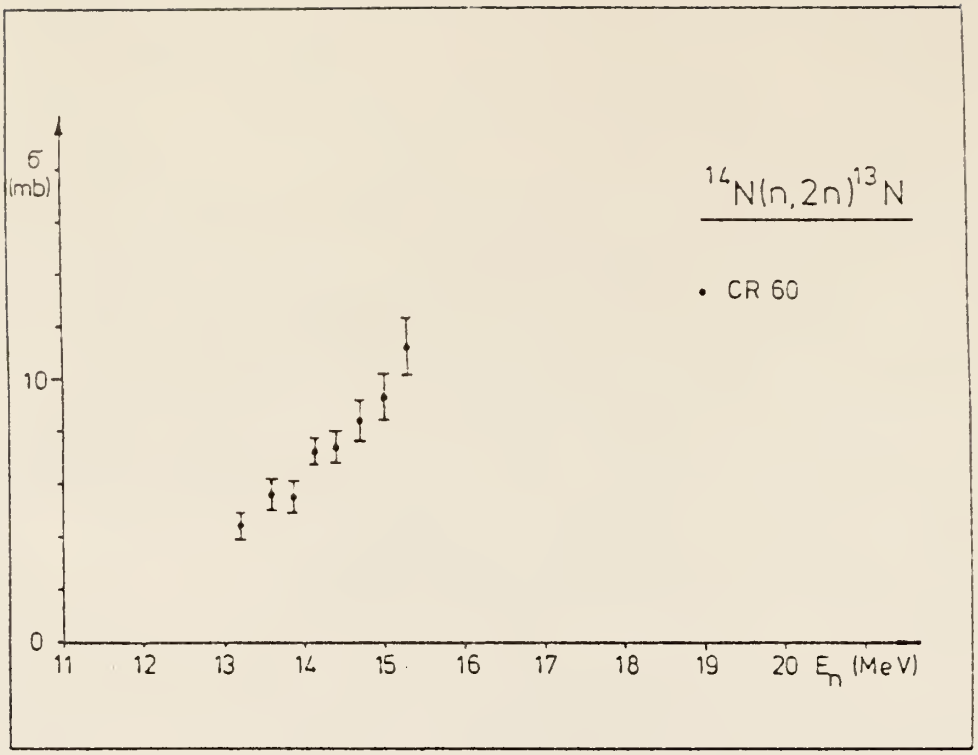

Figure 1.5-2. Graph of nuclear corss section for $^{14}N(n,2n)^{13}N$. CR60 means the data are obtained from the reference explained in (66).

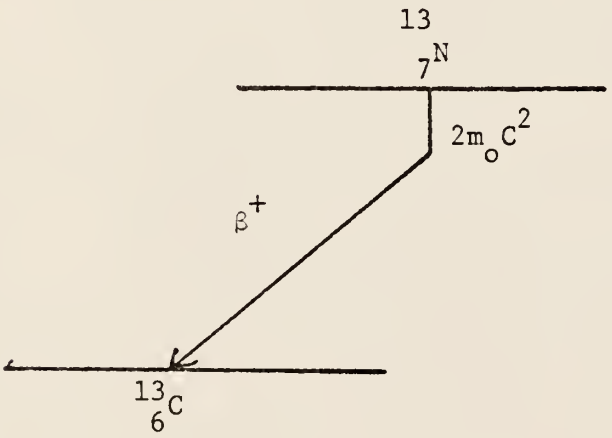

Figure 1.5-3. Decay scheme of 10-m ^{13}N to the ground state of ^{13}C is illustrated.

1.6 Problem and Purpose

There are several types of problems in many branches of science which involve the resolution of experimental observations (data) represented by the sum of linear independent exponential curves of the form

$$f(t) = \sum_{i=1}^{n} N_i \exp(-\lambda_i t) \qquad (1.6\text{-}1)$$

In these problems the parameters N_i and λ_i are physically significant, e.g., the annihilation photopeak is composed of counts which emanate from several radioactive isotopes, each with a characteristic decay constant (λ_i) and abundance (N_i). So the problem is not mere curve fitting, but the parameters should be estimated accurately. The number of components n must also be determined, if n is not known. In most cases and in particular for this work the exponentials are assumed to be separate and independent, i.e., none of the components are produced as the result of the decay of another component. The difficulty that is inherent in the problem is that approximate data of f(t) over a finite range in t must be used. The exponential series has such a strongly nonorthogonal property that the parameters are extremely sensitive to minor fluctuations in the data.

The major purpose of this work was to evaluate the Fourier Decay Analysis (FDA) method for the analysis of multicomponent time-dependent gamma-ray spectra. The FDA method was to be compared to a transform

(logarithm) and an iterative least squares analysis methods for determining the parameters, N_i and λ_i, of Eq. (1.6-1). The other major task of this work was to determine the half-life of ^{13}N using NH_4NO_3 and wheat samples as the source of nitrogen. The measured half lives were compared to published values.

1.7 Other Methods for Resolution of Decay Curves

The most common method which has been used thus far for resolution of a decay curve into its components is the graphical approach (or the stripping method). In this method of analysis, the data are plotted on semilog graph paper, and the resolution of the curve is performed by repeated subtraction of "fitted" straight lines. Judgement of which data are fit with straight lines can play a great role here. The procedure is easy to perform, but there are limitations in applying the method, e.g., it is nearly impossible to determine the decay constants for more than three or four components.

The stripping method can be improved by using the least-squares technique for fitting the straight lines. Thus, some estimation of error is possible. Many mathematical approaches to this problem have been suggested. Proney (24), Hudson (25), Household (26), Cornell (27), and Ziegler (28), have proposed methods which attempt to solve the problems inherent in the stripping method. Simple and straightforward mathematical solutions are available for solution of the problem of separating exponentials, but data which contain fluctuations cause many practical problems to arise. Due to the strong property of nonorthognality of exponential functions, a slight error in taking the data, will result in much error in the results. Thus, the data must be extremely precise, if more than two exponentials are to be separated. In most cases the precision required of the data is

beyond that usually available. Hence, this method often yields only an approximate estimate of the parameters N_i and λ_i (of Eq. 1.6-1).

Computer solutions in several forms have been programmed for the analysis of multicomponent decay curve. In curve fitting and in the quantitative treatment of experimental data the method of least squares is widely used. During the past years many people have developed computer codes, based on the least squares method, for analyzing multicomponent radioactive decay curves. Some codes have limited capabilities, while later modifications became increasingly complex and more sophisticated.

One code used for analysis of multicomponent decay curves is called "Brunhilde". This method described by Nervik (29) is based on the least squares procedure. Operation of the Brunhilde code may be broken into three general categories: (1) acceptance and storage of input data; (2) calculation and resolution of the decay curve; (3) printout of data. For more details see references (29,30).

A modification of this method of least squares is described by Cumming (29). The procedure described by Cumming is an iterative determination of the decay constants.

Another program for the analysis of multicomponent decay curves by a least squares procedure has been developed. This code is called CLSQ which was written by G. Lutz (30). In this code, which was prepared by a change of the original "CLSQ" of Cumming, determination of half-lives of the nuclear species are provided by an iterative routine starting

from trial values. Many people have modified the "CLSQ" code with different approaches (30).

Another mathematical approach has been developed by Shafer (31). As mentioned, in most of the methods the process of iteration is used. In this process initial estimates of the parameters (N_i and λ_i in Eq. 1.6-1) are made. Change parameters (ΔN_i and $\Delta\lambda_i$) are calculated in the least square sense. This change parameters are added to the initial estimates. New change parameters are calculated. This iterative procedure is continued until the decimal precision is obtained.

2.0 Fourier Decay Analysis Method

2.1 Theory

There are several types of problems in many branches of science in which data can be represented by a sum of independent exponential functions of the form

$$f(t) = \sum_{i=1}^{n} N_i \exp(-\lambda_i t) \qquad (2.1\text{-}1)$$

and physically significant parameters N_i and λ_i are desired to be estimated. The FDA approach is based on the fact that the exponential series may be represented by an integral equation (32). The function f(t) in Eq. (2.1-1) is in the form of a Dirichlet series (33) which may be expressed as a Stieltjes intergal (Appendix A).

$$f(t) = \sum_{i=1}^{n} N_i \exp(-\lambda_i t) = \int_0^\infty \exp(-\lambda t)\, dh(\lambda) \qquad (2.1\text{-}2)$$

where $h(\lambda)$ is step function (34).

The function f(t) may also be expressed in the form of a Laplace integral equation.

$$f(t) = \int_0^\infty \exp(-\lambda t) g(\lambda) d\lambda. \qquad (2.1\text{-}3)$$

The function $g(\lambda)$ is a sum of delta functions (Appendix B). A plot of $g(\lambda)$ vs λ is expected to be in form of a histogram, but due to error inherent in the experimental estimate of f(t) and in numerical computations necessary to obtain $g(\lambda)$, a plot of $g(\lambda)$ vs λ

will appear in the form of frequency spectrum. Each true peak in the spectrum indicates a component, the abscissa value at the center of the peak is the decay constant λ_i, while the height of the peak is directly proportional to N_i/λ_i. So, by having f(t), the problem is in the determination of $g(\lambda)$. The method used here is based on a general approach for solving linear equations (35,36,37). More description about this method can be obtained in references (29,32). The function $g(\lambda)$, actually $g(\lambda)/\lambda$, is obtained as follows

$$f(t) = \int_0^\infty \exp(-\lambda t) g(\lambda) d\lambda. \qquad (2.1\text{-}3)$$

The variables λ and t are transformed by letting $\lambda = e^{-y}$ and $t = e^x$. Then

$$d\lambda = -e^{-y}\, dy, \qquad (2.1\text{-}4)$$

$$e^{-\lambda t} = \exp[-e^{(x-y)}], \qquad (2.1\text{-}5)$$

$$f(t) = f(e^x), \qquad (2.1\text{-}6)$$

$$g(\lambda) = g(e^{-y}). \qquad (2.1\text{-}7)$$

While λ varies from zero to ∞, y varies from ∞ to $-\infty$. Hence,

$$f(e^x) = \int_{-\infty}^{+\infty} \exp\,[-e^{(x-y)}]\, e^{-y} g(e^{-y}) dy. \qquad (2.1\text{-}8)$$

Multiply both sides by e^x.

$$e^x f(e^x) = \int_{-\infty}^{+\infty} \exp\,[-e^{(x-y)}] e^{(x-y)} g(e^{-y}) dy \qquad (2.1\text{-}9)$$

From the definition of a Fourier transform (38), the function $F(\psi)$ is the Fourier transform of $g(x)$ when

$$F(\psi) = \frac{1}{\sqrt{2\pi}} \int_{-\infty}^{+\infty} g(x) e^{i\psi x} dx. \qquad (2.1\text{-}10)$$

Now if $F(\mu)$ is the Fourier transform of $e^x f(e^x)$, then

$$F(\mu) = \frac{1}{\sqrt{2\pi}} \int_{-\infty}^{+\infty} e^x f(e^x)\, e^{i\mu x} dx \qquad (2.1\text{-}11)$$

By substitution of $e^x f(e^x)$ from (2.1-9) into (2.1-11), we obtain

$$F(\mu) = \frac{1}{\sqrt{2\pi}} \int_{x=-\infty}^{x=+\infty} \left\{ \int_{y=-\infty}^{y=+\infty} \exp[e^{(x-y)}]\, e^{(x-y)} g(e^{-y}) dy \right\} e^{i\mu x} dx \qquad (2.1\text{-}12)$$

Let $s = x-y$, or $x = s+y$, then

$$F(\mu) = \frac{1}{\sqrt{2\pi}} \int_{s=-\infty}^{s=+\infty} \left\{ \int_{y=-\infty}^{y=+\infty} \exp[-e^s]\, e^s g(e^{-y})\, dy \right\} e^{i\mu(s+y)} ds \qquad (2.1\text{-}13)$$

By rearranging terms, we have

$$F(\mu) = \frac{1}{\sqrt{2\pi}} \int_{y=-\infty}^{y=+\infty} g(e^{-y})\, e^{i\mu y}\, dy \int_{s=-\infty}^{x=+\infty} \exp(-e^s)\, e^s\, e^{i\mu s} ds. \qquad (2.1\text{-}14)$$

Defining $G(\mu)$ and $K(\mu)$ as Fourier transform of $g(e^{-y})$ and $\exp(-e^s)e^s$, respectively, yields

$$G(\mu) \equiv \frac{1}{\sqrt{2\pi}} \int_{-\infty}^{+\infty} g(e^{-y})\, e^{i\mu y}\, dy \qquad (2.1\text{-}15)$$

$$K(\mu) \equiv \frac{1}{\sqrt{2\pi}} \int_{-\infty}^{+\infty} \exp(-e^{s}) e^{s} e^{i\mu s} ds \qquad (2.1\text{-}16)$$

Then by substituting Eqs. (2.1-15) and ((2.1-16) into Eq. (2.1-14), we obtain

$$F(\mu) = \sqrt{2\pi}\ G(\mu)\ K(\mu) \qquad (2.1\text{-}17)$$

and

$$G(\mu) = \frac{1}{\sqrt{2\pi}}\ F(\mu)/K(\mu) \qquad (2.1\text{-}18)$$

Now, by multiplying both sides by $e^{-i\mu y}$ and integrating over all μ space, we obtain

$$\int_{-\infty}^{+\infty} G(\mu) e^{-i\mu y} d\mu = \frac{1}{\sqrt{2\pi}} \int_{-\infty}^{+\infty} \frac{F(\mu)}{K(\mu)}\ e^{-i\mu y} d\mu \qquad (2.1\text{-}19)$$

By multiplying both sides by $\frac{1}{\sqrt{2\pi}}$, it is seen that the right-hand side is the inverse Fourier transform of $G(\mu)$, namely, $g(e^{-y})$. Then

$$g(e^{-y}) = \frac{1}{2\pi} \int_{-\infty}^{+\infty} \frac{F(\mu)}{K(\mu)}\ e^{-i\mu y} d\mu, \qquad (2.1\text{-}20)$$

but

$$g(e^{-y})\ dy = \frac{g(\lambda)}{\lambda}\ d\lambda. \qquad (2.1\text{-}21)$$

This means that a plot of $g(e^{-y})$ vs y is equivalent to a plot of $g(\lambda)/\lambda$ vs λ.

To evaluate $g(e^{-y})$, $F(\mu)$ and $K(\mu)$ are evaluated first. In this case, $K(\mu)$ can be evaluated analytically, because $K(\mu)$ is the Euler integral for the complex gamma function (Appendix C).

$$K(\mu) = \frac{1}{\sqrt{2\pi}} \Gamma(1+ i\mu) \qquad (2.1\text{-}22)$$

The function $F(\mu)$ can be evaulated numerically by using Eq. (2.1-11). These evaluations for $K(\mu)$ and $F(\mu)$ are used in Eq. (2.1-20) to determine $g(e^{-y})$ as y or equivalently $g(\lambda)/\lambda$ vs λ.

2.2 Cutoff Error

One of the difficulties which we have in evaluating Eq. (2.1-20) is that we must deal with data that only approximate f(t) over a finite range in t. Thus, Eqs. (2.1-11) and (2.1-20) can not be integrated numerically from $-\infty$ to $+\infty$, but must be evaluated between cutoff points $\pm x_o$ ($\pm \ln t_o$) and $\pm\mu_o$.

$$F(\mu) = \frac{1}{\sqrt{2\pi}} \int_{-\infty}^{+\infty} e^{x} f(e^{x})\, e^{i\mu x} dx \tag{2.2-1}$$

or

$$F(\mu) = \frac{1}{\sqrt{2\pi}} \int_{-\infty}^{-x_o} e^{x} f(e^{x})\, e^{i\mu x} dx + \frac{1}{\sqrt{2\pi}} \int_{-x_o}^{+x_o} e^{x} f(e^{x}) e^{i\mu x} dx$$

$$+ \frac{1}{\sqrt{2\pi}} \int_{+x_o}^{+\infty} e^{x} f(e^{x}) e^{i\mu x} dx \tag{2.2-2}$$

Let

$$E(x_o,\mu) \equiv \frac{1}{\sqrt{2\pi}} \int_{-\infty}^{-x_o} e^{x} f(e^{x})\, e^{i\mu x} dx + \frac{1}{\sqrt{2\pi}} \int_{+x_o}^{+\infty} e^{x} f(e^{x})\, e^{i\mu x} dx \tag{2.2-3}$$

then

$$F(\mu) = \frac{1}{\sqrt{2\pi}} \int_{-x_o}^{+x_o} e^{x} f(e^{x})\, e^{i\mu x} dx + E(x_o,\mu) \tag{2.2-4}$$

Thus, the calculated F(μ) will be in error by at least the amount of

$E(x_o,\mu)$. The value for x_o should be chosen such that the value of $E(x_o,\mu)$ becomes sufficiently small. It may be necessary to extrapolate the experimental data to larger values of t in order to reduce $E(x_o,\mu)$ to sufficiently small value.

The other cutoff at $\mu = \pm\mu_o$ in Eq. (2.1-20) produces errors which effects the ability to determine $g(\lambda)/\lambda$ vs.λ. The function $K(\mu)$ dies off rapidly with increasing μ, so for some value of μ the quotient $F(\mu)/K(\mu)$ in Eq. (2.1-20) begins to grow without bound. The greater the value in μ at which $F(\mu)/K(\mu)$ remains well-behaved, the narrower and more well-defined are the components.

2.3 Numerical Integration

To evaluate $g(\lambda)/\lambda$ vs λ two integrations must be performed. First, the Fourier transform, $F(\mu)$, is found by using Eq. (2.1-11). This function is divided by the complex gamma function given in Eq. (2.1-22), and $g(e^{-y})$ is found by using the result of the first integration in Eq. (2.1-20):

$$F(\mu) = \frac{1}{\sqrt{2\pi}} \int_{-x_o}^{+x_o} e^{x} f(e^{x}) e^{i\mu x} dx + E(\mu, x_o)$$

Since it is assumed $E(\mu, x_o) \simeq o$, then

$$F(\mu) \simeq \int_{-x_o}^{+x_o} e^{x} f(e^{x}) e^{i\mu x} dx \qquad (2.3\text{-}1)$$

Next the following algebraic operations are performed.

$$F(\mu) = \frac{1}{\sqrt{2\pi}} \int_{-x_o}^{+x_o} e^{x} f(e^{x}) e^{i\mu x} dx \qquad (2.3\text{-}2)$$

$$= \frac{1}{\sqrt{2\pi}} \int_{-x_o}^{o} e^{x} f(e^{x}) e^{i\mu x} dx + \frac{1}{\sqrt{2\pi}} \int_{o}^{x_o} e^{x} f(e^{x}) \, e^{i\mu x} dx$$

$$= \frac{1}{\sqrt{2\pi}} \int_{o}^{x_o} e^{-x} f(e^{-x}) e^{-i\mu x} dx + \frac{1}{\sqrt{2\pi}} \int_{o}^{x_o} e^{x} f(e^{x}) e^{i\mu x} dx$$

then

$$F(\mu) = \frac{1}{\sqrt{2\pi}} \int_{o}^{x_o} [e^{x} f(e^{x}) e^{i\mu x} + e^{-x} f(e^{-x}) e^{-i\mu x}] dx \qquad (2.3\text{-}3)$$

Define $f^*(x) \equiv e^{x} f(e^{x})$ and $f^*(-x) \equiv e^{-x} f(e^{-x})$

so,

$$F(\mu) = \frac{1}{\sqrt{2\pi}} \int_{o}^{x_o} [f^*(x) e^{i\mu x} + f^*(-x) e^{-i\mu x}] dx \qquad (2.3\text{-}4)$$

By using Euler's formula (39),

$$e^{i\mu x} = \cos(\mu x) + i \sin(\mu x), \qquad (2.3\text{-}5)$$

$$e^{-i\mu x} = \cos(\mu x) - i \sin(\mu x), \qquad (2.3\text{-}6)$$

substituting into Eq. (2.2-4), simplifying, and separating the real and imaginary parts, we obtain

$$F(\mu) = \frac{1}{\sqrt{2\pi}} \int_{o}^{x_o} [f^*(x) + f^*(-x)] \cos(\mu x) dx + \frac{i}{\sqrt{2\pi}} \int_{o}^{x_o} [f^*(x) - f^*(-x)] \sin(\mu x)\, dx \qquad (2.3\text{-}7)$$

$$F_c = \frac{1}{\sqrt{2\pi}} \int_{o}^{x_o} [f^*(x) + f^*(-x)] \cos(\mu x) dx, \qquad (2.3\text{-}8)$$

$$F_s = \frac{1}{\sqrt{2\pi}} \int_{o}^{x_o} [f^*(x) - f^*(-x)] \sin(\mu x)\, dx, \qquad (2.3\text{-}9)$$

where F_c and F_s are real and imaginary parts of $F(\mu)$, respectively.

But $K(\mu)$ also consists of an imaginary part, K_s, and real part, K_c. So $K(\mu)$ can be written

$$K(\mu) = K_c(\mu) + iK_s(\mu) \tag{2.3-10}$$

An expression for $F(\mu)/K(\mu)$ is obtained:

$$\frac{F(\mu)}{K(\mu)} = \frac{F_c(\mu) + iF_s(\mu)}{K_c(\mu) + iK_s(\mu)}$$

$$= \frac{[F_c(\mu) + iF_s(\mu)]\,[K_c(\mu) - iK_s(\mu)]}{[K_c(\mu) + iK_s(\mu)]\,[K_c(\mu) - iK_s(\mu)]}$$

$$= \frac{F_c(\mu)K_c(\mu) + F_s(\mu)K_s(\mu)}{K_c^2(\mu) + K_s^2(\mu)} + i\,\frac{F_s(\mu)K_c(\mu) - F_c(\mu)K_s(\mu)}{K_c^2(\mu) + K_s^2(\mu)} \tag{2.3-11}$$

By substituting Eq. (2.3-11) into Eq. (2.1-20) and using Eq. (2.3-6), we obtain

$$g(e^{-y}) = \frac{1}{2\pi}\int_{-\mu_o}^{+\mu_o} \left(\frac{F_c(\mu K_c(\mu) + F_s(\mu)\,K_s(\mu)}{K_c^2(\mu) + K_s^2(\mu)} + i\,\frac{F_s(\mu)K_c(\mu) - F_c(\mu)K_x(\mu)}{K_c^2(\mu) + K_s^2(\mu)}\right)$$

$$(\cos(y\mu) - i\sin(y\mu))d\mu \tag{2.3-12}$$

Define

$$H(\mu) \equiv \frac{F_c(\mu)K_c(\mu) + F_s(\mu)K_s(\mu)}{K_c^2(\mu) + K_s^2(\mu)}$$

and

$$J(\mu) \equiv \frac{F_s(\mu)K_c(\mu) - F_c(\mu)K_s(\mu)}{K_c^2(\mu) + K_s^2(\mu)}$$

Thus,

$$g(e^{-y}) = \frac{1}{2\pi}\left\{\int_o^{\mu o}[H(\mu)\cos(y\mu) + J(\mu)\sin(y\mu)]d\mu + \int_o^{\mu o}[H(-\mu)\cos(y\mu) - J(-\mu)\sin(y\mu)]d\mu\right\} + \frac{i}{2\pi}\left\{\int_o^{\mu o}[J(\mu)\cos(y\mu) - H(\mu)\sin(y\mu)]d\mu + \int_o^{\mu o}[J(-\mu)\cos(y\mu) - H(-\mu)\sin(y\mu)]d\mu\right\} \quad (2.3\text{-}13)$$

but (see Appendix H)

$$F_c(\mu) = F_c(-\mu), \quad (2.3\text{-}14\text{-}a)$$

$$F_s(\mu) = -F_s(-\mu), \quad (2.3\text{-}14\text{-}b)$$

$$K_c(\mu) = K_c(-\mu), \quad (2.3\text{-}14\text{-}c)$$

$$K_s(\mu) = -K_s(-\mu). \quad (2.3\text{-}14\text{-}d)$$

Thus,

$$g(e^{-y}) = \frac{1}{\pi}\int_o^{\mu o}[H(\mu)\cos(y\mu) + J(\mu)\sin(y\mu)]d\mu \quad (2.3\text{-}15)$$

Thus, all the imaginary terms vanish and a real value for $g(e^{-y})$ is obtained.

3.0 Testing the FDA Method

In order to test the method, one-, two-, and three-component decay curves were constructed. Table (3-1) contains data for one, two, and three component decay curves. In all three cases, time ranged from 0 to 1096.600 (arbitrary units). The points between t = 0 and t = 1 are omitted from the table since they were usually obtained by interpolation.

3.1 Effect of Cutoff with Respect to μ

Several plots of $g(\lambda)/\lambda$ for different values of μ were made. These plots were obtained by integration of Eq. (2.3-14) from 0 to μ_o for each desired value of λ. Figures (3.1-1,2,3,4 and 5) are plots of $g(\lambda)/\lambda$ vs λ for μ_o values equal to 2,4,6,8 and 9, respectively, using the data for a single component curve (Table 3-1,a) where λ = 0.02. For the above calculations, the trapezoidal method for numerical integration for Eqs. (2.3-1) and (2.3-14) was used. The effect of increasing the value of μ_o can be observed. It is seen that the principal peak falls in the same place on each curve, at the proper λ value. By comparing Figs. (3.1-1,2,3,4,5), we can see that as the μ_o value increases, the resolution increases progressively, i.e., the width of the principal peak decreases. In the curve obtained for $\mu_o = 9$ (Fig. 3.1-5), the center of the major peak falls at the proper place and the improvement in resolution has nearly saturated (see Table 3-2).

The major peak, which is theoretically a spike, has been broadened primarily because of the numerics of the calculation, i.e., round-off

Table 3.1. Input data for the accurate decay curve

t	f(t)[a]	f(t)[b]	f(t)[c]
0.000	100.000	1100.000	1200.00
1.000	98.020	1003.842	1101.862
1.284	97.465	978.226	1075.690
1.648	96.758	946.429	1043.186
2.117	95.854	907.113	1002.967
2.718	94.709	859.302	954.010
3.490	93.257	801.942	895.199
4.482	91.427	734.413	825.840
5.755	89.128	656.854	745.982
7.389	86.262	570.511	656.773
9.488	82.716	478.166	560.882
12.182	78.377	384.293	462.670
15.643	73.135	294.754	367.889
20.086	66.917	215.979	282.896
25.790	59.702	153.117	212.820
33.115	51.566	108.271	159.838
42.521	42.724	79.598	122.321
54.598	33.556	62.182	95.738
70.105	24.608	50.509	75.117
90.017	16.524	40.773	57.298
115.584	9.909	31.489	41.398
148.413	5.139	22.670	27.810
190.566	2.212	14.872	17.084
244.692	0.749	8.656	9.405
314.191	0.187	4.320	4.507
403.429	0.031	1.770	1.801
518.013	0.003	0.563	0.566
665.420	0.000	0.129	0.129
1096.600	0.000	0.002	0.002

Table 3.1 cont.

a. $f(t) = 100\ e^{-0.02t}$

b. $f(t) = 1000\ e^{-0.1t} + 100\ e^{-0.01t}$

c. $f(t) = 1000\ e^{-0.1t} + 100\ e^{-0.02t} + 100\ e^{-0.01t}$

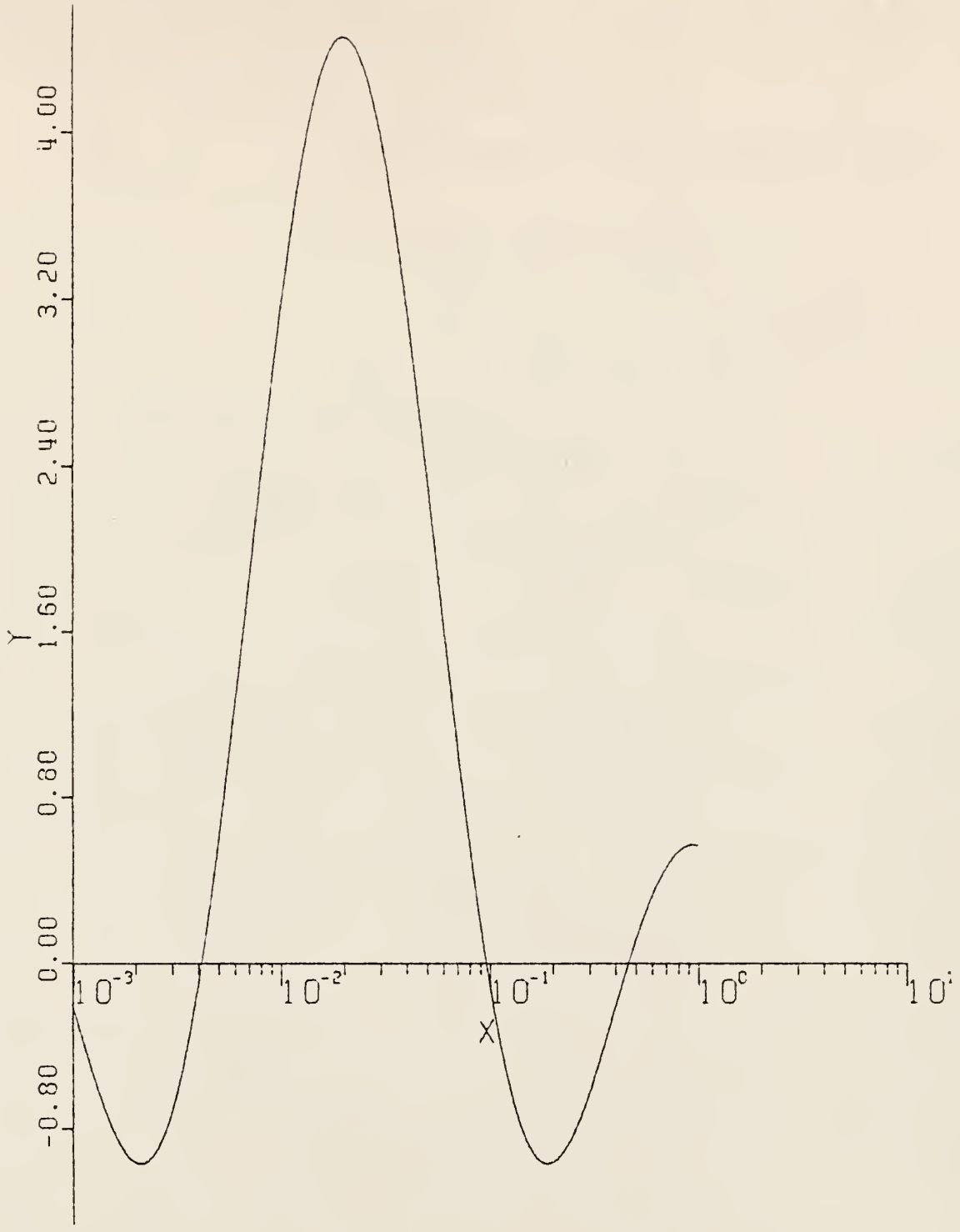

Figure 3.1-1. Result of the analysis of a single-component decay curve (trapezoidal integration routine). Details of the analysis are explained in Appendix E. ($Y = G(\lambda)/\lambda$, $X = \lambda$, $\mu_o = 2$, $X_o = 7$)

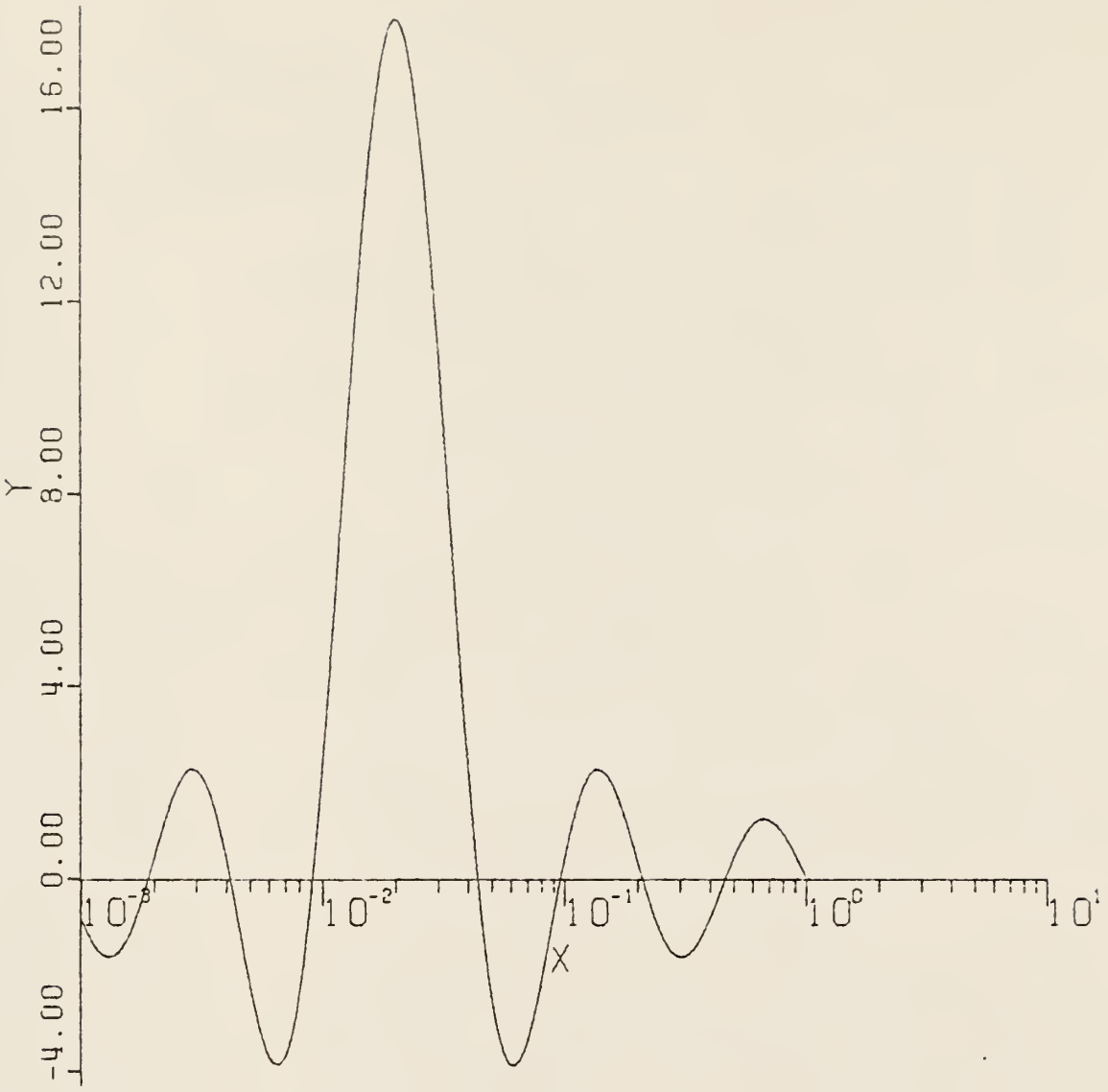

Figure 3.1-2. Result of the analysis of a single-component decay curve (trapezoidal integration routine). Details of the analysis are explained in Appendix E. ($Y = G(\lambda)/\lambda$, $X = \lambda$, $\mu_o = 4$, $X_o = 7$)

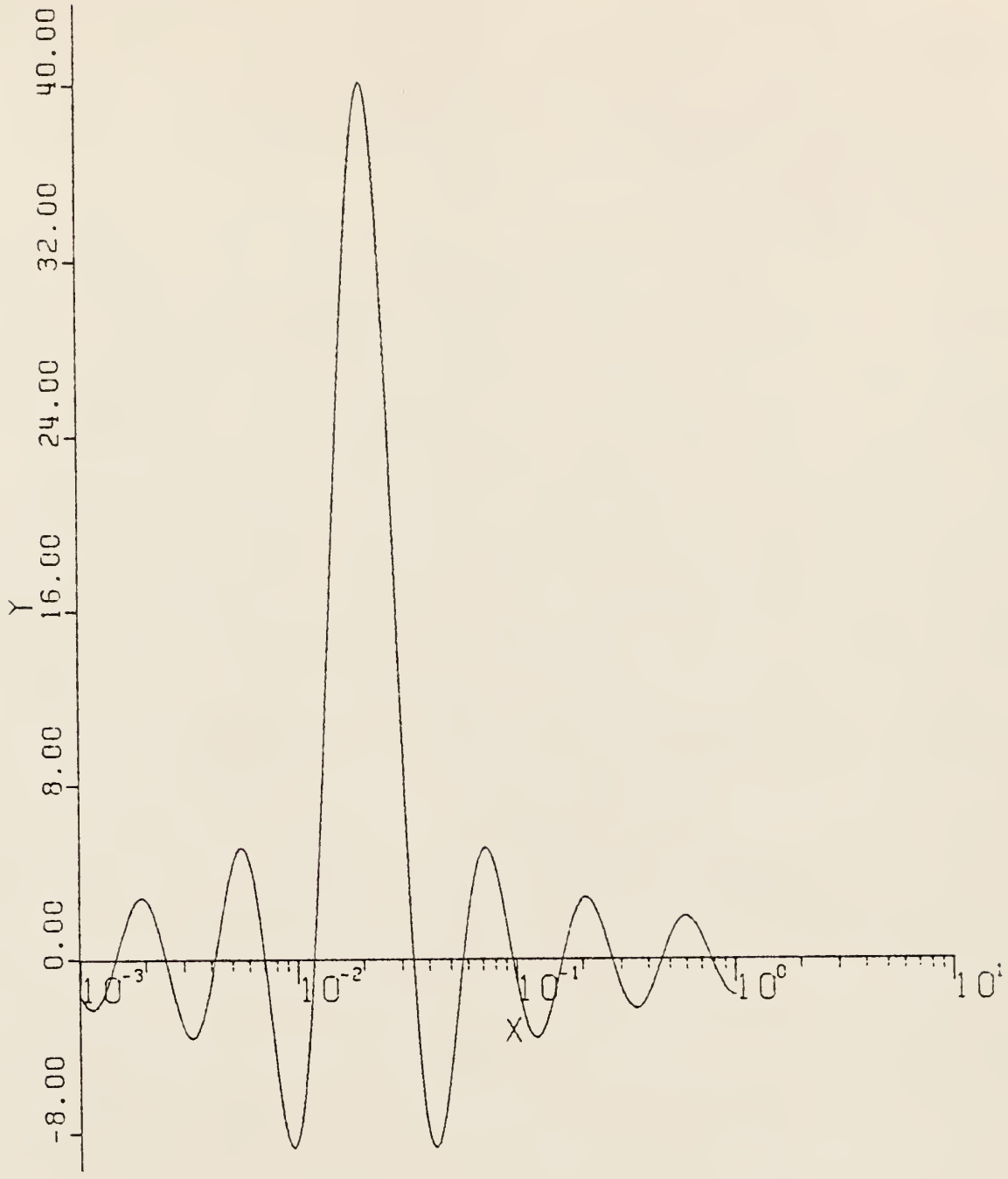

Figure 3.1-3. Result of the analysis of a single-component decay curve (trapezoidal integration routine). Details of the analysis are explained in Appendix E. ($Y = G(\lambda)/\lambda$, $X = \lambda$, $\mu_o = 6$, $X_o = 7$)

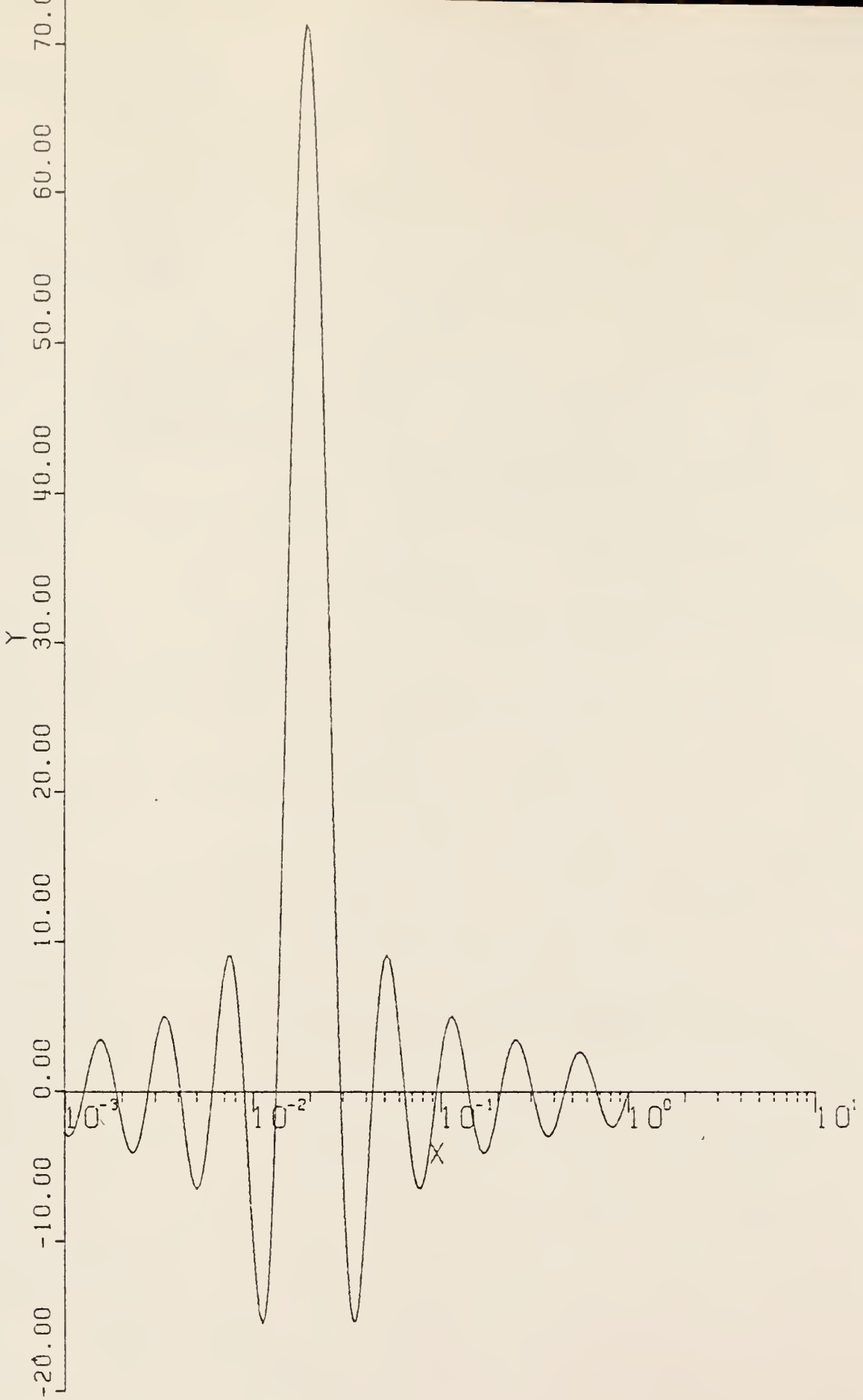

Figure 3.1-4. Result of the analysis of a single-component decay curve (trapezoidal integration routine). Details of the analysis are explained in Appendix E. ($Y = G(\lambda)/\lambda$, $X = \lambda$, $\mu_o = 8$, $X_o = 7$)

Figure 3.1-5. Result of the analysis of a single-component decay curve (trapezoidal integration routine). Details of the analysis are explained in Appendix E. ($Y = G(\lambda)/\lambda$, $X = \lambda$, $\mu_o = 9$, $X_o = 7$)

Table (3-2). Comparison of principal features of each $g(\lambda)/\lambda$ versus λ plot for $f(t) = 100 \exp(-0.02t)$ and $\mu_o = 2,4,6,8,9$ (trapezoidal integration routine, $x_o \cong 7$)

Fig. No.	fwhm	(K) |height| of under shoot on 1st error peak	(H) height of major peak	Ratio $\frac{H}{K}$	No. of error peaks (to 10°)
3.1-1	1.903	1	4.5	4.5	1 Post. 1 Neg.
3.1-2	0.931	4	18	4.5	2 Post. 2 Neg.
3.1-3	0.767	9	40	4.4	3 Post. 3 Neg.
3.1-4	0.498	16	72	4.5	4 Post. 5 Neg.
3.1-5	0.287	20	90	4.5	5 Post. 5 Neg.

error, inaccuracies within the numerical integration scheme, the interpolation routine, the order of interpolation, and cut-off or the fact that the integration is carried out only over a finite range instead of an infinite range as is called for by theory. Also the $g(\lambda)/\lambda$ plot does not go to zero as theory predicts. Remember $g(\lambda)/\lambda$ versus λ is supposed to be a spike at the λ root and zero all other places.

There is a "ringing" or series of "error ripples" which are nearly symmetrically placed about the major peaks. The ratio of the amplitude of these ripples is nearly constant with respect to the amplitude of the major peaks; the number of ripples increases as μ_o increases. Finally the width of these ripples decreases as the width of the major peaks decreases. Apparently these are caused by the numerics of the calculations, as noted above. The positions of the peaks in the error ripples changes as a function of μ_o, whereas the position of the true peak does not. By using this fact we can distinguish small true peaks from error ripples. Also, the width of the base of true peak is wider than the base width of an error ripple. The error ripples are symmetrical with respect to the true peaks and as μ_o increases the symmetry does not change.

Following the same procedure but by using Simpson's rule for integration of the Eqs. (2.3-1) and (2.3-14), we obtain Figs. (3.1-6,7,8,9 and 10) which are plots of $g(\lambda)/\lambda$ vs λ for μ_o values of 2,4,6,8 and 9, using the data for the single-component decay curve, where $\lambda = 0.02$. Again, the effect of increasing the value of μ_o can be observed. As the μ_o value increases, the resolution increases progressively and the breadth of the true peak decreases also (see Table 3-3). For cases of μ_o equal

to 2, 4, and 6 (Figs. 3.1-6,7, and 8) good results (< %2.5 error) are observed. As seen for μ_o = 8 and 9 (Figs. 3.1-9 and 10) the error ripples completely mask the results, and the error ripples are no longer symmetrical with respect to the true peak.

Once the approximate position of the true peak is found, the position can be determined more accurately by taking a smaller interval in λ. The curves shown in Figs. (3.1-11 and 12) are an expanded view of the μ_o = 6 and 8 peaks of Figs. (3.1-3 and 4).

The case of two-component decay curve with μ_o increasing from 3 to 6 was studied next. By using the trapezoidal method for integration, the plots for μ_o values 3 and 6 (Figs. 3.1-13 and 14) were obtained. The true peaks approximately fall in proper place (Table 3-4). According to the theory, in both curves the height of the true peaks should be equal, because $g(\lambda)/\lambda$ vs λ was plotted and both the coefficient and the λ value of the second component are a factor of 10 smaller than those of the first component, but due to errors in λ_1 and λ_2 the heights of two peaks are not equal (Table 3-4). The order of interpolation used for the analysis was increased from 3 to 6 in order to study the effect of interpolation on the results. This increase improved the results (Table 3-4). As seen, due to improvement of results, the heights of the true peaks become equal (Fig. 3.1-15 and 16).

The same procedure was followed by using the Simpson's method for integration. Again, fairly good results (< %5 error) for μ_o = 3 were obtained, while for μ_o = 6 the error ripples completely masked the true peaks (Figs. 3.1-17 and 18).

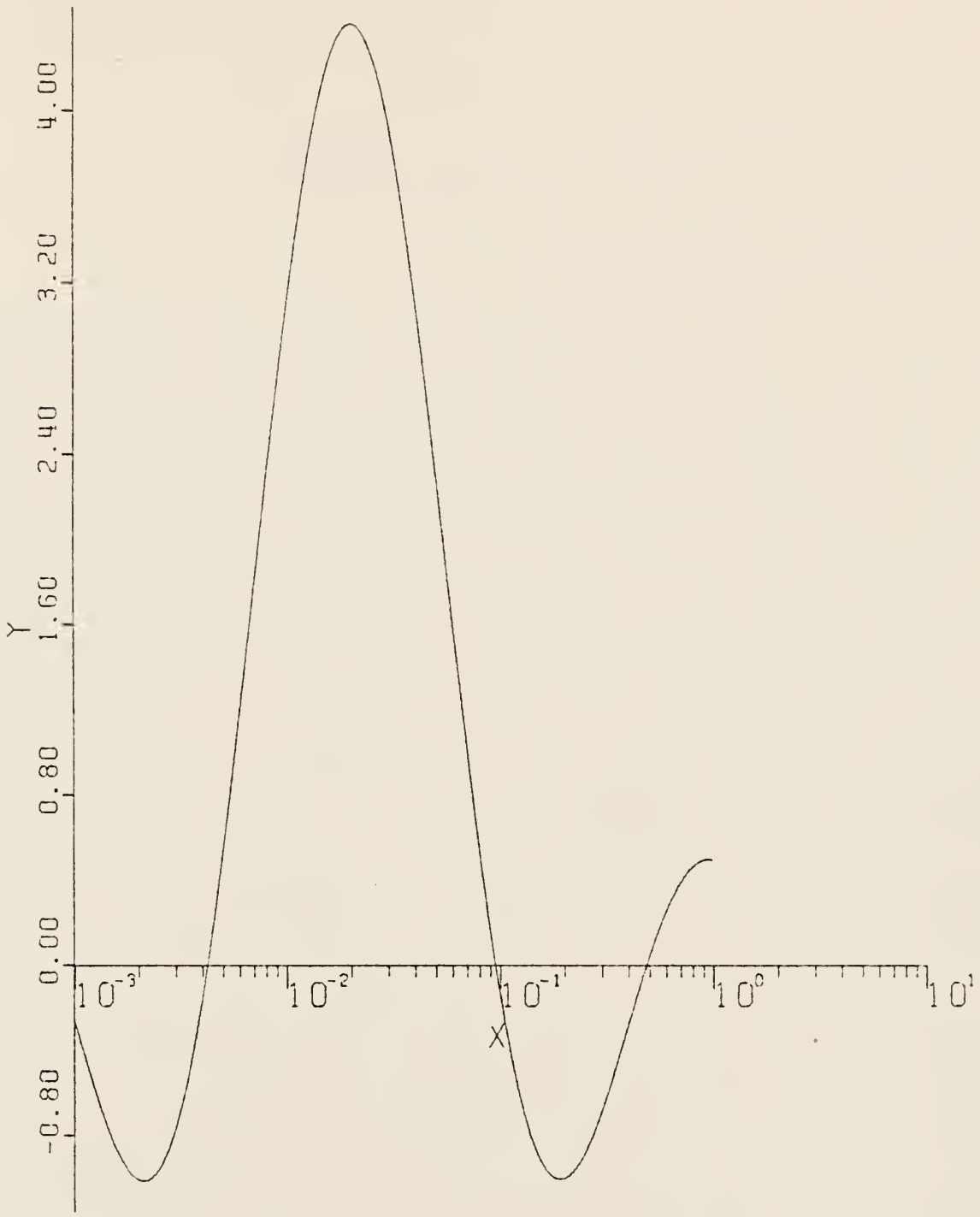

Figure 3.1-6. Result of the analysis of a single-component decay curve (Simpson's integration routine). Details of the analysis are explained in Appendix E. ($Y = G(\lambda)/\lambda$, $X = \lambda$, $\mu_o = 2$, $X_o = 7$)

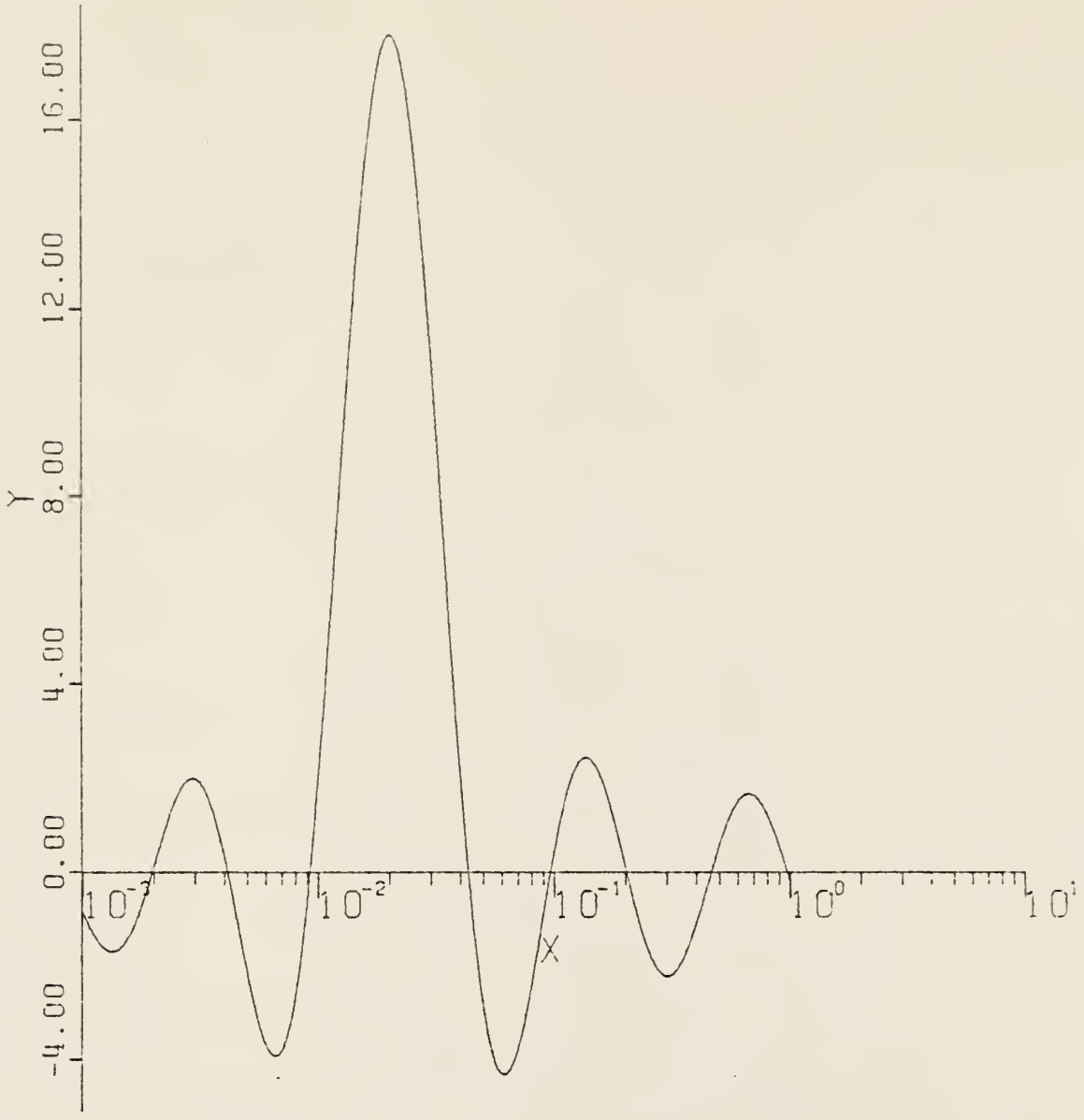

Figure 3.1-7. Result of the analysis of a single-component decay curve (Simpson's integration routine). Details of the analysis are explained in Appendix E. ($Y = G(\lambda)/\lambda$, $X = \lambda$, $\mu_o = 4$ $X_o = 7$)

Figure 3.1-8. Result of the analysis of a single-component decay curve (Simpson's integration routine). Details of the analysis are explained in Appendix E. ($Y = G(\lambda)/\lambda$, $X = \lambda$, $\mu_o = 6$, $X_o = 7$)

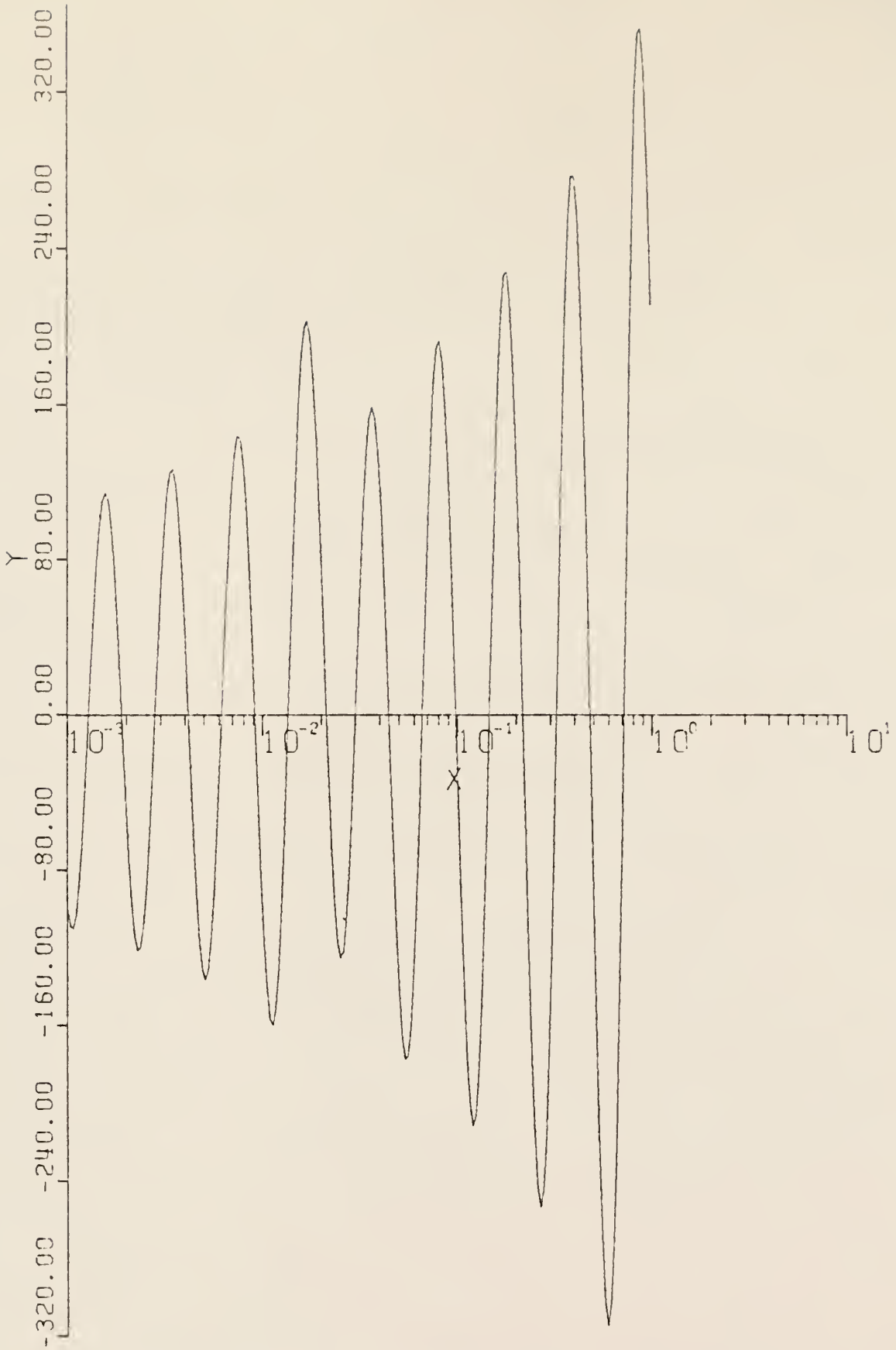

Figure 3.1-9. Result of the analysis of a single-component decay curve (Simpson's integration routine). Details of the analysis are explained in Appendix E. ($Y = G(\lambda)/\lambda$, $X = \lambda$, $\mu_o = 8$, $X_o = 7$)

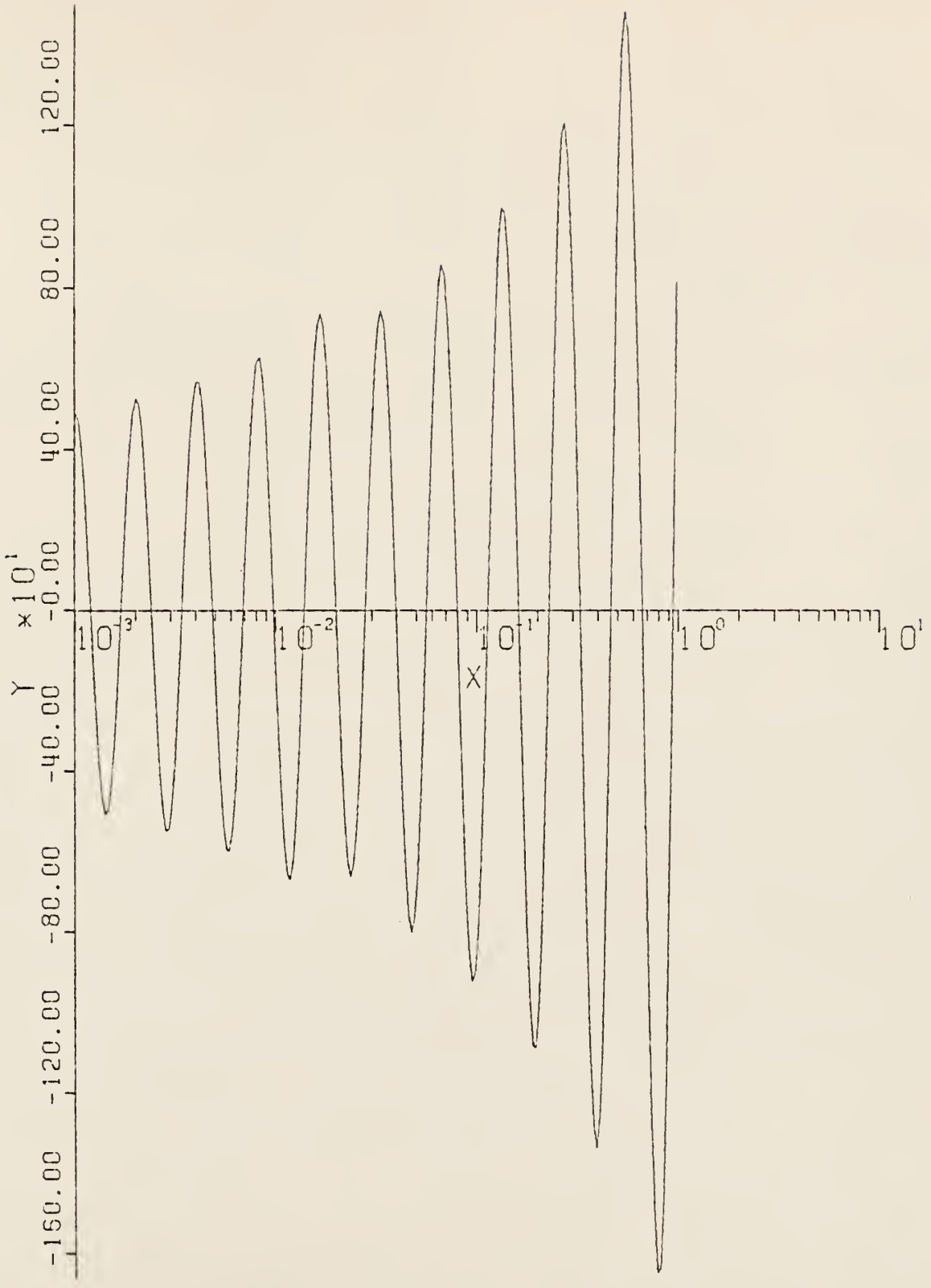

Figure 3.1-10. Result of the analysis of a single-component decay curve (Simpson's integration routine). Details of the analysis are explained in Appendix E. ($Y = G(\lambda)/\lambda$, $X = \lambda$, $\mu_o = 9$, $X_o = 7$)

Table (3-3). Comparison of principal features of each $g(\lambda)/\lambda$ versus λ plot for $f(t) = 100 \exp(-0.02t)$ and $\mu_o = 2,4,6,8,9$ (Simpson's integration routine)

Fig. No.	fwhm	(K) |height| of under shoot on 1st error peak	(H) height of major peak	Ratio = $\frac{H}{K}$	No. of error peaks (to 10°)
3.1-6	1.742	1.1	4.4	4	1 Post. 1 Neg.
3.1-7	0.653	4.5	18	4	2 Post. 2 Neg.
3.1-8	0.485	9	45	5	3 Post. 4 Neg.
3.1-9	Error ripples completely masked the results.				
3.1-10	Error ripples completely masked the results.				

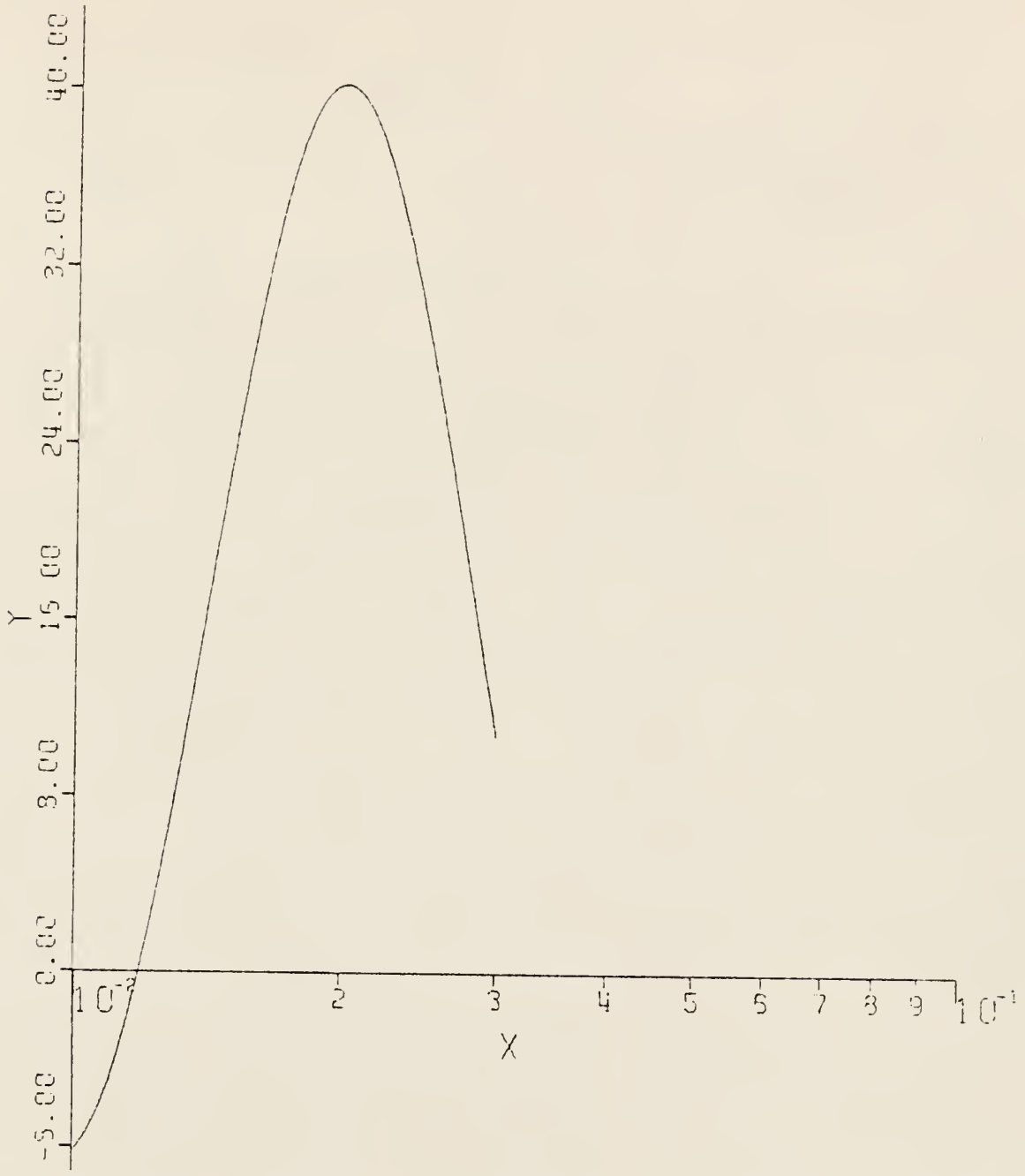

Figure 3.1-11. Results of the analysis of single-component decay curve (trapezoidal integration routine). Details of the analysis are explained in Appendix E. ($Y = G(\lambda)/\lambda$, $X = \lambda$, $\mu_o = 6$, $X_o = 7$)

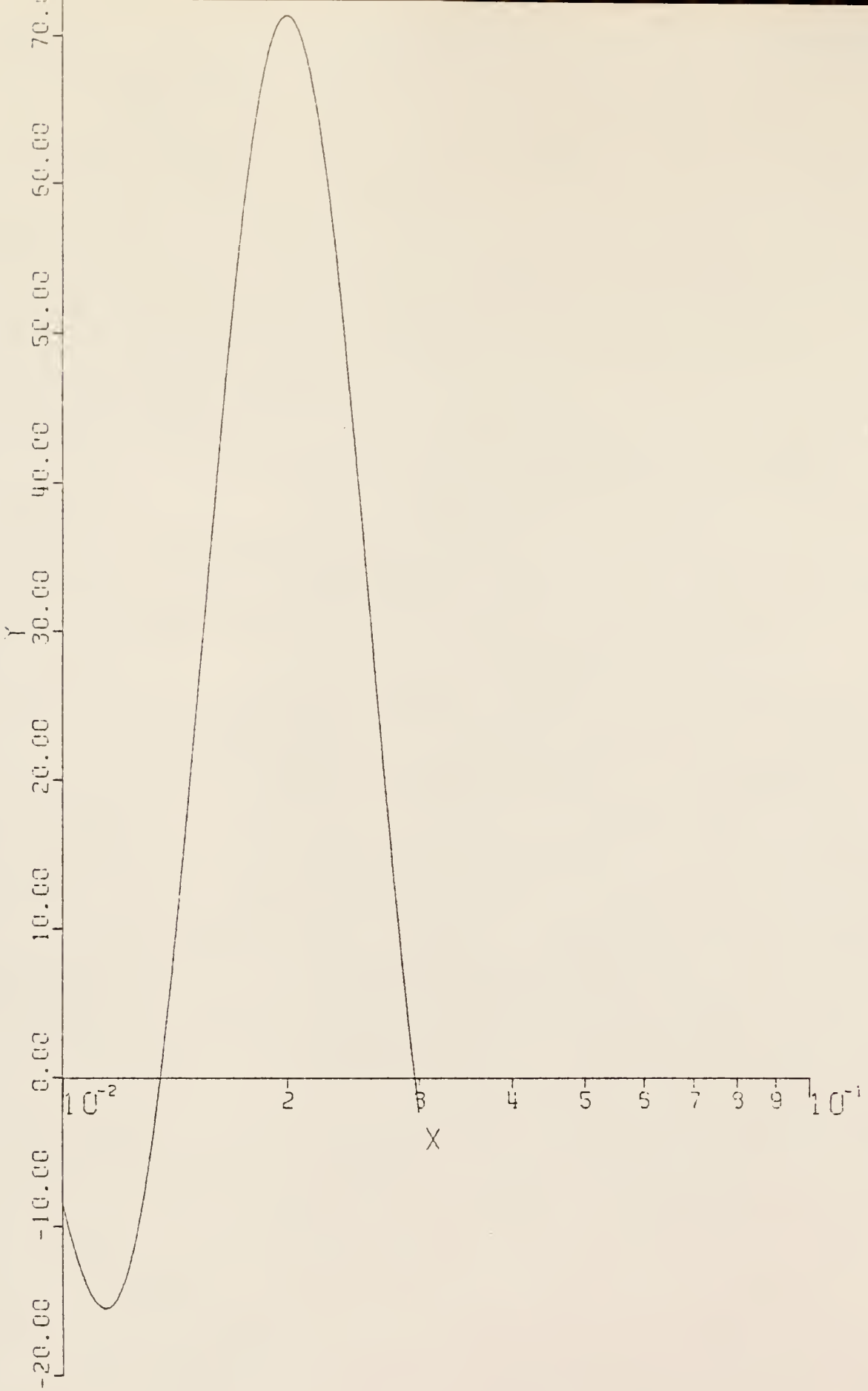

Figure 3.1-12. Results of the analysis of single-component decay curve (trapezoidal integration routine). Details of the analysis are explained in Appendix E. ($Y = G(\lambda)/\lambda$, $X = \lambda$, $\mu_o = 8$, $X_o = 7$)

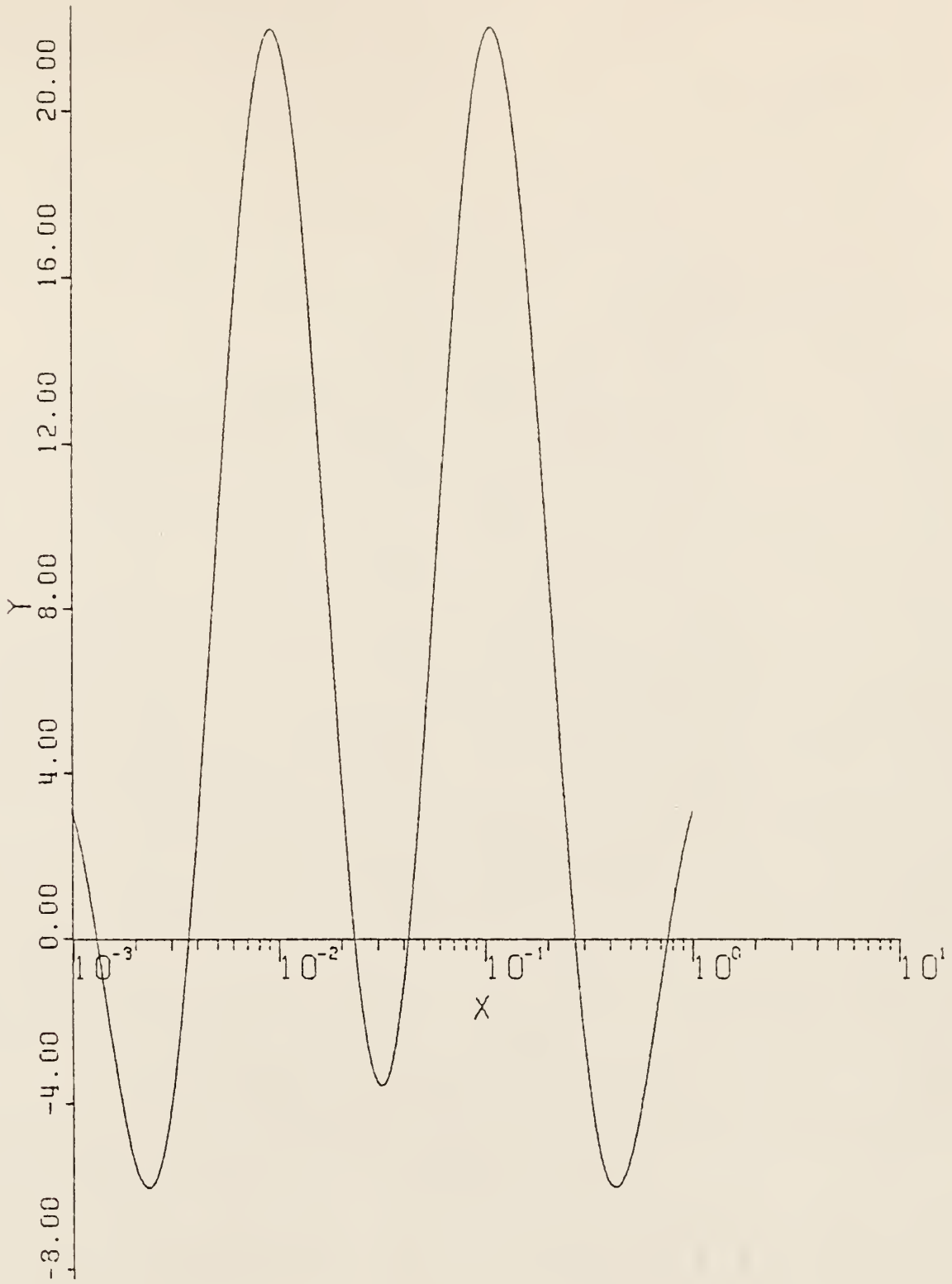

Figure 3.1-13. Results of the analysis of double-component decay curve (Trapezoidal integration routine). Details of the analysis are explained in Appendix E. ($Y = G(\lambda)/\lambda$, $X = \lambda$, $\mu_o = 3$, $X_o = 7$)

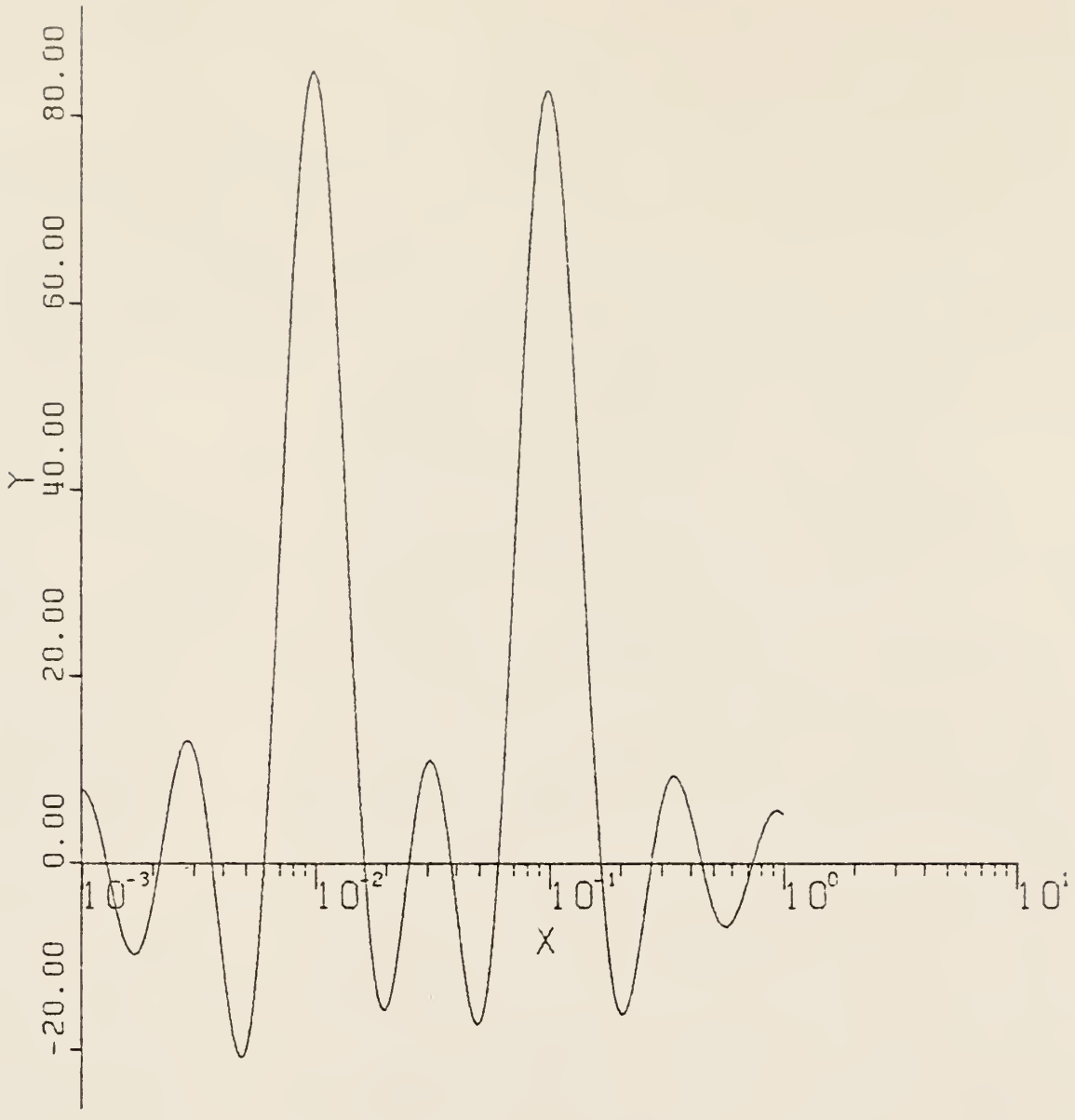

Figure 3.1-14. Results of the analysis of double-component decay curve (Trapezoidal integration routine). Details of the analysis are explained in Appendix E. ($Y = G(\lambda)/\lambda$, $X = \lambda$, $\mu_o = 6$, $X_o = 7$)

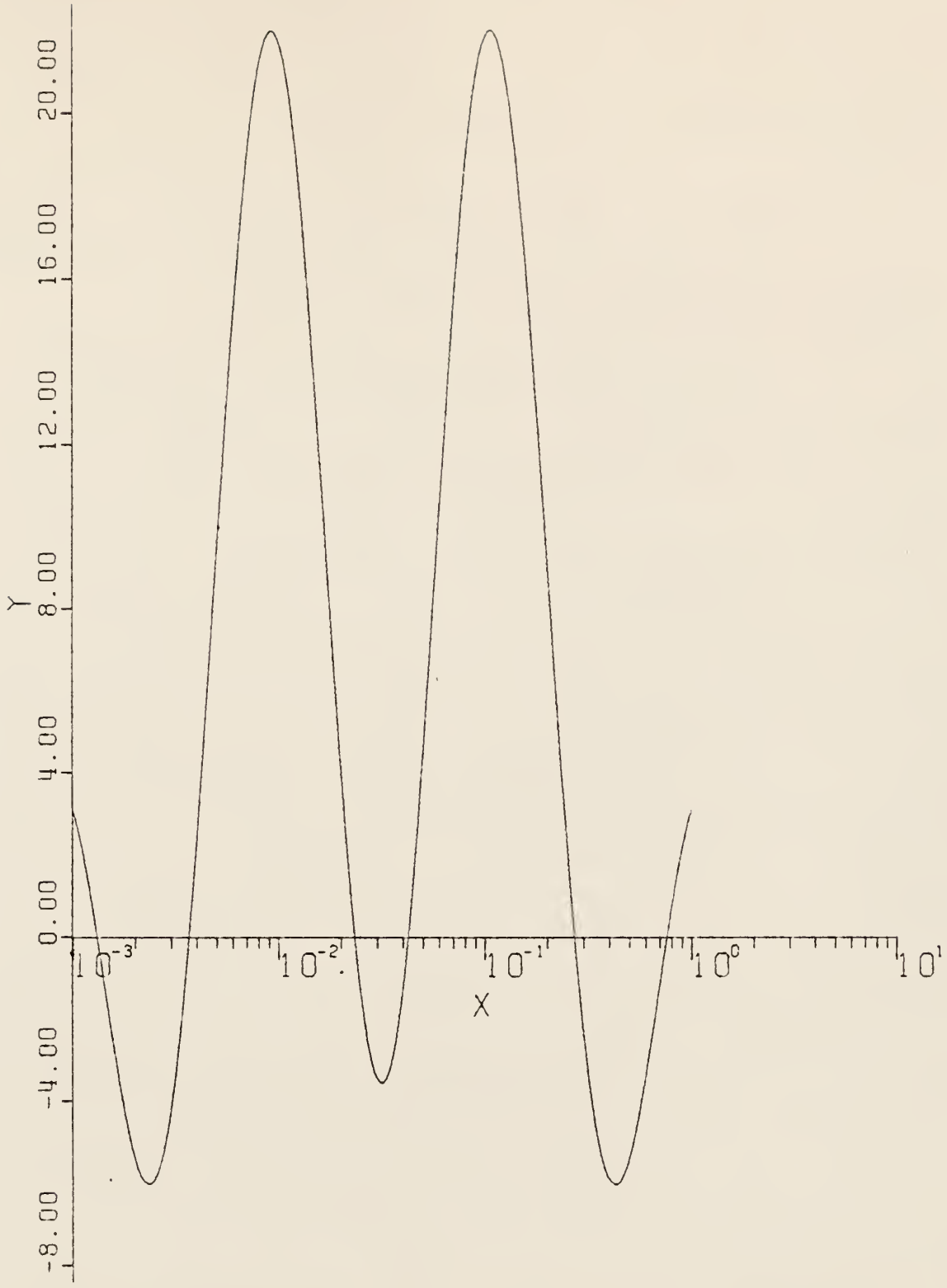

Figure 3.1-15. Results of the analysis of double-component decay curve (Trapezoidal integration routine). Details of the analysis are explained in Appendix E. ($Y = G(\lambda)/\lambda$, $X = \lambda$, $\mu_o = 3$, $X_o = 7$)

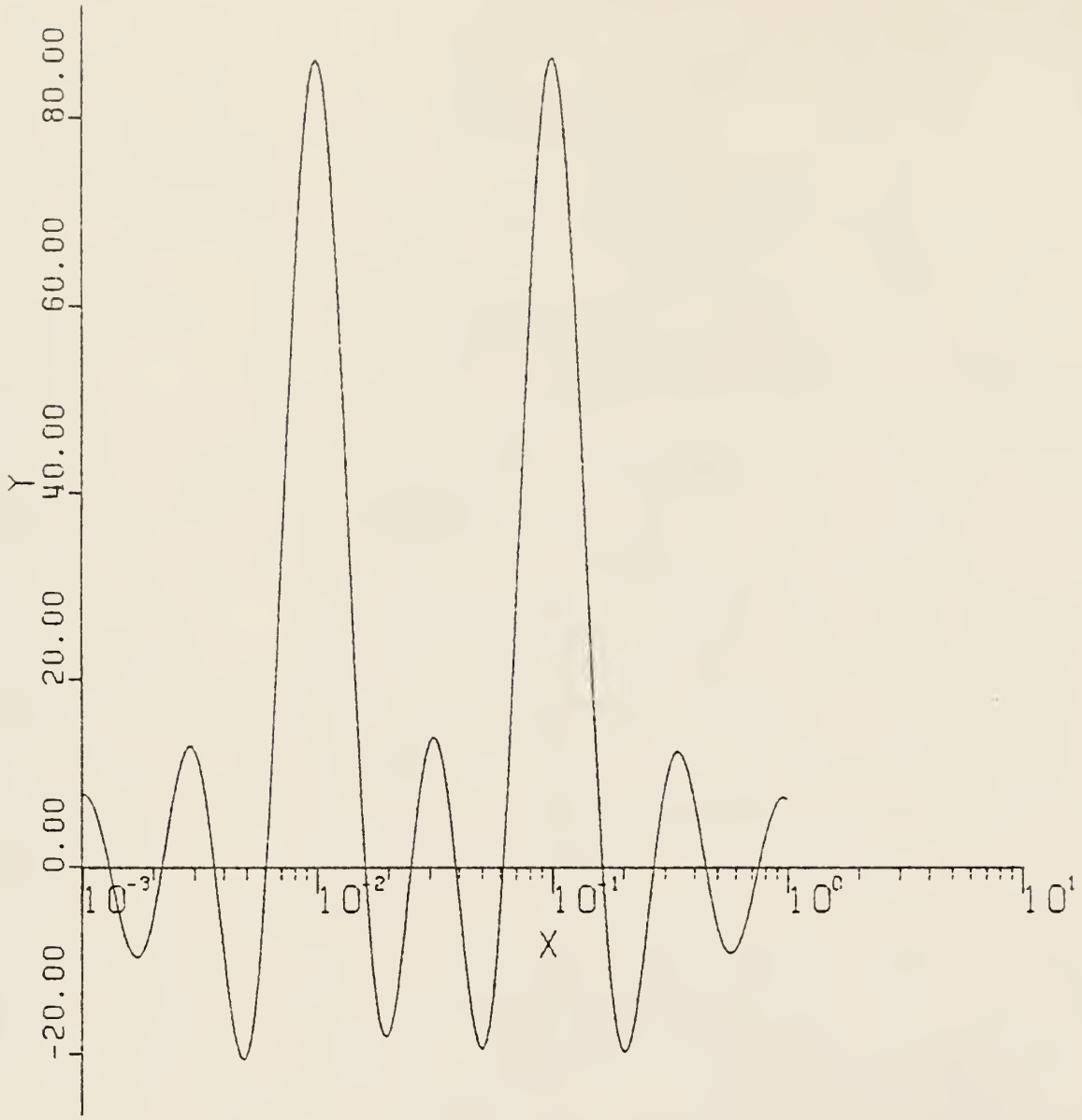

Figure 3.1-16. Results of the analysis of double-component decay curve (Trapezoidal integration routine). Details of the analysis are explained in Appendix E. ($Y = G(\lambda)/\lambda$, $X = \lambda$, $\mu_o = 6$, $X_o = 7$)

Table 3.4. Comparison of results for different interpolation order for $f(t) = 1000\ e^{-0.1t} + 100\ e^{-0.01t}$ and $\mu_o = 6$ (trapezoidal integration routine).

Fig. No.	Order of Interpolation	λ_1	λ_2	$H(\lambda_1)$	$H(\lambda_2)$
3.1-14	3	0.00988	0.09771	84.756	82.574
3.1-16	6	0.00988	0.10116	86.174	86.271

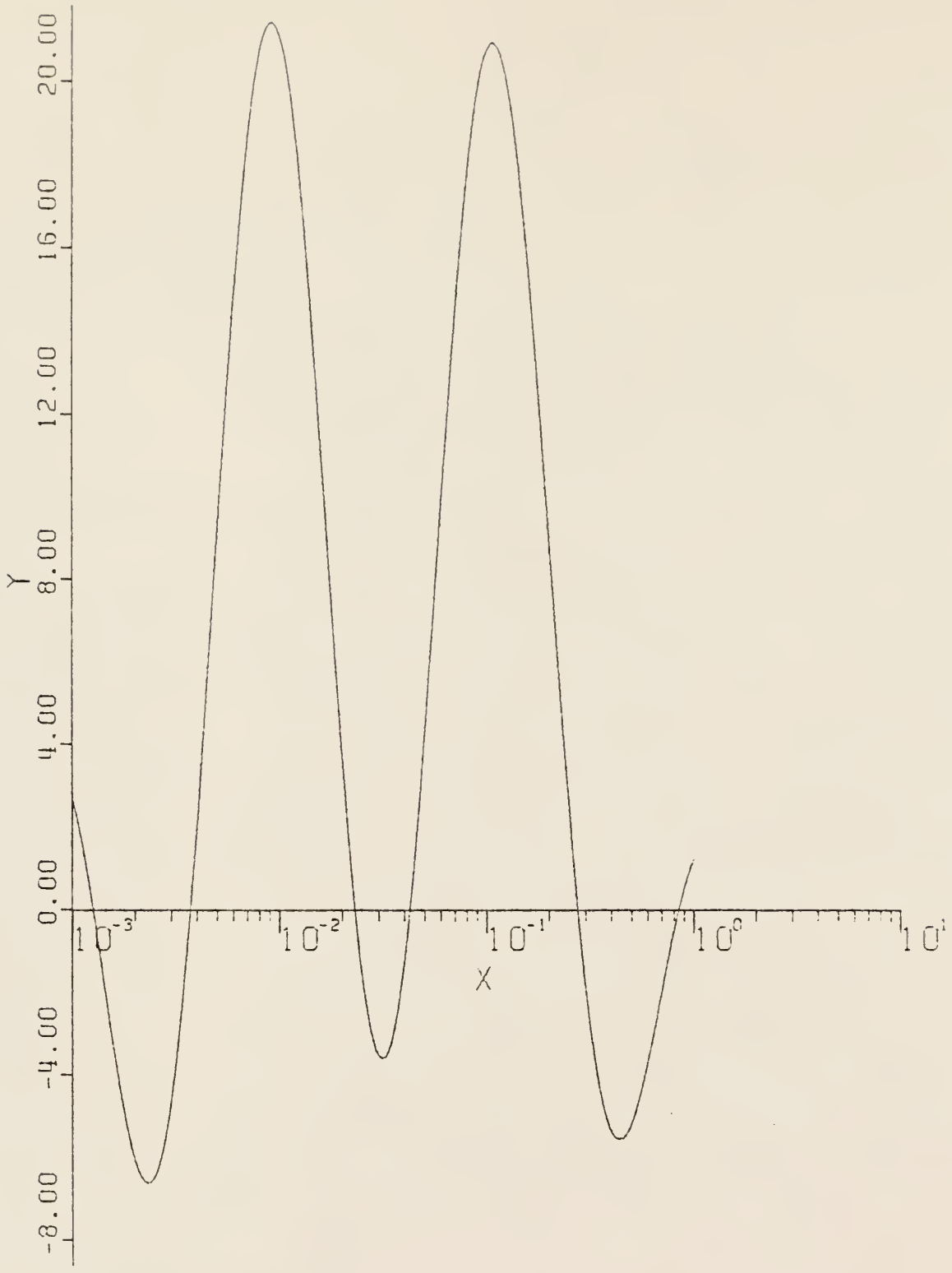

Figure 3.1-17. Result of the analysis of a double-component decay curve (Simpson's integration routine). Details of the analysis are explained in Appendix E. ($Y = G(\lambda)/\lambda$, $X = \lambda$, $\mu_o = 3$, $X_o = 7$)

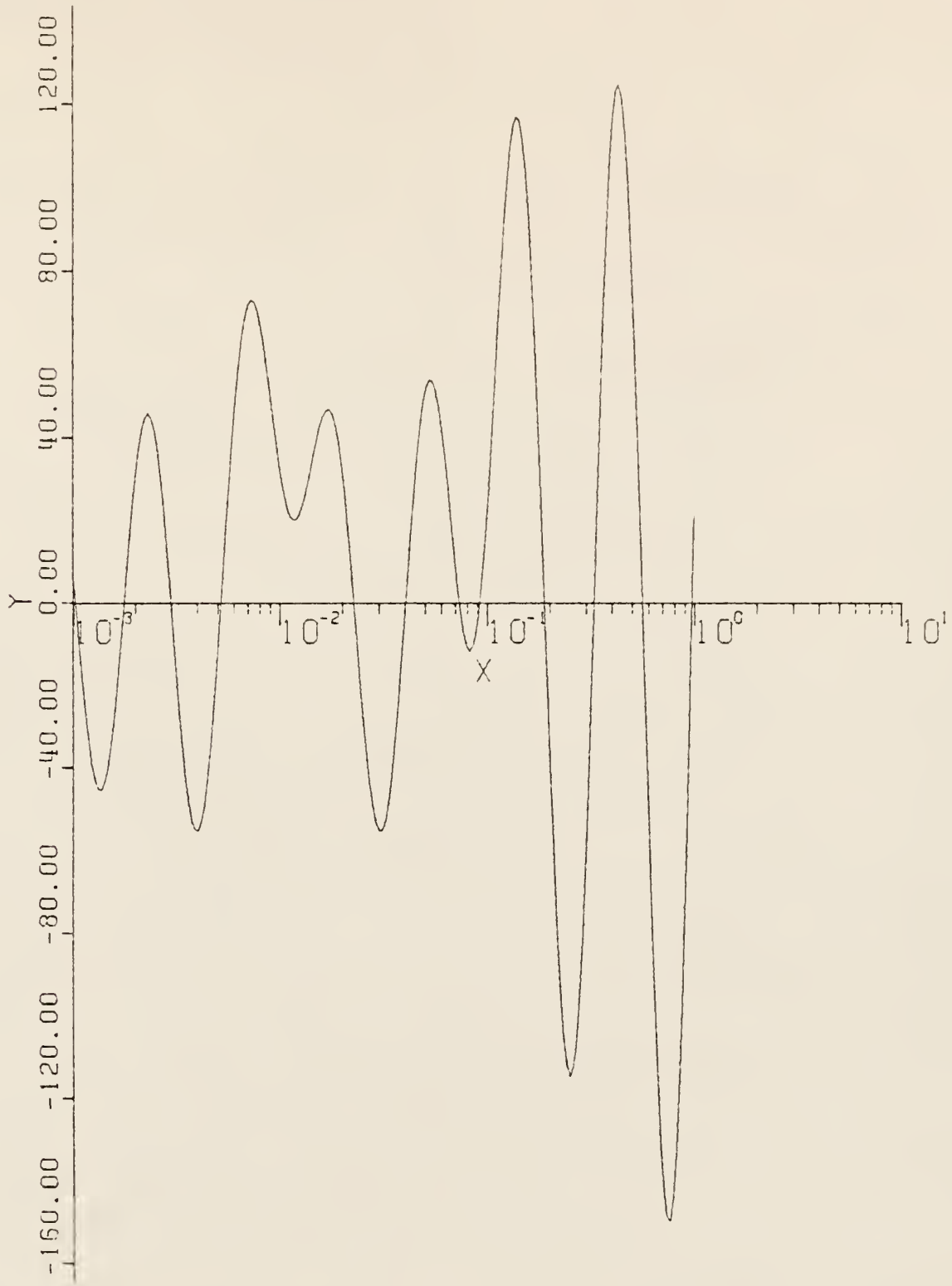

Figure 3.1-18. Result of the analysis of a double-component decay curve (Simpson's integration routine). Details of the analysis are explained in Appendix E. ($Y = G(\lambda)/\lambda$, $X = \lambda$, $\mu_o = 6$, $X_o = 7$)

In the third case, the results for a three-component decay curve was studied. Figures (3.1-19 and 20) are the plots for μ_o = 6 and 8. Again by increasing the value of μ_o the resolution improves, but more error ripples appear. The increase of μ_o from 6 to 8 greatly improves the accuracy of the final results. For μ_o = 8 good results were obtained, however, a shift in the positions of the true peaks occurred. The result of analysis has been explained in Table (3-5). This shift might be due to many factors in our analysis, e.g., integration scheme, interpolation, large error ripples which push the true peaks, gamma function calculation, truncation errors and roundoff errors in the calculations. In all cases, it was observed that the cutoff at $\pm\mu_o$, in Eq. (2.3-14) tends to increase the frequency of the error ripples and the breadth of the true peaks.

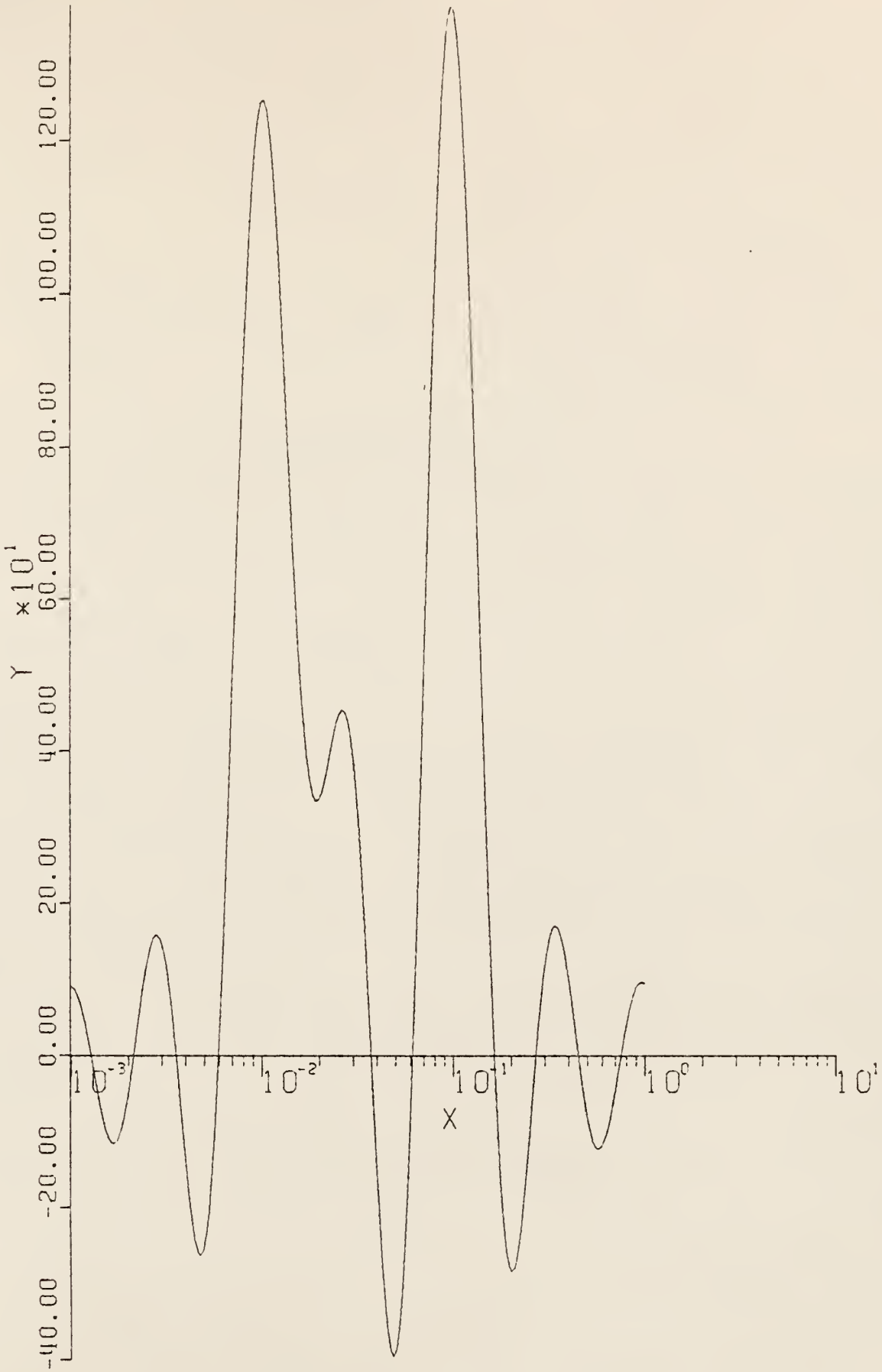

Figure 3.1-19. Result of the analysis of a three-component decay curve (trapezoidal integration routine). Details of the analysis are explained in Appendix E. ($Y = G(\lambda)/\lambda$, $X = \lambda$, $\mu_o = 6$, $X_o = 7$)

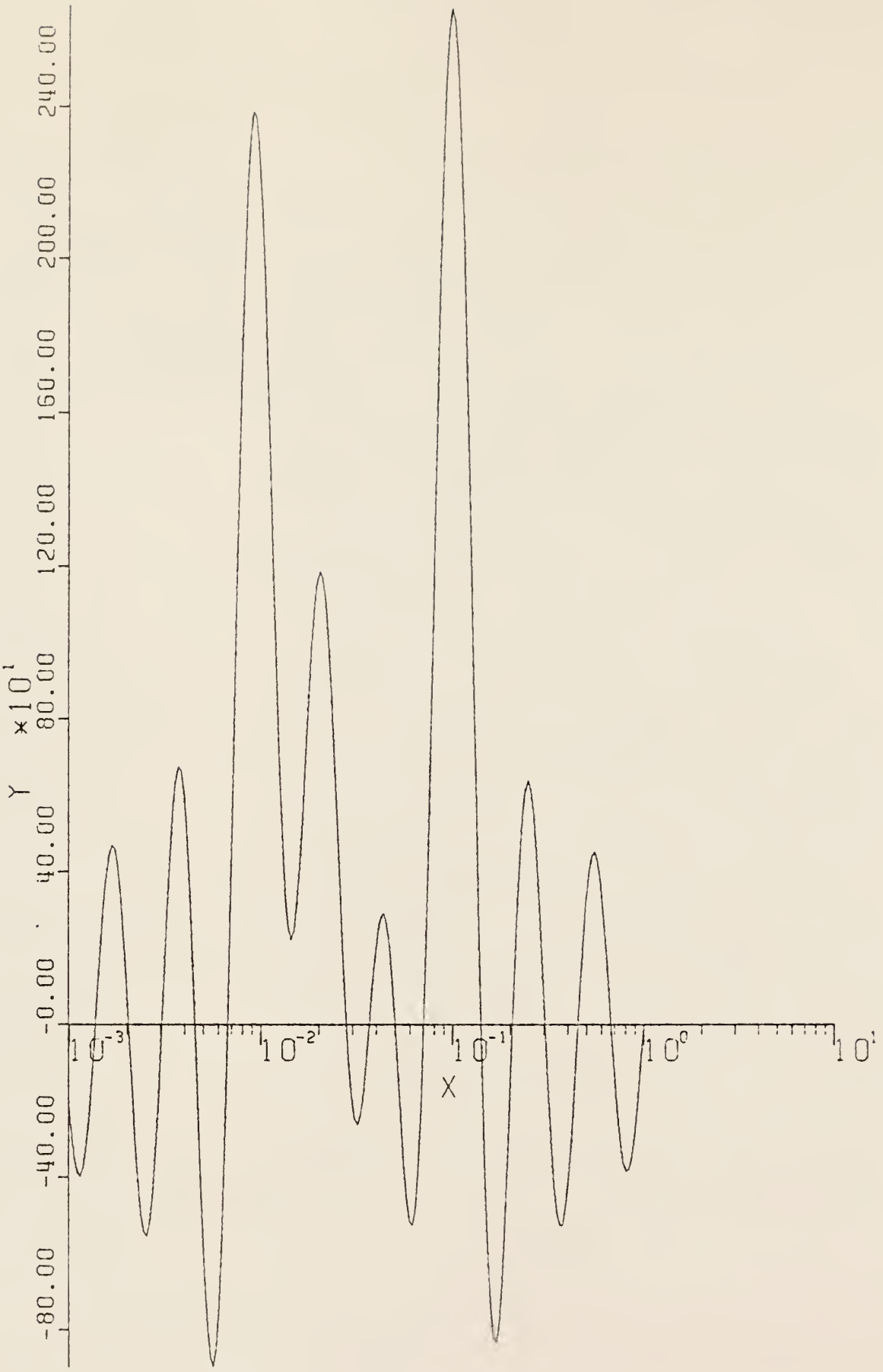

Figure 3.1-20. Result of the analysis of a three-component decay curve (trapezoidal integration routine). Details of the analysis are explained in Appendix E. ($Y = G(\lambda)/\lambda$, $X = \lambda$, $\mu_o = 8$, $X_o = 7$)

Table (3.5). Comparison of the results obtained by FDA method from Figs. (3.1-19) and (3.1-20) for the three-component decay curve.

Fig. No.	μ	λ_1	λ_2	λ_3	$H(\lambda_1)$	$H(\lambda_2)$	$H(\lambda_3)$
3.1-19	6	0.0102	0.0261	0.0977	1253.09	453.28	1374.78
3.1-20	8	0.0092	0.0204	0.1011	2383	1184	2656

3.2 Effect of Cutoff with Respect to x

The function f(t) determined experimentally must be cutoff at some finite value of t (or, $t = e^x$). Thus, one cannot integrate numerically from $-\infty$ to $+\infty$, as required in Eq. (2.1-20). The effect of cutoff with respect to x was studied, namely what happens when the original data do not span a large range in t (recall $t = e^x$)?

First, the case of a single-component ($f(t) = 100\ e^{-0.02t}$) was studied by using the trapezoidal method for the integration. Again the value of μ_o was increased in order to determine how the principal peaks and error ripples change. The previous curves have used data cutoff $|x_o| = 7$. Figures (3.2-1,2,3,4 and 5) show results of a cutoff of $|x_o| = 6.25$ for μ_o values fo 2,4,6,8 and 9. In all cases good results (< 2.5% error) are obtained and the principal peak falls in proper place (see Table 3-6). The error ripples with respect to the principal peak remain symmetrical, but for $\mu_o = 6$ and 8 (Figs. 3.2-3 and 4), it was observed that the error ripples are no longer symmetrical with respect to the true peaks.

The same procedure was repeated using Simpson's method for the integration for $\mu_o = 2,4,6,8$ and 9 (Figs. 3.2-6,7,8,9 and 10). Good results (< %5 error) were obtained, but when the final integration was carried out to $\mu_o = 6$ (Fig. 3.2-8), the error ripples completely masked the true peaks.

Then the cutoff were taken at $x_o = 5.5$, and the effect of the cut-off was studied. Figures (3.2-11,12 and 13) are plots of $g(\lambda)/\lambda$ vs λ

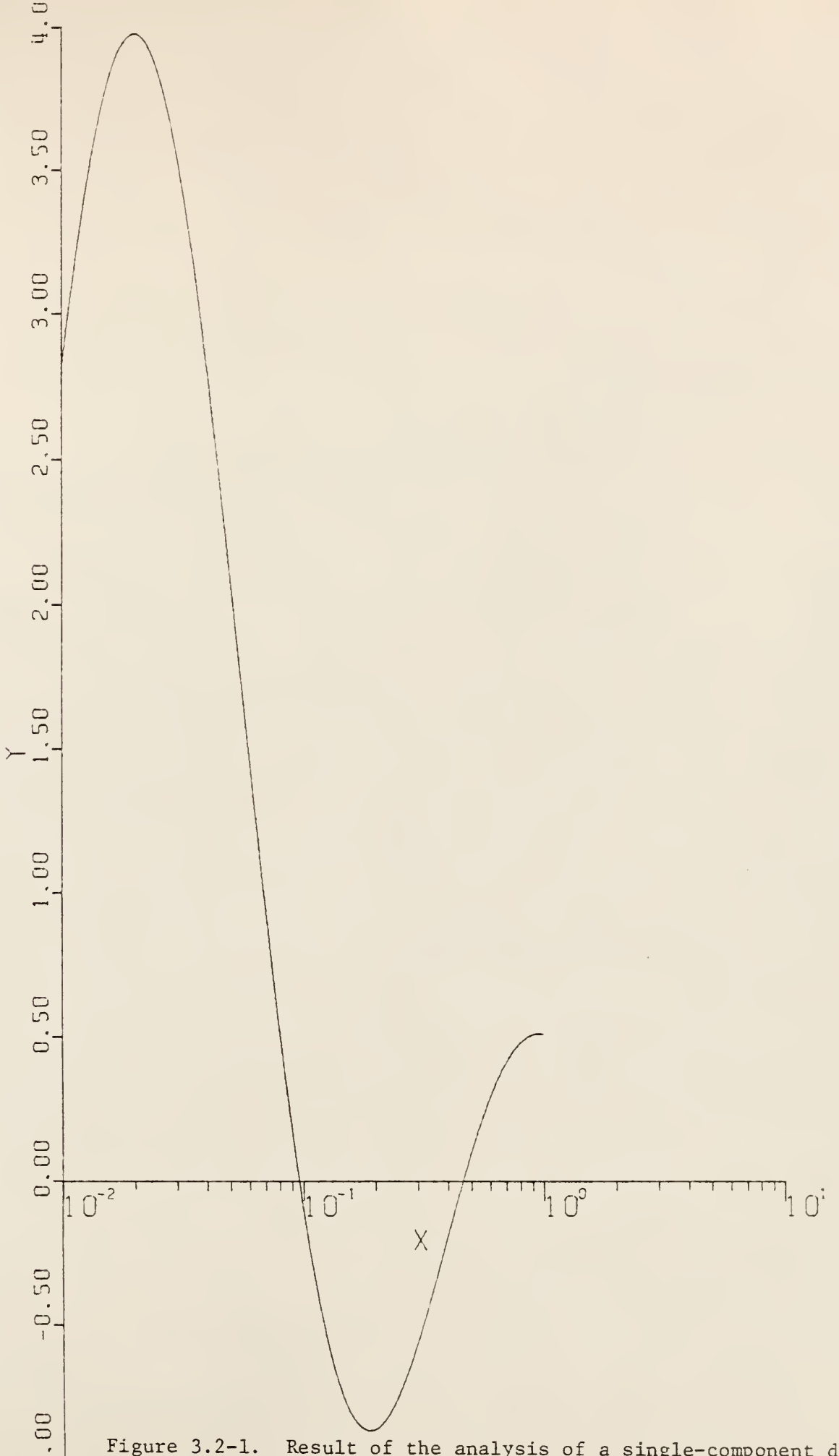

Figure 3.2-1. Result of the analysis of a single-component decay curve (trapezoidal integration routine). Details of the analysis

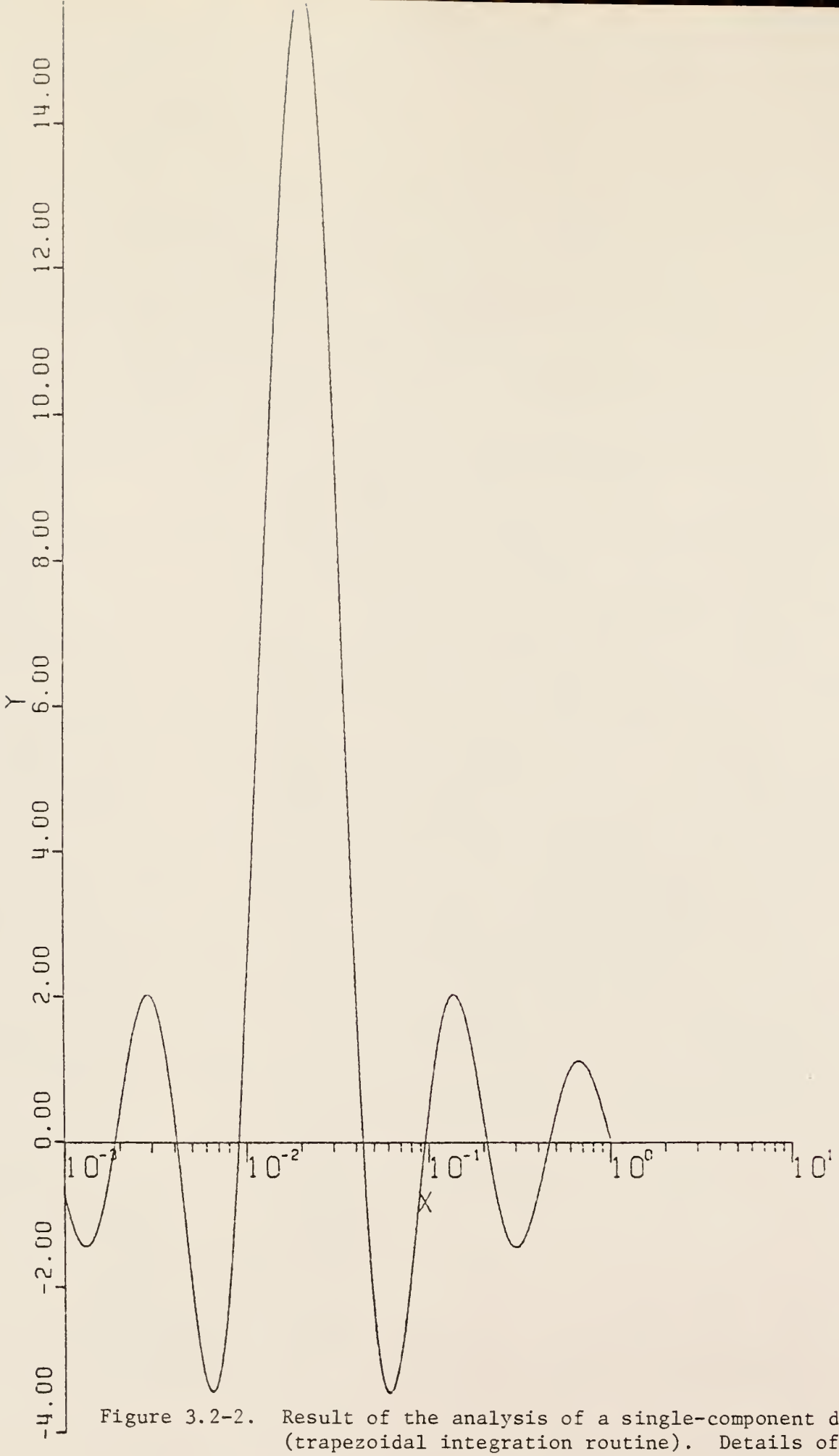

Figure 3.2-2. Result of the analysis of a single-component decay curve (trapezoidal integration routine). Details of the analysis are explained in Appendix E. ($Y = G(\lambda)/\lambda$, $X = \lambda$, $\mu_o = 4$, $X_o = 6.25$)

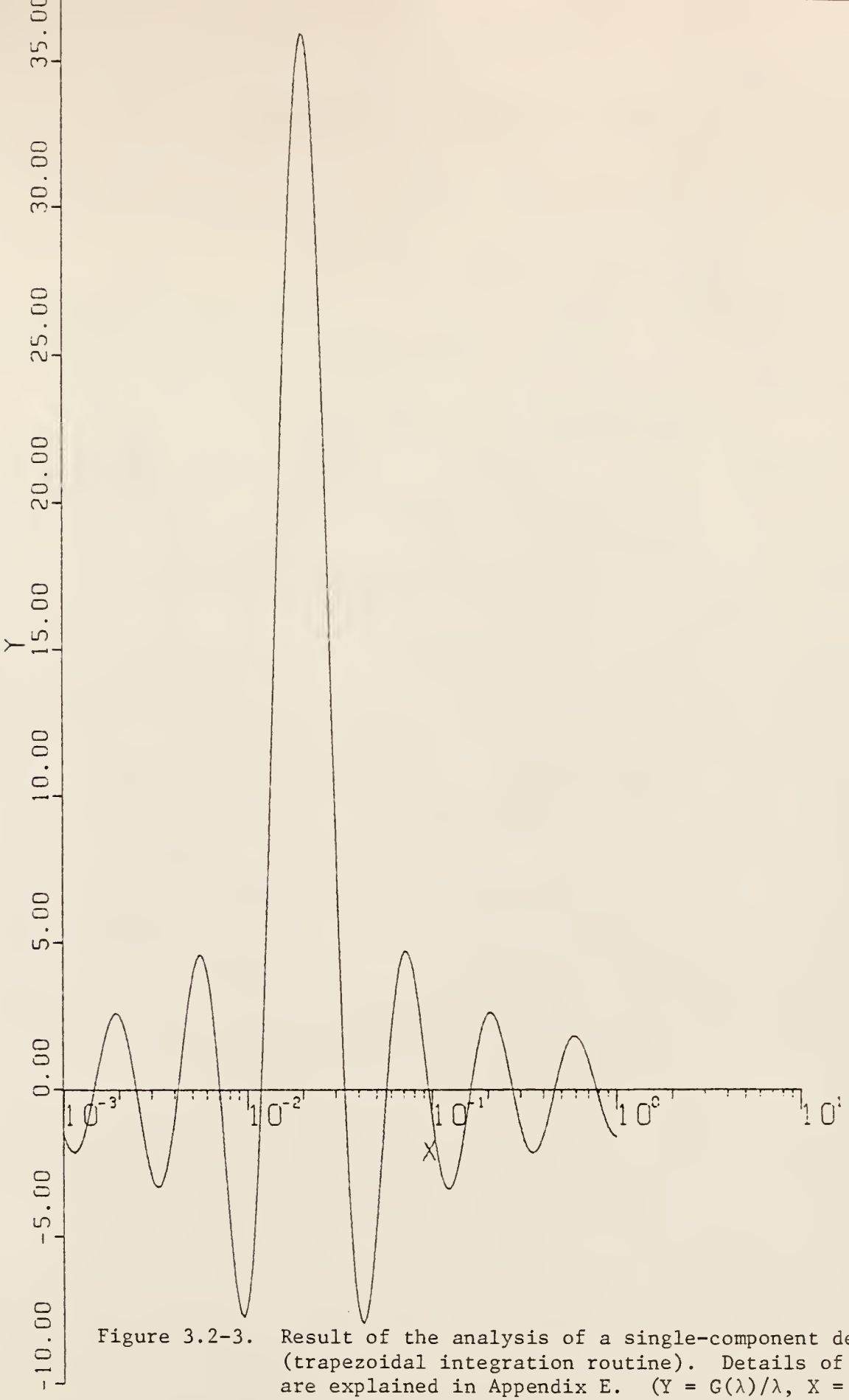

Figure 3.2-3. Result of the analysis of a single-component decay curve (trapezoidal integration routine). Details of the analysis are explained in Appendix E. ($Y = G(\lambda)/\lambda$, $X = \lambda$, $\mu_o = 6$, $X_o = 6.25$)

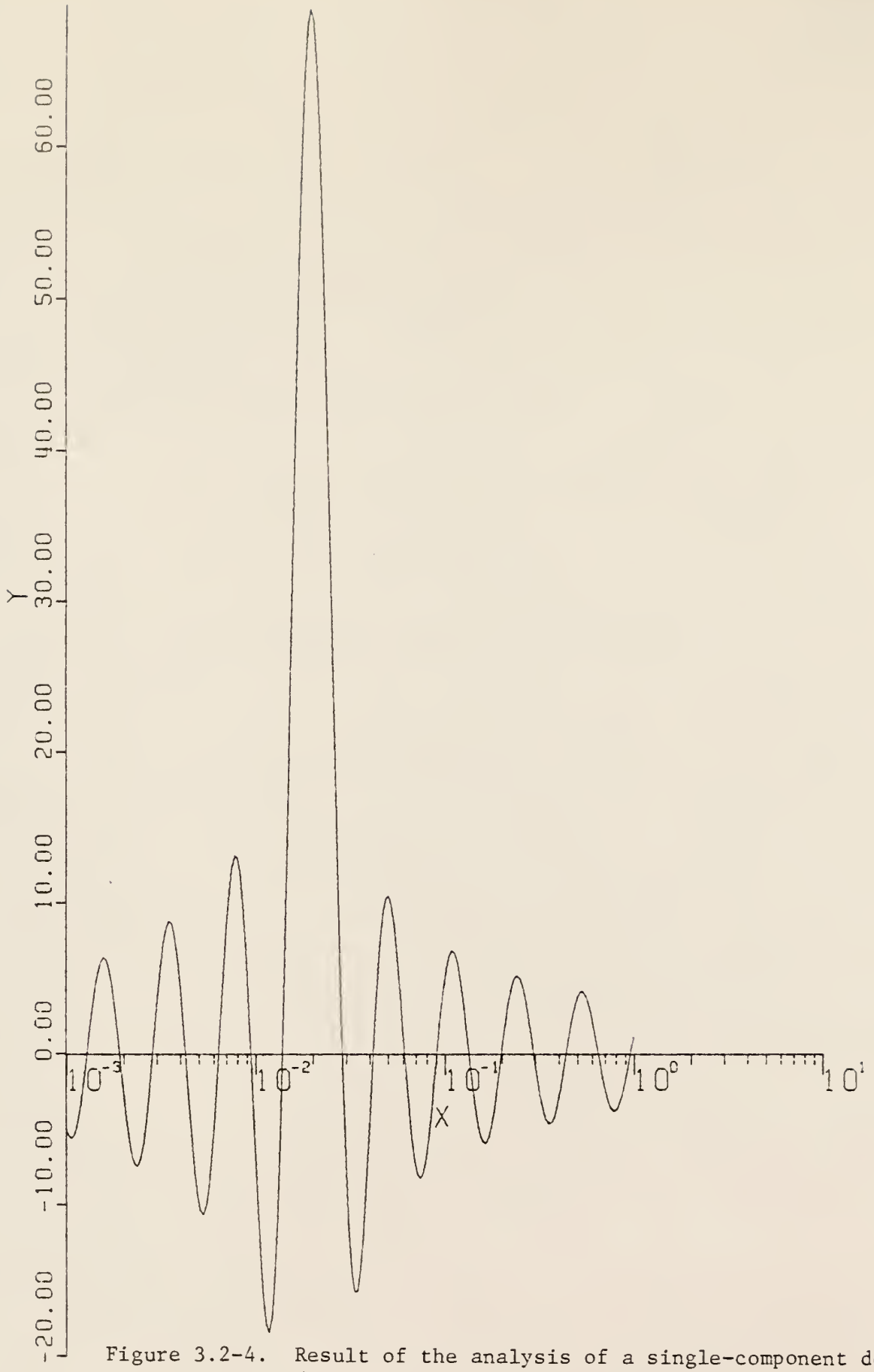

Figure 3.2-4. Result of the analysis of a single-component decay curve (trapezoidal integration routine). Details of the analysis are explained in Appendix E. ($Y = G(\lambda)/\lambda$, $X = \lambda$, $\mu_o = 8$, $X_o = 6.25$)

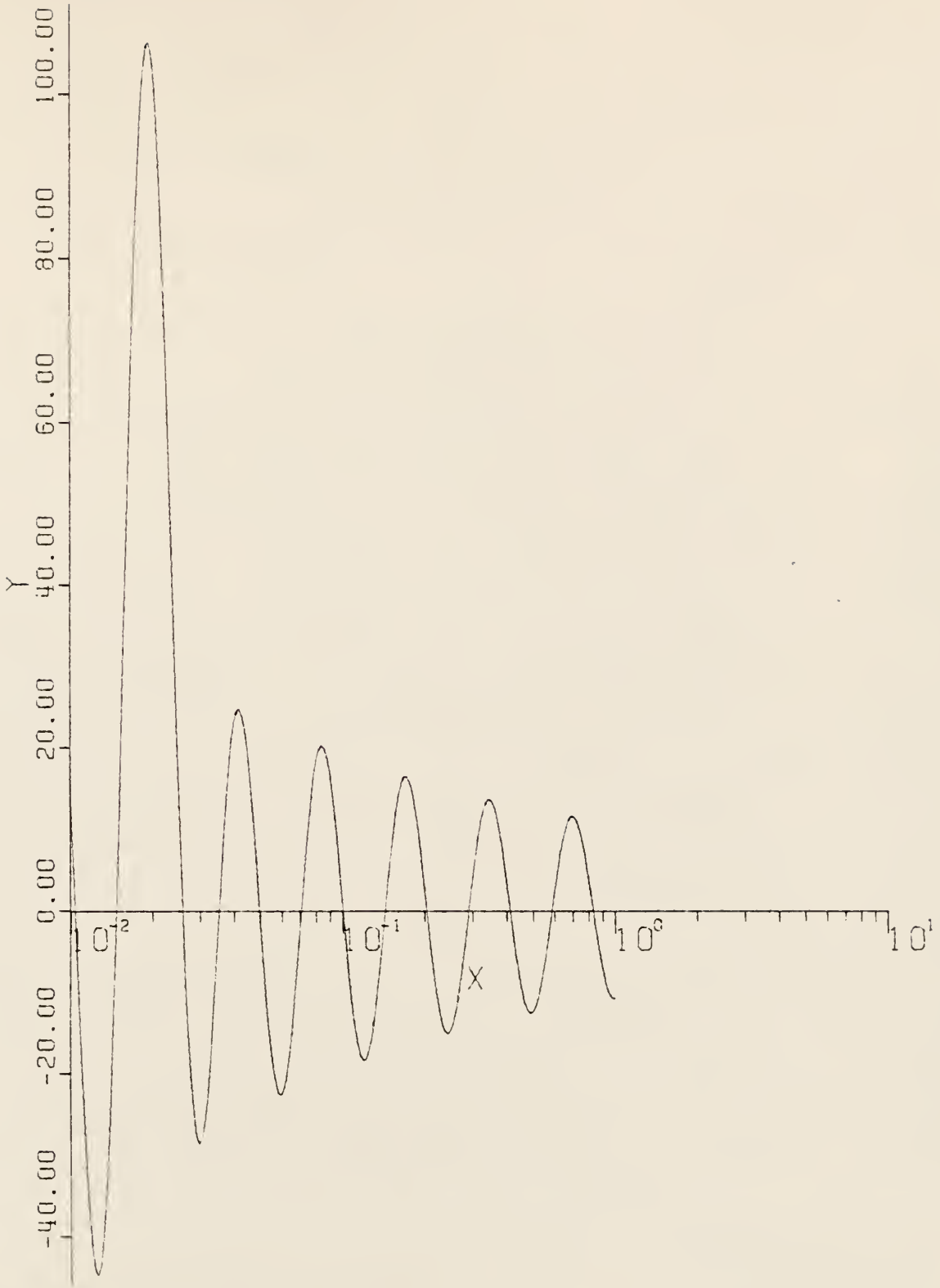

Figure 3.2-5. Result of the analysis of a single-component decay curve (trapezoidal integration routine). Details of the analysis are explained in Appendix E. ($Y = G(\lambda)/\lambda$, $X = \lambda$, $\mu_o = 9$, $X_o = 6.25$)

Table 3.6. Comparison of principal features of each $g(\lambda)/\lambda$ versus λ for $f(t) = 100 \exp(-0.02t)$ and $\mu_o = 2,4,6,8,9$ (trapezoidal integration routine, $x_o = 6.25$).

Fig. No.	fwhm	(K) |height| of under shoot on 1st error peak	(H) height of major peak	Ratio = $\frac{H}{K}$	No. of error peaks (to 10°)
3.2-1	3.2	0.80	4.	4.	1 Post. 1 Neg.
3.2-2	0.98	3.5	16	4.2	2 Post. 2 Neg.
3.2-3	0.42	7.8	35.75	4.5	3 Post. 3 Neg.
3.2-4	0.28	16	70	4.37	4 Post. 5 Neg.
3.2-5	0.19	29	108	3.7	5 Post. 6 Neg.

Figure 3.2-6. Result of the analysis of a single-component decay curve (Simpson's integration routine). Details of the analysis are explained in Appendix E. ($Y = G(\lambda)/\lambda$, $X = \lambda$, $\mu_o = 2$, $X_o = 6.25$)

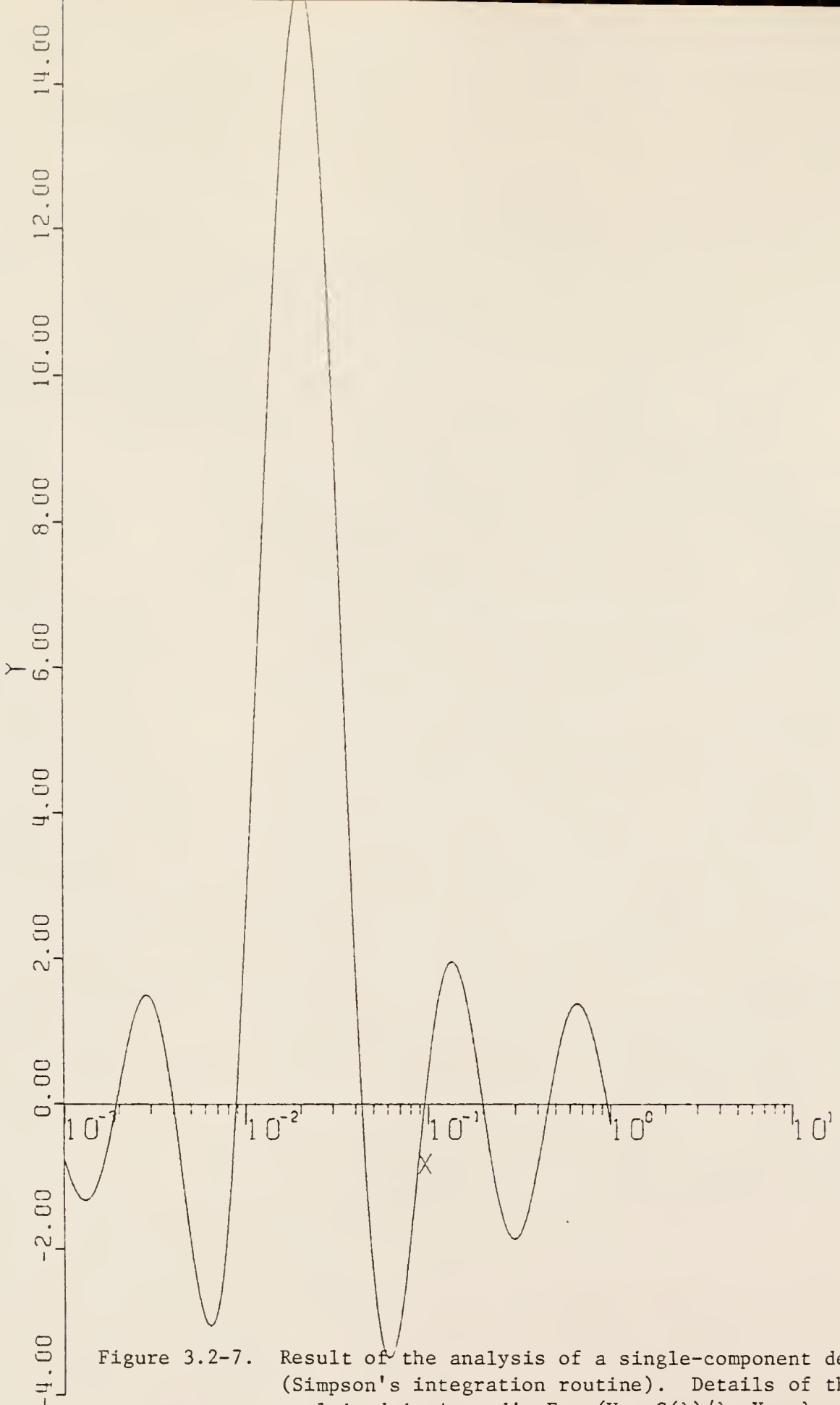

Figure 3.2-7. Result of the analysis of a single-component decay curve (Simpson's integration routine). Details of the analysis are explained in Appendix E. ($Y = G(\lambda)/\lambda$, $X = \lambda$, $\mu_o = 4$, $X_o = 6.25$)

Figure 3.2-8. Result of the analysis of a single-component decay curve (Simpson's integration routine). Details of the analysis are explained in Appendix E. ($Y = G(\lambda)/\lambda$, $X = \lambda$, $\mu_o = 6$, $X_o = 6.25$)

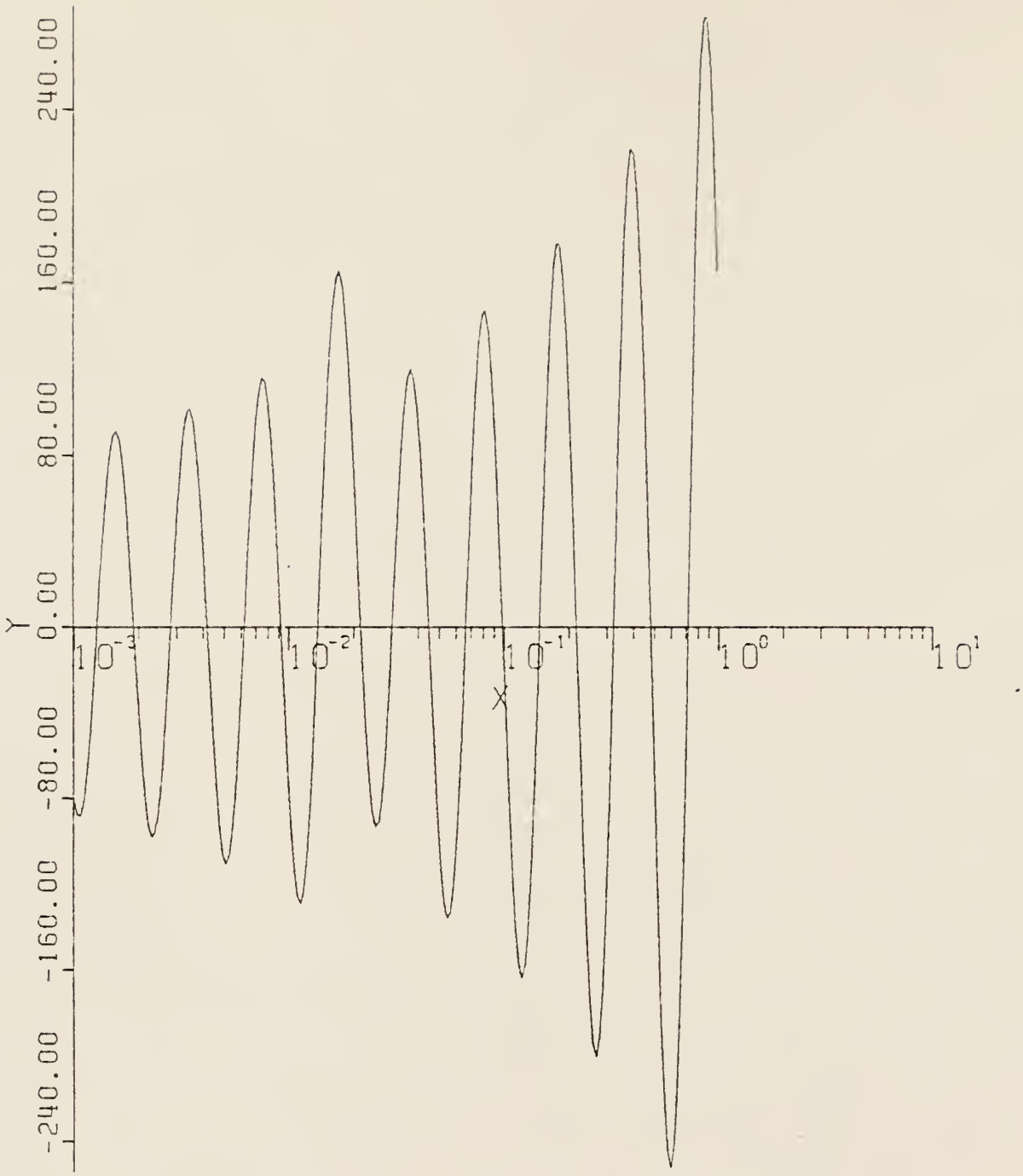

Figure 3.2-9. Result of the analysis of a single-component decay curve (Simpson's integration routine). Details of the analysis are explained in Appendix E. ($Y = G(\lambda)/\lambda$, $X = \lambda$, $\mu_o = 8$, $X_o = 6.25$)

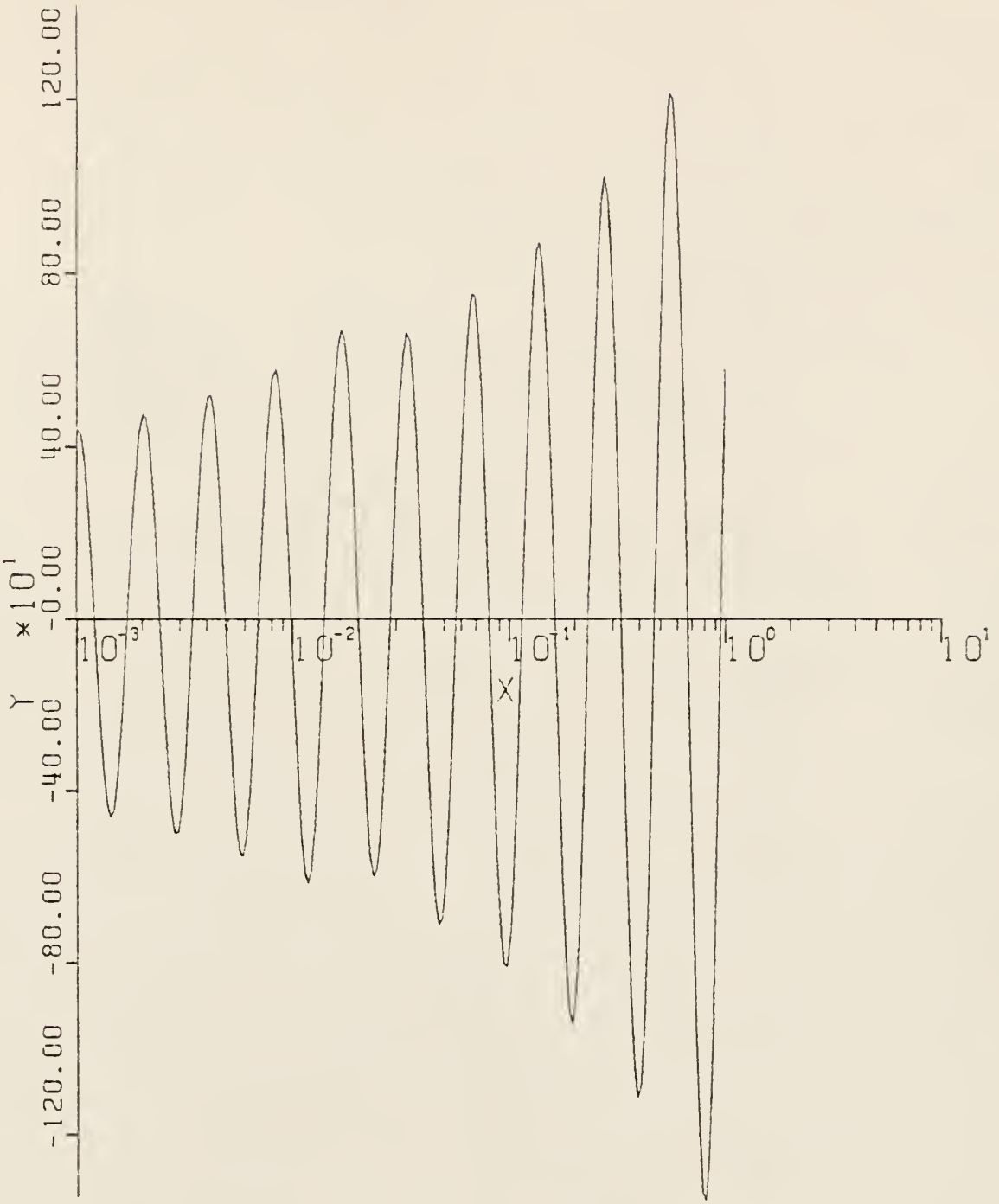

Figure 3.2-10. Result of the analysis of a single-component decay curve (Simpson's integration routine). Details of the analysis are explained in Appendix E. ($Y = G(\lambda)/\lambda$, $X = \lambda$, $\mu_o = 9$, $X_o = 6.25$)

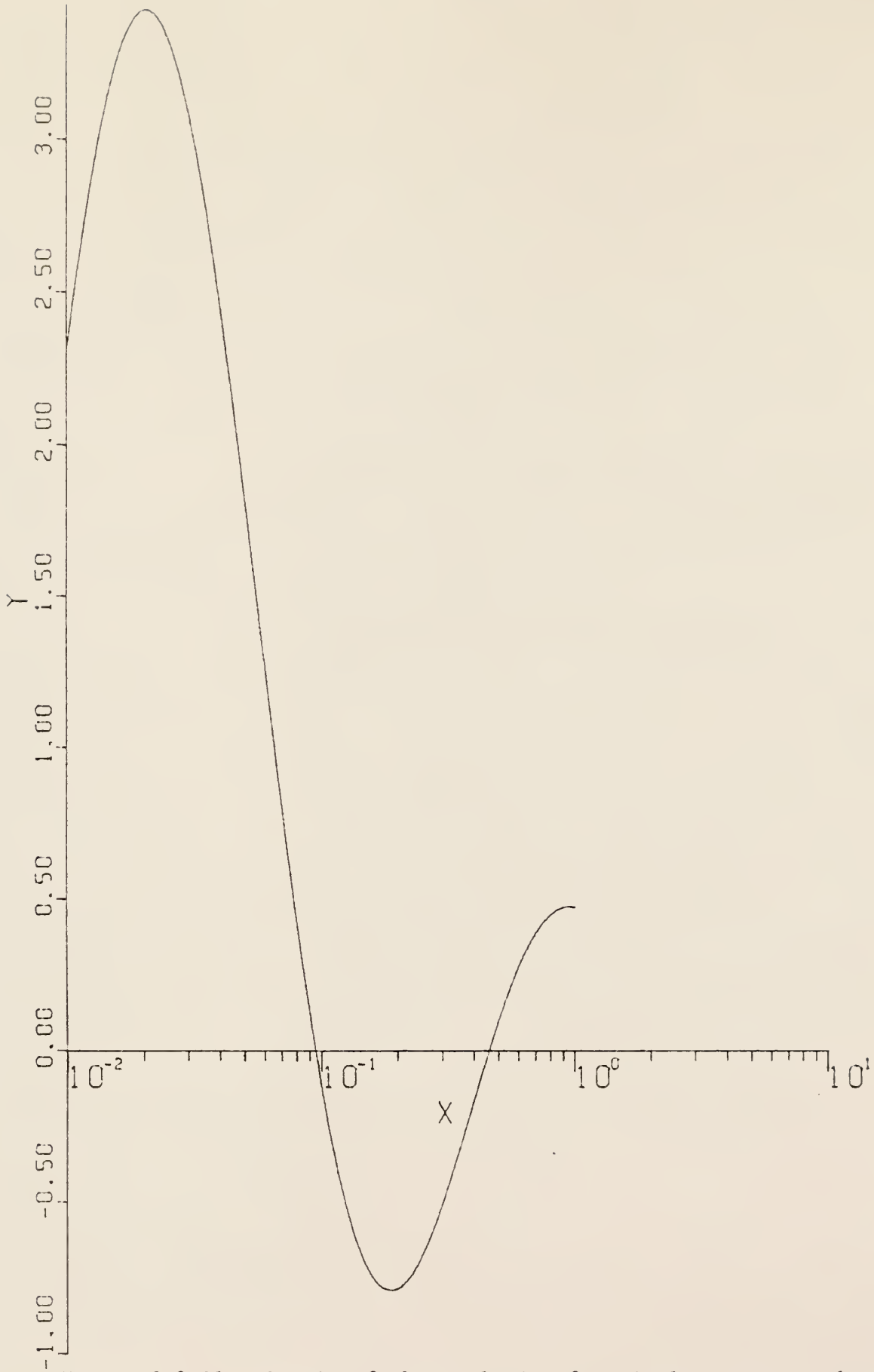

Figure 3.2-11. Result of the analysis of a single-component decay curve (trapezoidal integration routine). Details of the analysis are explained in Appendix E. ($Y = G(\lambda)/\lambda$, $X = \lambda$, $\mu_o = 2$, $X_o = 5.25$)

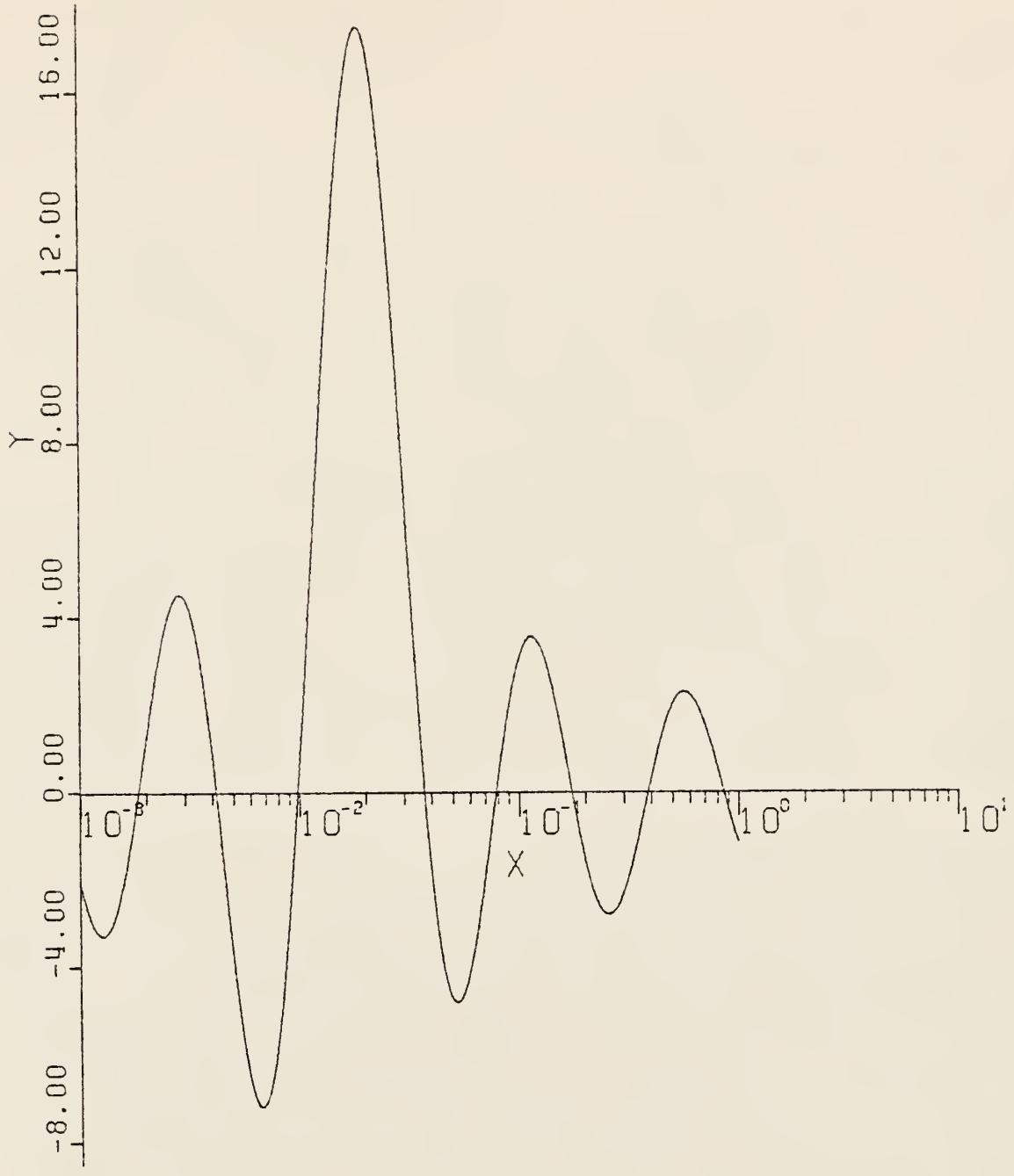

Figure 3.2-12. Result of the analysis of a single-component decay curve (trapezoidal integration routine). Details of the analysis are explained in Appendix E. ($Y = G(\lambda)/\lambda$, $X = \lambda$, $\mu_o = 4$, $X_o = 5.25$)

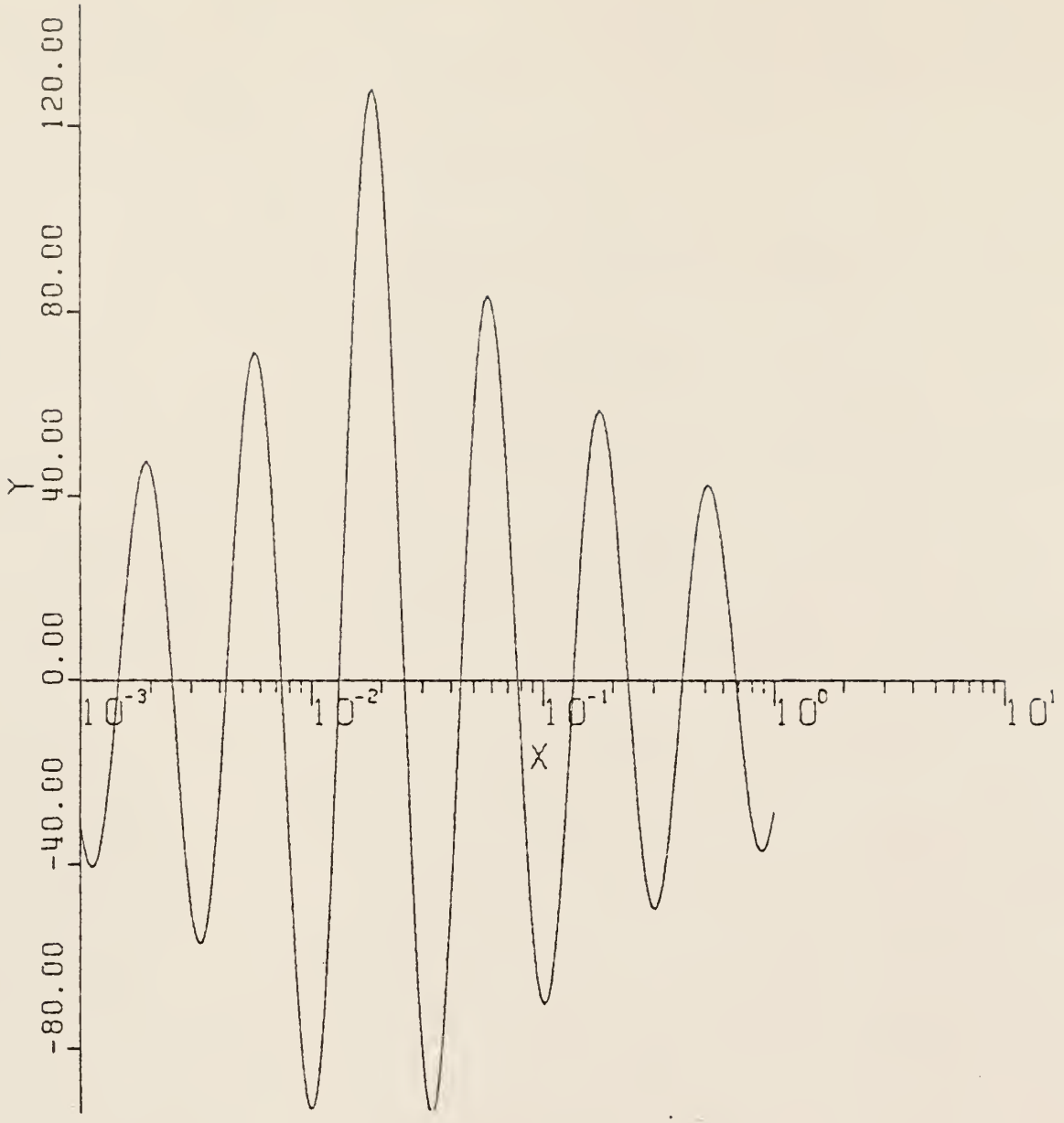

Figure 3.2-13. Result of the analysis of a single-component decay curve (trapezoidal integration routine). Details of the analysis are explained in Appendix E. ($Y = G(\lambda)/\lambda$, $X = \lambda$, $\mu_o = 6$, $X_o = 5.25$)

for μ_o = 2,4 and 6, using the trapezoidal method for the integration. The improvement of resolution is observed with increasing μ_o values (see Table 3-7).

The same procedure were done by using Simpson's rule for cutoff $|x_o|$ = 5.5. The result obtained was poorer than those obtained by trapezoidal scheme.

The results of the analysis showed that, the results for trapezoidal method are fairly good and better than the results obtained using Simpson's method for integration. Also it was found that a large cut-off in the initial data has a strong effect on the final results.

Table 3.7. Comparison of principal features of each $g(\lambda)/\lambda$ versus λ plot for $f(t) = 100 \exp(-0.02t)$ and $\mu_o = 2,4,6$ (trapezoidal integration routine, $x_o = 5.25$)

Fig. No.	fwhm	(K) |height| of under shoot on 1st error peak	(H) height of major peak	Ratio = $\frac{H}{K}$	No. of error peaks (to 10°)
3.2-11	2.05	0.80	3.40	4.25	1 Post. 1 Neg.
3.2-12	0.84	4.8	17.5	3.64	2 Post. 2 Neg.
3.2-13	error ripples completely masked the results.				

3.3 Height of True Peaks

The heigh of true peak is directly proportional to N_i/λ_i (see Eq. 2.1-3). Thus it is only necessary to run a standard decay curve with a known coefficient at the same value μ_o to determine what the proportionality factor is, e.g., for decay curve ($f(t) = 100\ e^{-0.02t}$), the height of the peak is 71.275 (arbitrary unit) (see Table 3-8). So a characteristic decay curve ($f(t) = 50\ e^{-0.02t}$) should have the height of 35.6 (arbitrary unit). Figures (3.3-1 and 2) are plots of $g(\lambda)/\lambda$ for $\mu_o = 8$, using trapezoidal method for the integration and using decay scheme $f(t) = 50\ e^{-0.02t}$ and $f(t) = 150\ e^{-0.02t}$.

The height of peaks were measured. The same procedure ($\mu_o = 6$) was performed using Simpson's method for integration and the same results were obtained (Figs. 3.3-3 and 4). The results in Table (3-8), indicate that the height of the resultant peaks are proportional to the number of atoms of the species.

Figure 3.3-1. Result of the analysis of a single-component decay curve ($f(t) = 50\ e^{0.02t}$, trapezoidal integration routine). Detials of the analysis are explained in Appendix E. ($Y = G(\lambda)/\lambda$, $X = \lambda$, $\mu_o = 8$, $X_o = 7$)

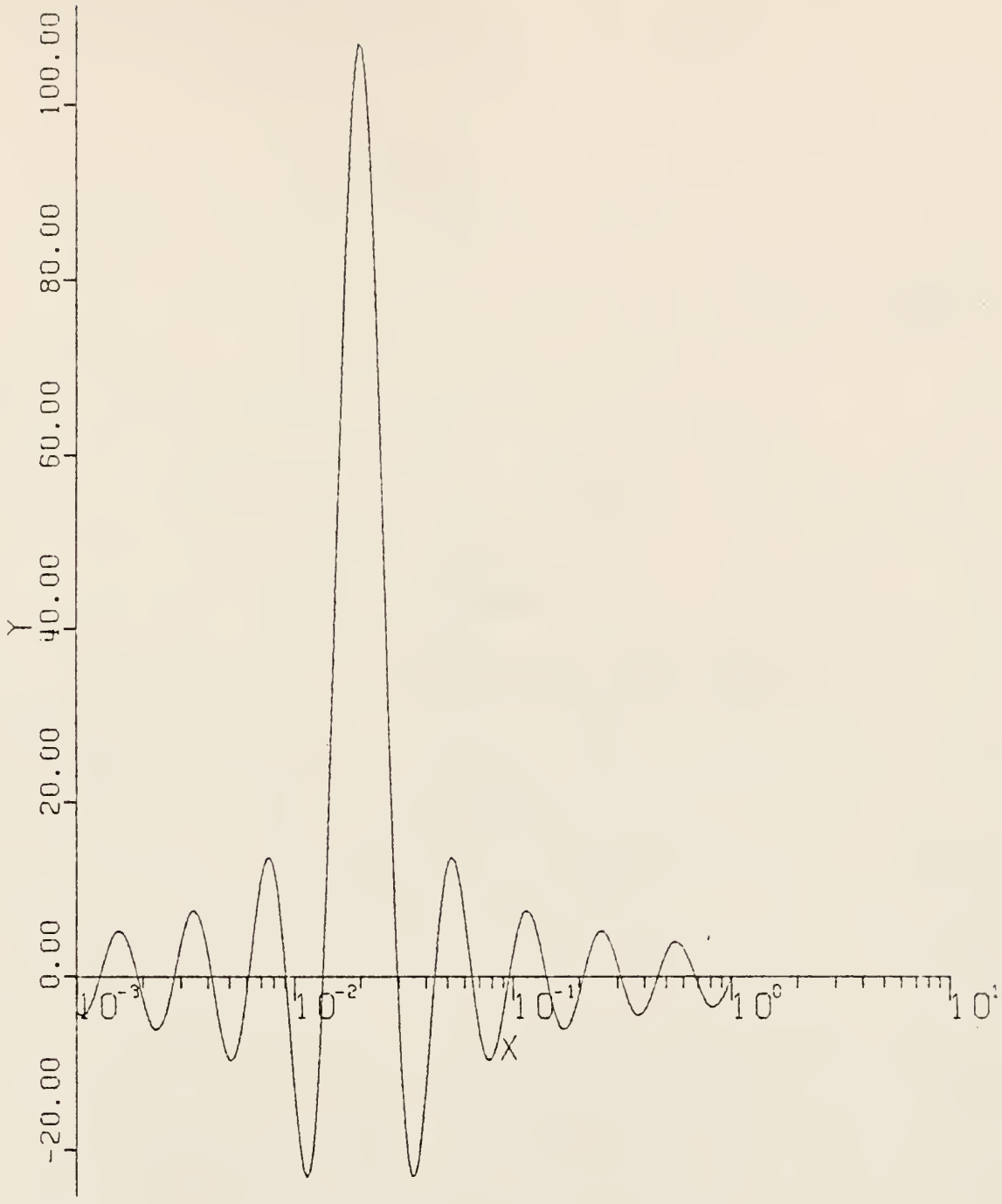

Figure 3.3-2. Result of the analysis of a single-component decay curve $f(t) = 150\ e^{-0.02t}$, trapezoidal integration routine). Details of the analysis are explained in Appendix E. ($Y = G(\lambda)/\lambda$, $\mu_o = 8$, $X_o = 7$)

Figure 3.3-3. Result of the analysis of a single-component decay curve ($f(t) = 50\ e^{-0.02t}$, Simpson's integration routine). Details of the analysis are explained in Appendix E. ($Y = G(\lambda)/\lambda$, $X = \lambda$, $\mu_o = 6$, $X_o = 7$)

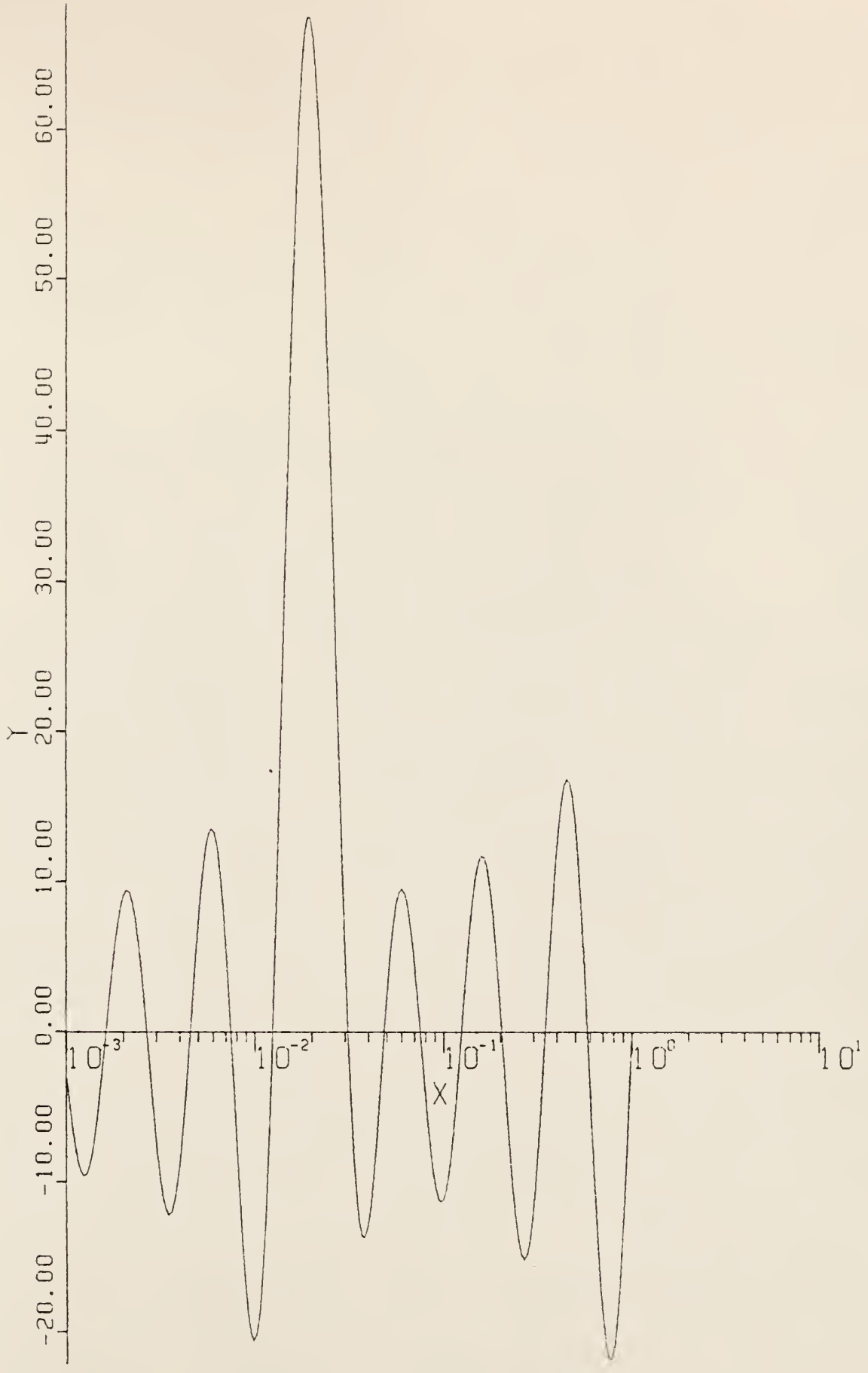

Figure 3.3-4. Result of the analysis of a single-component decay curve ($f(t) = 150\ e^{-0.02t}$, Simpson's integration routine). Details of the analysis are explained in Appendix E. ($Y = G(\lambda)/\lambda$, $X = \lambda$, $\mu_o = 6$, $X_o = 7$)

Table 3.8. Comparison of the amplitudes of the major peaks for the single-component decay curve.

Decay Curve Formula	Height of True Peak (a)	Height of True Peak (b)
$f(t) = 50\ e^{-0.02t}$	35.63 Fig. (3.3-1)	22.48 Fig. (3.3-3)
$f(t) = 100\ e^{-0.02t}$	71.275 Fig. (3.1-4)	44.96 Fig. (3.1-8)
$f(t) = 150\ e^{-0.02t}$	106.912 Fig. (3.3-2)	67.4 Fig. (3.3-4)

a. Trapezoidal integration routine

b. Simpson's integration routine

4.0 The Least Squares (LS) method

A least square method can be used to determine the coefficients and exponents of a multicomponent decay curve. In this section the mathematical expressions needed for fitting the postulated models to data are given.

4.1 Model $y = a + bx$

Our data consist of n paired observations (x_i, y_i) of an independent variable x and a dependent variable y. We wish to fit the data with an equation of the form

$$y = a + bx \tag{4.1-1}$$

For arbitrary values of a and b, we can calculate the deviations e_i between each observed value, y_i, and the value obtained from the model by calculation

$$e_i = y_i - (a + bx_i) \tag{4.1-2}$$

The parameters a and b are to be determined such that the estimated errors are, in some sense, as small as possible. Since we cannot minimize each of the e_i individually, we could try to make the sum, $\sum_{i=1}^{n} e_i$, minimum. However, the sum of these deviations is not a good measure of how well we have approximated the data with our calculated straight line because large positive deviations can be balanced by large negative deviations to yield a small sum even when

the fit is bad. Thus, we might consider minimizing the sum of the absolute values of the deviations, but this leads to difficulties in obtaining an analytical solution. Therefore, we are led to consider the minimization of the sum of the squares of deviations, which has many nice mathematical and statistical benefits (40).

The sum of the squares of the deviations, E, is

$$E = \sum_i w_i e_i^2 = \sum_i [w_i (y_i - a - bx_i)^2], \qquad (4.1\text{-}3)$$

where w_i is a weight, which will be discussed later.

A measure of the "goodness of fit" of the straight line to the data is provided by the quantity E. In a qualitative sense, if E is small, the fit is good; if E is large, the fit is bad. If E is minimized, the fit is optimum (40,41).

In our case the quantity y is a count rate measured with a detector system and a radioactive source; thus, we assume the fluctuations in the data are due to instrumental and source fluctuations only. In order to find the values of coefficients a and b which yields the minimum value for E, we use basic calculus concepts. E is a function of a and b, hence, a necessary condition for this to be a minimum (or a maximum) is that

$$\frac{\partial E}{\partial a} = 0, \qquad (4.1\text{-}4)$$

$$\frac{\partial E}{\partial b} = 0. \qquad (4.1\text{-}5)$$

So

$$\frac{\partial E}{\partial a} = \frac{\partial}{\partial a} \sum_i [w_i(y_i-a-bx_i)^2]$$

$$= -2 \sum_i [w_i(y_i-a-bx_i)] = 0, \qquad (4.1\text{-}6)$$

and

$$\frac{\partial E}{\partial b} = \frac{\partial}{\partial b} \sum_i [w_i(y_i-a-bx_i)^2]$$

$$= -2 \sum_i [w_i x_i(y_i-a-bx_i)] = 0. \qquad (4.1\text{-}7)$$

Differentiating Eq. (4.1-6) with respect to a and Eq. (4.1-7) with respect to b yields

$$\frac{\partial^2 E}{\partial a^2} = 2 \sum_i w_i \qquad (4.1\text{-}8)$$

$$\frac{\partial^2 E}{\partial b^2} = 2 \sum_i w_i x_i \qquad (4.1\text{-}9)$$

Thus, if $\sum_i w_i$ and $\sum_i w_i x_i$ are both greater than zero, we are guaranteed that the values found for a and b by solving Eqs. (4.1-6) and (4.1-7), simultaneously, will minimize E.

Rewriting Eqs. (4.1-6) and (4.1-7) in a somewhat more convenient form yields the following equations, called the normal (or canonical) equations:

$$\sum_i w_i y_i = a \sum_i w_i + b \sum_i w_i x_i \qquad (4.1\text{-}10)$$

$$\sum_i w_i x_i y_i = a \sum_i w_i x_i + b \sum_i w_i x_i^2 \qquad (4.1\text{-}11)$$

The normal equations are a set of two linear equations in the unknowns a and b and their simultaneous solution gives the values of a and b.

$$a = \frac{1}{\Delta} \left(\sum_i w_i x_i^2 \sum_i w_i y_i - \sum_i w_i x_i \sum_i w_i x_i y_i \right) \qquad (4.1\text{-}12)$$

$$b = \frac{1}{\Delta} \left(\sum_i w_i \sum_i w_i x_i y_i - \sum_i w_i x_i \sum_i w_i y_i \right) \qquad (4.1\text{-}13)$$

$$\Delta = \sum_i w_i \sum_i w_i x_i^2 - \left(\sum_i w_i x_i \right)^2 \qquad (4.1\text{-}14)$$

In order to make an exact statement about the goodness of the fit, it is necessary to make some assumptions about the y_i observations and true model of regression, namely, for a given x the true mean value of the y is of the form $\alpha + \beta x$. Estimates of α and β, a and b, obtained from the normal equations are called regression (least squares) estimators. These estimators are linear in the observations y_i and are unbiased estimates of α and β. With these properties, we can refer to the Gauss-Markov theorm (42,43) which states that among all unbiased estimators for α and β which are linear in the y_i, the least squares estimators have the smallest variance. Knowing that the appropriate

weighting factor for statistics of radioactive decay is inversely proportional to the variance of the number of counts, yields the simple form of solutions for a and b.

$$a = \frac{1}{\Delta} \left(\sum_i \frac{x_i^2}{\sigma_i^2} \sum_i \frac{y_i}{\sigma_i^2} - \sum_i \frac{x_i}{\sigma_i^2} \sum_i \frac{x_i y_i}{\sigma_i^2} \right) \tag{4.1-15}$$

$$b = \frac{1}{\Delta} \left(\sum_i \frac{1}{\sigma_i^2} \sum_i \frac{x_i y_i}{\sigma_i^2} - \sum_i \frac{x_i}{\sigma_i^2} \sum_i \frac{y_i}{\sigma_i^2} \right) \tag{4.1-16}$$

$$\Delta = \sum_i \frac{1}{\sigma_i^2} \sum_i \frac{x_i^2}{\sigma_i^2} - \left(\sum_i \frac{x_i}{\sigma_i^2} \right)^2 \tag{4.1-17}$$

The variance σ_z^2 of a function z, which is a function of uncorrelated variables $y_1, y_2, \ldots y_i, \ldots$, is given by (40)

$$\sigma_z^2 = \sum_i \sigma_i^2 \left(\frac{\partial z}{\partial y_i} \right)^2 \tag{4.1-18}$$

To find the uncertainty in the estimation of the coefficients, a and b in our fitting procedure, take derivatives of Eqs. (4.1-15) and (4.1-16).

$$\frac{\partial a}{\partial y_j} = \frac{1}{\Delta} \left(\frac{1}{\sigma_j^2} \sum_i \frac{x_i^2}{\sigma_i^2} - \frac{x_i}{\sigma_j^2} \sum_i \frac{x_i}{\sigma_j^2} \right) \tag{4.1-19}$$

$$\frac{\partial b}{\partial y_j} = \frac{1}{\Delta} \left(\frac{x_i}{\sigma_j^2} \sum_i \frac{1}{\sigma_i^2} - \frac{1}{\sigma_j^2} \sum_i \frac{x_i}{\sigma_j^2} \right) \tag{4.1-20}$$

Substituting Eqs. (4.1-19) and (4.1-20) into Eq. (4.1-18), simplifying, and rearranging the result yields

$$\sigma_a^2 \cong \frac{1}{\Delta} \sum_i \frac{x_i^2}{\sigma_i^2} \tag{4.1-21}$$

$$\sigma_b^2 \cong \frac{1}{\Delta} \sum_i \frac{1}{\sigma_i^2} \tag{4.1-22}$$

Within the errors of the experiment, the uncertainties, σ_i, in the observations may be approximated by (40)

$$\sigma_i^2 \cong y_i \tag{4.1-23}$$

Hence,

$$\sigma_a^2 \cong \frac{1}{\Delta} \sum_i \frac{x_i^2}{y_i} \tag{4.1-24}$$

$$\sigma_b^2 \cong \frac{1}{\Delta} \sum_i \frac{1}{y_i} \tag{4.1-25}$$

4.2 Model $y = a_o e^{b_o x}$ (linearized by transformation)

Count data from a decaying radioactive source follows an exponential function, i.e.,

$$C = C_o e^{-\lambda t}, \tag{4.2-1}$$

where C = counts (at time, t) from a radioactive source taken with an appropriate detector system,

C_o = counts (at time zero),

λ = characteristic decay constant (time^{-1}).

To find estimates for C_o and λ, the simplest approach is to linearize by logarithmic transformation, which yields

$$\ln C = \ln C_o - \lambda t \tag{4.2-2}$$

or in general notation

$$\ln y = \ln a_o + b_o x \tag{4.2-3}$$

Equation (4.2-3) is linear, with ln y as the dependent variable, x as the independent variable, and parameters, ln a_o and b_o. Thus, the regression condition is:

$$E_o = \sum_{i=1}^{n} w_{oi}(\ln y_i - \ln a_o + b_o x_i)^2 \tag{4.2-4}$$

To minimize (or maximize) E_o, the derivatives of E_o with respect to a_o and b_o should be zero. If $\frac{\partial^2 E_o}{\partial a_o^2}$ and $\frac{\partial^2 E_o}{\partial^2 b_o}$ are both greater than zero, we are guaranteed that the values found for ln a_o and b_o obtained by normal equations will minimize E_o. Equation (4.2-4) yields two equations to be solved for ln a_o and b_o. After rearrangement, this process (i.e., the same procedure as was shown in section 4.1) yields

$$b_o = \frac{(\sum_{i=1}^{n} w_{oi})(\sum_{i=1}^{n} w_{oi}x_i \ln y_i) - (\sum_{i=1}^{n} w_{oi}x_i)(\sum_{i=1}^{n} w_{oi}\ln y_i)}{(\sum_{i=1}^{n} w_{oi})(\sum_{i=1}^{n} w_{oi}x_i^2) - (\sum_{i=1}^{n} w_{oi}x_i)^2} \quad (4.2\text{-}5)$$

by having b_o, $\ln a_o$ can be obtained by:

$$\ln a_o = \frac{(\sum_{i=1}^{n} w_{oi}\ln y_i) - (\sum_{i=1}^{n} w_{oi}x_i)b_o}{(\sum_{i=1}^{n} w_{oi})} \quad (4.2\text{-}6)$$

To fulfill the condition of the Gauss-Markov theorm (42), the weights (w_{io}) are the reciprocal variances of the logarithm of data.

$$w_{oi} = \frac{1}{\sigma^2(\ln y_i)} \quad (4.2\text{-}7)$$

Since

$$\sigma^2(\ln y_i) = \left(\frac{\partial \ln y_i}{\partial y_i}\right)^2 \sigma^2(y_i) = \frac{1}{y_i^2}\sigma^2(y_i) \quad (4.2\text{-}8)$$

but for a counting experiment goverened by Poisson distribution;

$$\sigma^2(y_i) = y_i \quad (4.2\text{-}9)$$

then, by Eq. (4.1-18),

$$\sigma^2(\ln y_i) = \frac{1}{y_i} \quad (4.2\text{-}10)$$

Hence,

$$w_{oi} = y_i \tag{4.2-11}$$

4.3 Model $y = a_1 e^{b_1 x}$ (iterative procedure)

Assume a model, which represents the data, is

$$y = a_1 e^{b_1 x} \tag{4.3-1}$$

To estimate the parameter a_1 and b_1 we can minimize the sum of square residuals, E_1:

$$E_1 = \sum_{i=1}^{n} w_i (a_1 e^{b_1 x_i} - y_i)^2 \tag{4.3-2}$$

Equating the partial differentiation of E_1 with respect to the parameters a_1 and b_1 simultaneously to zero yields Eqs. (4.3-3) and (4.3-4)

$$\sum_{i=1}^{n} w_i (a_1 e^{b_1 x_i} - y_i) e^{b_1 x_i} = 0, \tag{4.3-3}$$

$$\sum_{i=1}^{n} w_i (a_1 e^{b_1 x_i} - y_i) e^{b_1 x_i} = 0 \tag{4.3-4}$$

Rearranging, we obtain the normal equations.

$$a_1 \sum_{i=1}^{n} w_i (e^{b_1 x_i})^2 = \sum_{i=1}^{n} w_i y_i e^{b_1 x_i} \qquad (4.3\text{-}5)$$

$$a_1 \sum_{i=1}^{n} w_i x_i (e^{b_1 x_i})^2 = \sum_{i=1}^{n} w_i x_i y_i e^{b_1 x_i} \qquad (4.3\text{-}6)$$

By elimination of the parameter a_1, the following equation for b_1 is obtained.

$$[\sum_{i=1}^{n} w_i x_i y_i e^{b_1 x_i}] [\sum_{i=1}^{n} w_i (e^{b_1 x_i})^2] - [\sum_{i=1}^{n} w_i y_i e^{b_1 x_i}] [\sum_{i=1}^{n} w_i x_i (e^{b_1 x_i})^2] = 0 \qquad (4.3\text{-}7)$$

The parameter b_1 can be obtained by numerical solution of Eq. (4.2-7) By substitution of Eq. (4.3-1) into Eq. (4.3-7), we obtain expression for a_1.

$$a_1 = [\sum_{i=1}^{n} w_i y_i e^{b_1 x_i}] / [\sum_{i=1}^{n} w_i (e^{b_1 x_i})^2] \qquad (4.3\text{-}8)$$

For the numerical solution of Eq. (4.3-7), let

$$f(b_1) = [\sum_{i=1}^{n} w_i x_i y_i e^{b_1 x_i}] [\sum_{i=1}^{n} w_i (e^{b_1 x_i})] - [\sum_{i=1}^{n} w_i y_i e^{b_1 x_i}]$$

$$[\sum_{i=1}^{n} w_i x_i (e^{b_1 x_i})^2], \qquad (4.3\text{-}9)$$

for which the root of $f(b_1)$ is desired. The equation $f(b_1)$ is a non-

linear equation, and there are many methods for solving these kinds of equations, e.g., Newton's method (44,45,46).

Newton's method can be used for find the real zero of $f(b_1)$. By using the Newton-Raphson method, successive approximations of the root, $b_{1,0}$, $b_{1,1}$, $b_{1,2}$,... can be obtained by using the following relation:

$$b_{i,i+1} = b_{1,i} - \frac{f(b_{1,i})}{f'(b_{1,i})} \tag{4.3-10}$$

where $f'(b_1) = \partial f/\partial b_1$. By differentiation of $f(b_1)$ (Eq. (4.3-9)), $f'(b_1)$ can be obtained:

$$f'(b_1) = [\sum_{i=1}^{n} w_i x_i^2 y_i e^{b_1 x_i}][\sum_{i=1}^{n} w_i (e^{b_1 x_i})^2] + [\sum_{i=1}^{n} w_i x_i y_i e^{b_1 x_i}]$$

$$[2\sum_{i=1}^{n} w_i x_i (e^{b_1 x_i})^2] - [\sum_{i=1}^{n} w_i x_i y_i e^{b_1 x_i}][\sum_{i=1}^{n} w_i x_i (e^{b_1 x_i})^2]$$

$$- [\sum_{i=1}^{n} w_i y_i e^{b_1 x_i}] [\sum_{i=1}^{n} w_i x_i^2 (e^{b_1 x_i})^2] \tag{4.3-11}$$

After simplifying, we obtain for $f'(b_1)$

$$f'(b_1) = [\sum_{i=1}^{n} w_i x_i^2 y_i e^{b_1 x_i}] [\sum_{i=1}^{n} w_i (e^{b_1 x_i})^2] + [\sum_{i=1}^{n} w_i x_i y_i e^{b_1 x_i}]$$

$$[\sum_{i=1}^{n} w_i x_i (e^{b_1 x_i})^2] - 2[\sum_{i=1}^{n} w_i y_i e^{b_1 x_i}] [\sum_{i=1}^{n} w_i x_i^2 (e^{b_1 x_i})^2] \tag{4.3-12}$$

To fulfill the condition of the Gauss-Markov theorm (42,43) the weights (w_i) are the reciprocal variances of the data.

$$w_i = \frac{1}{\sigma^2(y_i)} \tag{4.3-13}$$

but for a counting experiment governed by the Poisson distribution, the variances of data are

$$\sigma^2(y_i) = y_i. \tag{4.3-14}$$

Hence,

$$w_i = \frac{1}{y_i} \tag{4.3-15}$$

The model $f(t) = a_1 e^{b_1 t} + a_2 e^{b_2 t} + a_3 e^{b_3 t}$ which is the more sophisticated case of that explained above, has been explained in Appendix F.

5.0 Description of Experimental Apparatus

The Kansas State University 250 - kW TRIGA Mark II pulsing Nuclear Reactor was used as a source of fast neutrons for this work. The physical specifications of this reactor are described in reference (64). The TRIGA Nuclear Reactor (Fig. 5.1) is a research reactor and it supplies a sufficient neutron flux for activation analysis. Thermal and fast neutron flux levels at several locations in reactor are shown in Table (5.1). The irradiation position throughout this work was the F-7 position of the Triga Reactor. The F-7 position was used since a greater fast neutron flux)/(thermal neutron flux) is available in the F-ring of the reactor core than in other position, e.g., RSR. Access to the F-7 is provided by an aluminum tube which extends from the top of the reactor to the F-7. Standard polyethylene sample vials were used to hold the samples during irradiation in the F-7. The polyethylene vials were approximately 1 inch long and 7/16 inch in diameter. These small vials were placed inside polystyrene irradiation vials.

A coaxially lithium-drifted germanium [Ge(Li)] semiconductor detector (Canberra, model 7227 (37.5 mm diameter, and 22.5 mm length)) was used for gamma ray detection. The Ge(Li) detector normally is a p-i-n device. When a gamma-ray enters the intristic (i) region, ions result and produce induced voltage pulses, which are received at the pre-amplifier. Because of high mobility of the lithium contained in the germanium crystal at room temperature (20°C) which causes diffusion of the lithium, the detector always should be cooled by liquid nitrogen.

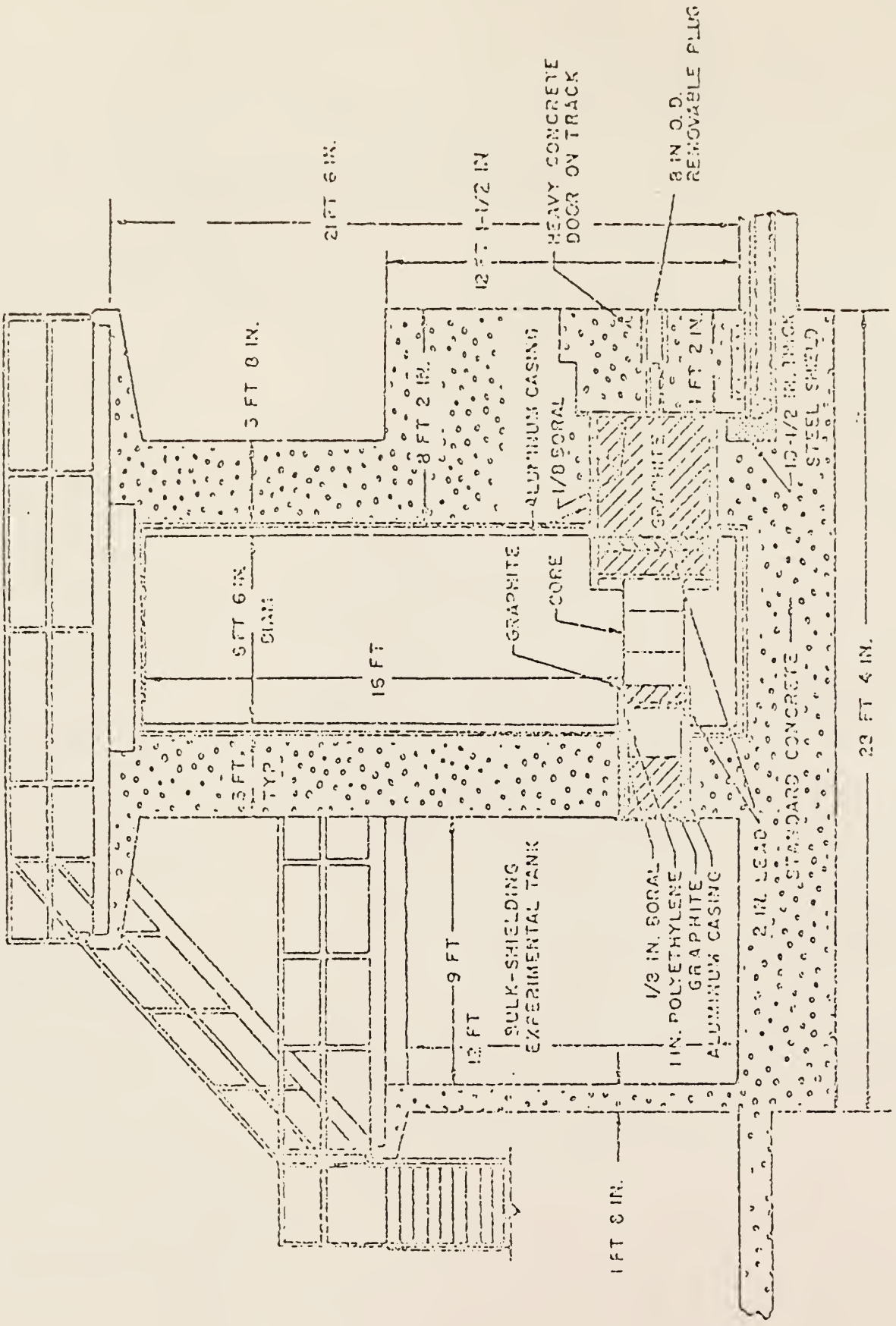

Figure 5.1. Vertical section view of TRIGA Mark II Nuclear Reactor (64).

Table 5.1. Thermal and Fast Neutron Flux Values for the TRIGA Mark II Nuclear Reactor (250 kW) (65). (thermal < 0.21 eV, Fast > 10 keV)

Irradiation Position	Reactor Pool Above Reflector	RSR	Fuel-Element Ring E	Fuel-Element Ring D	Fuel-Element Ring F	Reactor Pool Outside Reflector
Thermal neutron flux (n/cm^2-sec)	3.4×10^{11}	$1.8 \times .10^{12}$	4.1×10^{12}	4.9×10^{12}	4.3×10^{12}	6.8×10^{11}
Fast neutron flux (n/cm^2-sec)	1.1×10^{11}	1.5×10^{12}	6.4×10^{12}	4.25×10^{12}	3.5×10^{12}	6.8×10^{10}

The detector was located within the Neutron Activation Analysis Laboratory. A preamplifier (Canberra, model 979) was coupled directly to the Ge(Li) detector. The input of the main amplifier (spectroscopy amplifier, ORTEC model 451) was connected to the preamplifier by a coaxial cable. The maximum energy range of the gamma-ray spectrum was controlled with the amplifier gain. The power for the detector was supplied by a high voltage power supply, Fluke, model 415B. The main amplifier was coupled directly to a Northern Scientific Analog-to-Digital Convertor (ADC), model NS-623, and its associated multichannel analyzer equipment. A multichannel analyzer is used to sort and store voltage pulses according to their respective heights.

Output from the multichannel analyzer can be in the form of a live display of data on an oscilloscope, a printed paper tape unit, and a magnetic tape device. The output from the multichannel analyzer can be plotted as the number of pulses per unit time per unit pulse height vs pulse height. This display of data indicates the various interaction processes that occur in the detector.

The data are transferred to and stored on magnetic tape through the Northern Scientific, Model NS-408. An IBM 370/158 digital computer was used in processing the data for this work.

The Ge(Li) detector used in this work has the chief advantage of improved resolution relative to NaI(Tl) scintillator detector. The major disadvantage for Ge(Li) is its efficiency.

5.1 Experimental Procedure

5.1-1 Sample Preparation

Four samples of standard wheat of different protein content (9.55%, 10.7%, 13.8%, and 15.3% protein) and one sample of NH_4NO_3 were irradiated three times (in order to determine reproducibility of results) in this work. The samples were placed into polyethylene sample vials (obtained from Olympic Plastic Co.). All vials were cleaned before filling the samples. The polyethylene sample vials were placed inside the polystyrene irradiation vial.

5.1-2 Irradiation Conditions

The samples were irradiated after manual insertion into the F-7 position of the KSU TRIGA Mark II Nuclear Reactor. The typical irradiation time was 10 minutes at a reactor power level of about 225 kW (3.5×10^{12}), the maximum obtainable. There was about 2 to 8 minutes decay between the end of an irradiation and the beginning of the first gamma-ray spectrum measurement. A stop watch was started when the sample was taken out and was used to measure the elapsed time between the end of the irradiation and the counting sample. The irradiated samples disintegration rates after removal from the reactor were about 0.1 to 10 μCi.

5.1-3 Counting Procedure

The samples were transported manually to the detector system. A Ge(Li) semiconductor detector was used for the counting of all samples.

Additional details on the equipment can be found in "Description of Experimental Apparatus". The samples were placed on the Ge(Li) detector with constant geometry between sample and detector, and the spectrum for the reference was accumulated for the desired interval of time, in the 2048 channels configuration of the multichannel analyzer. The analyzer dead time was never greater than 10% for any of the measurements. Wheat and NH_4NO_3 were measured using amplifier gain of 5. Spectrum data were transferred from the memory system of the analyzer to magnetic tape which was then used to store the data and also for data processing.

5.1-4 Computer Operations

After the data for each sample were collected on magnetic tape, the spectra were removed by use of the KSU IBM 350/158 (ITEL Advanced Systems 5, after April 22, 1978), computer (WATID computer code). A copy of the WATID code is included in Appendix G. The data were analyzed by using the FDA code. The FDA consists of different steps, such as; numerical integration, gamma function calculation, intepolation, and plotting the results.

The details of computer codes are explained in Appendix D. The theory related to gamma function calculation is explained in Appendix I. Fourier decay analysis codes, using trapezoidal and Simpson's inegration routines are given in Appendices, J and K, respectively. A code for numerical solution of Eq. (4.3-7) has been written (Appendix M), which were used for half life determination.

6.0 Analysis and Discussion of Experimental Data

6.1 Analysis of NH_4NO_3 Data

Samples of NH_4NO_3 were irradiated and the data were analyzed by using the FDA method, the iterative method and the transformed least squares (TLS) method. In the case of NH_4NO_3, results obtained by FDA were obtained primarily in the form of a table of numbers ($G(\lambda)/\lambda$ vs λ). Getting results in form of numbers has some advantages and disadvantages. By looking at a plot, the number of real components and distribution of error ripples can be specified easily; but the use of numbers gives us exact results.

In the FDA method, the results for NH_4NO_3 shown in coming tables, a shift of position of the true peak is observed when the cutoff μ_o changes. The shift in position of the true peak for different values of μ_o is due to many factors. As shown section 3 for two or three components even if the data were purposefully constructed, we would have the problem of shift of true peaks. Most data obtained for analysis contain statistical and instrumental errors. As time increases the scatter in data obtained from a radioisotope will increase too, such that after several half lives of time had elapsed too much scatter appeared in the data. Since the data appeared to indicate more than one component and the scatter of data was severe, the problem of shift of the position of true peaks became particularly difficult. As is true with all data analysis procedure the less scatter in the data,

the better the FDA method is going to work. Although for the data analyzed in this study which included data with a large amount of scatter, the results obtained from FDA method are much better than the iterative method or transformed least squares (TLS) method. In some cases, when the data were really scattered badly, it was smoothed by ignoring certain points which caused a dramatic improvement.

By increasing the value of μ_o the accuracy of the results increases, in general. However, in most of the cases when the cutoff value of μ_o reaches 5, the error ripples completely mask the results. Thus, in most cases the results were obtained by the FDA method with $\mu_o = 4$.

For each set of data, results have been analyzed and discussed in the following sections.

(a) NH_4NO_3 - Data set #1

Data set #1 is tabulated in Table (6.1). The data have been plotted in Fig. (6.1). By using the FDA method, the data were analyzed for $\mu_o = 2$ and 4. The half-life for ^{13}N was obtained (see Table 6.4). The result of the FDA analysis is in form of two columns; $G(\lambda)/\lambda$ vs λ are given. Also included in the analysis table is a listing of the parameters used in computer program for the FDA; these parameters are explained in Appendix E. Tables (6.2 and 6.3) are the results of the FDA for $\mu_o = 2$ and 4, respectively. The half-life obtained by FDA for $\mu_o = 2$ and 4 are 8.53 m and 8.99 m, respectively. As seen by increasing

Table 6.1. Data set #1 (NH_4NO_3).

Decay Time (min.)	Counts per 2.133 minutes
8.000	11730.598
10.150	9845.098
13.950	8088.898
16.750	6939.000
19.950	5638.000
22.700	4904.398
25.500	4214.199
28.100	3630.100
31.850	2988.100
34.550	2530.500

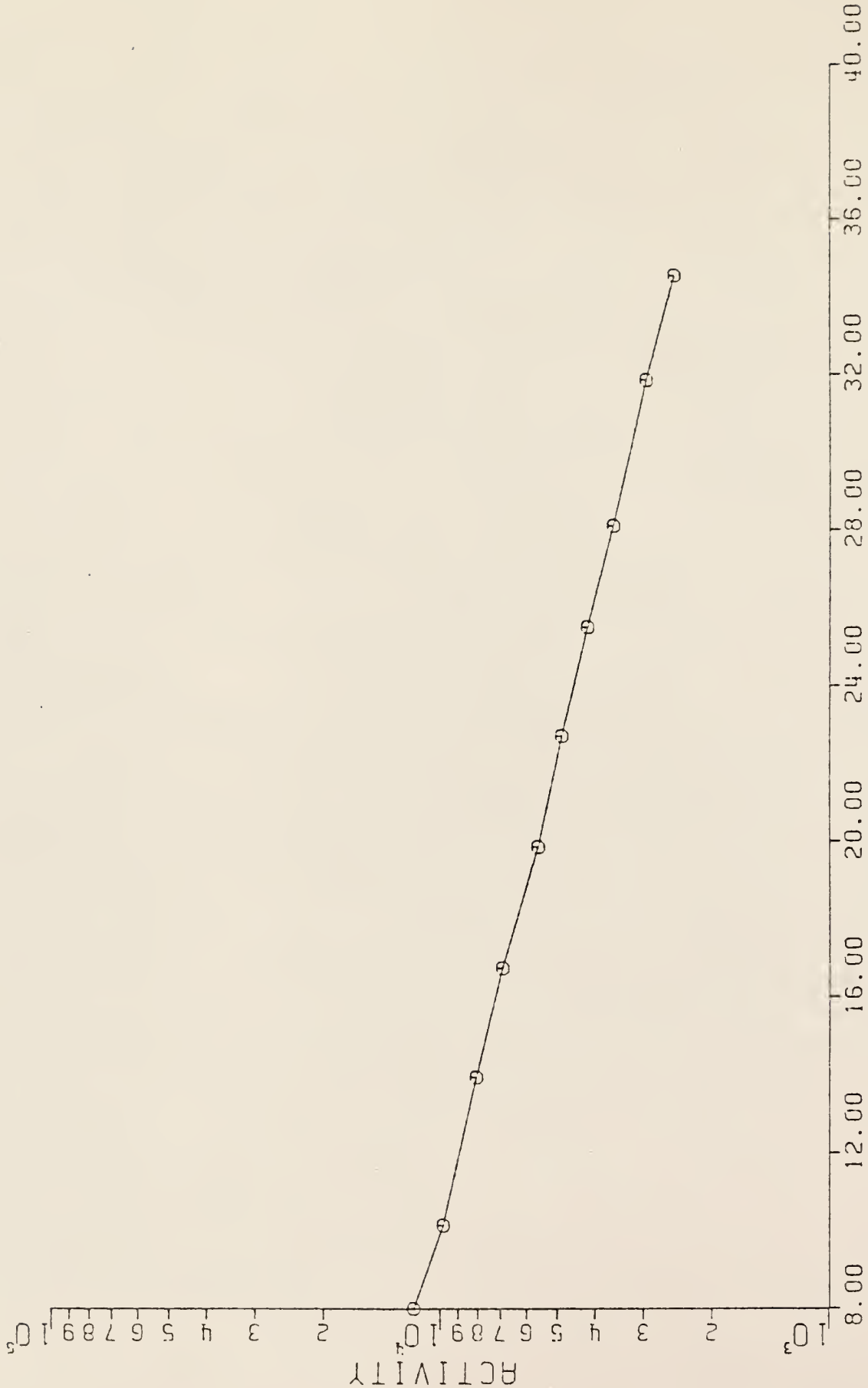

Figure 6.1. A plot of activity (counts, total area of the 0.511 MeV photopeaks, per 2.133 minutes) versus decay time (in minutes) for NH_4NO_3 (Data Set #1).

Table 6.2. Fourier Decay Analysis results for NH_4NO_3, data set #1.

G(λ)/λ	λ
0.62908371E 05	0.20000000E-01
0.71949563E 05	0.20470615E-01
0.81107313E 05	0.20952318E-01
0.90370563E 05	0.21445330E-01
0.99730875E 05	0.21949977E-01
0.10917663E 06	0.22466466E-01
0.11869913E 06	0.22995126E-01
0.12828669E 06	0.23536220E-01
0.13792925E 06	0.24090059E-01
0.14761650E 06	0.24656922E-01
0.15733688E 06	0.25237121E-01
0.16708019E 06	0.25830973E-01
0.17683531E 06	0.26438806E-01
0.18659144E 06	0.27060926E-01
0.19633738E 06	0.27697694E-01
0.20606281E 06	0.28349455E-01
0.21575594E 06	0.29016551E-01
0.22540606E 06	0.29699322E-01
0.23500244E 06	0.30398194E-01
0.24453406E 06	0.31113487E-01
0.25399063E 06	0.31845625E-01
0.26336063E 06	0.32594983E-01
0.27263369E 06	0.33361968E-01
0.28179981E 06	0.34147013E-01
0.29084819E 06	0.34950521E-01
0.29976806E 06	0.35772931E-01
0.30855038E 06	0.36614701E-01
0.31718513E 06	0.37476290E-01
0.32566206E 06	0.38358133E-01
0.33397206E 06	0.39260749E-01
0.34210550E 06	0.40184591E-01
0.35005338E 06	0.41130178E-01
0.35780744E 06	0.42098004E-01
0.36535869E 06	0.43088604E-01
0.37269988E 06	0.44102531E-01
0.37982144E 06	0.45140300E-01
0.38671694E 06	0.46202485E-01
0.39337388E 06	0.47289673E-01
0.39979981E 06	0.48402458E-01
0.40597313E 06	0.49541414E-01
0.41189175E 06	0.50707165E-01
0.41755131E 06	0.51900364E-01
0.42294575E 06	0.53121623E-01
0.42806794E 06	0.54371603E-01
0.43291325E 06	0.55650994E-01
0.43748231E 06	0.56960523E-01
0.44176325E 06	0.58300894E-01
0.44575644E 06	0.59672773E-01
0.44945744E 06	0.61076906E-01
0.45286494E 06	0.62514067E-01
0.45597450E 06	0.63985050E-01

Table 6.2, cont'd.

$G(\lambda)/\lambda$	λ
0.45878394E 06	0.65490663E-01
0.46129156E 06	0.67031801E-01
0.46349775E 06	0.68609118E-01
0.46539938E 06	0.70223570E-01
0.46699725E 06	0.71875989E-01
0.46828900E 06	0.73567271E-01
0.46927700E 06	0.75298429E-01
0.46996138E 06	0.77070236E-01
0.47034431E 06	0.78883767E-01
0.47042644E 06	0.80739975E-01
0.47020744E 06	0.82639873E-01
0.46969175E 06	0.84584475E-01
0.46888069E 06	0.86574852E-01
0.46777906E 06	0.88612020E-01
0.46638794E 06	0.90697169E-01
0.46471756E 06	0.92831314E-01
0.46276219E 06	0.95015705E-01
0.46053113E 06	0.97251534E-01
0.45803081E 06	0.99540055E-01
0.45526406E 06	0.10188228E 00
0.45223694E 06	0.10427964E 00
0.44895419E 06	0.10673344E 00
0.44542350E 06	0.10924494E 00
0.44165056E 06	0.11181569E 00
0.43764175E 06	0.11444682E 00
0.43340413E 06	0.11713982E 00
0.42894556E 06	0.11989623E 00
0.42427369E 06	0.12271744E 00
0.41939463E 06	0.12560511E 00
0.41431663E 06	0.12856084E 00
0.40904800E 06	0.13158596E 00
0.40359819E 06	0.13468236E 00
0.39797400E 06	0.13785148E 00
0.39218581E 06	0.14109522E 00
0.38624169E 06	0.14441532E 00
0.38014925E 06	0.14781368E 00
0.37391994E 06	0.15129179E 00
0.36756075E 06	0.15485185E 00
0.36108219E 06	0.15849560E 00
0.35449219E 06	0.16222513E 00
0.34780163E 06	0.16604245E 00
0.34101944E 06	0.16994971E 00
0.33415506E 06	0.17394876E 00
0.32721894E 06	0.17804193E 00
0.32021988E 06	0.18223137E 00
0.31316456E 06	0.18651944E 00
0.30606669E 06	0.19090855E 00
0.29893481E 06	0.19540077E 00
0.29177581E 06	0.19999874E 00

NLAM= 100 LAMS= 0.020 LAMF= 0.20000

TEND= 34.550 NXPTS= 100 MUEND= 2.000

MUPTS= 100 IMAXTP= 10 NPTSTP= 6

Table 6.3. Fourier Decay Analysis results for NH_4NO_3, data set #1.

$G(\lambda)/\lambda$	λ
-0.15964881E 06	0.20000000E-01
-0.25972519E 06	0.20470615E-01
-0.35976094E 06	0.20952318E-01
-0.45899781E 06	0.21445330E-01
-0.55666231E 06	0.21949977E-01
-0.65197194E 06	0.22466466E-01
-0.74417869E 06	0.22995126E-01
-0.83251356E 06	0.23536220E-01
-0.91624338E 06	0.24090059E-01
-0.99465806E 06	0.24656922E-01
-0.10670630E 07	0.25237121E-01
-0.11328070E 07	0.25830973E-01
-0.11912770E 07	0.26438806E-01
-0.12419010E 07	0.27060926E-01
-0.12841550E 07	0.27697694E-01
-0.13175700E 07	0.28349455E-01
-0.13417280E 07	0.29016551E-01
-0.13562770E 07	0.29699322E-01
-0.13609250E 07	0.30398194E-01
-0.13554470E 07	0.31113487E-01
-0.13396870E 07	0.31845625E-01
-0.13135550E 07	0.32594983E-01
-0.12770380E 07	0.33361968E-01
-0.12301940E 07	0.34147013E-01
-0.11731480E 07	0.34950521E-01
-0.11061110E 07	0.35772931E-01
-0.10293469E 07	0.36614701E-01
-0.94319756E 06	0.37476290E-01
-0.84808556E 06	0.38358133E-01
-0.74446175E 06	0.39260749E-01
-0.63292619E 06	0.40184591E-01
-0.51403231E 06	0.41130178E-01
-0.38845113E 06	0.42098004E-01
-0.25690413E 06	0.43088604E-01
-0.12013219E 06	0.44102531E-01
0.21045695E 05	0.45140300E-01
0.16579438E 06	0.46202485E-01
0.31324388E 06	0.47289673E-01
0.46248844E 06	0.48402458E-01
0.61260750E 06	0.49541414E-01
0.76267250E 06	0.50707165E-01
0.91173831E 06	0.51900364E-01
0.10588610E 07	0.53121623E-01
0.12031030E 07	0.54371603E-01
0.13435370E 07	0.55650994E-01
0.14792540E 07	0.56960523E-01
0.16093750E 07	0.58300894E-01
0.17330330E 07	0.59672773E-01
0.18494220E 07	0.61076906E-01
0.19577460E 07	0.62514067E-01
0.20573010E 07	0.63985050E-01

Table 6.3, cont'd.

G(λ)/λ	λ
0.21474030E 07	0.65490663E-01
0.22274380E 07	0.67031801E-01
0.22968440E 07	0.68609118E-01
0.23551380E 07	0.70223570E-01
0.24018970E 07	0.71875989E-01
0.24367780E 07	0.73567271E-01
0.24595110E 07	0.75298429E-01
0.24699070E 07	0.77070236E-01
0.24678500E 07	0.78883767E-01
0.24533090E 07	0.80739975E-01
0.24263330E 07	0.82639873E-01
0.23870510E 07	0.84584475E-01
0.23356720E 07	0.86574852E-01
0.22724880E 07	0.88612020E-01
0.21978560E 07	0.90697169E-01
0.21122310E 07	0.92831314E-01
0.20161140E 07	0.95015705E-01
0.19100840E 07	0.97251534E-01
0.17947920E 07	0.99540055E-01
0.16709510E 07	0.10188228E 00
0.15393150E 07	0.10427964E 00
0.14006900E 07	0.10673344E 00
0.12559550E 07	0.10924494E 00
0.11059750E 07	0.11181569E 00
0.95171550E 06	0.11444682E 00
0.79411706E 06	0.11713982E 00
0.63416413E 06	0.11989623E 00
0.47285513E 06	0.12271744E 00
0.31117156E 06	0.12560511E 00
0.15012600E 06	0.12856084E 00
-0.92793555E 04	0.13159596E 00
-0.16006788E 06	0.13468230E 00
-0.31927806E 06	0.13785148E 00
-0.46797100E 06	0.14109522E 00
-0.61124231E 06	0.14441532E 00
-0.74823175E 06	0.14781368E 00
-0.87810063E 06	0.15129179E 00
-0.10000926E 07	0.15485185E 00
-0.11134780E 07	0.15849560E 00
-0.12176010E 07	0.16222513E 00
-0.13118660E 07	0.16604245E 00
-0.13957440E 07	0.16994971E 00
-0.14688760E 07	0.17394876E 00
-0.15305790E 07	0.17804193E 00
-0.15808430E 07	0.18223137E 00
-0.16193410E 07	0.18651944E 00
-0.16459190E 07	0.19090855E 00
-0.16605050E 07	0.19540077E 00
-0.16631090E 07	0.19999874E 00

NLAM= 100 LAMS= 0.020 LAMF= 0.20000

TEND= 34.550 NXPTS= 100 MUEND= 4.000

MUPTS= 100 IMAXTP= 10 NPTSTP= 6

Table 6.4. Comparison of half lives obtained from the three analysis methods for NH_4NO_3 data set #1 and reported half lives (53-56), (57-59), (60), and (61).

		9.96 m	10.05m	10.08 m	9.93 m
	$T_{1/2}$	error (%)	error (%)	error (%)	error (%)
FDA Method	8.99	9.73	10.54	10.81	9.46
Iterative Method	12.07	21.18	20.09	19.74	21.55
TLS Method	12.24	22.89	21.79	21.42	23.26

the μ_o, the cutoff integration, a shift in the position of the true peak is observed. For $\mu_o = 5$, the error ripples completely masked the results.

The data were analyzed also by the iterative method and TLS method. The half life of ^{13}N obtained from different references are 9.06 m (53,54,55,56), 10.05 m (57,58,59), 10.08 m (60) and 9.93 m (61). Results of the analysis of the data set No. 1 and a percentage error of these results compared to those obtained from published reports are tabulated in Table (6.4). As seen the result obtained by FDA is better than that obtained by the iterative method or the TLS method.

(b) NH_4NO_3 - Data Set #2

Data set #2 is tabulated in Table (6.5). Again the data were analyzed by, FDA, iterative, and TLS methods. The first fifteen data points had very little scatter, but significant scatter in the rest of the data appeared after about 45 minutes of decay. The data were analyzed by FDA for μ_o = 2 and 4; the results are given in Tables (6.6) and (6.7), respectively. Half lives obtained by FDA for μ_o = 2 and 4, are 11.9 m and 13.0 m, respectively. For μ_o = 5 error ripples completely masked the results.

The data were smoothed by ignoring certain points (Table 6.8). These smoothed data (Table (6.8)) were analyzed by FDA for μ_o = 2 and 4, and the results are given in Tables (6.9) and (6.10), respectively. The half lives were 10.3 m and 10.3 m for μ_o = 2 and 4, respectively. As seen the results were improved significantly and there is no longer shift in the position of true peaks. The data (Table 6.8) were analyzed also by the iterative and TLS methods. The results of the analysis by the three methods are given in Table (6.11). As seen the results of the FDA are better than the results of the other methods.

Table 6.5. Data set #2 (NH_4NO_3).

Decay Time (min.)	Counts per 2.133 minutes
2.500	11380.398
4.750	9876.457
6.990	8609.316
9.230	7480.207
11.470	6702.617
13.690	5754.379
15.920	4997.648
18.150	4562.719
20.370	3911.900
22.580	3455.410
24.800	3121.000
29.240	2343.640
31.440	2142.280
33.650	1902.100
35.850	1621.470
38.060	1406.610
40.270	1427.610
42.470	1187.010
44.670	1116.450
46.870	973.460

Table 6.5 contd.

Decay Time (min.)	Counts per 2.133 minutes
49.070	974.100
51.270	777.020
53.460	697.840
55.650	696.990
57.840	596.060

Table 6.6. Fourier Decay Analysis results for NH_4NO_3, data set #2.

G(λ)/λ	λ
0.13006350E 06	0.20000000E-01
0.13782344E 06	0.20470615E-01
0.14559344E 06	0.20952318E-01
0.15336313E 06	0.21445330E-01
0.16112469E 06	0.21949977E-01
0.16886725E 06	0.22466466E-01
0.17658281E 06	0.22995126E-01
0.18426125E 06	0.23536226E-01
0.19189313E 06	0.24090059E-01
0.19946956E 06	0.24656922E-01
0.20698050E 06	0.25237121E-01
0.21441725E 06	0.25830973E-01
0.22177038E 06	0.26438806E-01
0.22903056E 06	0.27060926E-01
0.23618875E 06	0.27697694E-01
0.24323656E 06	0.28349455E-01
0.25016431E 06	0.29016551E-01
0.25696350E 06	0.29699322E-01
0.26362556E 06	0.30398194E-01
0.27014231E 06	0.31113487E-01
0.27650531E 06	0.31845625E-01
0.28270631E 06	0.32594983E-01
0.28873744E 06	0.33361968E-01
0.29459088E 06	0.34147013E-01
0.30025956E 06	0.34950521E-01
0.30573569E 06	0.35772931E-01
0.31101263E 06	0.36614701E-01
0.31608369E 06	0.37476290E-01
0.32094194E 06	0.38358133E-01
0.32558125E 06	0.39260749E-01
0.32999594E 06	0.40184591E-01
0.33417988E 06	0.41130178E-01
0.33812788E 06	0.42098004E-01
0.34183494E 06	0.43088604E-01
0.34529625E 06	0.44102531E-01
0.34850700E 06	0.45140300E-01
0.35146444E 06	0.46202485E-01
0.35416275E 06	0.47289673E-01
0.35659975E 06	0.48402458E-01
0.35877250E 06	0.49541414E-01
0.36067825E 06	0.50707165E-01
0.36231306E 06	0.51900364E-01
0.36367675E 06	0.53121623E-01
0.36476725E 06	0.54371603E-01
0.36558213E 06	0.55650994E-01
0.36612231E 06	0.56960523E-01
0.36638525E 06	0.58300894E-01
0.36637250E 06	0.59672773E-01
0.36608250E 06	0.61076906E-01
0.36551688E 06	0.62514067E-01
0.36467625E 06	0.63985050E-01

G(λ)/λ	λ
0.36356213E 06	0.65490663E-01
0.36217556E 06	0.67031801E-01
0.36051975E 06	0.68609118E-01
0.35859494E 06	0.70223570E-01
0.35640556E 06	0.71875985E-01
0.35395363E 06	0.73567271E-01
0.35124325E 06	0.75298429E-01
0.34827788E 06	0.77070236E-01
0.34506163E 06	0.78883767E-01
0.34159875E 06	0.80739975E-01
0.33789363E 06	0.82639873E-01
0.33395200E 06	0.84584475E-01
0.32977900E 06	0.86574852E-01
0.32537969E 06	0.88612020E-01
0.32076000E 06	0.90697169E-01
0.31592681E 06	0.92831314E-01
0.31088600E 06	0.95015705E-01
0.30564425E 06	0.97251534E-01
0.30020981E 06	0.99540055E-01
0.29458700E 06	0.10188228E 00
0.28878581E 06	0.10427964E 00
0.28281275E 06	0.10673344E 00
0.27667631E 06	0.10924494E 00
0.27038344E 06	0.11181569E 00
0.26394356E 06	0.11444682E 00
0.25736463E 06	0.11713982E 00
0.25065469E 06	0.11989623E 00
0.24382306E 06	0.12271744E 00
0.23687769E 06	0.12560511E 00
0.22982794E 06	0.12856084E 00
0.22268300E 06	0.13158596E 00
0.21545175E 06	0.13468230E 00
0.20814331E 06	0.13785148E 00
0.20076694E 06	0.14109522E 00
0.19333181E 06	0.14441532E 00
0.18584688E 06	0.14781368E 00
0.17832244E 06	0.15129179E 00
0.17076656E 06	0.15485185E 00
0.16318931E 06	0.15849560E 00
0.15559950E 06	0.16222513E 00
0.14800663E 06	0.16604245E 00
0.14041950E 06	0.16994971E 00
0.13284788E 06	0.17394876E 00
0.12530019E 06	0.17804193E 00
0.11778556E 06	0.18223137E 00
0.11031275E 06	0.18651944E 00
0.10289013E 06	0.19090855E 00
0.95526875E 05	0.19540077E 00
0.88231000E 05	0.19999874E 00

NLAM= 100 LAMS= 0.020 LAMF= 0.20000

TEND= 57.840 NXPTS= 100 MUEND= 2.000

MUPTS= 100 IMAXTP= 25 NPTSTP= 6

Table 6.7. Fourier Decay Analysis results for NH_4NO_3, data set #2.

$G(\lambda)/\lambda$	λ
-0.50677363E 06	0.20000000E-01
-0.50099725E 06	0.20470615E-01
-0.49142119E 06	0.20952318E-01
-0.47803244E 06	0.21445330E-01
-0.46083381E 06	0.21949977E-01
-0.43986200E 06	0.22466466E-01
-0.41517006E 06	0.22995126E-01
-0.38684394E 06	0.23536220E-01
-0.35498975E 06	0.24090059E-01
-0.31973725E 06	0.24656922E-01
-0.28124325E 06	0.25237121E-01
-0.23968394E 06	0.25830973E-01
-0.19525750E 06	0.26438806E-01
-0.14818300E 06	0.27060926E-01
-0.98698188E 05	0.27697694E-01
-0.47055938E 05	0.28349455E-01
0.64682891E 04	0.29016551E-01
0.61591262E 05	0.29699322E-01
0.11801475E 06	0.30398194E-01
0.17543138E 06	0.31113487E-01
0.23352625E 06	0.31845625E-01
0.29196831E 06	0.32594983E-01
0.35043756E 06	0.33361968E-01
0.40860075E 06	0.34147013E-01
0.46613531E 06	0.34950521E-01
0.52270088E 06	0.35772931E-01
0.57798556E 06	0.36614701E-01
0.63166398E 06	0.37476290E-01
0.68343913E 06	0.38358133E-01
0.73300000E 06	0.39260749E-01
0.78006944E 06	0.40184591E-01
0.82437150E 06	0.41130178E-01
0.86565281E 06	0.42098004E-01
0.90367588E 06	0.43088604E-01
0.93822938E 06	0.44102531E-01
0.96910863E 06	0.45140300E-01
0.99614456E 06	0.46202485E-01
0.10191854E 07	0.47289673E-01
0.10381010E 07	0.48402458E-01
0.10527960E 07	0.49541414E-01
0.10631900E 07	0.50707165E-01
0.10692380E 07	0.51900364E-01
0.10709150E 07	0.53121623E-01
0.10682240E 07	0.54371603E-01
0.10611970E 07	0.55650994E-01
0.10498940E 07	0.56960523E-01
0.10343934E 07	0.58300894E-01
0.10148052E 07	0.59672773E-01
0.99126238E 06	0.61076906E-01
0.96392588E 06	0.62514067E-01
0.93296963E 06	0.63985050E-01

G(λ)/λ	λ
0.89859438E 06	0.65490663E-01
0.86102139E 06	0.67031801E-01
0.82048906E 06	0.68609118E-01
0.77725588E 06	0.70223570E-01
0.73158925E 06	0.71875989E-01
0.68377463E 06	0.73567271E-01
0.63410525E 06	0.75298429E-01
0.58288500E 06	0.77070236E-01
0.53042594E 06	0.78883767E-01
0.47704375E 06	0.80739975E-01
0.42305525E 06	0.82639873E-01
0.36878369E 06	0.84584475E-01
0.31454613E 06	0.86574852E-01
0.26065688E 06	0.88612020E-01
0.20742306E 06	0.90697169E-01
0.15515306E 06	0.92831314E-01
0.10413213E 06	0.95015705E-01
0.54640328E 05	0.97251534E-01
0.69499844E 04	0.99540055E-01
-0.38685797E 05	0.10188228E 00
-0.82036750E 05	0.10427964E 00
-0.12288306E 06	0.10673344E 00
-0.16102131E 06	0.10924494E 00
-0.19628094E 06	0.11181569E 00
-0.22849706E 06	0.11444682E 00
-0.25753856E 06	0.11713982E 00
-0.28329319E 06	0.11989623E 00
-0.30567256E 06	0.12271744E 00
-0.32461469E 06	0.12560511E 00
-0.34007756E 06	0.12856084E 00
-0.35204506E 06	0.13158596E 00
-0.36052575E 06	0.13468230E 00
-0.36555188E 06	0.13785148E 00
-0.36717781E 06	0.14109522E 00
-0.36548056E 06	0.14441532E 00
-0.36056013E 06	0.14781368E 00
-0.35253650E 06	0.15129179E 00
-0.34154844E 06	0.15485185E 00
-0.32775494E 06	0.15849560E 00
-0.31133081E 06	0.16222513E 00
-0.29246731E 06	0.16604245E 00
-0.27136863E 06	0.16994971E 00
-0.24825369E 06	0.17394870E 00
-0.22335075E 06	0.17804193E 00
-0.19689681E 06	0.18223137E 00
-0.16913638E 06	0.18651944E 00
-0.14031831E 06	0.19090855E 00
-0.11069844E 06	0.19540077E 00
-0.80530625E 05	0.19999874E 00

NLAM= 100 LAMS= 0.020 LAMF= 0.20000

TEND= 57.840 NXPTS= 100 MUEND= 4.000

MUPTS= 100 IMAXTP= 25 NPTSTP= 6

G(LAMBDA) LAMBDA

Table 6.8. Data set #2 (smoothed NH_4NO_3).

Decay Time (min.)	Counts per 2.133 minutes
2.500	11380.398
4.750	9876.457
6.990	8609.316
9.230	7480.207
11.470	6702.617
13.690	5754.379
15.920	4997.648
18.150	4562.719
20.370	3911.900
22.580	3455.410
24.800	3121.000
29.240	2343.640
31.440	2142.280
33.650	1902.100
35.850	1621.470
38.060	1406.610
42.470	1187.010

Table 6.9. Fourier Decay Analysis results for NH_4NO_3, data set #2.

G(λ)/λ	λ
0.76677938E 05	0.20000000E-01
0.84555688E 05	0.20470615E-01
0.92502938E 05	0.20952318E-01
0.10050938E 06	0.21445330E-01
0.10856656E 06	0.21949977E-01
0.11666394E 06	0.22466466E-01
0.12479256E 06	0.22995126E-01
0.13294206E 06	0.23536220E-01
0.14110256E 06	0.24090059E-01
0.14926431E 06	0.24656922E-01
0.15741669E 06	0.25237121E-01
0.16554975E 06	0.25830973E-01
0.17365344E 06	0.26438806E-01
0.18171750E 06	0.27060926E-01
0.18973213E 06	0.27697694E-01
0.19768694E 06	0.28349455E-01
0.20557163E 06	0.29016551E-01
0.21337613E 06	0.29699322E-01
0.22109081E 06	0.30398194E-01
0.22870538E 06	0.31113487E-01
0.23621063E 06	0.31845625E-01
0.24359600E 06	0.32594983E-01
0.25085263E 06	0.33361968E-01
0.25797056E 06	0.34147013E-01
0.26494144E 06	0.34950521E-01
0.27175463E 06	0.35772931E-01
0.27840231E 06	0.36614701E-01
0.28487588E 06	0.37476290E-01
0.29116644E 06	0.38358133E-01
0.29726563E 06	0.39260749E-01
0.30316575E 06	0.40184591E-01
0.30885863E 06	0.41130178E-01
0.31433675E 06	0.42098004E-01
0.31959281E 06	0.43088604E-01
0.32462075E 06	0.44102531E-01
0.32941281E 06	0.45140300E-01
0.33396313E 06	0.46202485E-01
0.33826538E 06	0.47289673E-01
0.34231400E 06	0.48402458E-01
0.34610381E 06	0.49541414E-01
0.34962906E 06	0.50707165E-01
0.35288631E 06	0.51900364E-01
0.35587019E 06	0.53121623E-01
0.35857706E 06	0.54371603E-01
0.36100419E 06	0.55650994E-01
0.36314738E 06	0.56960523E-01
0.36500406E 06	0.58300894E-01
0.36657113E 06	0.59672773E-01
0.36784725E 06	0.61076906E-01
0.36883144E 06	0.62514067E-01
0.36952156E 06	0.63985050E-01

G(λ)/λ	λ
0.36991625E 06	0.65490663E-01
0.37001619E 06	0.67031801E-01
0.36982138E 06	0.68609118E-01
0.36933119E 06	0.70223570E-01
0.36854656E 06	0.71875989E-01
0.36746969E 06	0.73567271E-01
0.36610131E 06	0.75298429E-01
0.36444356E 06	0.77070236E-01
0.36249900E 06	0.78883767E-01
0.36026956E 06	0.80739975E-01
0.35775900E 06	0.82639873E-01
0.35497063E 06	0.84584475E-01
0.35190913E 06	0.86574852E-01
0.34857738E 06	0.88612020E-01
0.34498081E 06	0.90697169E-01
0.34112444E 06	0.92831314E-01
0.33701319E 06	0.95015705E-01
0.33265288E 06	0.97251534E-01
0.32804900E 06	0.99540055E-01
0.32320869E 06	0.10188228E 00
0.31813794E 06	0.10427964E 00
0.31284344E 06	0.10673344E 00
0.30733325E 06	0.10924494E 00
0.30161356E 06	0.11181569E 00
0.29569331E 06	0.11444682E 00
0.28958000E 06	0.11713982E 00
0.28328181E 06	0.11989623E 00
0.27680750E 06	0.12271744E 00
0.27016463E 06	0.12560511E 00
0.26336300E 06	0.12856084E 00
0.25641163E 06	0.13158596E 00
0.24931944E 06	0.13468230E 00
0.24209606E 06	0.13785148E 00
0.23475069E 06	0.14109522E 00
0.22729300E 06	0.14441532E 00
0.21973275E 06	0.14781368E 00
0.21208019E 06	0.15129179E 00
0.20434456E 06	0.15485185E 00
0.19653625E 06	0.15849560E 00
0.18866531E 06	0.16222513E 00
0.18074188E 06	0.16604245E 00
0.17277544E 06	0.16994971E 00
0.16477688E 06	0.17394876E 00
0.15675619E 06	0.17804193L 00
0.14872300E 06	0.18223137E 00
0.14068769E 06	0.18651944E 00
0.13265981E 06	0.19090855E 00
0.12465000E 06	0.19540077E 00
0.11666750E 06	0.19999874E 00

NLAM= 100 LAMS= 0.020 LAMF= 0.20000

TEND= 42.470 NXPTS= 100 MUENC= 2.000

MUPTS= 100 IMAXTP= 17 NPTSTP= 6

Table 6.10. Fourier Decay Analysis results for NH_4NO_3, data set #2.

G(λ)/λ	λ
-0.49492231E 06	0.20000000E-01
-0.53902256E 06	0.20470615E-01
-0.57997663E 06	0.20952318E-01
-0.61741813E 06	0.21445330E-01
-0.65100875E 06	0.21949977E-01
-0.68042219E 06	0.22466466E-01
-0.70536781E 06	0.22995126E-01
-0.72557225E 06	0.23536220E-01
-0.74079919E 06	0.24090059E-01
-0.75083938E 06	0.24656922E-01
-0.75551656E 06	0.25237121E-01
-0.75469119E 06	0.25830973E-01
-0.74825944E 06	0.26438806E-01
-0.73615350E 06	0.27060926E-01
-0.71834438E 06	0.27697694E-01
-0.69484131E 06	0.28349455E-01
-0.66569300E 06	0.29016551E-01
-0.63098644E 06	0.29699322E-01
-0.59084656E 06	0.30398194E-01
-0.54543806E 06	0.31113487E-01
-0.49495919E 06	0.31845625E-01
-0.43965094E 06	0.32594983E-01
-0.37978388E 06	0.33361968E-01
-0.31566238E 06	0.34147013E-01
-0.24762031E 06	0.34950521E-01
-0.17603231E 06	0.35772931E-01
-0.10128275E 06	0.36614701E-01
-0.23788613E 05	0.37476290E-01
0.56001320E 05	0.38358133E-01
0.13763681E 06	0.39260749E-01
0.22064563E 06	0.40184591E-01
0.30453319E 06	0.41130178E-01
0.38880825E 06	0.42098004E-01
0.47295956E 06	0.43089604E-01
0.55649550E 06	0.44102531E-01
0.63889706E 06	0.45140300E-01
0.71966888E 06	0.46202485E-01
0.79831463E 06	0.47289673E-01
0.87434681E 06	0.48402458E-01
0.94729963E 06	0.49541414E-01
0.10167157E 07	0.50707165E-01
0.10821670E 07	0.51900364E-01
0.11432410E 07	0.53121623E-01
0.11995540E 07	0.54371603E-01
0.12507500E 07	0.55650994E-01
0.12965090E 07	0.56960523E-01
0.13365390E 07	0.58300894E-01
0.13705800E 07	0.59672773E-01
0.13984190E 07	0.61076906E-01
0.14198740E 07	0.62514067E-01
0.14348100E 07	0.63985050E-01

G(λ)/λ	λ
0.14431220E 07	0.65490663E-01
0.14447600E 07	0.67031801E-01
0.14397060E 07	0.68609118E-01
0.14279850E 07	0.70223570E-01
0.14096740E 07	0.71875989E-01
0.13848770E 07	0.73567271E-01
0.13537480E 07	0.75298429E-01
0.13164830E 07	0.77070236E-01
0.12733080E 07	0.78883767E-01
0.12244940E 07	0.80739975E-01
0.11703360E 07	0.82639873E-01
0.11111790E 07	0.84584475E-01
0.10473849E 07	0.86574852E-01
0.97934931E 06	0.88612020E-01
0.90748956E 06	0.90697169E-01
0.83226113E 06	0.92831314E-01
0.75411156E 06	0.95015705E-01
0.67352313E 06	0.97251534E-01
0.59099238E 06	0.99540055E-01
0.50702825E 06	0.10188228E 00
0.42213150E 06	0.10427964E 00
0.33681294E 06	0.10673344E 00
0.25159550E 06	0.10924494E 00
0.16697181E 06	0.11181569E 00
0.83460875E 05	0.11444682E 00
0.15462266E 04	0.11713982E 00
-0.78298125E 05	0.11989623E 00
-0.15560650E 06	0.12271744E 00
-0.22994700E 06	0.12560511E 00
-0.30089594E 06	0.12856084E 00
-0.36805825E 06	0.13158596E 00
-0.43107281E 06	0.13468230E 00
-0.48960588E 06	0.13785148E 00
-0.54335600E 06	0.14109522E 00
-0.59205581E 06	0.14441532E 00
-0.63547588E 06	0.14781368E 00
-0.67341650E 06	0.15129179E 00
-0.70572813E 06	0.15485185E 00
-0.73228981E 06	0.15849560E 00
-0.75302488E 06	0.16222513E 00
-0.76789600E 06	0.16604245E 00
-0.77690575E 06	0.16994971E 00
-0.78009456E 06	0.17394876E 00
-0.77754394E 06	0.17804193E 00
-0.76937294E 06	0.18223137E 00
-0.75573400E 06	0.18651944E 00
-0.73682000E 06	0.19090855E 00
-0.71285513E 06	0.19540077E 00
-0.68409450E 06	0.19999874E 00

NLAM= 100 LAMS= 0.020 LAMF= 0.20000

TEND= 42.470 NXPTS= 100 MUEND= 4.000

MUPTS= 100 IMAXTP= 17 NPTSTP= 6

Table 6.11. Comparison of half lives obtained from the three analysis methods for NH_4NO_3, data set #2 and reported half lives (53-56), (57-59), (60), and (61).

		9.96 m	10.05 m	10.08 m	9.93 m
	$T_{1/2}$	error (%)	error (%)	error (%)	error (%)
FDA Method	10.34	3.81	2.88	2.57	4.12
Iterative Method	11.24	12.85	11.84	11.50	13.19
TLS Method	12.12	21.68	20.59	20.23	22.05

(c) NH_4NO_3 - Data Set #3

Data set No. 3 is tabulated in Table (6.12). By using the FDA method, the data were analyzed for μ_o = 2 and 4; and the results are given in Tables (6.13) and (6.14), respectively. Half lives obtained by FDA method for μ_o = 2 and 4 are 9.9 m and 9.6 m, respectively.

The results of the analysis are tabulated in Table (6.15). Again the results of the FDA are better than the result of others.

Table 6.12. Data set #3 (NH_4NO_3).

Decay Time (min.)	Counts per 4.267 minutes
6.260	29285.000
10.670	23038.098
15.030	17036.797
19.390	13351.898
23.760	11391.398
28.111	8257.500
32.450	6688.500
36.790	5545.398

Table 6.13. Fourier Decay Analysis results for NH_4NO_3, data set #3.

$G(\lambda)/\lambda$	λ
0.16064463E 06	0.20000000E-01
0.18616300E 06	0.20470615E-01
0.21201975E 06	0.20952318E-01
0.23818031E 06	0.21445330E-01
0.26461544E 06	0.21949977E-01
0.29129038E 06	0.22466466E-01
0.31818081E 06	0.22995126E-01
0.34524719E 06	0.23536220E-01
0.37245919E 06	0.24090059E-01
0.39978581E 06	0.24656922E-01
0.42718975E 06	0.25237121E-01
0.45463600E 06	0.25830973E-01
0.48209219E 06	0.26438806E-01
0.50952475E 06	0.27060926E-01
0.53689813E 06	0.27697694E-01
0.56417569E 06	0.28349455E-01
0.59132563E 06	0.29016551E-01
0.61830944E 06	0.29699322E-01
0.64509675E 06	0.30398194E-01
0.67164831E 06	0.31113487E-01
0.69793369E 06	0.31845625E-01
0.72391544E 06	0.32594983E-01
0.74955881E 06	0.33361968E-01
0.77483613E 06	0.34147013E-01
0.79970663E 06	0.34950521E-01
0.82414138E 06	0.35772931E-01
0.84810563E 06	0.36614701E-01
0.87157206E 06	0.37476290E-01
0.89450281E 06	0.38358133E-01
0.91687106E 06	0.39260749E-01
0.93864856E 06	0.40184591E-01
0.95979994E 06	0.41130178E-01
0.98030138E 06	0.42098004E-01
0.10001234E 07	0.43088604E-01
0.10192405E 07	0.44102531E-01
0.10376255E 07	0.45140300E-01
0.10552520E 07	0.46202485E-01
0.10720990E 07	0.47289673E-01
0.10881420E 07	0.48402458E-01
0.11033570E 07	0.49541414E-01
0.11177270E 07	0.50707165E-01
0.11312290E 07	0.51900364E-01
0.11438440E 07	0.53121623E-01
0.11555570E 07	0.54371603E-01
0.11663520E 07	0.55650994E-01
0.11762110E 07	0.56960523E-01
0.11851220E 07	0.58300894E-01
0.11930740E 07	0.59672773E-01
0.12000530E 07	0.61076906E-01
0.12060500E 07	0.62514067E-01
0.12110570E 07	0.63985050E-01

G(λ)/λ	λ
0.12150680E 07	0.65490663E-01
0.12180760E 07	0.67031801E-01
0.12200770E 07	0.68609118E-01
0.12210660E 07	0.70223570E-01
0.12210430E 07	0.71875989E-01
0.12200090E 07	0.73567271E-01
0.12179620E 07	0.75298429E-01
0.12149070E 07	0.77070236E-01
0.12108480E 07	0.78883767E-01
0.12057910E 07	0.80739975E-01
0.11997380E 07	0.82639873E-01
0.11927030E 07	0.84584475E-01
0.11846880E 07	0.86574852E-01
0.11757130E 07	0.88612020E-01
0.11657820E 07	0.90697169E-01
0.11549130E 07	0.92831314E-01
0.11431200E 07	0.95015705E-01
0.11304170E 07	0.97251534E-01
0.11168200E 07	0.99540055E-01
0.11023540E 07	0.10188228E 00
0.10870310E 07	0.10427964E 00
0.10708740E 07	0.10673344E 00
0.10539070E 07	0.10924494E 00
0.10361479E 07	0.11181569E 00
0.10176248E 07	0.11444682E 00
0.99836225E 06	0.11713982E 00
0.97838256E 06	0.11989623E 00
0.95771725E 06	0.12271744E 00
0.93639050E 06	0.12560511E 00
0.91443000E 06	0.12856084E 00
0.89186819E 06	0.13158596E 00
0.86873119E 06	0.13468230E 00
0.84505400E 06	0.13785148E 00
0.82086369E 06	0.14109522E 00
0.79619663E 06	0.14441532E 00
0.77108069E 06	0.14781368E 00
0.74555381E 06	0.15129179E 00
0.71964431E 06	0.15485185E 00
0.69338825E 06	0.15849560E 00
0.66681950E 06	0.16222513E 00
0.63997263E 06	0.16604245E 00
0.61288156E 06	0.16994971E 00
0.58558494E 06	0.17394876E 00
0.55811256E 06	0.17804193E 00
0.53050363E 06	0.18223137E 00
0.50279188E 06	0.18651944E 00
0.47500819E 06	0.19090855E 00
0.44719456E 06	0.19540077E 00
0.41938225E 06	0.19999874E 00

NLAM= 100 LAMS= 0.020 LAMF= 0.20000

TEND= 36.790 NXPTS= 100 MUEND= 2.000

MUPTS= 100 IMAXTP= 8 NPTSTP= 6

Table 6.14. Fourier Decay Analysis results for NH_4NO_3, data set #3.

G(λ)/λ	λ
-0.10871750E 07	0.20000000E-01
-0.12829200E 07	0.20470615E-01
-0.14728000E 07	0.20952318E-01
-0.16552690E 07	0.21445330E-01
-0.18288670E 07	0.21949977E-01
-0.19921140E 07	0.22466466E-01
-0.21436430E 07	0.22995126E-01
-0.22821080E 07	0.23536220E-01
-0.24062550E 07	0.24090059E-01
-0.25149190E 07	0.24656922E-01
-0.26070140E 07	0.25237121E-01
-0.26815700E 07	0.25830973E-01
-0.27377170E 07	0.26438806E-01
-0.27747090E 07	0.27060926E-01
-0.27919240E 07	0.27697694E-01
-0.27888650E 07	0.28349455E-01
-0.27651730E 07	0.29016551E-01
-0.27206240E 07	0.29699322E-01
-0.26551410E 07	0.30398194E-01
-0.25687770E 07	0.31113487E-01
-0.24617390E 07	0.31845625E-01
-0.23343810E 07	0.32594983E-01
-0.21871910E 07	0.33361968E-01
-0.20207990E 07	0.34147013E-01
-0.18359640E 07	0.34950521E-01
-0.16336050E 07	0.35772931E-01
-0.14147260E 07	0.36614701E-01
-0.11804760E 07	0.37476290E-01
-0.93213213E 06	0.38358133E-01
-0.67105175E 06	0.39260749E-01
-0.39868763E 06	0.40184591E-01
-0.11661850E 06	0.41130178E-01
0.17354194E 06	0.42098004E-01
0.47008013E 06	0.43088604E-01
0.77128188E 06	0.44102531E-01
0.10753090E 07	0.45140300E-01
0.13803480E 07	0.46202485E-01
0.16845590E 07	0.47289673E-01
0.19860580E 07	0.48402456E-01
0.22830090E 07	0.49541414E-01
0.25735710E 07	0.50707165E-01
0.28559460E 07	0.51900364E-01
0.31283680E 07	0.53121623E-01
0.33891330E 07	0.54371603E-01
0.36365950E 07	0.55650994E-01
0.38691940E 07	0.56960523E-01
0.40854630E 07	0.58300894E-01
0.42840100E 07	0.59672773E-01
0.44635790E 07	0.61076906E-01
0.46229990E 07	0.62514067E-01
0.47612750E 07	0.63985050E-01

G(λ)/λ	λ
0.48774970E 07	0.65490663E-01
0.49709220E 07	0.67031801E-01
0.50409240E 07	0.68609118E-01
0.50870530E 07	0.70223570E-01
0.51089380E 07	0.71875989E-01
0.51065810E 07	0.73567271E-01
0.50798270E 07	0.75298429E-01
0.50288780E 07	0.77070236E-01
0.49540420E 07	0.78883767E-01
0.48557790E 07	0.80739975E-01
0.47346910E 07	0.82639873E-01
0.45915380E 07	0.84584475E-01
0.44272150E 07	0.86574852E-01
0.42427400E 07	0.88612020E-01
0.40392590E 07	0.90697169E-01
0.38180700E 07	0.92831314E-01
0.35805280E 07	0.95015705E-01
0.33281090E 07	0.97251534E-01
0.30623960E 07	0.99540055E-01
0.27850620E 07	0.10188228E 00
0.24977930E 07	0.10427964E 00
0.22023590E 07	0.10673344E 00
0.19006210E 07	0.10924494E 00
0.15943670E 07	0.11181569E 00
0.12855260E 07	0.11444682E 00
0.97595356E 06	0.11713982E 00
0.66751950E 06	0.11989623E 00
0.36208231E 06	0.12271744E 00
0.61431352E 05	0.12560511E 00
-0.23262919E 06	0.12856084E 00
-0.51837344E 06	0.13158596E 00
-0.79415531E 06	0.13468230E 00
-0.10583960E 07	0.13785148E 00
-0.13096110E 07	0.14109522E 00
-0.15464050E 07	0.14441532E 00
-0.17675040E 07	0.14781368E 00
-0.19717090E 07	0.15129179E 00
-0.21580100E 07	0.15485185E 00
-0.23254590E 07	0.15849560E 00
-0.24732790E 07	0.16222513E 00
-0.26008220E 07	0.16604245E 00
-0.27075900E 07	0.16994971E 00
-0.27932090E 07	0.17394876E 00
-0.28574730E 07	0.17804193E 00
-0.29003090E 07	0.18223137E 00
-0.29217920E 07	0.18651944E 00
-0.29221460E 07	0.19090855E 00
-0.29017320E 07	0.19540077E 00
-0.28610470E 07	0.19999874E 00

NLAM= 100 LAMS= 0.020 LAMF= 0.20000

TEND= 36.790 NXPTS= 100 MUEND= 4.000

MUPTS= 100 IMAXTP= 8 NPTSTP= 6

Table 6.15. Comparison of half lives obtained from the three analysis methods for NH_4NO_3, data set #3 and reported half lives (53-56), (57-59), (60), and (61).

	$T_{1/2}$	9.96 m	10.05 m	10.08 m	9.93 m
		error (%)	error (%)	error (%)	error (%)
FDA Method	9.64	% 3.17	% 4.03	% 4.52	% 2.88
Iterative Method	12.38	%24.28	%23.17	%22.80	%24.66
TLS Method	12.63	%26.84	%25.71	%25.33	%27.23

(d) NH_4NO_3 - Data Set #4

The data in Table (6.16) were used for this analysis. The data are plotted in Fig. (6.2). From this plot there appears to be more than one component in the data. The data were analyzed by FDA for $\mu_o = 3$ and 4. Tables (6.17) and (6.18) are the results of the analysis for $\mu_o = 3$ and 4, respectively. Half-lives obtained by FDA for $\mu_o = 3$ and 4 are 15.7 m and 10.6 m. The big shift in the principal peak is due to the reasons explained at the beginning of the Section 6. For $\mu_o = 5$, error ripples completely masked the results.

The data which looked to fit a straight line (11 points from the beginning of the data) were used for iterative and TLS methods. The results of the analysis are given in Table (6.19).

Table 6.16. Data set #4 (NH_4NO_3).

Decay Time (min.)	Counts per 4.267 minutes
19.000	10323.297
24.100	8314.098
28.750	6390.000
33.500	5014.500
38.200	3810.500
42.850	3127.400
47.600	2341.600
54.100	1828.300
59.150	1448.000
63.850	1165.000
68.550	935.400
73.350	932.700
78.350	735.800
83.000	590.100
87.750	477.900
95.550	403.700
100.200	340.500
104.950	313.400
110.200	217.000
114.000	242.800
119.600	221.400

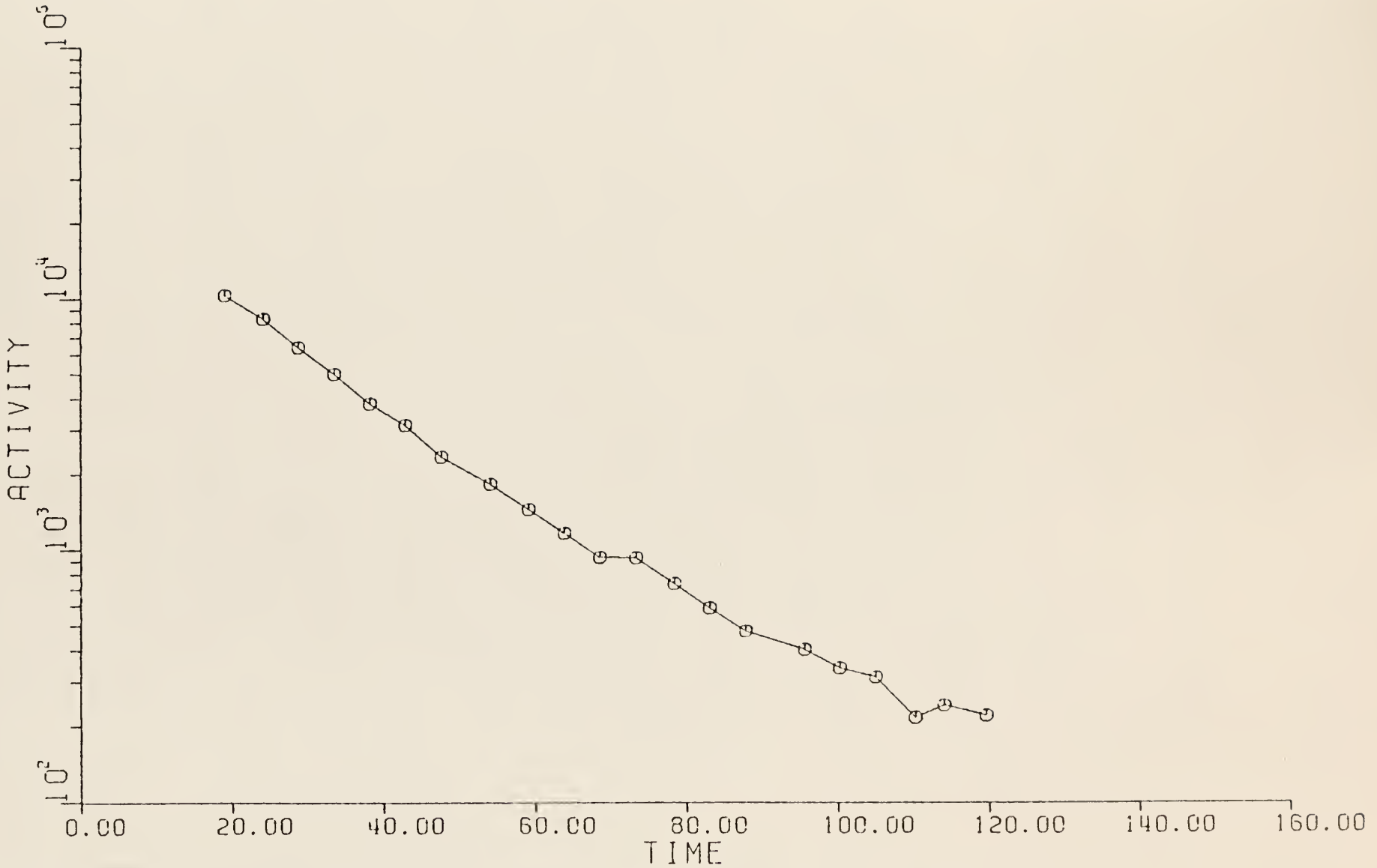

Figure 6.2. A plot of activity (counts, total area of the 0.511 MeV photopeaks, per 4.267 minutes) versus decay time (in minutes) for NH_4NO_3 (Data Set #4).

Table 6.17. Fourier Decay Analysis results for NH_4NO_3, data set #4.

G(λ)/λ	λ
0.10557763E 06	0.20000000E-01
0.10496638E 06	0.20470615E-01
0.22595900E 06	0.20952318E-01
0.28836388E 06	0.21445330E-01
0.35199950E 06	0.21949977E-01
0.41665844E 06	0.22466466E-01
0.48214150E 06	0.22995126E-01
0.54823569E 06	0.23536220E-01
0.61472269E 06	0.24090059E-01
0.68138538E 06	0.24656922E-01
0.74799588E 06	0.25237121E-01
0.81432756E 06	0.25830973E-01
0.88015244E 06	0.26438806E-01
0.94524081E 06	0.27060926E-01
0.10093646E 07	0.27697694E-01
0.10722910E 07	0.28349455E-01
0.11337930E 07	0.29016551E-01
0.11936470E 07	0.29699322E-01
0.12516280E 07	0.30398194E-01
0.13075190E 07	0.31113487E-01
0.13611090E 07	0.31845625E-01
0.14121870E 07	0.32594983E-01
0.14605550E 07	0.33361968E-01
0.15060170E 07	0.34147013E-01
0.15483920E 07	0.34950521E-01
0.15874980E 07	0.35772931E-01
0.16231730E 07	0.36614701E-01
0.16552620E 07	0.37476290E-01
0.16836160E 07	0.38358133E-01
0.17081020E 07	0.39260749E-01
0.17285990E 07	0.40184591E-01
0.17449990E 07	0.41130178E-01
0.17572060E 07	0.42098004E-01
0.17651400E 07	0.43088604E-01
0.17687290E 07	0.44102531E-01
0.17679230E 07	0.45140300E-01
0.17626810E 07	0.46202485E-01
0.17529810E 07	0.47289673E-01
0.17388130E 07	0.48402458E-01
0.17201850E 07	0.49541414E-01
0.16971130E 07	0.50707165E-01
0.16696380E 07	0.51900364E-01
0.16378120E 07	0.53121623E-01
0.16017030E 07	0.54371603E-01
0.15613870E 07	0.55650994E-01
0.15169690E 07	0.56960523E-01
0.14685500E 07	0.58300894E-01
0.14162620E 07	0.59672773E-01
0.13602390E 07	0.61076906E-01
0.13006440E 07	0.62514067E-01
0.12376270E 07	0.63985050E-01

G(λ)/λ	λ
0.11713730E 07	0.65490663E-01
0.11020630E 07	0.67031801E-01
0.10299061E 07	0.68609118E-01
0.95510300E 06	0.70223570E-01
0.87788069E 06	0.71875989E-01
0.79846519E 06	0.73567271E-01
0.71709056E 06	0.75298429E-01
0.63400113E 06	0.77070236E-01
0.54944625E 06	0.78883767E-01
0.46368081E 06	0.80739575E-01
0.37696106E 06	0.82639873E-01
0.28955700E 06	0.84584475E-01
0.20173113E 06	0.86574852E-01
0.11375225E 06	0.88612020E-01
0.25885441E 05	0.90697169E-01
-0.61590527E 05	0.92831314E-01
-0.14841825E 06	0.95015705E-01
-0.23433263E 06	0.97251534E-01
-0.31906731E 06	0.99540055E-01
-0.40235581E 06	0.10188228E 00
-0.48395650E 06	0.10427964E 00
-0.56362088E 06	0.10673344E 00
-0.64109819E 06	0.10924494E 00
-0.71616938E 06	0.11181569E 00
-0.78859375E 06	0.11444682E 00
-0.85816263E 06	0.11713982E 00
-0.92466744E 06	0.11989623E 00
-0.98791056E 06	0.12271744E 00
-0.10477178E 07	0.12560511E 00
-0.11039060E 07	0.12856084E 00
-0.11563190E 07	0.13158596E 00
-0.12048090E 07	0.13468230E 00
-0.12492450E 07	0.13785148E 00
-0.12895060E 07	0.14109522E 00
-0.13254900E 07	0.14441532E 00
-0.13571070E 07	0.14781368E 00
-0.13842800E 07	0.15129179E 00
-0.14069540E 07	0.15485185E 00
-0.14250850E 07	0.15849560E 00
-0.14386430E 07	0.16222513E 00
-0.14476180E 07	0.16604245E 00
-0.14520130E 07	0.16994971E 00
-0.14518490E 07	0.17394876E 00
-0.14471600E 07	0.17804193E 00
-0.14379980E 07	0.18223137E 00
-0.14244290E 07	0.18651944E 00
-0.14065310E 07	0.19090855E 00
-0.13844020E 07	0.19540077E 00
-0.13581510E 07	0.19999874E 00

NLAM= 100 LAMS= 0.020 LAMF= 0.20000

TEND= 119.600 NXPTS= 100 MUEND= 3.000

MUPTS= 100 IMAXTP= 21 NPTSTP= 6

Table 6.18. Fourier Decay Analysis results for NH_4NO_3, data set #4.

G(λ)/λ	λ
-0.12968038E 06	0.20000000E-01
-0.21684294E 06	0.20470615E-01
-0.30125813E 06	0.20952318E-01
-0.38202250E 06	0.21445330E-01
-0.45828194E 06	0.21949977E-01
-0.52916669E 06	0.22466466E-01
-0.59387019E 06	0.22995126E-01
-0.65159156E 06	0.23536220E-01
-0.70159394E 06	0.24090059E-01
-0.74317606E 06	0.24656922E-01
-0.77570319E 06	0.25237121E-01
-0.79859319E 06	0.25830973E-01
-0.81134275E 06	0.26438806E-01
-0.81350981E 06	0.27060926E-01
-0.80473750E 06	0.27697694E-01
-0.78474700E 06	0.28349455E-01
-0.75334731E 06	0.29016551E-01
-0.71043181E 06	0.29699322E-01
-0.65599000E 06	0.30398194E-01
-0.59009663E 06	0.31113487E-01
-0.51291825E 06	0.31845625E-01
-0.42473019E 06	0.32594983E-01
-0.32588069E 06	0.33361968E-01
-0.21681988E 06	0.34147013E-01
-0.98080688E 05	0.34950521E-01
0.29697320E 05	0.35772931E-01
0.16582063E 06	0.36614701E-01
0.30950681E 06	0.37476290E-01
0.45987825E 06	0.38358133E-01
0.61600994E 06	0.39260749E-01
0.77691594E 06	0.40184591E-01
0.94152706E 06	0.41130178E-01
0.11087480E 07	0.42098004E-01
0.12774310E 07	0.43088604E-01
0.14464130E 07	0.44102531E-01
0.16144640E 07	0.45140300E-01
0.17803730E 07	0.46202485E-01
0.19429090E 07	0.47289673E-01
0.21008200E 07	0.48402458E-01
0.22528950E 07	0.49541414E-01
0.23979190E 07	0.50707165E-01
0.25347110E 07	0.51900364E-01
0.26621240E 07	0.53121623E-01
0.27790570E 07	0.54371603E-01
0.28844590E 07	0.55650994E-01
0.29773420E 07	0.56960523E-01
0.30567910E 07	0.58300894E-01
0.31219520E 07	0.59672773E-01
0.31720780E 07	0.61076906E-01
0.32064880E 07	0.62514067E-01
0.32246200E 07	0.63985050E-01

Table 6.18, cont'd.

G(λ)/λ	λ
0.32259950E 07	0.65490663E-01
0.32102480E 07	0.67031801E-01
0.31771230E 07	0.68609118E-01
0.31264710E 07	0.70223570E-01
0.30582710E 07	0.71875989E-01
0.29726050E 07	0.73567271E-01
0.28696830E 07	0.75293429E-01
0.27498240E 07	0.77070236E-01
0.26134690E 07	0.78883767E-01
0.24611690E 07	0.80739975E-01
0.22935820E 07	0.82639873E-01
0.21114970E 07	0.84584475E-01
0.19157850E 07	0.86574852E-01
0.17074230E 07	0.88612020E-01
0.14874740E 07	0.90697169E-01
0.12571210E 07	0.92831314E-01
0.10175780E 07	0.95015705E-01
0.77015188E 06	0.97251534E-01
0.51622900E 06	0.99540055E-01
0.25725950E 06	0.10188228E 00
-0.53138438E 04	0.10427964E 00
-0.26997719E 06	0.10673344E 00
-0.53515988E 06	0.10924494E 00
-0.79936031E 06	0.11181569E 00
-0.10609630E 07	0.11444682E 00
-0.13184360E 07	0.11713982E 00
-0.15702350E 07	0.11989623E 00
-0.18148320E 07	0.12271744E 00
-0.20507800E 07	0.12560511E 00
-0.22766190E 07	0.12856084E 00
-0.24909650E 07	0.13158596E 00
-0.26925110E 07	0.13468230E 00
-0.28800180E 07	0.13785148E 00
-0.30523290E 07	0.14109522E 00
-0.32083780E 07	0.14441532E 00
-0.33472040E 07	0.14781368E 00
-0.34679260E 07	0.15129179E 00
-0.35698140E 07	0.15485185E 00
-0.36522210E 07	0.15849560E 00
-0.37146380E 07	0.16222513E 00
-0.37566770E 07	0.16604245E 00
-0.37780820E 07	0.16994971E 00
-0.37787170E 07	0.17394876E 00
-0.37585900E 07	0.17804193E 00
-0.37178290E 07	0.18223137E 00
-0.36567030E 07	0.18651944E 00
-0.35755990E 07	0.19090855E 00
-0.34750460E 07	0.19540077E 00
-0.33556840E 07	0.19999874E 00

NLAM= 100 LAMS= 0.020 LAMF= 0.20000

TEND= 119.600 NXPTS= 100 MUEND= 4.000

MUPTS= 100 IMAXTP= 21 NPTSTP= 6

(e) NH_4NO_3 - Data set #5

Data set #5 are given in Table (6.20). The data are plotted in Fig. (6.3). As seen a lot of scatter exists in the data. The data were analyzed by FDA for μ_o = 2 and 4. Tables (6.21) and (6.22) are the results obtained by FDA for μ_o = 2 and 4, respectively. Half lives obtained by FDA for μ_o = 2 and 4 were 14.0 m and 9.2 m.

Again the data were analyzed by the iterative and TLS methods. For the iterative and TLS methods the first twelve data points were used. The results of the analysis of the data by the three methods are tabulated in Table (6.23).

Table 6.19. Comparison of half lives obtained from the three analysis methods for NH_4NO_3 data set #4 and reported half lives (53-56), (57-59), (60), and (61).

	$T_{1/2}$	9.96 m	10.05 m	10.08 m	9.93 m
		error (%)	error (%)	error (%)	error (%)
FDA Method	10.58	6.22	5.27	4.96	6.54
Iterative Method	11.18	12.24	11.24	10.91	12.58
TLS Method	14.18	42.36	41.09	40.67	42.79

Table 6.20. Data set #5 (NH_4NO_3)

Decay Time (min.)	Counts per 4.267 minutes
14.150	17859.500
18.950	13645.898
23.650	10285.297
28.600	7860.199
33.450	6230.000
39.100	4433.797
44.950	3747.200
48.800	2951.100
53.550	2208.100
59.150	1753.700
64.250	1518.600
69.160	1054.500
73.950	1074.100
79.150	928.800
83.850	646.300
88.550	540.500
93.300	524.500
98.150	381.000
103.000	484.000
108.150	298.000
112.900	283.200
117.800	253.500
122.550	297.900

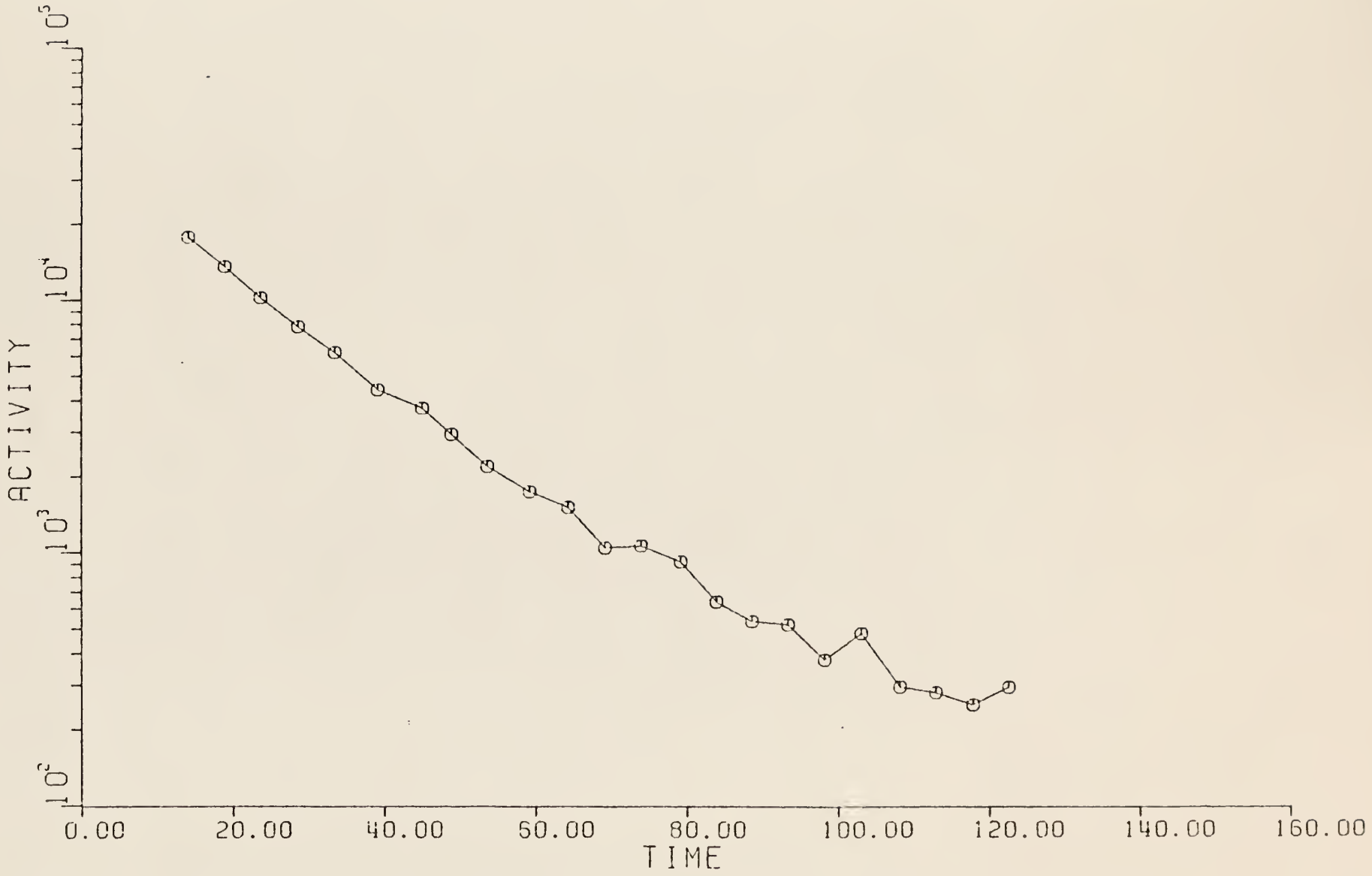

Figure 6.3. A plot of activity (counts, total area of the 0.511 MeV photopeaks, per 4.267 minutes) versus decay time (in minutes) for NH_4NO_3 (Data Set #5).

Table 6.21. Fourier Decay Analysis results for NH_4NO_3, data set #5.

G(λ)/λ	λ
0.58511156E 06	0.20000000E-01
0.60732356E 06	0.20470615E-01
0.62937481E 06	0.20952318E-01
0.65123950E 06	0.21445330E-01
0.67289381E 06	0.21949977E-01
0.69430556E 06	0.22466466E-01
0.71545381E 06	0.22995126E-01
0.73630531E 06	0.23536220E-01
0.75683950E 06	0.24090059E-01
0.77702513E 06	0.24656922E-01
0.79684150E 06	0.25237121E-01
0.81625681E 06	0.25830973E-01
0.83525100E 06	0.26438806E-01
0.85380019E 06	0.27060926E-01
0.87187513E 06	0.27697694E-01
0.88945631E 06	0.28349455E-01
0.90651931E 06	0.29016551E-01
0.92304219E 06	0.29699322E-01
0.93900000E 06	0.30398194E-01
0.95437725E 06	0.31113487E-01
0.96914906E 06	0.31845625E-01
0.98329794E 06	0.32594983E-01
0.99680256E 06	0.33361968E-01
0.10096460E 07	0.34147013E-01
0.10218093E 07	0.34950521E-01
0.10332768E 07	0.35772931E-01
0.10440340E 07	0.36614701E-01
0.10540630E 07	0.37476296E-01
0.10633540E 07	0.38358133E-01
0.10718910E 07	0.39260749E-01
0.10796630E 07	0.40184591E-01
0.10866560E 07	0.41130178E-01
0.10928650E 07	0.42098004E-01
0.10982760E 07	0.43088604E-01
0.11028830E 07	0.44102531E-01
0.11066800E 07	0.45140300E-01
0.11096610E 07	0.46202485E-01
0.11118180E 07	0.47289673E-01
0.11131480E 07	0.48402458E-01
0.11136500E 07	0.49541414E-01
0.11133230E 07	0.50707165E-01
0.11121630E 07	0.51900364E-01
0.11101720E 07	0.53121623E-01
0.11073520E 07	0.54371603E-01
0.11037070E 07	0.55650994E-01
0.10992360E 07	0.56960523E-01
0.10939490E 07	0.58300894E-01
0.10878480E 07	0.59672773E-01
0.10809410E 07	0.61076906E-01
0.10732380E 07	0.62514067E-01
0.10647460E 07	0.63985050E-01

G(λ)/λ	λ
0.10554750E 07	0.65490663E-01
0.10454365E 07	0.67031801E-01
0.10346419E 07	0.68609118E-01
0.10231026E 07	0.70223570E-01
0.10108378E 07	0.71875989E-01
0.99785775E 06	0.73567271E-01
0.98418094E 06	0.75298429E-01
0.96982006E 06	0.77070236E-01
0.95479900E 06	0.78883767E-01
0.93912989E 06	0.80739975E-01
0.92283494E 06	0.82639873E-01
0.90593238E 06	0.84584475E-01
0.88844794E 06	0.86574852E-01
0.87039750E 06	0.88612020E-01
0.85180538E 06	0.90697169E-01
0.83269431E 06	0.92831314E-01
0.81308994E 06	0.95015705E-01
0.79301163E 06	0.97251534E-01
0.77248569E 06	0.99540055E-01
0.75154219E 06	0.10188228E 00
0.73020206E 06	0.10427964E 00
0.70848756E 06	0.10673344E 00
0.68643569E 06	0.10924494E 00
0.66406106E 06	0.11181569E 00
0.64140088E 06	0.11444682E 00
0.61847813E 06	0.11713982E 00
0.59532106E 06	0.11989623E 00
0.57196000E 06	0.12271744E 00
0.54841619E 06	0.12560511E 00
0.52472313E 06	0.12856084E 00
0.50090906E 06	0.13158596E 00
0.47700206E 06	0.13468230E 00
0.45302588E 06	0.13785148E 00
0.42901781E 06	0.14109522E 00
0.40499975E 06	0.14441532E 00
0.38099756E 06	0.14781368E 00
0.35704506E 06	0.15129179E 00
0.33316406E 06	0.15485185E 00
0.30938688E 06	0.15849560E 00
0.28573831E 06	0.16222513E 00
0.26224631E 06	0.16604245E 00
0.23893425E 06	0.16994971E 00
0.21583100E 06	0.17394876E 00
0.19296094E 06	0.17804193E 00
0.17034906E 06	0.18223137E 00
0.14802275E 06	0.18651944E 00
0.12599919E 06	0.19090855E 00
0.10431025E 06	0.19540077E 00
0.82972938E 05	0.19999874E 00

NLAM= 100 LAMS= 0.020 LAMF= 0.20000

TEND= 122.550 NXPTS= 100 MUEND= 2.000

MUPTS= 100 IMAXTP= 23 NPTSTP= 6

Table 6.22. Fourier Decay Analysis results for NH_4NO_3, data set #5.

G(λ)/λ	λ
0.48506075E 06	0.20000000E-01
0.51785844E 06	0.20470615E-01
0.54975181E 06	0.20952318E-01
0.58067119E 06	0.21445330E-01
0.61056331E 06	0.21949977E-01
0.63937900E 06	0.22466466E-01
0.66708438E 06	0.22995126E-01
0.69365625E 06	0.23536220E-01
0.71908125E 06	0.24090059E-01
0.74335938E 06	0.24656922E-01
0.76649794E 06	0.25237121E-01
0.78851513E 06	0.25830973E-01
0.80944213E 06	0.26438806E-01
0.82931769E 06	0.27060926E-01
0.84819094E 06	0.27697694E-01
0.86611306E 06	0.28349455E-01
0.88314775E 06	0.29016551E-01
0.89936375E 06	0.29699322E-01
0.91483744E 06	0.30398194E-01
0.92964456E 06	0.31113487E-01
0.94386506E 06	0.31845625E-01
0.95758450E 06	0.32594983E-01
0.97089081E 06	0.33361968E-01
0.98386263E 06	0.34147013E-01
0.99658956E 06	0.34950521E-01
0.10091485E 07	0.35772931E-01
0.10216228E 07	0.36614701E-01
0.10340859E 07	0.37476290E-01
0.10466038E 07	0.38358133E-01
0.10592430E 07	0.39260749E-01
0.10720580E 07	0.40184591E-01
0.10850980E 07	0.41130178E-01
0.10983990E 07	0.42098004E-01
0.11119940E 07	0.43088604E-01
0.11259000E 07	0.44102531E-01
0.11401240E 07	0.45140300E-01
0.11546670E 07	0.46202485E-01
0.11695150E 07	0.47289673E-01
0.11846360E 07	0.48402458E-01
0.11999990E 07	0.49541414E-01
0.12155510E 07	0.50707165E-01
0.12312340E 07	0.51900364E-01
0.12469680E 07	0.53121623E-01
0.12626760E 07	0.54371603E-01
0.12782600E 07	0.55650994E-01
0.12936150E 07	0.56960523E-01
0.13086260E 07	0.58300894E-01
0.13231710E 07	0.59672773E-01
0.13371120E 07	0.61076906E-01
0.13503130E 07	0.62514067E-01
0.13626340E 07	0.63985050E-01

Table 6.22, cont'd.

$G(\lambda)/\lambda$	λ
0.13739170E 07	0.65490663E-01
0.13840120E 07	0.67031801E-01
0.13927640E 07	0.68609118E-01
0.14000090E 07	0.70223570E-01
0.14055970E 07	0.71875985E-01
0.14093660E 07	0.73567271E-01
0.14111640E 07	0.75298429E-01
0.14108410E 07	0.77070236E-01
0.14082530E 07	0.78883767E-01
0.14032650E 07	0.80739575E-01
0.13957430E 07	0.82639873E-01
0.13855740E 07	0.84584475E-01
0.13726460E 07	0.86574852E-01
0.13568640E 07	0.88612020E-01
0.13381400E 07	0.90697169E-01
0.13164110E 07	0.92831314E-01
0.12916200E 07	0.95015705E-01
0.12637260E 07	0.97251534E-01
0.12327150E 07	0.99540055E-01
0.11985810E 07	0.10188228E 00
0.11613370E 07	0.10427964E 00
0.11210160E 07	0.10673344E 00
0.10776760E 07	0.10924494E 00
0.10313796E 07	0.11181569E 00
0.98222169E 06	0.11444682E 00
0.93031075E 06	0.11713982E 00
0.87577694E 06	0.11989623E 00
0.81876444E 06	0.12271744E 00
0.75943338E 06	0.12560511E 00
0.69796650E 06	0.12856084E 00
0.63456775E 06	0.13158596E 00
0.56944563E 06	0.13468230E 00
0.50282688E 06	0.13785148E 00
0.43495075E 06	0.14109522E 00
0.36606975E 06	0.14441532E 00
0.29644619E 06	0.14781368E 00
0.22635938E 06	0.15129179E 00
0.15607556E 06	0.15485185E 00
0.85892000E 05	0.15849560E 00
0.16096063E 05	0.16222513E 00
-0.53022238E 05	0.16604245E 00
-0.12117063E 06	0.16994971E 00
-0.18805200E 06	0.17394876E 00
-0.25337919E 06	0.17804193E 00
-0.31686788E 06	0.18223137E 00
-0.37823781E 06	0.18651944E 00
-0.43722350E 06	0.19090855E 00
-0.49355963E 06	0.19540077E 00
-0.54699938E 06	0.19999874E 00

NLAM= 100 LAMS= 0.020 LAMF= 0.20000

TEND= 122.550 NXPTS= 100 MUEND= 4.000

MUPTS= 100 IMAXTP= 23 NPTSTP= 6

Table 6.23. Comparison of half lives obtained from the three analysis methods for NH_4NO_3 data set #5 and reported half lives (53-56), (57-59), (60), and (61).

	$T_{1/2}$	9.96 m	10.05 m	10.08 m	9.93 m
		error (%)	error (%)	error (%)	error (%)
FDA Method	9.21	7.57	8.39	8.67	7.29
Iterative Method	11.19	12.31	11.31	10.97	12.65
TLS Method	12.98	30.29	29.12	28.24	30.68

(f) NH_4NO_3 - Data Set #6

Data set #6 is given in Table (6.24). The data are plotted in Fig. (6.4). Again a lot of scatter is observed in the data. The data were analyzed by FDA method for μ_o = 2 and 4. Tables (6.25) and (6.26) are the results obtained by FDA for μ_o = 2 and 4, respectively. Half lives obtained by FDA method for μ_o = 2 and 4 are, 12.7 m and 11.0 m, respectively. For μ_o = 5 the error ripples completely masked the results.

Because of the scatter in the data, the data were smoothed by ignoring very bad points. Then the smoothed data (Table (6.27)) were analyzed by FDA for μ_o = 2 and 4. Tables (6.28) and (6.29) are the results for μ_o = 2 and 4, respectively. Half lives obtained by FDA method for μ_o = 2 and 4 are, 12.7 m and 10.8 m, respectively.

By using the first eight points of the beginning of Table (6.24) the data were analyzed by the iterative and TLS methods. Results of the analysis by the different methods are tabulated in Table (6.30).

Table 6.24. Data set #6 (NH_4NO_3)

Decay Time (min.)	Counts per 8.533 minutes
3.500	51539.297
13.300	28699.699
22.500	16791.898
32.400	9926.898
41.450	6235.598
50.750	4173.699
59.900	2708.800
68.900	1700.800
78.400	1525.000
87.400	1077.300
96.400	860.500
105.800	769.500
114.700	521.400
123.900	365.900
132.900	484.600
142.000	401.500
151.000	249.200
160.300	329.700
169.700	201.000
179.000	264.900
189.000	270.400
198.000	223.700
207.000	185.600

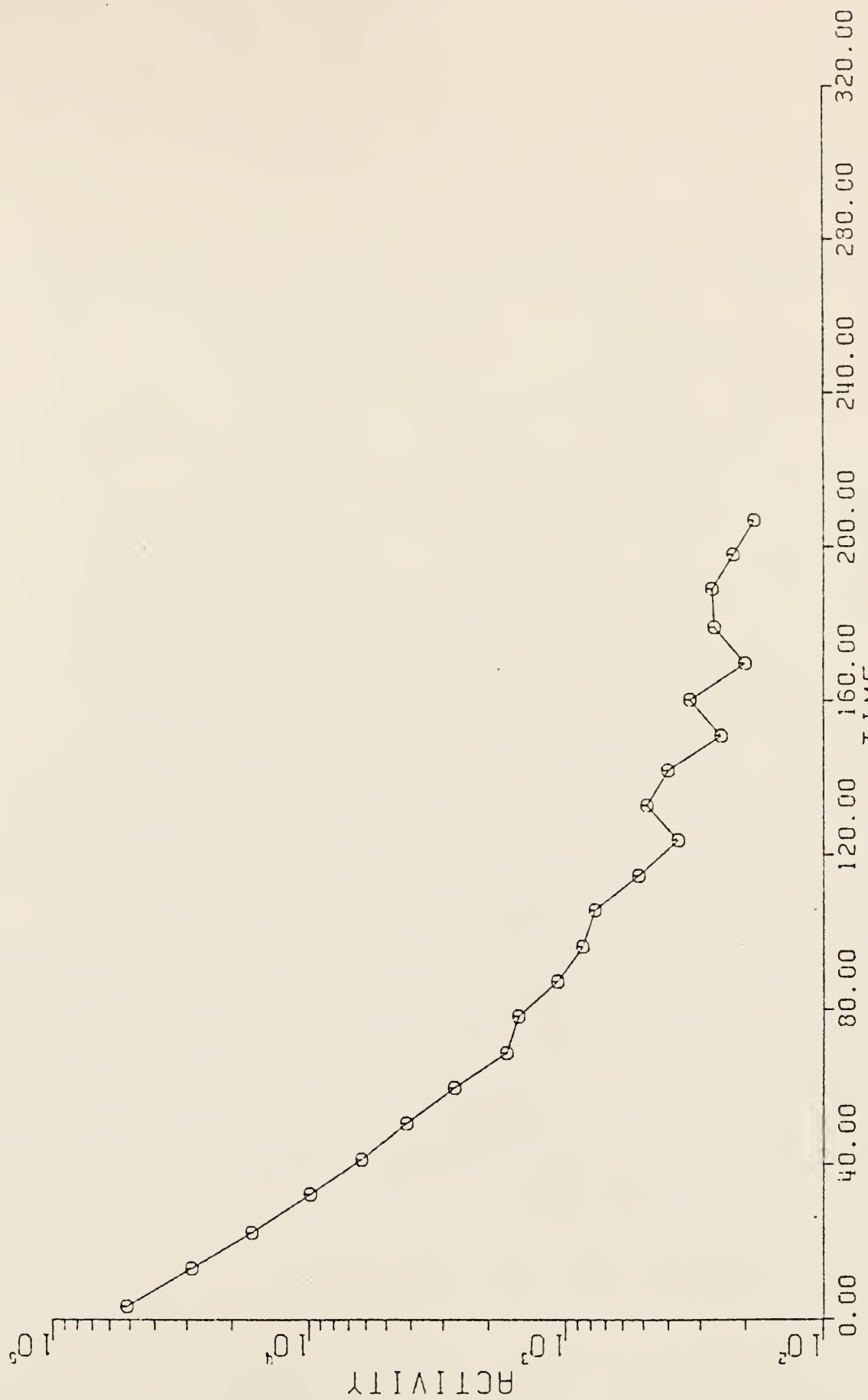

Figure 6.4. A plot of activity (counts, total area of the 0.511 MeV photopeaks, per 8.533 minutes) versus decay time (in minutes) for NH_4NO_3 (Data Set #6).

Table 6.25. Fourier Decay Analysis results for NH_4NO_3, data set #6.

G(λ)/λ	λ
0.83958513E 06	0.20000000E-01
0.86778006E 06	0.20470615E-01
0.89585788E 06	0.20952318E-01
0.92378000E 06	0.21445330E-01
0.95152294E 06	0.21949977E-01
0.97904688E 06	0.22466466E-01
0.10063276E 07	0.22995126E-01
0.10333328E 07	0.23536220E-01
0.10600250E 07	0.24090059E-01
0.10863810E 07	0.24656922E-01
0.11123660E 07	0.25237121E-01
0.11379510E 07	0.25830973E-01
0.11631070E 07	0.26438806E-01
0.11878000E 07	0.27060926E-01
0.12120020E 07	0.27697694E-01
0.12356890E 07	0.28349455E-01
0.12588270E 07	0.29016551E-01
0.12813890E 07	0.29699322E-01
0.13033490E 07	0.30398194E-01
0.13246800E 07	0.31113487E-01
0.13453540E 07	0.31845625E-01
0.13653500E 07	0.32594983E-01
0.13846370E 07	0.33361968E-01
0.14031940E 07	0.34147013E-01
0.14210010E 07	0.34950521E-01
0.14380340E 07	0.35772931E-01
0.14542660E 07	0.36614701E-01
0.14696860E 07	0.37476290E-01
0.14842670E 07	0.38358133E-01
0.14979930E 07	0.39260749E-01
0.15108470E 07	0.40184591E-01
0.15228100E 07	0.41130178E-01
0.15338690E 07	0.42098004E-01
0.15440080E 07	0.43088604E-01
0.15532120E 07	0.44102531E-01
0.15614730E 07	0.45140300E-01
0.15687780E 07	0.46202485E-01
0.15751140E 07	0.47289673E-01
0.15804760E 07	0.48402458E-01
0.15848560E 07	0.49541414E-01
0.15882430E 07	0.50707165E-01
0.15906380E 07	0.51900364E-01
0.15920310E 07	0.53121623E-01
0.15924260E 07	0.54371603E-01
0.15918110E 07	0.55650994E-01
0.15901980E 07	0.56960523E-01
0.15875780E 07	0.58300894E-01
0.15839590E 07	0.59672773E-01
0.15793420E 07	0.61076906E-01
0.15737280E 07	0.62514067E-01
0.15671300E 07	0.63985050E-01

Table 6.25, cont'd.

G(λ)/λ	λ
0.15595510E 07	0.65490663E-01
0.15509970E 07	0.67031801E-01
0.15414780E 07	0.68609118E-01
0.15310080E 07	0.70223570E-01
0.15195950E 07	0.71875989E-01
0.15072540E 07	0.73567271E-01
0.14939990E 07	0.75298429E-01
0.14798420E 07	0.77070236E-01
0.14648040E 07	0.78883767E-01
0.14488980E 07	0.80739975E-01
0.14321400E 07	0.82639873E-01
0.14145570E 07	0.84584475E-01
0.13961630E 07	0.86574852E-01
0.13769810E 07	0.88612020E-01
0.13570330E 07	0.90697169E-01
0.13363420E 07	0.92831314E-01
0.13149320E 07	0.95015705E-01
0.12928260E 07	0.97251534E-01
0.12700510E 07	0.99540055E-01
0.12466350E 07	0.10188228E 00
0.12226030E 07	0.10427964E 00
0.11979790E 07	0.10673344E 00
0.11727980E 07	0.10924494E 00
0.11470800E 07	0.11181569E 00
0.11208660E 07	0.11444682E 00
0.10941760E 07	0.11713982E 00
0.10670460E 07	0.11989623E 00
0.10395044E 07	0.12271744E 00
0.10115817E 07	0.12560511E 00
0.98330875E 06	0.12856084E 00
0.95472194E 06	0.13158596E 00
0.92585063E 06	0.13468230E 00
0.89672463E 06	0.13785148E 00
0.86737706E 06	0.14109522E 00
0.83784269E 06	0.14441532E 00
0.80815231E 06	0.14781368E 00
0.77834419E 06	0.15129179E 00
0.74844119E 06	0.15485185E 00
0.71848094E 06	0.15849560E 00
0.68849613E 06	0.16222513E 00
0.65851800E 06	0.16604245E 00
0.62857713E 06	0.16994971E 00
0.59870913E 06	0.17394876E 00
0.56894238E 06	0.17804193E 00
0.53930744E 06	0.18223137E 00
0.50983763E 06	0.18651944E 00
0.48056113E 06	0.19090855E 00
0.45150738E 06	0.19540077E 00
0.42270856E 06	0.19999874E 00

NLAM= 100 LAMS= 0.020 LAMF= 0.20000

TEND= 207.000 NXPTS= 100 MUEND= 2.000

MUPTS= 100 IMAXTP= 23 NPTSTP= 6

Table 6.26. Fourier Decay Analysis results for NH_4NO_3, data set #6.

G(λ)/λ	λ
-0.973900000E 05	0.20000000E-01
-0.127063C6E 06	0.20470615E-01
-0.151676B8E 06	0.20952318E-01
-0.170848C5E 06	0.21445330E-01
-0.184234B1E 06	0.21949977E-01
-0.191523C0E 06	0.22465466E-01
-0.192444C1E 06	0.22995126E-01
-0.186770C0E 06	0.23536220E-01
-0.174312C6E 06	0.24090059E-01
-0.154929C9E 06	0.24656922E-01
-0.128528C0E 06	0.25237121E-01
-0.950600C0E 05	0.25830973E-01
-0.545298C6E 05	0.26438806E-01
-0.698501C7E 04	0.27060926E-01
0.474764C6E 05	0.27697694E-01
0.108707C3E 06	0.28349455E-01
0.176507C6E 06	0.29016551E-01
0.250636C9E 06	0.29699322E-01
0.330800C4E 06	0.30398194E-01
0.416673C5E 06	0.31113487E-01
0.507876C5E 06	0.31845625E-01
0.603984C9E 06	0.32594983E-01
0.704552C0E 06	0.33361968E-01
0.809081C1E 06	0.34147013E-01
0.917061C3E 06	0.34950521E-01
0.102792C5E 07	0.35772931E-01
0.114110C0E 07	0.36614701E-01
0.125601C0E 07	0.37476290E-01
0.137201C0E 07	0.38358133E-01
0.148849C0E 07	0.39260749E-01
0.160480C0E 07	0.40184591E-01
0.172029C0E 07	0.41130178E-01
0.183431C0E 07	0.42098004E-01
0.194623C0E 07	0.43088604E-01
0.205540C0E 07	0.44102531E-01
0.216121C0E 07	0.45140300E-01
0.226302C0E 07	0.46202485E-01
0.236027C0E 07	0.47289673E-01
0.245236C0E 07	0.48402458E-01
0.253876C0E 07	0.49541414E-01
0.261897C0E 07	0.50707165E-01
0.269249C0E 07	0.51900364E-01
0.275889C0E 07	0.53121623E-01
0.281777C0E 07	0.54371603E-01
0.286877C0E 07	0.55650994E-01
0.291157C0E 07	0.56960523E-01
0.294591C0E 07	0.58300894E-01
0.297157C0E 07	0.59672773E-01
0.298838C0E 07	0.61076906E-01
0.299622C0E 07	0.62514067E-01
0.299502C0E 07	0.63985050E-01

Table 6.26, cont'd.

$G(\lambda)/\lambda$	λ
0.29847930E 07	0.65490663E-01
0.29655460E 07	0.67031801E-01
0.29373850E 07	0.68609118E-01
0.29004450E 07	0.70223570E-01
0.28549250E 07	0.71875989E-01
0.28010660E 07	0.73567271E-01
0.27391540E 07	0.75298429E-01
0.26695250E 07	0.77070236E-01
0.25925550E 07	0.78883767E-01
0.25086620E 07	0.80739975E-01
0.24182940E 07	0.82639873E-01
0.23219500E 07	0.84584475E-01
0.22201480E 07	0.86574852E-01
0.21134350E 07	0.88612020E-01
0.20023770E 07	0.90697169E-01
0.18875860E 07	0.92831314E-01
0.17696550E 07	0.95015705E-01
0.16492040E 07	0.97251534E-01
0.15268690E 07	0.99540055E-01
0.14032950E 07	0.10188228E 00
0.12791020E 07	0.10427964E 00
0.11549170E 07	0.10673344E 00
0.10313831E 07	0.10924494E 00
0.90908494E 06	0.11181569E 00
0.78864150E 06	0.11444682E 00
0.67061981E 06	0.11713982E 00
0.55557081E 06	0.11989623E 00
0.44402800E 06	0.12271744E 00
0.33647588E 06	0.12560511E 00
0.23339100E 06	0.12856084E 00
0.13520400E 06	0.13158596E 00
0.42304324E 05	0.13468230E 00
-0.44952723E 05	0.13785148E 00
-0.12625581E 06	0.14109522E 00
-0.20133725E 06	0.14441532E 00
-0.26997131E 06	0.14781368E 00
-0.33197119E 06	0.15129179E 00
-0.38721031E 06	0.15485185E 00
-0.43559475E 06	0.15849560E 00
-0.47708231E 06	0.16222513E 00
-0.51167525E 06	0.16604245E 00
-0.53942331E 06	0.16994971E 00
-0.56040944E 06	0.17394876E 00
-0.57477413E 06	0.17804193E 00
-0.58268831E 06	0.18223137E 00
-0.58436131E 06	0.18651944E 00
-0.58004919E 06	0.19090855E 00
-0.57002975E 06	0.19540077E 00
-0.55462450E 06	0.19999874E 00

NLAM= 100 LAMS= 0.020 LAMF= 0.20000

TEND= 207.000 NXPTS= 100 MUEND= 4.000

MUPTS= 100 IMAXTP= 23 NPTSTP= 6

Table 6.27. Data set #6 (smoothed, NH_4NO_3)

Decay Time (min.)	Counts per 8.533 minutes
3.500	51539.297
13.300	28699.699
22.500	16791.898
32.400	9926.989
41.450	6235.598
50.750	4173.699
59.900	2708.800
68.900	1700.800
78.400	1525.000
87.400	1077.300
96.400	860.500
105.800	769.500
114.700	521.400
123.900	365.900
151.000	249.200
169.700	201.000
207.000	185.600

Table 6.28. Fourier Decay Analysis results for NH_4NO_3, smoothed set #6.

G(λ)/λ	λ
0.84316769E 06	0.2000000CE-01
0.87211638E 06	0.20470615E-01
0.90093169E 06	0.2095231 8E-01
0.92957831E 06	0.21445330E-01
0.95803019E 06	0.21949977E-01
0.98624581E 06	0.22466466E-01
0.10142036E 07	0.22995126E-01
0.10418651E 07	0.23536220E-01
0.10691980E 07	0.24090059E-01
0.10961750E 07	0.24656922E-01
0.11227580E 07	0.25237121E-01
0.11489200E 07	0.25830973E-01
0.11746270E 07	0.26438806E-01
0.11998570E 07	0.27060926E-01
0.12245710E 07	0.27697694E-01
0.12487430E 07	0.28349455E-01
0.12723420E 07	0.29016551E-01
0.12953410E 07	0.29699322E-01
0.13177110E 07	0.30398194E-01
0.13394280E 07	0.31113487E-01
0.13604610E 07	0.31845625E-01
0.13807890E 07	0.32594983E-01
0.14003820E 07	0.33361968E-01
0.14192210E 07	0.34147013E-01
0.14372770E 07	0.34950521E-01
0.14545330E 07	0.3577293 1E-01
0.14709650E 07	0.36614701E-01
0.14865510E 07	0.3747629CE-01
0.15012730E 07	0.38358133E-01
0.15151120E 07	0.3926074 9E-01
0.15280500E 07	0.40184591E-01
0.15400710E 07	0.41130178E-01
0.15511590E 07	0.42098004E-01
0.15612990E 07	0.43088604E-01
0.15704820E 07	0.44102531E-01
0.15786910E 07	0.4514030CE-01
0.15859180E 07	0.46202485E-01
0.15921500E 07	0.47289673E-01
0.15973820E 07	0.48402458E-01
0.16016050E 07	0.49541414E-01
0.16048140E 07	0.50707165E-01
0.16070030E 07	0.51900364E-01
0.16081700E 07	0.53121623E-01
0.16083120E 07	0.54371603E-01
0.16074250E 07	0.55650994E-01
0.16055130E 07	0.56960523E-01
0.16025770E 07	0.58300894E-01
0.15986190E 07	0.59672773E-01
0.15936400E 07	0.61076906E-01
0.15876520E 07	0.62514067E-01
0.15806560E 07	0.63985050E-01

Table 6.28, cont'd.

G(λ)/λ	λ
0.15726630E 07	0.65490663E-01
0.15636780E 07	0.67031801E-01
0.15537130E 07	0.68609118E-01
0.15427810E 07	0.70223570E-01
0.15308940E 07	0.71875989E-01
0.15180650E 07	0.73567271E-01
0.15043080E 07	0.75298429E-01
0.14896390E 07	0.77070236E-01
0.14740780E 07	0.78883767E-01
0.14576380E 07	0.80739975E-01
0.14403420E 07	0.82639873E-01
0.14222100E 07	0.84584475E-01
0.14032610E 07	0.86574852E-01
0.13835210E 07	0.88612026E-01
0.13630070E 07	0.90697169E-01
0.13417500E 07	0.92831314E-01
0.13197690E 07	0.95015705E-01
0.12970910E 07	0.97251534E-01
0.12737440E 07	0.99540055E-01
0.12497580E 07	0.10188228E 00
0.12251530E 07	0.10427964E 00
0.11999630E 07	0.10673344E 00
0.11742180E 07	0.10924494E 00
0.11479390E 07	0.11181569E 00
0.11211700E 07	0.11444682E 00
0.10939320E 07	0.11713982E 00
0.10662600E 07	0.11989623E 00
0.10381863E 07	0.12271744E 00
0.10097380E 07	0.12560511E 00
0.98094975E 06	0.12856084E 00
0.95185812E 06	0.13158596E 00
0.92249181E 06	0.13468230E 00
0.89288581E 06	0.13785148E 00
0.86307100E 06	0.14109522E 00
0.83308175E 06	0.14441532E 00
0.80295050E 06	0.14781368E 00
0.77271231E 06	0.15129179E 00
0.74239838E 06	0.15485185E 00
0.71204406E 06	0.15849560E 00
0.68167825E 06	0.16222513E 00
0.65133950E 06	0.16604245E 00
0.62105325E 06	0.16994971E 00
0.59085706E 06	0.17394876E 00
0.56078156E 06	0.17804193E 00
0.53085881E 06	0.18223137E 00
0.50111663E 06	0.18651944E 00
0.47158763E 06	0.19090855E 00
0.44230344E 06	0.19540077E 00
0.41329075E 06	0.19999874E 00

NLAM= 100 LAMS= 0.020 LAMF= 0.20000

TEND= 207.000 NXPTS= 100 MUEND= 2.000

MUPTS= 100 IMAXTP= 17 NPTSTP= 6

Table 6.29. Fourier Decay Analysis results for NH_4NO_3, smoothed set #6

G(λ)/λ	λ
0.17151238E 06	0.20000000E-01
0.15956206E 06	0.20470615E-01
0.15085031E 06	0.20952318E-01
0.14565788E 06	0.21445330E-01
0.14424225E 06	0.21949977E-01
0.14684106E 06	0.22466466E-01
0.15366425E 06	0.22995126E-01
0.16489438E 06	0.23536220E-01
0.18068763E 06	0.24090059E-01
0.20117181E 06	0.24656922E-01
0.22644069E 06	0.25237121E-01
0.25655250E 06	0.25830973E-01
0.29154163E 06	0.26438806E-01
0.33139913E 06	0.27060926E-01
0.37608825E 06	0.27697694E-01
0.42553456E 06	0.28349455E-01
0.47962588E 06	0.29016551E-01
0.53821850E 06	0.29699322E-01
0.60113594E 06	0.30398194E-01
0.66816819E 06	0.31113487E-01
0.73907556E 06	0.31845625E-01
0.81357506E 06	0.32594983E-01
0.89136938E 06	0.33361968E-01
0.97212650E 06	0.34147013E-01
0.10554910E 07	0.34950521E-01
0.11410730E 07	0.35772931E-01
0.12284770E 07	0.36614701E-01
0.13172860E 07	0.37476290E-01
0.14070500E 07	0.38358133E-01
0.14973230E 07	0.39260749E-01
0.15876420E 07	0.40184591E-01
0.16775300E 07	0.41130178E-01
0.17665100E 07	0.42098004E-01
0.18541020E 07	0.43088604E-01
0.19398360E 07	0.44102531E-01
0.20232280E 07	0.45140300E-01
0.21038150E 07	0.46202485E-01
0.21811390E 07	0.47289673E-01
0.22547510E 07	0.48402458E-01
0.23242280E 07	0.49541414E-01
0.23891580E 07	0.50707165E-01
0.24491500E 07	0.51900364E-01
0.25038430E 07	0.53121623E-01
0.25529100E 07	0.54371603E-01
0.25960090E 07	0.55650994E-01
0.26328950E 07	0.56960523E-01
0.26633110E 07	0.58300894E-01
0.26870470E 07	0.59672773E-01
0.27039260E 07	0.61076906E-01
0.27138110E 07	0.62514067E-01
0.27166030E 07	0.63985050E-01

G(λ)/λ	λ
0.27122410E 07	0.65490663E-01
0.27007000E 07	0.67031801E-01
0.26820900E 07	0.68609118E-01
0.26561940E 07	0.70223570E-01
0.26233820E 07	0.71875989E-01
0.25836970E 07	0.73567271E-01
0.25373110E 07	0.75298429E-01
0.24844320E 07	0.77070236E-01
0.24253030E 07	0.78883767E-01
0.23602010E 07	0.80739975E-01
0.22894370E 07	0.82639873E-01
0.22133500E 07	0.84584475E-01
0.21323090E 07	0.86574852E-01
0.20467040E 07	0.88612020E-01
0.19569510E 07	0.90697169E-01
0.18634940E 07	0.92831314E-01
0.17667780E 07	0.95015705E-01
0.16672700E 07	0.97251534E-01
0.15654570E 07	0.99540055E-01
0.14618340E 07	0.10188228E 00
0.13568380E 07	0.10427964E 00
0.12511140E 07	0.10673344E 00
0.11450230E 07	0.10924494E 00
0.10390388E 07	0.11181569E 00
0.93382075E 06	0.11444682E 00
0.82968756E 06	0.11713982E 00
0.72715550E 06	0.11989623E 00
0.62667806E 06	0.12271744E 00
0.52867681E 06	0.12560511E 00
0.43357475E 06	0.12856084E 00
0.34176206E 06	0.13158596E 00
0.25360444E 06	0.13468230E 00
0.16943325E 06	0.13785148E 00
0.89563250E 05	0.14109522E 00
0.14272816E 05	0.14441532E 00
-0.56197820E 05	0.14781368E 00
-0.12162494E 06	0.15129179E 00
-0.18183681E 06	0.15485185E 00
-0.23668313E 06	0.15849560E 00
-0.28605450E 06	0.16222513E 00
-0.32987588E 06	0.16604245E 00
-0.36811081E 06	0.16994971E 00
-0.40075188E 06	0.17394876E 00
-0.42782956E 06	0.17804193E 00
-0.44940813E 06	0.18223137E 00
-0.46558400E 06	0.18651944E 00
-0.47648769E 06	0.19090855E 00
-0.48227519E 06	0.19540077E 00
-0.48313844E 06	0.19999874E 00

NLAM= 100 LAMS= 0.020 LAMF= 0.20000

TEND= 207.000 NXPTS= 100 MUEND= 4.000

MUPTS= 100 IMAXTP= 17 NPTSTP= 6

Table 6.30. Comparison of half lives obtained from the three analysis methods for NH_4NO_3 data set #6 and reported half lives (53-56), (57-59), (60), and (61).

	$T_{1/2}$	9.96 m	10.05 m	10.08 m	9.93 m
		error (%)	error (%)	error (%)	error (%)
FDA Method	10.83	8.76	7.79	7.47	9.09
Iterative Method	11.25	12.70	11.69	11.35	13.04
TLS Method	13.48	35.34	34.12	33.73	35.75

6.2 Analysis of Wheat Data

Existence of many elements in wheat results in many radioisotopes being produced by irradiation by neutrons; this causes difficulties in the analysis. The large number of radioisotopes causes the large error ripples which appear in the results and tend to mask true peaks. In the analysis of the wheat we had the problem of shifts of position of true peaks. The error ripples "push" the true peak aside and cause the shift of the principal peak. Theoretically, in the FDA method there are no error ripples. But in the application of the theory to data these error ripples appear. By looking at the plots of some analysis results, we can see that the error ripples are joined to true peaks at the base. So by increasing these error ripples in number and amplitude, the principal peaks are pushed from the proper place.

By increasing the μ_o value, the frequency of the error ripples increases. If we have much scatter or many components in data, the problem of the shift of the principal peaks increases (see the beginning of the Section 6).

Since all the problems explained above exist in the wheat data analysis, most of the data were analyzed for μ_o equal to 1. We have to be careful that there are no other components with half lives near to 10 minutes. In order to check this, we can run the data for μ_o values larger than 1, which will increase the resolution or cause the large width

peaks in the $G(\lambda)/\lambda$ vs λ spectrum to become narrower. Hence, other components should show up by introducing new principal peaks. The results of wheat analysis were obtained principally in form of plots. All the parameters for these plots are given in Appendix L. The data and results for each sample were analyzed as follows.

(a) Wheat - Data set #7

Data in Table (6.31) were used for the analysis. The FDA method for μ_o = 2 and 4 are half lives of 9.4 m and 8.4 m, respectively. The results of the analysis in form of plots are shown in Figs. (6.5) and (6.6). As can be seen, due to scatter in the data the error ripples are large in amplitude and by decreasing the μ_o value to 2, we minimize the error ripples, which causes trouble in wheat data analysis. Although by decreasing the μ_o value, we lose some resolution, i.e., the principal peaks become broader, but in comparison to reducing the error ripples with large amplitude and large frequency this decrease in resolution is acceptable.

By using the first five data points, the analysis was performed by using iterative and TLS method. The results of the analysis by these methods are tabulated in Table (6.32).

Table 6.31. Data set #7 (wheat)

Decay Time (min.)	Counts per 4.267 minutes
26307.63	6.667
19199.88	11.70
14347.0	16.45
10957.13	21.35
8575.13	26.03
2834.0	30.74
2054.34	35.45
1546.00	40.16

Figure 6.5. Fourier Decay Analysis results for wheat, data set #7. ($Y = G(\lambda)/\lambda$, $X = \lambda$)

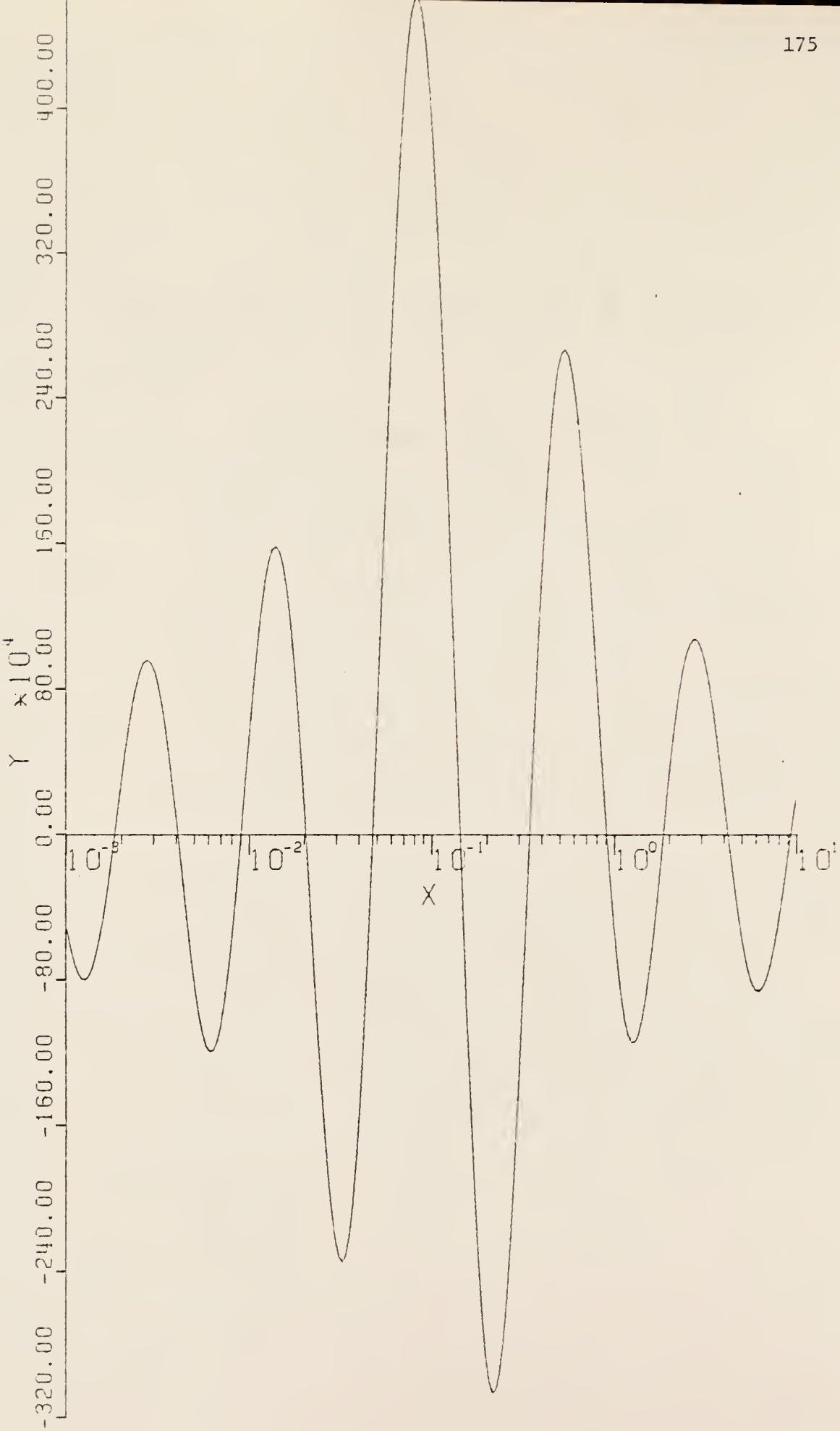

Figure 6.6. Fourier Decay Analysis results for wheat, data set #7. ($Y = G(\lambda)/\lambda$, $X = \lambda$)

Table 6.32. Comparison of half lives obtained from the three analysis methods for wheat data set #7 and reported half lives (53-56), (57-59), (60), and (61).

	$T_{1/2}$	9.96 m	10.05 m	10.08 m	9.93 m
		error (%)	error (%)	error (%)	error (%)
FDA Method	9.36	5.96	6.80	7.08	5.67
Iterative Method	11.77	18.23	17.17	18.82	18.59
TLS Method	11.95	19.97	18.99	18.55	20.34

(b) Wheat - Data set #8

The data used for the analysis are given in Table (6.33). The data are plotted in Fig. (6.7). Excessive scatter in the data was observed. By using FDA method for μ_o = 1 and 3, the half lives of 7.8 m and 4.5 m were obtained. The results of the FDA for μ_o = 2 and 3 are shown in Figs. (6.8) and (6.9).

By using the first nine data points of the Table (6.33), the data were analyzed by the iterative and TLS methods. The results of the analysis by the three methods are tabulated in Table (6.34). As seen the results obtained by FDA method are much better than those obtained by the iterative or TLS methods.

Table 6.33. Data set #8 (wheat)

Decay Time (min.)	Counts per 4.267 minutes
36.350	12964.699
41.500	10378.898
46.500	9394.598
51.500	8072.199
56.650	6354.500
61.700	5720.098
68.500	4362.398
73.400	4117.898
78.460	3114.600
83.450	3417.700
88.400	3223.600
93.350	2330.100
98.600	1975.600
104.450	2169.800
109.350	1879.700
119.100	1908.200
124.100	1572.700
129.050	1973.400
136.250	1846.900
141.100	1515.400
146.500	503.900
150.900	1433.800
156.700	1403.900

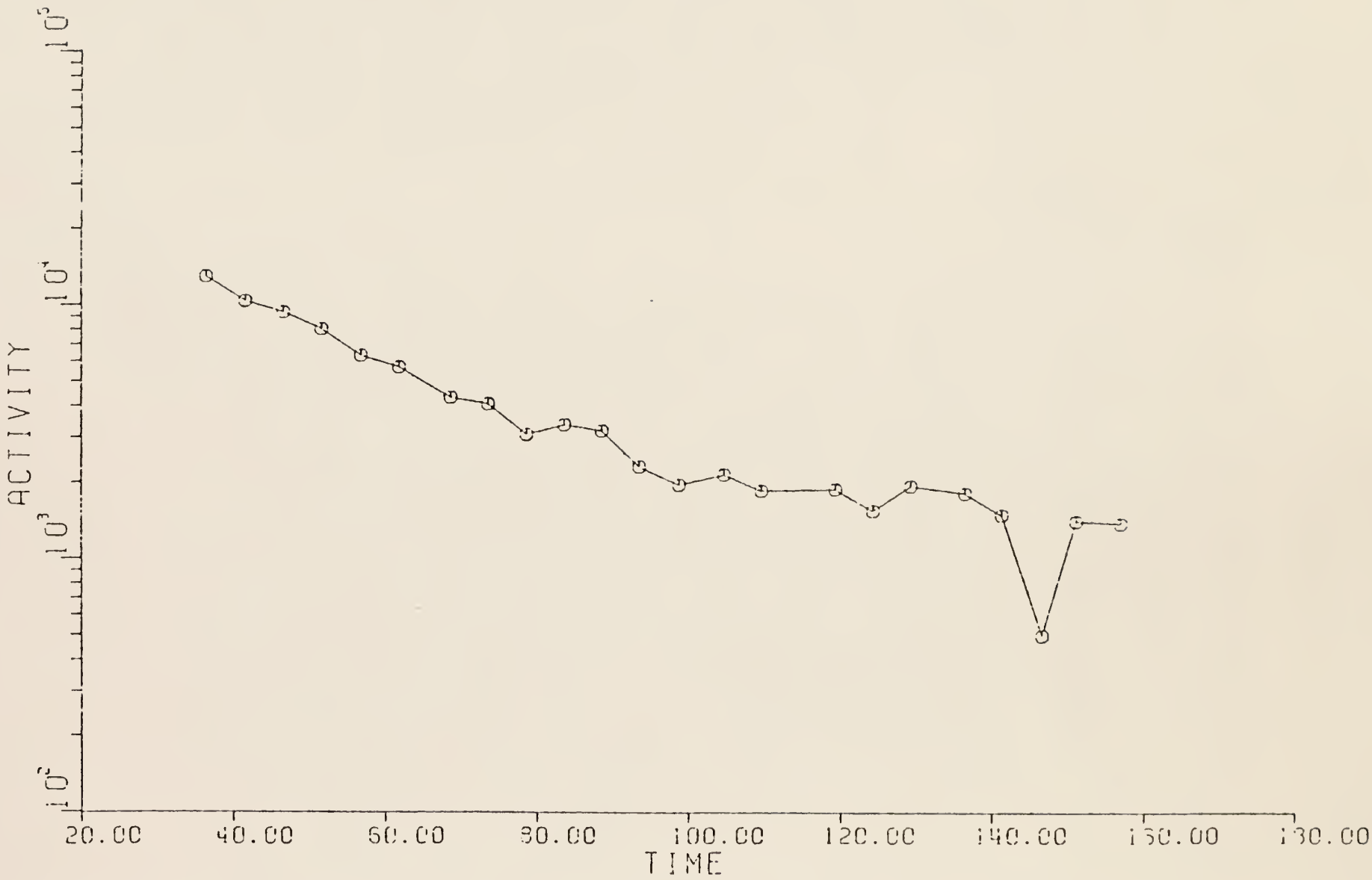

Figure 6.7. A plot of activity (counts, total area of the 0.511 MeV photopeaks, per 4.267 minutes) versus decay time (in minutes) for wheat (Data Set #8).

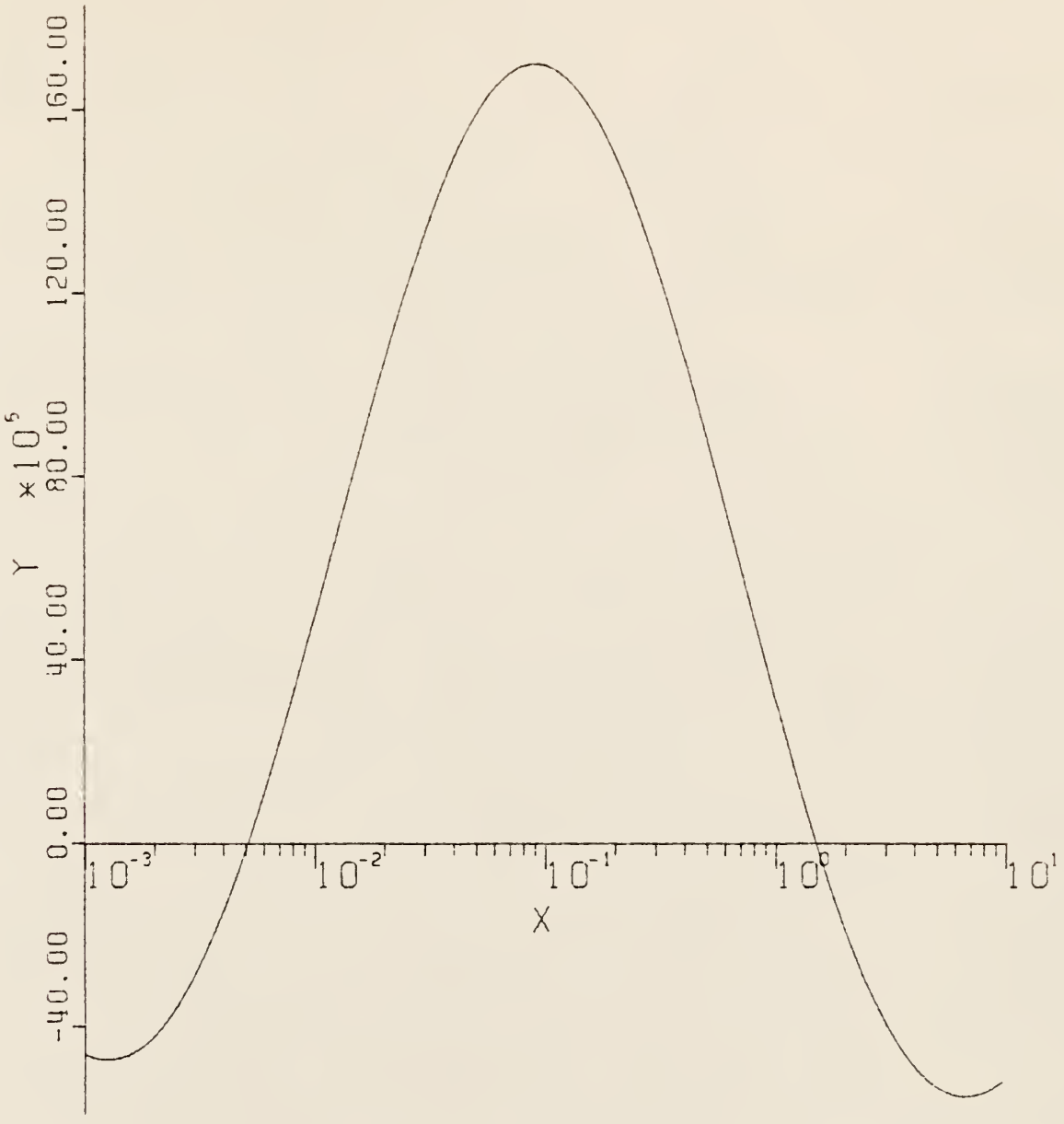

Figure 6.8. Fourier Decay Analysis results for wheat, data set #8. ($Y = G(\lambda)/\lambda$, $X = \lambda$)

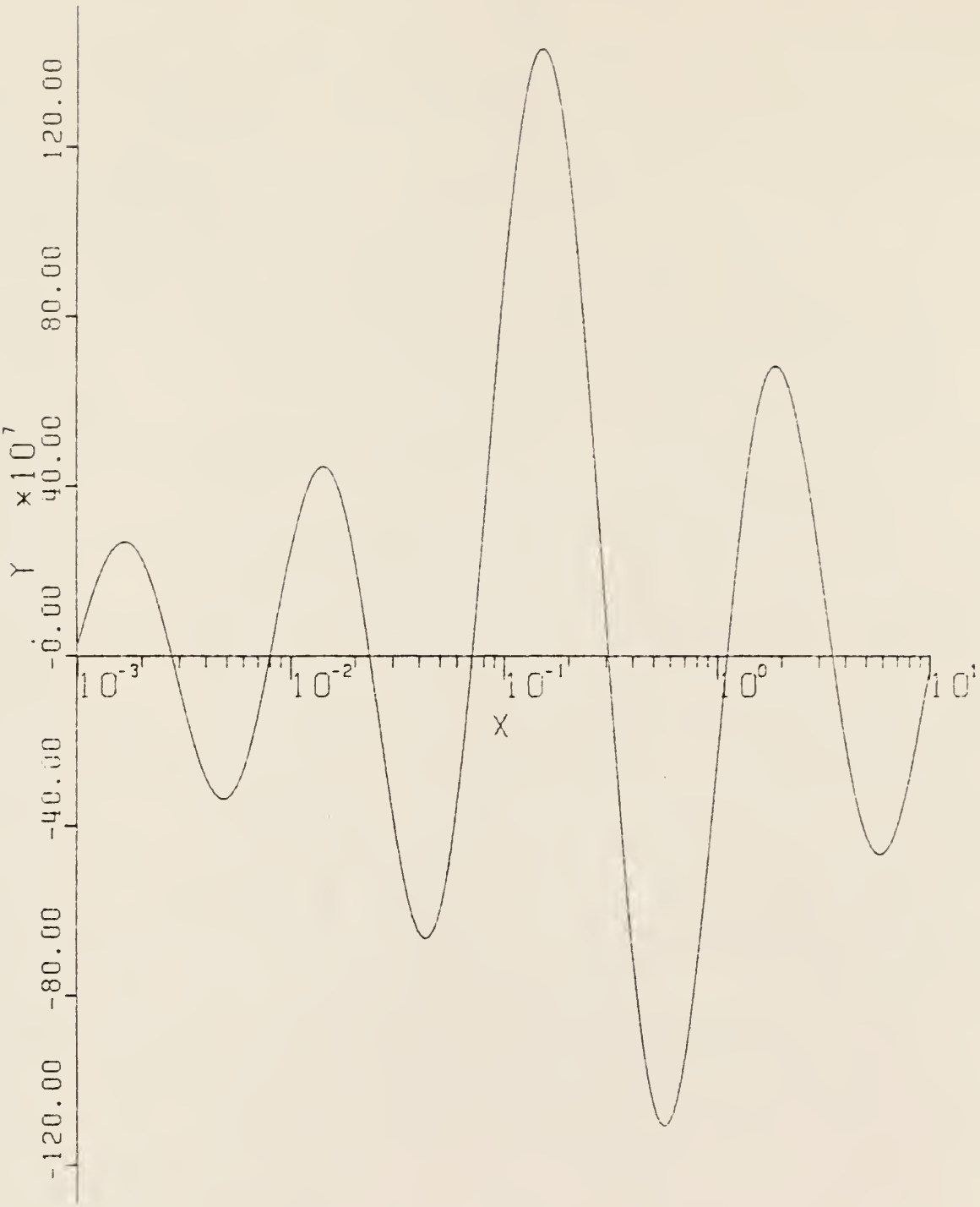

Figure 6.9. Fourier Decay Analysis results for wheat, data set #8. ($Y = G(\lambda)/\lambda$, $X = \lambda$)

Table 6.34. Comparison of half lives obtained from the three analysis methods for wheat data set #8 and reported half lives (53-56), (57-59), (60), and (61).

	$T_{1/2}$	9.96 m	10.05 m	10.08 m	9.93 m
		error (%)	error (%)	error (%)	error (%)
FDA Method	7.79	21.80	22.50	22.73	21.57
Iterative Method	21.33	114	112	111	114
TLS Method	21.30	113	111	111	114

(c) Wheat - Data Set #9

Data given in Table (6.35) were used for the analysis. By using FDA method for μ_o = 2 and 4, the half lives 9.4 m and 9.0 m were obtained. The results of FDA method for μ_o = 2 and 4 are shown in Figs. (6.10) and (6.11).

The data also were analyzed by the iterative and TLS methods. The results of the analysis by the three methods are tabulated in Table (6.36).

Table 6.35. Data set #9 (wheat)

Decay Time (min.)	Counts per 4.267 minutes
1.200	18556.000
6.360	14554.000
10.920	12277.699
16.500	10296.000
20.000	7748.500
25.550	6903.297
29.350	5483.898

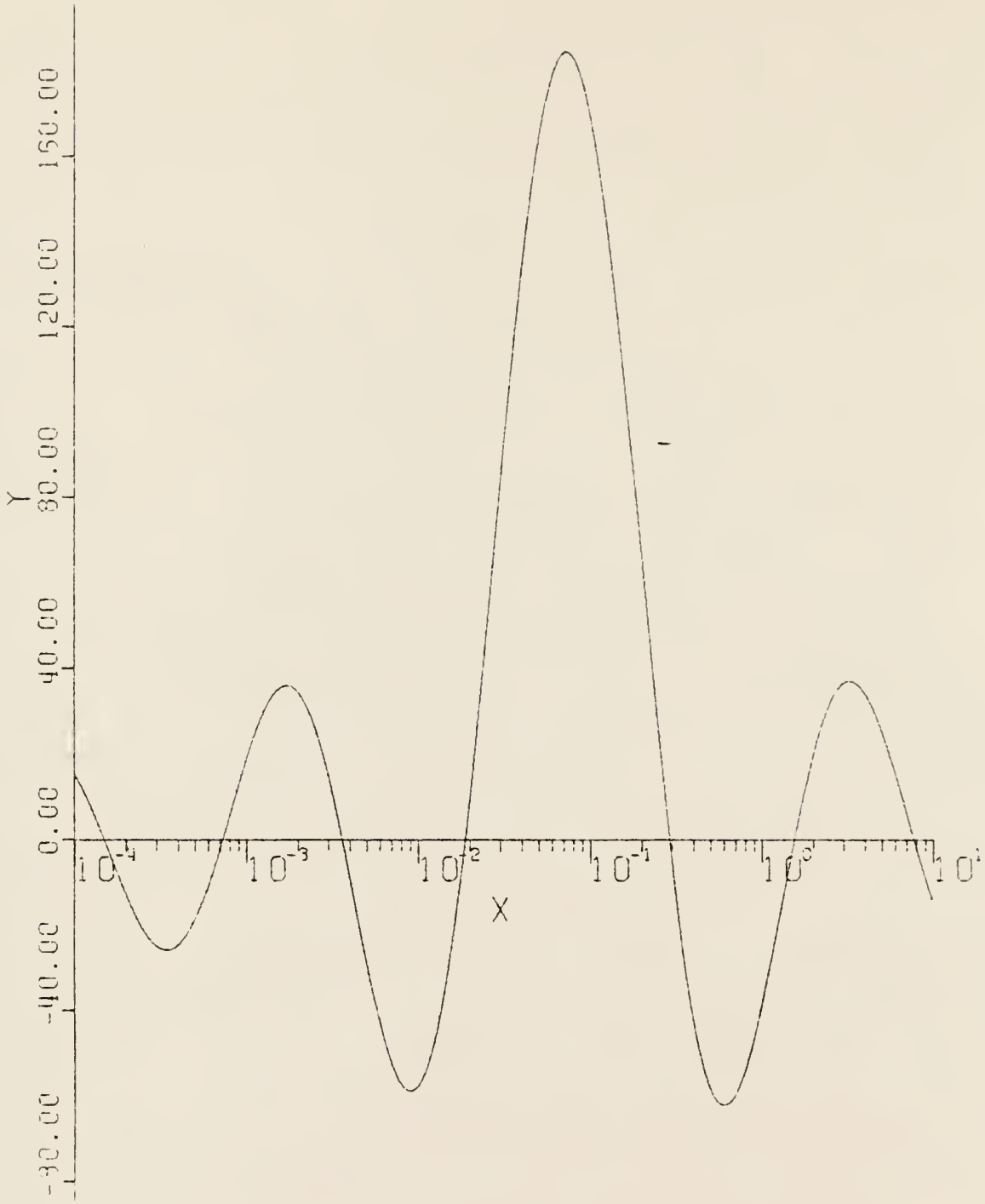

Figure 6.10. Fourier Decay Analysis results for wheat, data set #9. ($Y = G(\lambda)/\lambda$, $X = \lambda$)

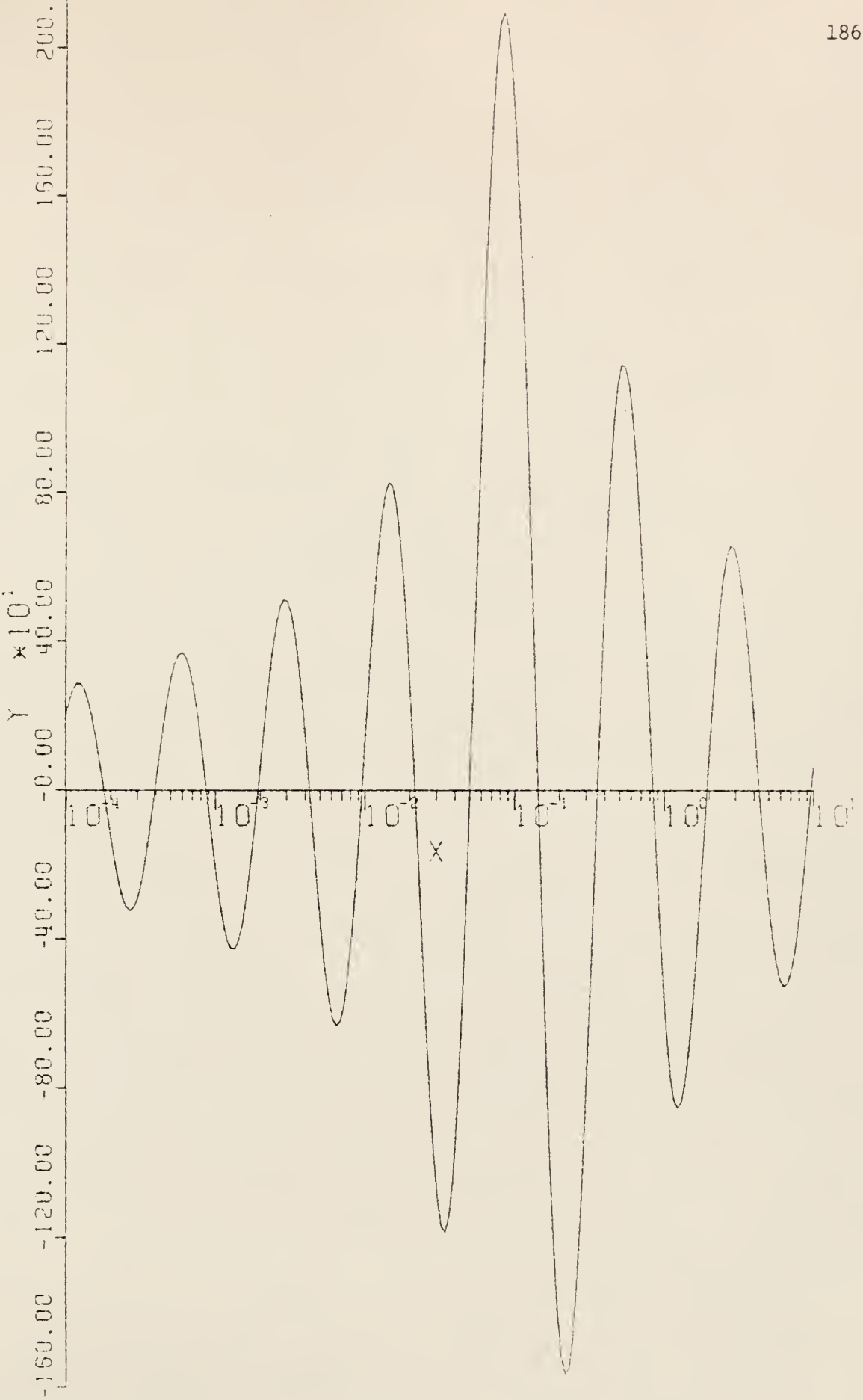

Figure 6.11. Fourier Decay Analysis results for wheat, data set #9. ($Y = G(\lambda)/\lambda$, $X = \lambda$)

Table 6.36. Comparison of half lives obtained from the three analysis methods for wheat data set #9 and reported half lives (53-56), (57-59), (60), and (61).

	$T_{1/2}$	9.96 m	10.05 m	10.08 m	9.93 m
		error (%)	error (%)	error (%)	error (%)
FDA Method	9.38	5.82	6.67	6.95	5.54
Iterative Method	16.38	64.51	63.04	62.55	65.01
TLS Method	16.33	63.96	62.49	62.01	64.45

(d) Wheat - Data Set #10

Data given in Table (6.37) were used for the analysis. By using FDA method for μ_o = 1 and 3, the results 9.4 m and 8.5 m were obtained. The results of FDA for μ_o = 1 and 3 in form of plots are shown in Figs. (6.12) and (6.13).

The data were also analyzed by the iterative and TLS method. The results of the analysis by the three methods are tabulated in Table (6.38).

Table 6.37. Data set #10 (wheat)

Decay Time (min.)	Counts per 4.267 minutes
1.650	22890.598
6.230	18155.098
10.780	14926.000
15.310	11786.398
19.820	10484.000
24.270	8810.297
28.220	7023.297

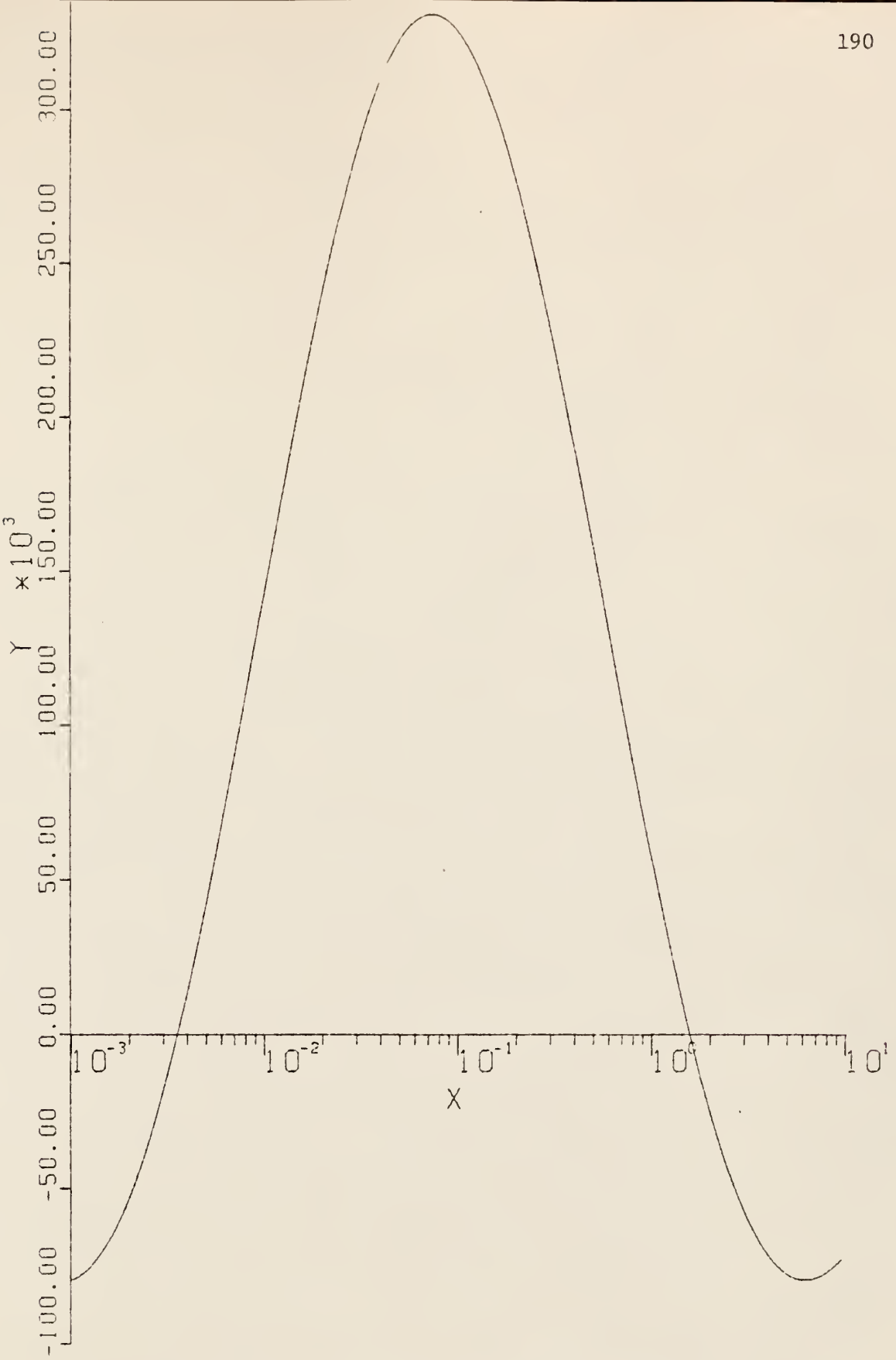

Figure 6.12. Fourier Decay Analysis results for wheat, data set #10. ($Y = G(\lambda)/\lambda$, $X = \lambda$)

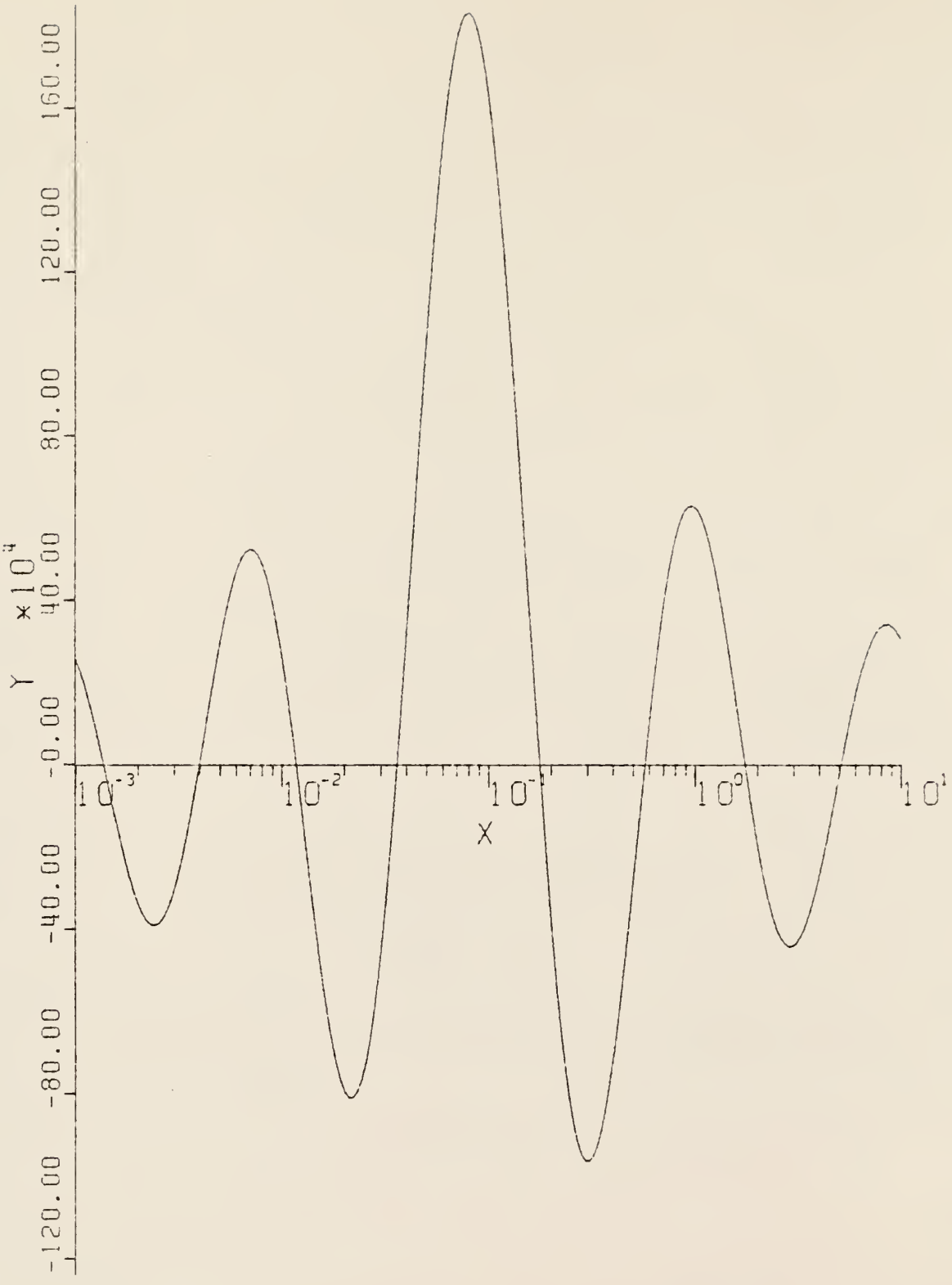

Figure 6.13. Fourier Decay Analysis results for wheat, data set #10. ($Y = G(\lambda)/\lambda$, $X = \lambda$)

Table 6.38. Comparison of half lives obtained from the three analysis methods for wheat data set #10 and reported half lives (53-56), (57-59), (60), and (61)

	$T_{1/2}$	9.96 m	10.05 m	10.08 m	9.93 m
		error (%)	error (%)	error (%)	error (%)
FDA Method	9.36	5.97	6.81	7.06	5.68
Iterative Method	16.04	61.94	59.60	59.12	61.53
TLS Method	16.17	62.34	60.17	60.41	62.83

(e) Wheat - Data Set #11

Data given in Table (6.39) were used for the analysis. The data were plotted in Fig. (6.14). This plot reveals much scatter in the data. By using FDA method for μ_o = 1 and 3, the half lives of 17.9 m and 24.8 m were obtained. The results obtained by FDA method for μ_o = 1 and 3 are shown in Figs. (6.15) and (6.16), respectively. By looking at Fig. (6.16), we can see that the principal peak is not symmetrical in form. This symmetry of principal peak should always exist. As seen in Fig. (6.16) this is not true for this analysis. Thus a false peak, which has a half life near 10 minutes must be present in data. Since this false peak is related to the principal peak by error ripples, it pushes the true peak and causes error in the analysis. By decreasing μ_o to 1, we minimize this problem, although we get less resolution in the results.

The first ten points of data listed in Table (6.39) the data were analyzed by the iterative and TLS methods. The results of the analysis are given in Table (6.40).

Table 6.39. Data set #11 (wheat)

Decay Time (min.)	Counts per 4.267 minutes
5.000	11387.898
9.800	9244.297
14.700	7197.098
19.500	5562.398
24.350	4828.398
29.200	4243.297
34.000	3062.700
39.500	2437.500
45.050	2008.000
50.100	1617.600
55.000	1443.800
59.800	1380.200
64.700	1191.000
69.500	1055.400
74.450	1214.400
79.350	921.800
84.300	745.900
90.900	753.500
95.550	594.800
100.350	766.100
105.250	472.400
109.900	530.900
114.600	524.700
119.550	529.700
124.250	466.100

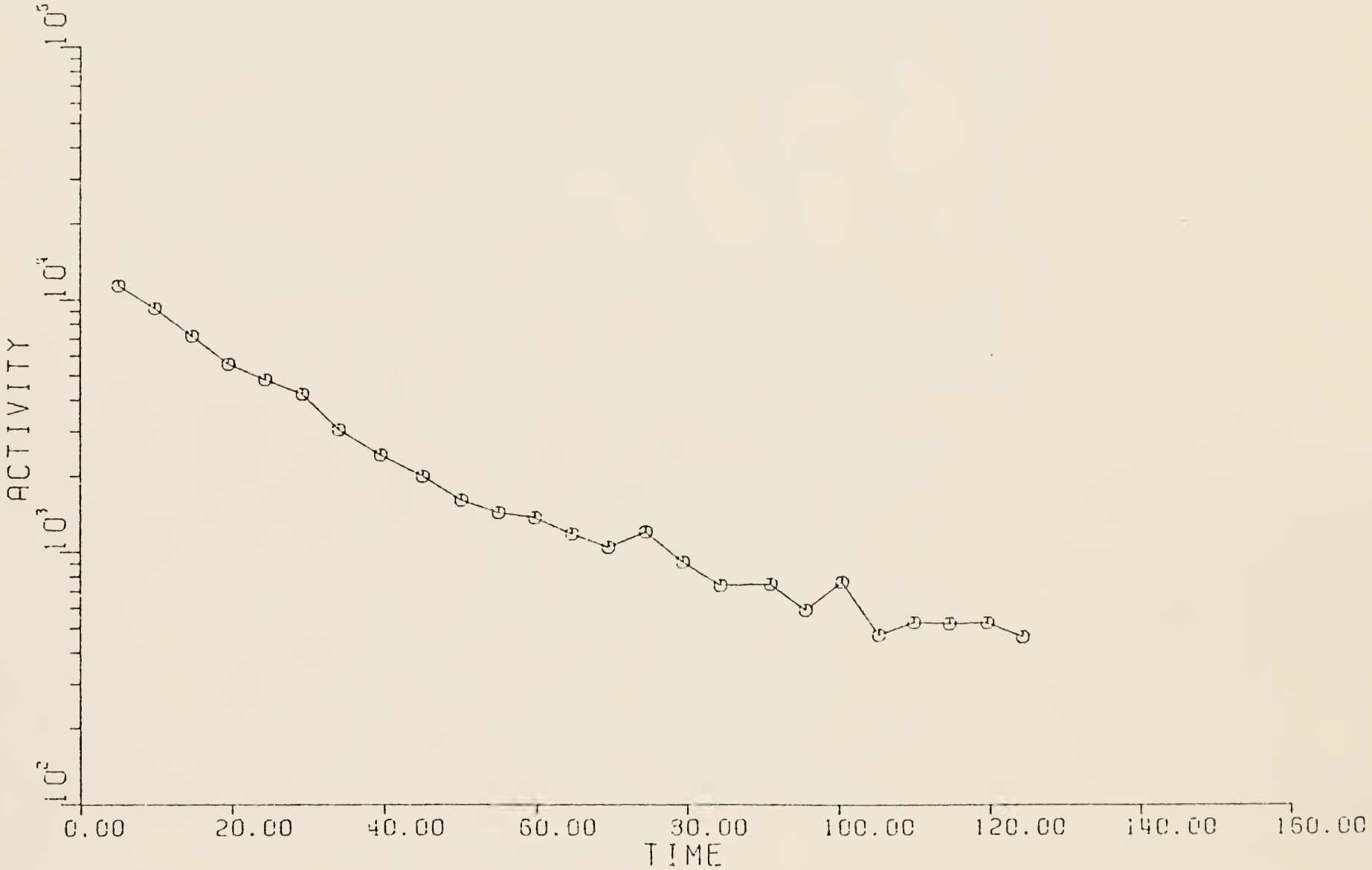

Figure 6.14. A plot of activity (counts, total area of the 0.511 MeV photopeaks, per 4.267 minutes) versus decay time (in minutes) for wheat (Data Set #11).

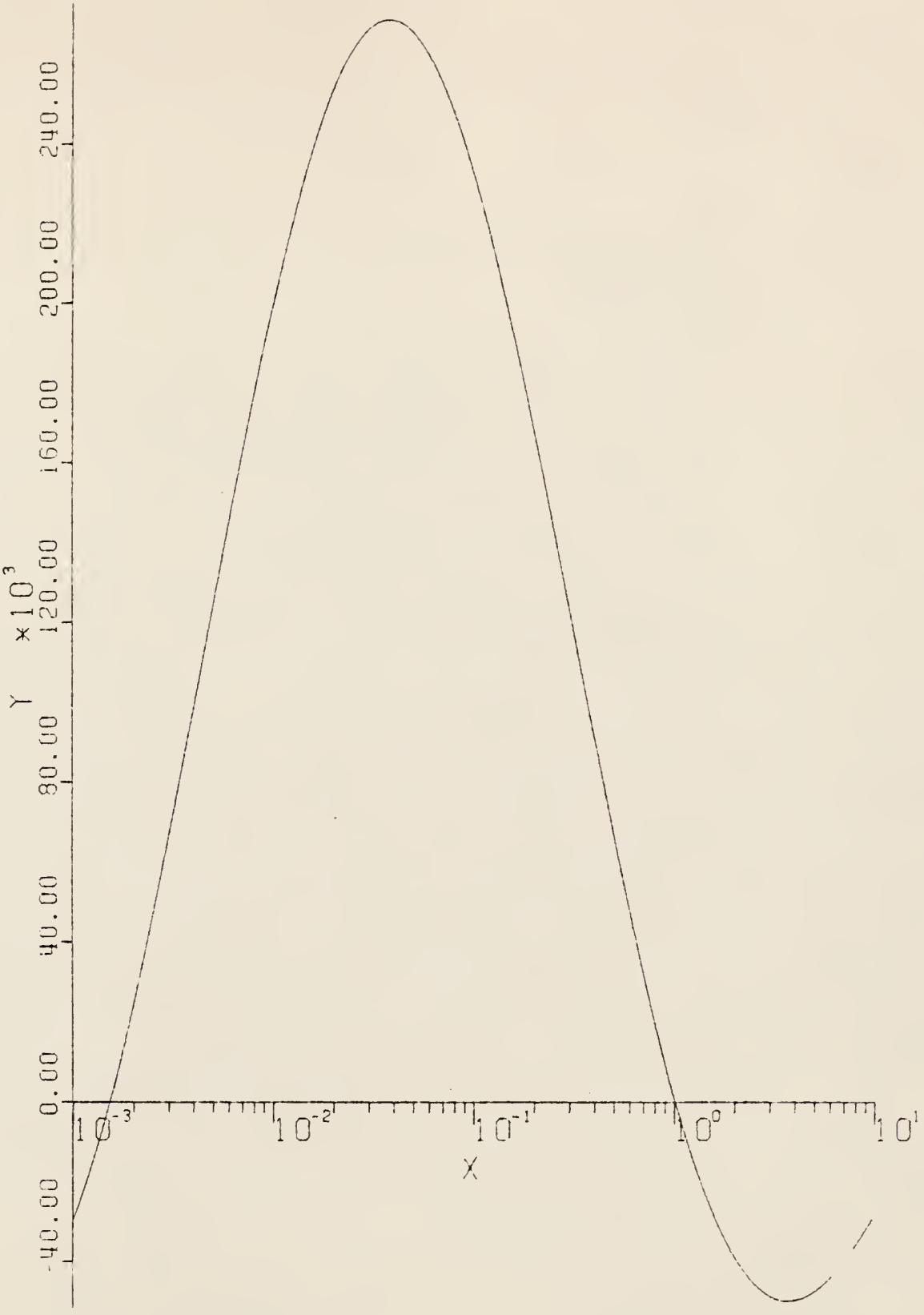

Figure 6.15. Fourier Decay Analysis results for wheat, data set #11. ($Y = G(\lambda)/\lambda$, $X = \lambda$)

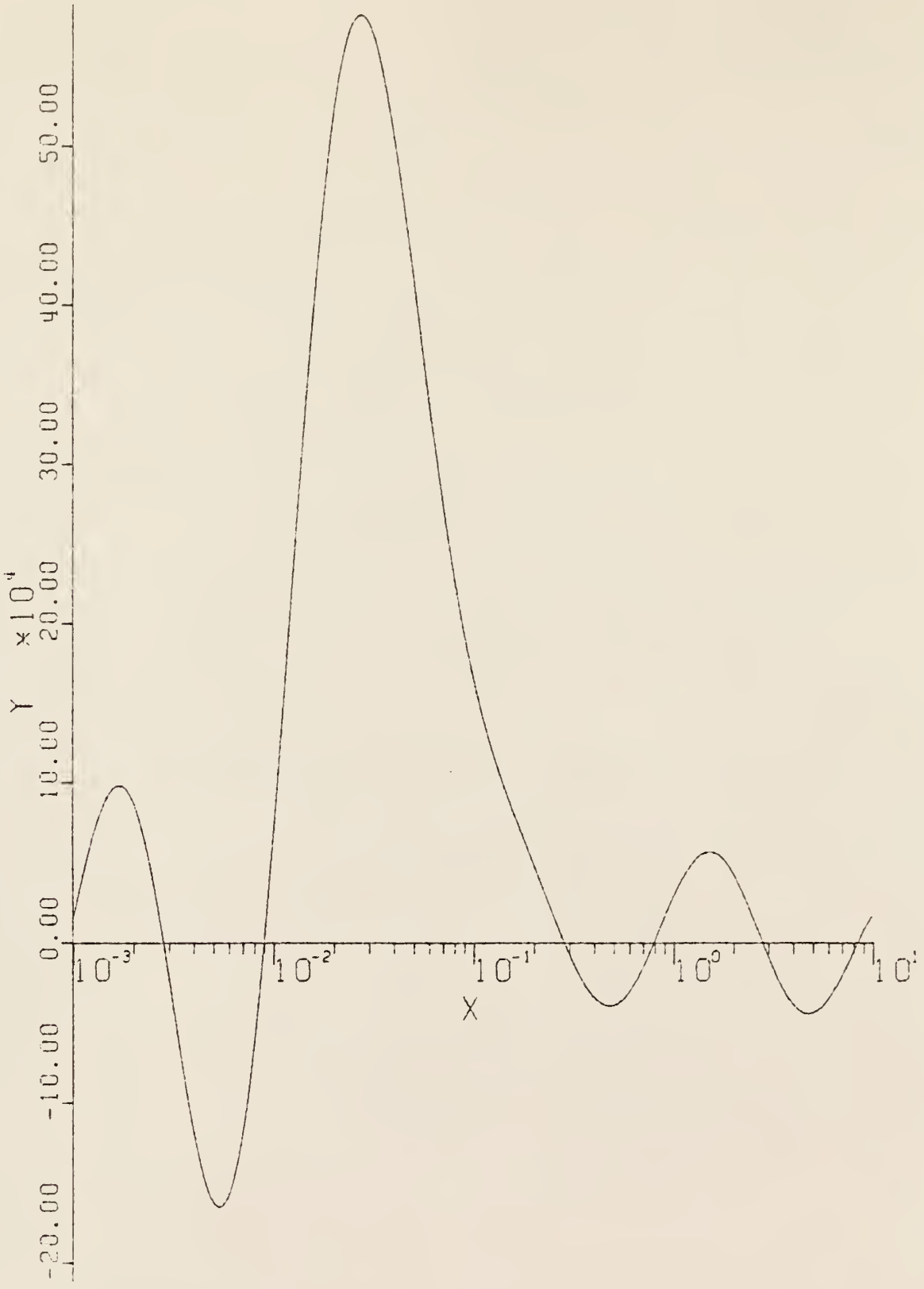

Figure 6.16. Fourier Decay Analysis results for wheat, data set #11. ($Y = G(\lambda)/\lambda$, $X = \lambda$)

Table 6.40. Comparison of half lives obtained from the three analysis methods for wheat data set #11 and reported half lives (53-56), (57-59), (60), and (61).

	$T_{1/2}$	9.96 m	10.05 m	10.08 m	9.93 m
		error (%)	error (%)	error (%)	error (%)
FDA Method	17.90	79.72	78.11	77.58	80.27
Iterative Method	15.89	59.57	58.14	57.67	60.06
TLS Method	15.87	59.35	57.93	57.46	59.83

(f) Wheat - Data Set #12

The data given in (6.41) were used in the analysis. By using FDA method, the half lives 8.2 m and 7.4 m for μ_o = 1 and 3 were obtained, respectively. The result of the analysis by the FDA method are given in Fig. (6.17) and (6.18) for μ_o = 1 and 3, respectively.

The data were analyzed by the iterative and TLS methods. The results of the analysis by the three methods are tabulated in Table (6.42).

Table 6.41. Data set #12 (wheat)

Decay Time (min.)	Counts per 4.267 minutes
1.600	18936.000
6.220	14934.098
10.750	12739.000
15.280	9866.500
19.790	8098.000
24.300	7022.797

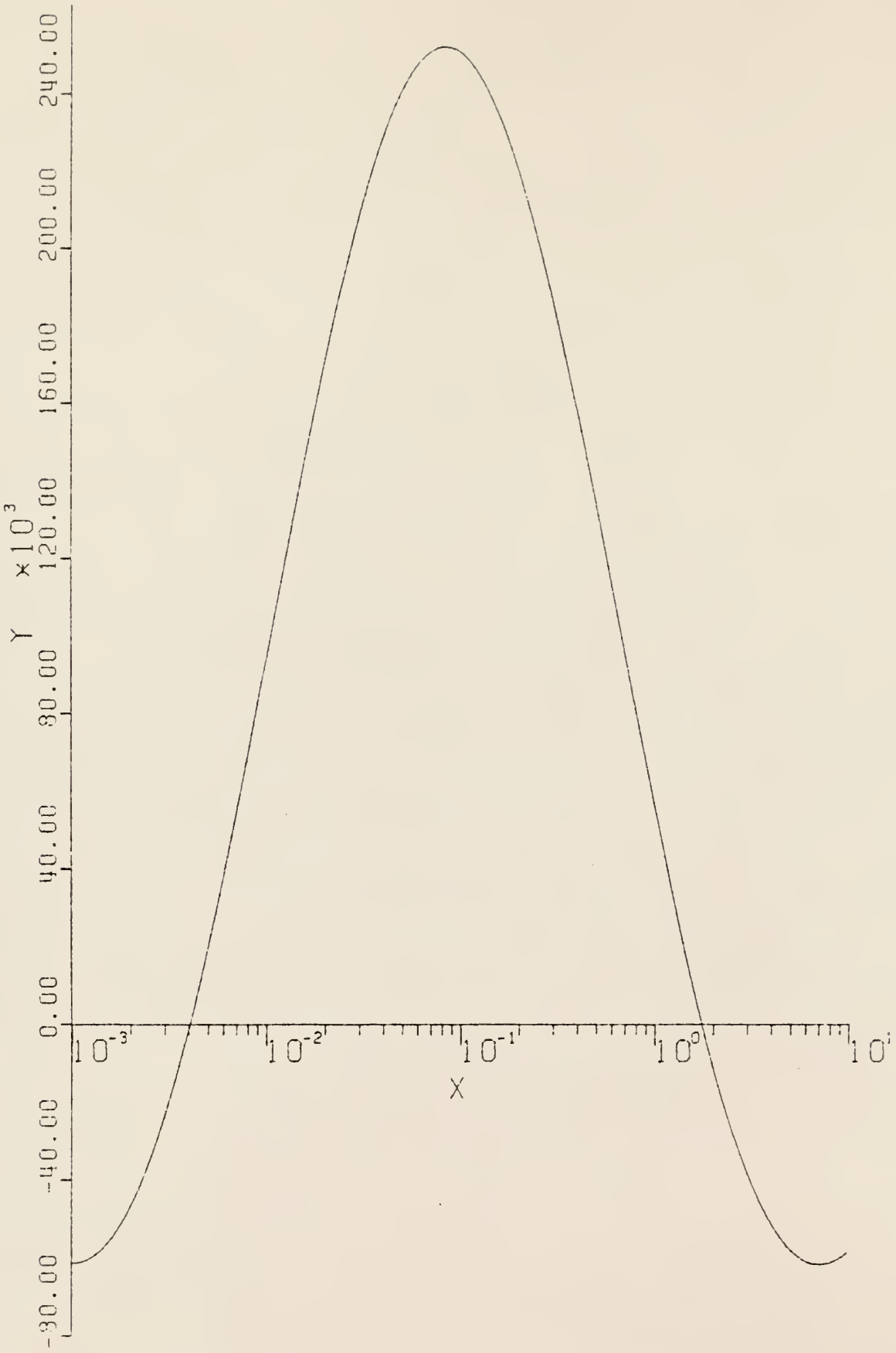

Figure 6.17. Fourier Decay Analysis results for wheat, data set #12. ($Y = G(\lambda)/\lambda$, $X = \lambda$)

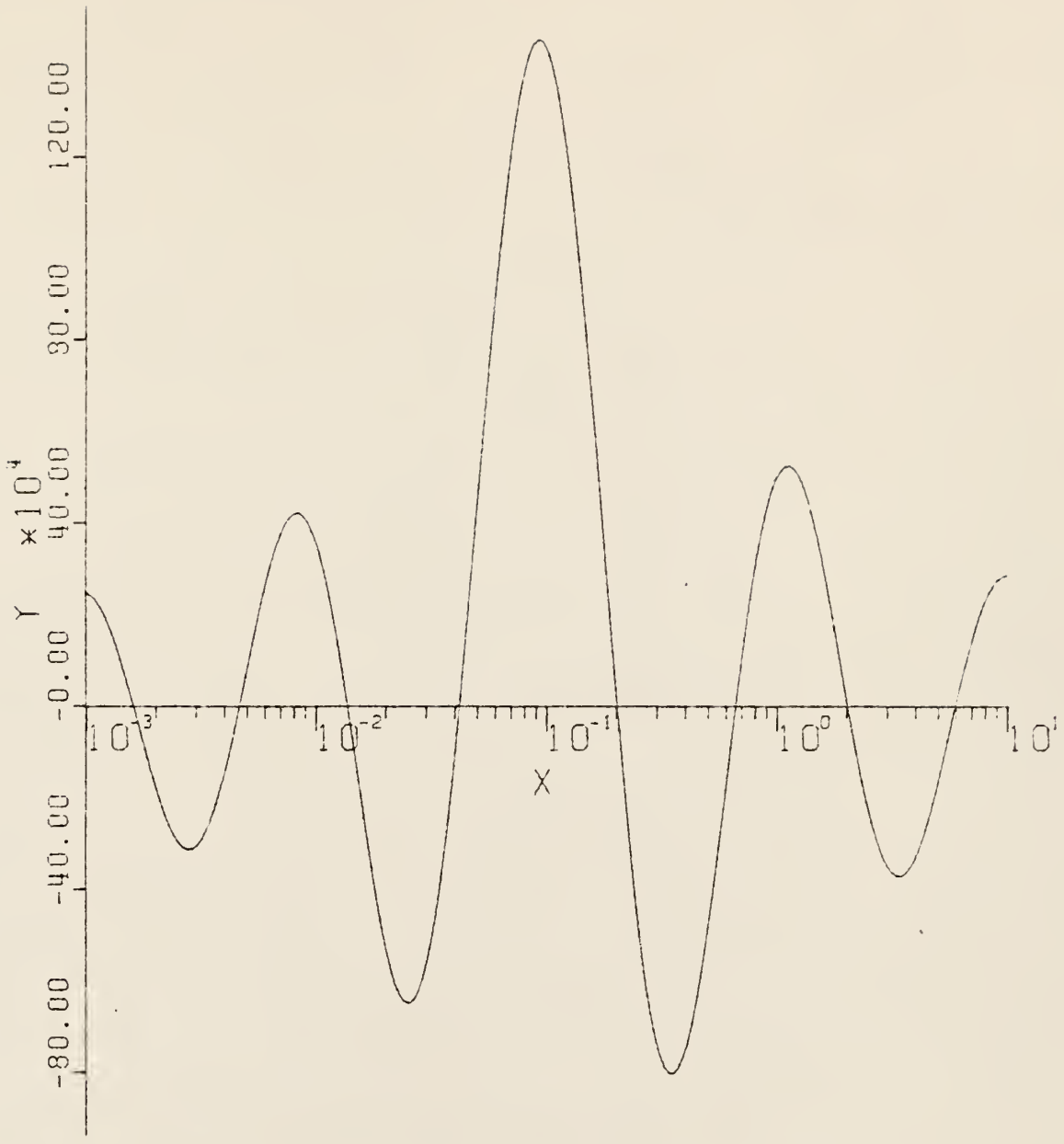

Figure 6.18. Fourier Decay Analysis results for wheat, data set #12. ($Y = G(\lambda)/\lambda$, $X = \lambda$)

Table 6.42. Comparison of half lives obtained from the three analysis methods for wheat data set #12 and reported half lives (53-56), (57-59), (60), and (61).

	$T_{1/2}$	9.96 m	10.05 m	10.08 m	9.93 m
		error (%)	error (%)	error (%)	error (%)
FDA Method	8.15	18.17	18.90	19.14	17.92
Iterative Method	15.26	53.28	51.84	51.38	53.67
TLS Method	15.68	57.44	56.01	55.55	57.99

(g) Wheat - Data Set #13

Data given in Table (6.43) were used for the analysis. By using FDA methods, for μ_o = 1 and 3, the half lives 8.9 m and 8.2 m were obtained. Results of the analysis by the FDA method are presented in the form of plots in Figs. (6.19) and (6.20) for μ_o = 1 and 3, respectively.

The data also were analyzed by using the iterative and TLS methods. Results of the analysis for the three methods are tabulated in Table (6.44).

Table 6.43. Data set #13 (wheat)

Decay Time (min.)	Counts per 4.267 minutes
2.250	4830.297
6.900	4052.900
11.500	3153.300
16.250	2675.000
25.500	2453.000

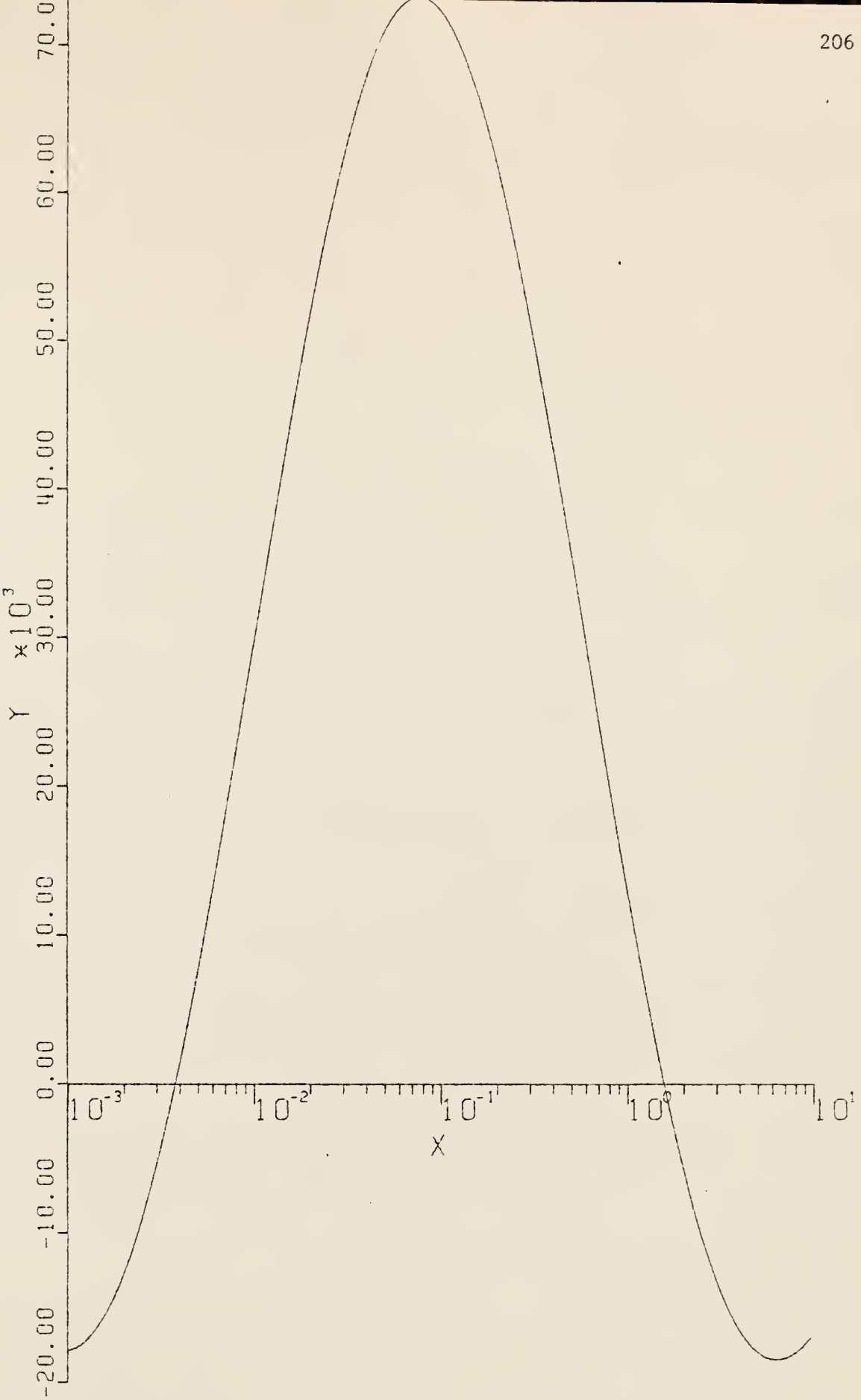

Figure 6.19. Fourier Decay Analysis results for wheat, data set #13. ($Y = G(\lambda)/\lambda$, $X = \lambda$)

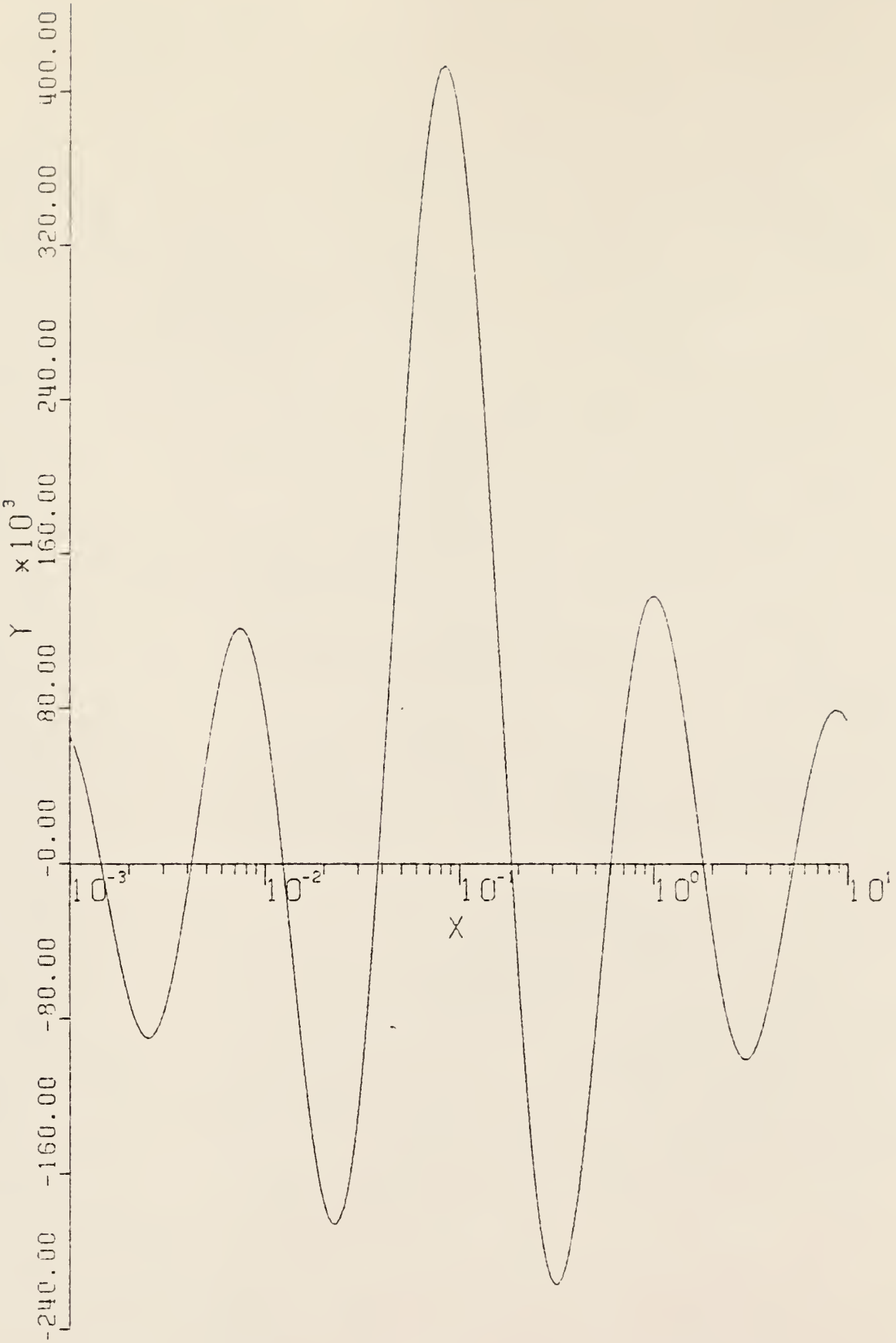

Figure 6.20. Fourier Decay Analysis results for wheat, data set #13. ($Y = G(\lambda)/\lambda$, $X = \lambda$)

Table 6.44. Comparison of half lives obtained from the three analysis methods for wheat data set #13 and reported half lives (53-56), (57-59), (60), and (61).

	$T_{1/2}$	9.96 m	10.05 m	10.08 m	9.93 m
		error (%)	error (%)	error (%)	error (%)
FDA Method	8.94	10.23	11.03	11.29	9.93
Iterative Method	15.92	59.83	58.22	57.93	60.32
TLS Method	15.96	60.24	58.80	58.33	60.72

6.3 CONCLUSIONS

As mentioned before, the problem of representation of a function using sums of exponentials with unknown exponents and coefficients is important since it arises frequently in practice. The FDA method, used in this work, can be used for the analysis of multicomponent decay curves. The two numerical integrations involved in the FDA method introduce two cutoff errors, x_o (Eq. 2.2-2) and u_o (Eq. 2.3-12). In section 3, all the problems related to the FDA method concerned with numerical integrations, cutoffs, interpolation, and other problems and in section 6, the problems concerned with real data were discussed. A summary of the principal conclusions are:

a - As the cutoff value u_o increases, the frequency of error ripples and the resolution of true peak increases.

b - As the cutoff value x_o decreases, the height of error ripples increases and they appear sooner.

c - Error ripples are symmetrical with respect to the true peaks.

d - As the number of components increases, the numerical integration of the two integrals (Eqs. 2.3-7 and 2.3-15) becomes more difficult and the accuracy of the FDA method decreases.

e - Non-symmetry of the error ripples with respect to the true peak indicate an analysis problem. Non-symmetry of the true peak indicates the presence of an unresolved true peak.

f - By increasing the order of interpolation, improvement of results was obtained.

g - The data must be taken for a time period equal to several half lives of the longest-lived component else that component will not be resolved in the analysis

h - The number of true peaks equals the number of exponential components present in the data.

i - In some situations in order to get rid of scatter in the data, the problems encountered due to cutoff (x_o) are unavoidable.

j - Some cases indicate in order to reduce error ripple interference, low resolution must be accepted.

k - Error ripples due to scatter in the data are much stronger than those due to cutoff (x_o), but the error ripples depend of the severity of scatter in data.

By using the FDA method the half life for ^{13}N was obtained by analyzing NH_4NO_3 and wheat data. The results obtained by the FDA method compared to the iterative and transformed least squares methods were the best.

6.4 Suggestions for Further Study

The principle objective of this work was to analyze the Fourier Decay Analysis Method for the analysis of multicomponent decay curves. Much work remains in the analysis and improvement of the FDA method for curve fitting. For increased accuracy and further work of the method, the following items should be considered.

1. Collection of data needs to be improved
    a. refined irradiation
    b. better detection equipment
2. The computer code for FDA needs improvement
    a. improvement in the numerical integration routine
    b. improvement in the interpolation method
    c. use of an extrapolution routine to improve the data
3. an error analysis of FDA needs study
4. mathematical techniques of smoothing data with high scatter need study.
5. study of dependent exponential decay curve

7.0 ACKNOWLEDGEMENTS

The author wishes to express his deepest and most sincere gratitude to Dr. N. Dean Eckhoff, Head of the Department of Nuclear Engineering at Kansas State University, for his guidance, assistance, and contribution to this work. The author also extends his gratitude to Dr. H. J. Donnert for his helpful discussions. The financial support provided by the Department of Nuclear Engineering under the GRA Program is greatly appreciated. The continued cooperation of the Kansas State University TRIGA Mark II Nuclear Reactor Facility personnel is acknowledged. Thanks are due to Mr. Q. Sharfuddin for his informative discussions. The assistance of Mr. S. Howe, and Mr. G. Nelson, students in the Nuclear Engineering Department, in the neutron activation analysis of the samples is deeply appreciated. To Mrs. S. Kemnitz, a special word of thanks is given for her diligence in typing this thesis.

Finally, the author's appreciation of the continued support, encouragement and advice of his parents, Mr. and Mrs. Jowzani Moghaddam, throughout many years of study, can never be adequately stated.

8.0 LITERATURE CITED

1. Corliss, R., Neutron Activation Analysis, U.S. Atomic Energy Commission, Division of Technical Information.

2. Kruger, P., Principles of Activation Analysis, John Wiley and Sons, Inc., 1971.

3. Price, W. J., Nuclear Radiation Detection, 2nd Edition, McGraw-Hill, 1964.

4. Evans, R. D., The Atomic Nucleus, McGraw-Hill, 1972.

5. Foster, A. R., and Wright, R. L., Basic Nuclear Engineering 2nd Edition, Allyn and Bacon, Inc., 1973.

6. Kaplan, I., Nuclear Physics, Addition-Wesley Publishing Company, Inc., 1964.

7. Lyon, w. S., Guide to Activation Analysis, D. Van Nostrand Co., Inc., 1964.

8. Glasstone, S., and Sesonske, A., Nuclear Reactor Engineering, D. Van Nostrand Co., Inc., 1967.

9. Crouthamel, C. E., Applied Gamma-Ray Spectrometry, Pergamon Press, 1969.

10. Lenihan, J. M. A. and S. J. Thomson, Eds., Activation Analysis: Principles and Applications, Academic Press, 1965.

11. Taylor, D., Neutron Irradiation and Activation Analysis, D. Van Nostrand, 1964.

12. Eckhoff, N. D., "Optimal Neutron Activation Analysis," a Ph.D. Dissertation, Kansas State University, 1967.

13. Fano, U., Nucleonics, 11,8 (August, 1953); 11,55 (September, 1953).

14. Heath, R. L., "Scintillation Spectrometry-Gamma-Ray Spectrum Catalogue," 2nd Edition, Vols. 1 of 1, IDO-16880-1, 1964.

15. Heath, R. L., "Scintillation Spectrometry: Gamma-Ray Spectrum Catalogue," 2nd Edition, Vols. 2 of 2, IDO-16880-2, 1964.

16. Chase, G. D., and Rabinowitz, J. L., Principles of Radioistope Methodology, 3rd Edition, Purgess Publishing Co., 1967.

17. Siegbahn, K., Alpha-, Beta- and Gamma-Ray Spectroscopy, North-Holland Publishing Company (1965).

18. "Modern Trends in Activation Analysis," Proceedings of 1961 International Conference, Texas A & M, April 19-22, 1965.

19. Hubbell, J. H., and Scofield, N. E., IRE Trans. on Nuclear Science, NS, 5, 155 (1958).

20. Burrus, W. R., IRE Trans. on Nuclear Science, NS, 7, 102 (1960).

21. West, H. I., and Johnson, B., IRE Trans. on Nuclear Science, NS, 7, 102 (1960).

22. Mollenaurer, J. F., Univ. Calif. Rept. UNRL-9748, 1961.

23. Heath, R. L., U. S. Atomic Energy Comm. Document ID016784, 1962.

24. Hildebrand, F. D., Introduction to Numerical Analysis, McGraw-Hill Book Company, Inc., New York, 1956.

25. Hudson, G. E., Am. J. Phys., 21, 362 (1953).

26. Householder, A. S., U.S. Atomic Energy Commission Report, ORNL-455 (Feb. 1950).

27. Cornell, R. G., U. S. Atomic Energy Commission Report. ORNL-2120 (Sept. 1956).

28. Lanczos, C., Applied Analysis, Prentice-Hall, Inc., New York, 1956.

29. O'Kelly, G. D., ed., "Application of Computers to Nuclear and Radiochemistry," Proc. Sympt. (Gatlinburg, Tennessee, Oct. 1962).

30. DeVoe, R., ed., Radiochemical Analysis, Technical Note, NBS-404.

31. Shafer, R. E., Analysis of Multicomponent Radioactive Decay Curve, UCRL-7084-T (1962).

32. Gardener, D. G., Gardner, J. C., Laush, G., and Meinke, W. W., J. Chem. Phys., 31, 978 (1959).

33. "International Dictionary of Applied Mathematics", D. Van Nostrand Co., Inc., 1960.

34. Wylie, C. R., Advanced Engineering Mathematics", 4th Edition, McGraw-Hill, Inc., 1975.

35. Titchmarsh, E. C., Introduction to the Theory of Fourier Integrals Oxford University Press, New York, 1937.

36. Perlis, A. J., U. S. Atomic Energy Commission Report, NP-786 (Sept., 1948).

37. Paley, R. E., and Wiener, N., Fourier Transform in the Complex Domain, American Mathematical Society, 1934.

38. Irving, J., and Mullineux, N., Mathematics in Physics and Engineering, Academic Press, Inc., 1967.

39. Taylor, A. E., Advanced Calculus, Ginn and Company, 1955.

40. Bevington, P. R., Data Reduction and Error Analysis for the Physical Sciences, McGraw-Hill, Inc., 1969.

41. Snedecor, G. W., and Cohran, W. G., Statistical Methods, The Iowa State University Press.

42. Irwin, M., and Freund, J. E., Probability and Statistics for Engineers, Prentice-Hall, Inc., 1965.

43. Chou, Y. L., Probability and Statistics for Decision Making, Holt, Rinehart and Winston, Inc., 1972.

44. Scheild, F., Numerical Analysis, Schaum's outline series, McGraw-Hill, Inc.

45. Carnahan, B., Luther, H. A., and Wilkes, J. O., Applied Numerical Methods, John Wiley and Sons, Inc., 1969.

46. Stark, P. A., Introduction to Numerical Methods, The Macmillan Co., 1972.

47. Abramowitz, M. and Stegun, I. A., Handbook of Mathematical Functions Dover Publications, Inc., New York, 1972.

48. Natl. Bur. Standards, Appl. Math. Ser. 34 (1954), "Tables of the gamma function for complex arguments".

49. Davis, H. T., Tables of the Higher Mathematical Functions, I, Principia Press, Bloomington, Ind., 1933.

50. Whittaker, E. T., and Watson, G. N., A Course of Modern Analysis, Cambridge University Press; Macmillan, New York, 1943.

51. Milne-Thomson, L. M., The Calculas of Finite Differences, Macmillan, London, 1933.

52. Copson, E. T., Theory of Function of a Complex Variable, Clarendon Press, Oxford, 1935.

53. Ebrey, T. G., and Gray, P. R., Nucl. Phys. 61, 479 (1965).

54. Arnell, S. E., Dubois, J., and Almen, O., Nucl. Phys. 6, 196 (1958).

55. Daniel, H., and Schmidt-Rohr, U., Nucl. Phys., 7, 516 (1958).

56. Daniel, H., Schmidt-Rohr, U., and Naturforsch, Z., 12A, 750 (1957).

57. Foley, K. J., Salmon, G. L., and Clegg, A. B., Nucl. Phys. 31, 43 (1962).

58. Bormann, M., Fretwurst, E., Schehka, P., Werge, G., Büttner, H., Lindner, A., and Meldner, H., Nucl. Phys. 63, 438 (1965).

59. Churchill, J. L. W., Jones, W. M., and Hunt, S. E., Nature 172, 460 (1953).

60. Wilkinson, D. H., Phys. Rev. 100, 32 (1955).

61. Ward, A. G., Proc. Cambridge Phil. Soc. 35, 523 (1939).

62. Miller, L. F., "Effects of Radiation Quality on the Radiolysis of Water," M.S. Thesis, Kansas State University, Department of Nuclear Engineering, (1966).

63. Hamming, R. W., Numerical Methods for Scientists and Engineers, McGraw-Hill, Inc., 1973.

64. "Hazards Summary Report" for the Kansas State University TRIGA Mark II Reactor (Jan. 1961).

65. Kansas State University TRIGA Mark II Calibration Data and Operation Notes.

66. Handbook on Nuclear Activation Cross-Section, Technical Reports Series No. 156, IAEA, Vienna, 1974.

APPENDICES

APPENDIX A

Explanation of Stieltjes Integral

The Stieltjes integral involves two functions f and g, each defined on a closed interval [a,b]. It is denoted by

$$\int_a^b f(x)dg(x) \qquad \text{(A-1)}$$

In the special case in which g is the simple function $g(x) = x$, the Stieltjes integral Eq. (A-1) becomes the Riemann integral

$$\int_a^b f(x)dx \qquad \text{(A-2)}$$

Let us divide the interval [a,b] into n number of subintervals. This is done by inserting points between a and b. Thus, suppose

$$a = x_o < x_1 < x_2 < \ldots < x_{n-1} < x_n = b \ .$$

Thus, we have subintervals:

$$[x_0,x_1],\ [x_1,x_2],\ldots,[x_{n-1},\ x_n]$$

Take a set of points x_1', x_2',..., x_n', one in each subinterval as explained above. We then define

$$\int_a^b f(x)dg(x) = \lim_{|p|\to o} \sum_{i=1}^{n} f(x_i') \left[g(x_i)-g(x_{i-1})\right] \qquad \text{(A-3)}$$

Here $|p|$ is the smallest interval of the defined subintervals. If

g is constant on [a,b], all differences $g(x_i) - g(x_{i-1})$ are zero and so we see that

$$\int_a^b f(x)\, dg(x) = 0 \qquad \text{(A-4)}$$

One of the important practical uses of Stieltjes integrals involves the case in which g is a discontinuous function which has a finite number of discontinuities at which it jumps suddenly in value, but remains constant in value in the open intervals between the points of discontinuity, e.g., step functions and impulse functions.

APPENDIX B

Explanation of Eqs. (2.1-2.3)

We want to prove the Eqs. (2.1-2) and (2.1-3); starting with

$$f(t) = \sum_{i=1}^{n} N_i \exp(-\lambda_i t) \ . \qquad \text{(B-1)}$$

According to the properties of the Dirac-delta function (38);

$$\int_0^{\infty} e^{-\lambda t} \delta(\lambda-\lambda_i)d\lambda = e^{-\lambda_i t} \ . \qquad \text{(B-2)}$$

Substitute $e^{-\lambda_i t}$ from Eq. (B-2) into Eq. (B-1)

$$f(t) = \sum_{i=1}^{n} N_i \int_0^{\infty} e^{-\lambda t}\delta(\lambda-\lambda_i)d\lambda \ . \qquad \text{(B-3)}$$

Then by rearrangement;

$$f(t) = \int_0^{\infty} e^{-\lambda t} \sum_{i=1}^{n} N_i\delta(\lambda-\lambda_i)\, d\lambda \ . \qquad \text{(B-4)}$$

Define $h(\lambda)$ such that

$$\frac{dh(\lambda)}{d\lambda} = \sum_{i=1}^{n} N_i\delta(\lambda-\lambda_i)d\lambda \ . \qquad \text{(B-5)}$$

Hence,

$$f(t) = \int_0^{\infty} e^{-\lambda t}\, dh(\lambda) \ . \qquad \text{(B-6)}$$

By looking at Eq. (B-6), we can see that $h(\lambda)$ is a step function with steps at $\lambda_1, \lambda_2,\ldots,\lambda_i$ and with amplitude values of $N_1, N_2,\ldots, N_i$, respectively.

To obtain Eq. (2.1-3), rewrite Eq. (B-4):

$$f(t) = \int_0^\infty e^{-\lambda t} \sum_{i=1}^{n} N_i \delta(\lambda-\lambda_i) d\lambda \ .$$

Define $g(\lambda) = \sum_{i=1}^{n} N_i \delta(\lambda-\lambda_i)$

Hence,

$$f(t) = \int_0^\infty e^{-\lambda t} g(\lambda) \ d\lambda \ . \qquad \text{(B-7)}$$

Thus, $g(\lambda)$ is a sum of delta functions with the values N_i at related points λ_i.

APPENDIX C

Explanation of Eq. (2.1-16)

We want to prove Eq. (2.1-22). According to Eq. (2.1-16)

$$K(\mu) \equiv \frac{1}{\sqrt{2\pi}} \int_{s=-\infty}^{s=+\infty} \exp(-e^s) e^s \, e^{i\mu s} \, ds \, . \tag{C-1}$$

The variable s is transformed by letting $t = e^s$:

$$\exp(-e^s) = \exp(-t) \tag{C-2}$$

$$e^s = t \tag{C-3}$$

$$e^{i\mu s} = t^{i\mu} \tag{C-4}$$

$$ds = dt/t \tag{C-5}$$

Note s varies from $-\infty$ to ∞, t varies from 0 to ∞. Hence,

$$K(\mu) = \frac{1}{\sqrt{2\pi}} \int_{t=0}^{t=+\infty} \exp(-t) t^{i\mu} dt \, . \tag{C-6}$$

But according to Euler's definition of the gamma function (39)

$$\Gamma(z) = \int_{x=0}^{x=+\infty} e^{-x} \, x^{(z-1)} \, dx \tag{C-7}$$

Hence,

$$K(\mu) = \frac{1}{\sqrt{2\pi}} \, \Gamma(1+i\mu) \, . \tag{C-8}$$

APPENDIX D

Explanation of the Computer Programs Used in This Work

D-1 Integration of F(μ)

The following expression

$$F(\mu) = \frac{1}{\sqrt{2\pi}} \int_{o}^{x_o} \{[f^*(x) + f^*(-x)] \cos\mu x + i[f^*(x) - f^*(-x)] \sin\mu x\}dx$$

was programmed for numerical integration. In order to evaluate F(μ) by a numerical method, F(μ) was written in the following form:

$$F(\mu_i) = \frac{1}{\sqrt{2\pi}} \{\sum_{K} [FXP(K) + FXN(K)] \cos(MU(I))\ X(K) + i[FXP(K) - FXN(K)]\ SIN(MU\ (I))\ X(K))\}WX(K)$$

Numerical integration was performed by two different schemes, Trapezoidal method and Simpson's method, respectively. For the first one, the integration weights (WX(K)) were found in the main program, while the second one, a subroutine "FATES" was used to generate the weights for the Simpson's integration method. Since f*(x) and f*(-x) are not usually obtained at the desired points corresponding to x, so a subroutine "INTERP" was used in order to evaluate f*(x) and f*(-x) at the desired points.

D-2 Integration of $G(e^{-y})$

The following expression

$$G(e^{-y}) = \frac{1}{\pi} \int_{o}^{\mu_o} \left(\frac{F_c K_c + F_s K_s}{K_c^2 + K_s^2}\right)\cos y\mu + \frac{F_s K_c - F_c K_s}{K_c^2 + K_s^2} \sin y\mu\right) d\mu$$

was programmed for numerical integration. In order to evaluate $G(e^{-y})$ by a numerical method, $G(e^{-y})$ was written in the following form:

$$G(e^{-LAD(J)}) = \frac{1}{\pi} \sum_{i} \left\{\frac{FR(I)KR(I) + FI(I)KI)I)}{KR^2(I) + KI^2(I)} COS(LAD(J)MU(I)) + \frac{FI(I)KR(I) - FR(I)KI(I)}{KR^2(I) + KI^2(I)} SIN(LAD(J)MU(I)\right\}WMU(I)$$

Numerical integration was performed by two different schemes, Trapezoidal method and Simpson's method. For the first one, the integration weights (WMU(I)) were found in the main program, while for the second one, a subroutine "FATES" was used to generate the weights for the Simpson's method. In the above expressions, F_c and F_s are the real and imaginary parts of $F(\mu)$ and K_c and K_s are the real part and imaginary parts of $\Gamma(1 + i\mu)$, respectively. The function $\Gamma(1 + i\mu)$ was obtained by using "FUNCTION CGAMMA" and K_s and K_c were obtained by using "FUNCTION DIMAG" and "FUNCTION DREAL", respectively.

D-3 Explanation of SUBPROGRAM FATES (IWT, NWT, WTAB, WATES)

The weights factor necessary in the calculation of the following integrals by the Simpson's integration method, were evaluated by this subprogram.

$$F(\mu) = \frac{1}{\sqrt{2\pi}} \int_{x=0}^{x=x_0} \{[f^*(x) + f^*(-x)] \cos\mu x + i\,[f^*(x) - f^*(-x)] \sin\mu x\}\, dx$$

$$G(e^{-y}) = \frac{1}{\pi} \int_{\mu=0}^{\mu=\mu_0} \left(\frac{F_c K_c + F_s K_s}{K_c^2 + K_s^2} \cos y\mu + \frac{F_s K_c - F_c K_s}{K_c^2 + K_s^2} \sin y\mu\right) d\mu$$

The subroutine, which has been used here in order to find weight factors, can be used for two cases, equally spaced points whose logarithms are equally spaced. In the latter case, the points are obtained from one another by successive multipication by a fixed factor.

The procedure is that of modified Simpson's rule (46). When integration weights for only two points are to be calculated, the Trapezoidal rule is applied, while for one point integration the weight is made equal zero.

In order to use Subroutine FATES, it is necessary to define IWT, NWT, WTAB, where the NWT is the number of points and the value of IWT depends on the scale chosen for the integration points. If a linear scale is used, IWT must be defined as IWT1; if logarithmic, IWT must be set equal to a number larger than 1. The following statement-by-statement description of this subroutine has been obtained from (62) and for more detailed discussion the reader is referred to (63).

```
819 WTA = NWT
```

This order makes a floating point number equal to NWT, the number of points in the abscissa list.

```
IF(NWT-2GE.0)GO TO 39
19 WATES(1) = .0
GO TO 259
```

These orders take care of the case in which the list consists of only a single value. The integral in this case is zero, and control goes to 259, which will return control to the main program.

```
39 IF (IWT-2GE.0)GO TO 79
59 WTDEL = (WTAB(1)-WTAB(NWT))/(WTA-1.)
GO TO 99
```

The first order determines whether the list progression is linear or geometric. The second calculates the interval between points of the list for the linear case. This is only one of many ways for doing this.

```
79 WTDEL = LOG(WTAB(1)/WTAB(NWT))/WTA-1.)
99 IF(WTDEL.GE.0.)GO TO 990
119 WTDEL = -WTDEL
```

The first order calculates the factor between points if the interval changes geometrically. The last two order make the interval size positive in all cases. This may or may not be desirable.

```
990 IF(NWT-2) 259,1190,139
1190 WATES(1) = .5*WTDEL
WATES(2) = WATES(1)
GO TO 199
```

This takes care of the case in which only two points are involved in the integration, which is then trapezoidal. The transfer to 199 permits either linear or geometric progression to be assumed. The two cases are not quite the same for two point integration, even though at first thought it would seem they should be.

```
139 NWTA = (WTA/2.+.1)
NWTB = (WTA/2.-1)
NWTC = (WTA/4.+.1)
NWTD = (WTA/4.-.1)
```

These four orders generate parameters to be used in determining whether the number of weights is odd, divisible by 4, or even. WTA is numerically almost identical with NWT, differing at most in the 8'th significant figure. The orders are to construct integers from the number in paranthesis. The important thing is that the integer is always the <u>smaller</u> of the two numbers bracketing the floating point value. Thus, a number divisible by 2 will yield NWTA larger by unity than NWTB. A number not divisible by 2 will yield NWTA = NWTB. The same trick is used also for divisibility by 4.

```
WATES(1) = WTDEL/3.
```

```
WTC = WATES(1)
WATES(NWT) = WATES (1)
```

The first and last weights are given their proper value, and WTC, to be used later, is assigned its value.

```
DO 159 I=1, NWTB
WATES(I+1) = WTDEL + WTC
INDX = NWT-I
WATES(INDX) = WTDEL + WTC
159 WTC = -WTC
```

This group of orders assigns the bulk of the weights their 1,4,2,4,.... structure. Notice the symmetry between WATES(I+1) and WATES(NWT-I). NWTB will be a value such that NWTB = 1 is either the middle value or the lower of two middle values. In the latter case, after this set of orders, the two middle values are either 2*WTDEL/3, so that the middle interval is given incorrectly, or on the low side, or they are 4*WTDEL/3, so that the middle values are weighted too heavily. We must either subtract or add WTDEL/3 to establish weights which either neglect or add in twice the middle interval. Then we must add or subtract weights for the middle interval, which are WTDEL*(-1/24, 13/24, 13/24, -1/24), corresponding to approximating by a cubic, with integration only over the middle interval.

```
WTD = 1./24.
IF(NWTC-NWTD.2E.0)GO TO 1790
```

```
1590 WTD=- WTD
```

The first order establishes the divisor for the correction. The other two orders determine the sign of the correction for the middle interval, which depends on divisibility of NWT by 4.

```
1790 IF(NWTA-NWTB.LE.0)GO TO 194
179 WATES(NWTB) = WATES(NWTB)-WTD*WTDEL
WATES(NWTB+1) = WATES(NWTB+1)+5.*WTD*WTDEL
WATES(NWTD+3) = WATES(NWTB)
WATES(NWTB+2) = WATES(NWTB+1)
```

These orders make the correction, which involves four middle values, when the number of points of inegration is even(i.e., divisible by 2). When NWT is odd, the correction is bypassed.

```
199 IF(IWT-2.LT.0)GO TO 259
219 DO 239 I=1, NWT
239 WATES(I) = WATES(I)*WTAB(I)
259 RETURN
```

These orders complete the subroutine proper. The final modification which they make is multiplication by values of the abscissa for the case in which the mesh is geometric.

```
      SUBROUTINE RATES(IWT,NWT,WTAB,WATES)
      DIMENSION WTAB(100),WATES(100)
  819 WTA=NWT
      IF(NWT-2.GE.0) GO TO 39
   19 WATES(1)=0.
      GO TO 259
   39 IF(IWT-2.GE.0) GO TO 79
   59 WTDEL=(WTAB(1)-WTAB(NWT))/(WTA-1.)
      GO TO 99
   79 WTDEL=ALOG(WTAB(1)/WTAB(NWT))/(WTA-1.)
   99 IF(WTDEL.GE.0.) GO TO 990
  119 WTDEL=-WTDEL
  990 IF(NWT-2) 259,1190,139
 1190 WATES(1)= .5*WTDEL
      WATES(2)=WATES(1)
      GO TO 199
  139 NWTA=(WTA/2.+.1)
      NWTB=(WTA/2.-.1)
      NWTC=(WTA/4.+.1)
      NWTD=(WTA/4.-.1)
      WATES(1)=WTDEL/3.
      WTC=WATES(1)
      WATES(NWT)=WATES(1)
      DO 159 I=1,NWTB
      WATES(I+1)=WTDEL+WTC
      INDX=NWT-I
      WATES(INDX)=WTDEL+WTC
  159 WTC=-WTC
      WTD=1./24.
      IF(NWTC-NWTD.LE.0) GO TO 1790
 1590 WTC=-WTD
 1790 IF(NWTA-NWTB.LE.0) GO TO 199
  179 WATES(NWTB)=WATES(NWTB)-WTD*WTDEL
      WATES(NWTB+1)=WATES(NWTB+1)+5.*WTC*WTDEL
      WATES(NWTB+3)=WATES(NWTB)
      WATES(NWTB+2)=WATES(NWTB+1)
  199 IF(IWT-2.LT.0) GO TO 259
  219 DO 239 I=1,NWT
  239 WATES(I)=WATES(I)*WTAB(I)
  259 RETURN
      END
```

D-4 Explanation of SUBPROGRAM INTERP (IMAXTP, XABCIS, FORDIN, NPTSTP, TVX, TVF)

This computer code was used to interpolate among the various parameters required for the main programs. This program was written by Mr. Cain (36), although it has been revised many times by different people to the form we have used here.

Interpolation for a given point-of-interest was made in this program over a number of interpolation points one less than the length of the interpolation list. The Gaussian arrangement was used whereby points on alternate sides of the point-of-interest were successively used. A polynomial of the same degree as the number of interpolation points minus one was passed through the list points. This subroutine form is SUBROUTINE INTERP(IMAXTP, XABCIS, FORDIN, NPTSTP, TVX, TVF). This subroutine accepts lists up to 101 points long and interpolation order up to order 8. Larger lists and greater order interpolation can be readily obtained by modifying the DIMENSION statement. Arrangements have been made for extremely short lists and for interpolations near one end of the list. Explanation of the computer program variables are given in Table (D-4).

Table D-4. Explanation of Computer Program Variables

Symbol	Explanation
INTERP	Symbolic Name of the Subroutine Subprogram
IMAXTP	Length of Interpolation List
XABCIS	Abcissa of Interpolation List; Must be Entered into Computer in Either Ascending or Descending Order
FORDIN	Ordinate of Interpolation List
NPTSTP	Number of Interpolation Points
TVX	Interpolation Point in Abscissa List
TVF	Desired Interpolated Value in Ordinate List
XOTP	Floating Point Variable Used in Ordering Interpolation Points
INTP	Fixed Point Variable Used in Ordering Interpolation Points; INTP = 1 is the Argument of the XABCIS (and FORDIN) Nearest TVX, INTP = 2 is Next Nearest, Etc.
ATP	Variable Used in Ordering Interpolation Points Made Equal to Absolute Value of Difference Between TVX and Each XABCIS
ITP	Position in List of XABCIS Nearest TVX
INNTP	Integer Oscillating Between +1 and -1 to Obtain the Gaussian Arrangement
XN	Abscissa List Ordered So That Successive Values are at Greater Distances from TVX
FN	Ordinate List Ordered So That Successive Values are at Greater Distances from TVF
IQTP	Variable Which Determines if End of List Has Been Reached
FACT	Factor which Modifies the Dividend Difference

LOGIC DIAGRAM FOR THE INTERPOLATION SUBROUTINE

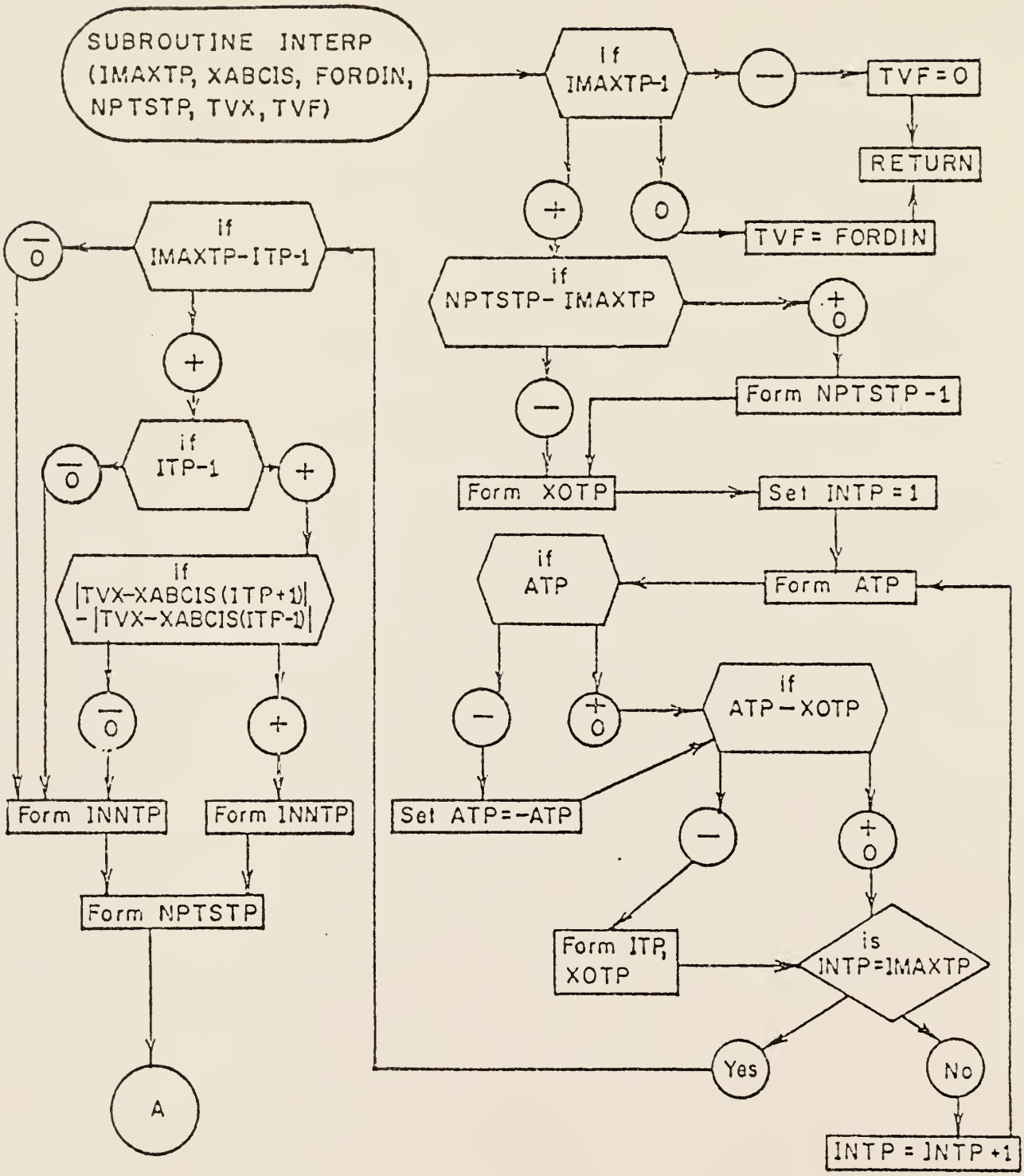

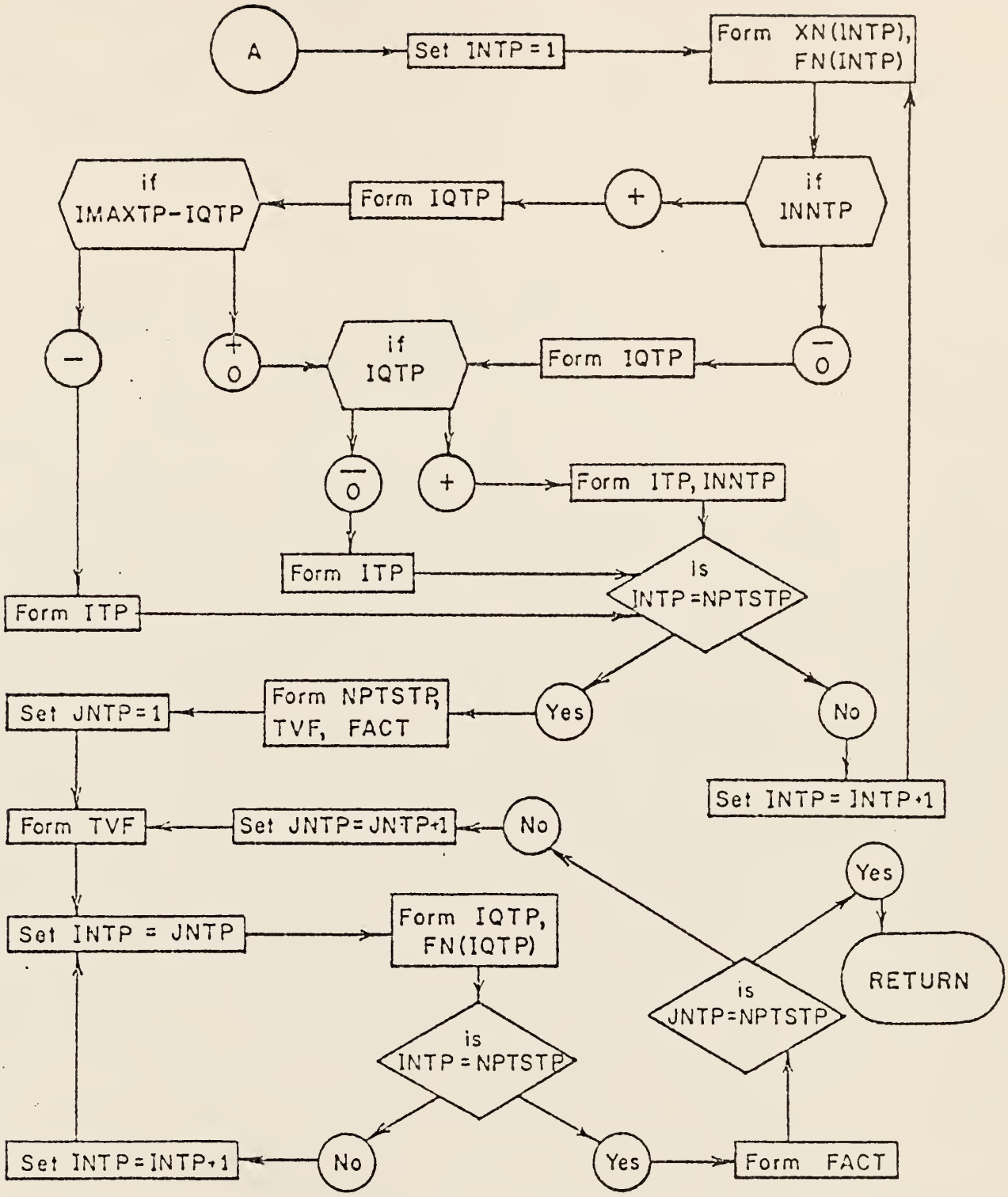
A
Set INTP = 1
Form XN(INTP), FN(INTP)
if INNTP
+
Form IQTP
if IMAXTP-IQTP
−
+ 0
if IQTP
Form IQTP
− 0
− 0
+
Form ITP, INNTP
Form ITP
Form ITP
Is INTP=NPTSTP
Yes
Form NPTSTP, TVF, FACT
Set JNTP=1
No
Set INTP=INTP+1
Form TVF
Set JNTP=JNTP+1
No
Yes
Set INTP = JNTP
Form IQTP, FN(IQTP)
RETURN
is JNTP=NPTSTP
is INTP=NPTSTP
Set INTP=INTP+1
No
Yes
Form FACT

```
      SUBROUTINE INTERP(IMAXTP,XABCIS,FORDIN,NPTSTP,TVX,TVF)
      DIMENSION XABCIS(101),FORDIN(101),XN(8),FN(8)
  800 IF(IMAXTP-1) 810,820,830
  810 TVF=0.
      GO TO 1000
  820 TVF=FORDIN(1)
      GO TO 1000
  830 IF(NPTSTP-IMAXTP) 850,840,840
  840 NPTSTP=IMAXTP-1
  850 XOTP=1.E25
      DO 890 INTP=1,IMAXTP
      ATP=TVX-XABCIS(INTP)
      IF(ATP)860,870,870
  860 ATP=-ATP
  870 IF(ATP-XOTP)880,890,890
  880 ITP=INTP
      XOTP=ATP
  890 CONTINUE
      IF(IMAXTP-ITP-1) 892,892,889
  889 IF(ITP-1) 892,892,891
  891 IF(ABS(TVX-XABCIS(ITP+1))-ABS(TVX-XABCIS(ITP-1))) 892,892,893
  892 INNTP=1
      GO TO 894
  893 INNTP=-1
  894 NPTSTP=NPTSTP+1
      DO 970 INTP=1,NPTSTP
      XN(INTP)=XABCIS(ITP)
      FN(INTP)=FORDIN(ITP)
      IF(INNTP) 900,900,910
  900 IOTP=ITP-INTP
      GO TO 940
  910 IOTP=ITP+INTP
  920 IF(IMAXTP-IOTP) 930,940,940
  930 ITP=ITP-1
      GO TO 970
  940 IF(IOTP) 950,950,960
  950 ITP=ITP+1
      GO TO 970
  960 ITP=IOTP
      INNTP=-INNTP
  970 CONTINUE
      NPTSTP=NPTSTP-1
      TVF=0.
      FAC =1.
      DO 990 JNTP=1,NPTSTP
      TVF=TVF+FAC *FN(1)
      DO 980 INTP=JNTP,NPTSTP
      IOTP=INTP-JNTP+1
  980 FN(IOTP)=(FN(IOTP+1)-FN(IOTP))/(XN(INTP+1)-XN(IOTP))
  990 FAC =FAC *(TVX-XN(JNTP))
 1000 RETURN
      END
```

D-5 Explanation of FUNCTION CGAMMA (R, XIMAG)

The $\Gamma(1 + i\mu)$ was calculated by use of the FUNCTION statement "CGAMMA (R,XIMAG)". However, this function can be used for evaluation of $\Gamma(x + iy)$, just by giving the correspondent value to R and XIMAG.

```
      FUNCTION CGAMMA(R,XIMAG)
C
C        THIS FUNCTION CALCULATES THE GAMMA FUNCTION OF A COMPLEX
C     ARGUMENT AND RETURNS IT IN A COMPLEX*8 VARIABLE.....
C
      COMPLEX*16 CGAMMA,Z,SUBT,DCMPLX,CDLOG
      REAL*8 D,TPI,R,XIMAG,SIGN,DLOG
      DIMENSION D(8)
      DATA D/12.0D0,360.0D0,1260.0D0,1680.0D0,1188.0D0,0.0D0,156.0D0,0.
     1D0/
      DATA TPI/6.283185306/
      D(8)=122400./3617.
      D(6)=360360./691.
      Z=DCMPLX(R,XIMAG)
      SUBT=(0.,0.)
      IF(R.GE.9) GO TO 1
      SUBT=CDLOG(Z)
      Z=Z+1.
1     CGAMMA=(Z-5.D-1)*CDLOG(Z)-Z+5.D-1*DLOG(TPI)
      KT=1
      DO 2 I=1,15,2
      SIGN=(-1)**(KT+1)
      CGAMMA=CGAMMA+SIGN/(D(KT)*Z**I)
2     KT=KT+1
      CGAMMA=CGAMMA-SUBT
      RETURN
      END
```

D-6 Explanation of FUNCTION DIMAG(X)

The imaginary part of $\Gamma(1 + i\mu)$ is evaluated by use of the FUNCTION statement DIMAG (X).

```
FUNCTION DIMAG(X)
COMPLEX*16  X,Y
REAL*8 DIMAG
Y=(0.,-1.0)
DIMAG=Y*X
RETURN
END
```

D-7 Explanation FUNCTION DREAL(X)

The real part of $\Gamma(1 + i\mu)$ were calculated by use of the FUNCTION statement "DREAL(X)".

```
FUNCTION DREAL(X)
COMPLEX*16 X,Y
REAL*8 DREAL
Y=(1.,0.)
DREAL=Y*X
RETURN
END
```

D-8 Computer Program for Plotting the Results

This program is written in Fortran IV language for IBM system 370/158, and CalComp plotter number 770. A complete listing of the program is given here.

```
SUBROUTINE SEMILG(A,B,NPTS)
DIMENSION IBUF(4000),A(250),B(250)
CALL LIMITS(48.,11.,25,6,5)
CALL PLOTS(IBUF,4000)
CALL PLOT(0.,-11.,23)
CALL SCALOG(A,5.0,NPTS,1)
CALL SCALE (B,10.,NPTS,1)
CALL PLOT(1.,.5,23)
CALL AXIS(0.,0.,'Y',+1,10.,90.,B(NPTS+1),B(NPTS+2))
R=-B(NPTS+1)/B(NPTS+2)
CALL LGAXIS(0.,R,'X',-1,5.0,0.,A(NPTS+1),A(NPTS+2))
CALL LGLINE(A,B,NPTS,1,0,1,-1)
CALL PLOT(12.,0.,999)
RETURN
END
```

D-9 Computer Program for Plotting the Data

This program is written in Fortran IV language for IBM system 370/158, and CalComp plotter number 770. A complete listing of the program is given here.

```
      DIMENSION IBUF(2000),T(25),XA(25),XB(25)
      READ(5,8)  (T(M),XA(M),M=1,23)
      CALL LIMITS(20.,24.,25,6,3)
    8 FORMAT(2F10.2)
      CALL PLOTS(IBUF,2000)
      CALL PLOT(0.0,-24.0,-3)
      CALL PLOT(2.0,2.0,-3)
      CALL SCALE(T,8.,23,1)
      CALL SCALOG(XA,5.,23,1)
      CALL AXIS (0.0,0.0,'TIME',-4,8.,0.0,T(24),T(25))
      CALL LGAXIS (0.0,0.0,'ACTIVITY',+8,5.,90.0,XA(24),XA(25))
      CALL LGLINE(T,XA,23,1,1,1,1)
      CALL PLOT(23.,0.,23)
      CALL PLOT (0.0,0.0,999)
      STOP
      END
```

APPENDIX E

Parameter Data for the Figures in Section 3

Explanation of Parameters Used in the FDA Code

1 - NLAM

Number of intervals of λ

2 - LAMS

The first starting value of λ

3 - LAMF

The final value of λ

4 - TEND

Period of time for obtaining data

5 - NXPTS

Number of equal intervals belonging to $[o,x_o]$

6 - MUEND

The value for μ_o

7 - MUPTS

Number of equal intervals belonging to $[o,\mu_o]$

8 - IMAXTP

The number of data points

9 - NPTSTP

The order of interpolation

Table E-1. Various Values of Necessary Parameters Involved in the Obtained Figures.

Fig. No.	NLAM	LAMS	LAMF	TEND	NXPTS	MUEND	MUPTS	IMAXTP	NPTSTP
3.1-1	200	0.001	1.0	1096.6	100	2.0	100	29	3
3.1-2	200	0.001	1.0	1066.6	100	4.0	100	29	3
3.1-3	200	0.001	1.0	1096.6	100	6.0	100	29	3
3.1-4	200	0.001	1.0	1096.6	100	8.0	100	29	3
3.1-5	200	0.001	1.0	1096.6	100	9.0	100	29	3
3.1-6	200	0.001	1.0	1096.6	100	2.0	100	29	3
3.1-7	200	0.001	1.0	1096.6	100	4.0	100	29	3
3.1-8	200	0.001	1.0	1096.6	100	6.0	100	29	3
3.1-9	200	0.001	1.0	1096.6	100	8.0	100	29	3
3.1-10	200	0.001	1.0	1096.6	100	9.0	100	29	3
3.1-11	200	0.010	0.3	1096.6	100	6.0	100	29	3
3.1-12	200	0.010	0.03	1096.6	100	8.0	100	29	3
3.1-13	200	0.001	1.0	1096.6	100	3.0	100	29	3
3.1-14	200	0.001	1.0	1096.6	100	6.0	100	29	3

Table E-1 (continued)

Fig. No.	NLAM	LAMS	LAMF	TEND	NXPTS	MUEND	MUPTS	IMAXTP	NPTSTP
3.1-15	200	0.001	1.0	1096.6	100	3.0	100	29	6
3.1-16	200	0.001	1.0	1096.6	100	6.0	100	29	6
3.1-17	200	0.001	1.0	1096.6	100	3.0	100	29	6
3.1-18	200	0.001	1.0	1096.6	100	6.0	100	29	6
3.1-19	200	0.001	1.0	1096.6	25	6.0	25	29	6
3.1-20	200	0.001	1.0	1096.6	25	8.0	25	29	6
3.2-1	200	0.01	1.0	518.013	100	2.0	100	27	3
3.2-2	200	0.010	1.0	518.013	100	4.0	100	27	3
3.2-3	200	0.001	1.0	518.013	100	6.0	100	27	3
3.2-4	200	0.001	1.0	518.013	100	8.0	100	27	3
3.2-5	200	0.010	1.0	518.013	100	9.0	100	27	3
3.2-6	200	0.001	1.0	518.013	100	2.0	100	27	3
3.2-7	200	0.001	1.0	518.013	100	4.0	100	27	3
3.2-8	200	0.001	1.0	518.013	100	6.0	100	27	3
3.2-9	200	0.001	1.0	518.013	100	8.0	100	27	3
3.2-10	200	0.001	1.0	518.013	100	9.0	100	27	3

Table E-1 (continued)

Fig. No.	NLAM	LAMS	LAMF	TEND	NXPTS	MUEND	MUPTS	IMAXTP	NPTSTP
3.2-11	200	0.01	1.0	190.566	100	2.0	100	23	3
3.2-12	200	0.001	1.0	190.566	100	4.0	100	23	3
3.2-13	200	0.001	1.0	190.566	100	6.0	100	23	3
3.3-1	200	0.001	1.0	1096.6	100	8.0	100	29	3
3.3-2	200	0.001	1.0	1096.6	100	8.0	100	29	3
3.3-3	200	0.001	1.0	1096.6	100	6.0	100	29	3
3.3-4	200	0.001	1.0	1096.6	100	6.0	100	29	3

APPENDIX F

$$\text{Model } f(t) = a_1 e^{b_1 t} + a_2 e^{b_2 t} + a_3 e^{b_3 t}$$

Assume our model, which represents the situation is

$$f(t) = a_1 e^{-b_1 t} + a_2 e^{-b_2 t} + a_3 e^{-b_3 t} \qquad \text{(F-1)}$$

Writing the regression condition

$$R = \sum_{i=1}^{n} (y_i - a_1 e^{-b_1 t_i} - a_2 e^{-b_2 t_i} - a_3 e^{-b_3 t_i})^2 \to \min \qquad \text{(F-2)}$$

Thus we can write

$$\frac{\partial R}{\partial a_1} = \frac{\partial R}{\partial a_2} = \frac{\partial R}{\partial a_3} = \frac{\partial R}{\partial b_1} = \frac{\partial R}{\partial b_2} = \frac{\partial R}{\partial b_3} = 0 \qquad \text{(F-3)}$$

By partial differentiation of R with respect to a_1, a_2, a_3, b_1, b_2 and b_3 and simplifying, we obtain the following normal equations.

$$\sum_{i=1}^{n} (y_i - a_1 e^{b_1 t_i} - a_2 e^{-b_2 t_i} - a_3 e^{-b_3 t_i})\ (e^{-b_1 t_i}) = 0 \qquad \text{(F-4)}$$

$$\sum_{i=1}^{n} (y_i - a_i e^{-b_1 t_i} - a_2 e^{-b_2 t_i} - a_3 e^{-b_3 t_i})\ (e^{-b_2 t_i}) = 0 \qquad \text{(F-5)}$$

$$\sum_{i=1}^{n} (y_i - a_1 e^{-b_1 t_i} - a_2 e^{-b_2 t_i} - a_3 e^{-b_3 t_i})\ (e^{-b_3 t_i}) = 0 \qquad \text{(F-6)}$$

$$\sum_{i=1}^{n} (y_i - a_1 e^{-b_1 t_i} - a_2 e^{-b_2 t_i} - a_3 e^{-b_3 t_i})\ (t_i e^{-b_1 t_i}) = 0 \qquad \text{(F-7)}$$

$$\sum_{i=1}^{n} (y_i - a_1 e^{-b_1 t_i} - a_2 e^{-b_2 t_i} - a_3 e^{-b_3 t_i})\ (t_i\ e^{-b_2 t_i}) = 0 \qquad \text{(F-8)}$$

$$\sum_{i=1}^{n} (y_i - a_1 e^{-b_1 t_i} - a_2 e^{-b_2 t_i} - a_3 e^{-b_3 t_i})\ (t_i\ e^{-b_3 t_i}) = 0 \qquad \text{(F-9)}$$

Let Eqs. F-4,5,6,7,8, and 9 be represented by f_1, f_2, f_3, f_4, f_5 and f_6 respectively. Then

$$f_1(a_1,a_2,a_3,b_1,b_2,b_3) = 0 \qquad \text{(F-10)}$$

$$f_2(a_1,a_2,a_3,b_1,b_2,b_3) = 0 \qquad \text{(F-11)}$$

$$f_3(a_1,a_2,a_3,b_1,b_2,b_3) = 0 \qquad \text{(F-12)}$$

$$f_4(a_1,a_2,a_3,b_1,b_2,b_3) = 0 \qquad \text{(F-13)}$$

$$f_5(a_1,a_2,a_3,b_1,b_2,b_3) = 0 \qquad \text{(F-14)}$$

$$f_6(a_1,a_2,a_3,b_1,b_2,b_3) = 0 \qquad \text{(F-15)}$$

Solution of the Equations by Newton-Raphson's Method

Equations F-10,11,12,13,14 and 15 can be solved numerically for a_1, a_2, a_3, b_1, b_2 and b_3 by using Newton-Rophson's Method. Assume equations f_1, f_2, f_3, f_4, f_5 and f_6 are continous and differentiable. Arrange to obtain the following system of equations.

$$\frac{\partial f_1}{\partial a_1} h + \frac{\partial f_1}{\partial a_2} k + \frac{\partial f_1}{\partial a_3} l + \frac{\partial f_1}{\partial b_1} m + \frac{\partial f_1}{\partial b_2} n + \frac{\partial f_1}{\partial b_3} p = - f_1 \qquad \text{(F-16)}$$

$$\frac{\partial f_2}{\partial a_1} h + \frac{\partial f_2}{\partial a_2} k + \frac{\partial f_2}{\partial a_3} l + \frac{\partial f_2}{\partial b_1} m + \frac{\partial f_2}{\partial b_2} n + \frac{\partial f_2}{\partial b_3} p = - f_2 \qquad \text{(F-17)}$$

$$\frac{\partial f_3}{\partial a_1} h + \frac{\partial f_3}{\partial a_2} k + \frac{\partial f_3}{\partial a_3} l + \frac{\partial f_3}{\partial b_1} m + \frac{\partial f_3}{\partial b_2} n + \frac{\partial f_3}{\partial b_3} p = - f_3 \qquad \text{(F-18)}$$

$$\frac{\partial f_4}{\partial a_1} h + \frac{\partial f_4}{\partial a_2} k + \frac{\partial f_4}{\partial a_3} l + \frac{\partial f_4}{\partial b_1} m + \frac{\partial f_4}{\partial b_2} n + \frac{\partial f_4}{\partial b_3} p = - f_4 \qquad \text{(F-19)}$$

$$\frac{\partial f_5}{\partial a_1} h + \frac{\partial f_5}{\partial a_2} k + \frac{\partial f_5}{\partial a_3} l + \frac{\partial f_5}{\partial b_1} m + \frac{\partial f_5}{\partial b_2} n + \frac{\partial f_5}{\partial b_3} p = - f_5 \qquad \text{(F-20)}$$

$$\frac{\partial f_6}{\partial a_1} h + \frac{\partial f_6}{\partial a_2} k + \frac{\partial f_6}{\partial a_3} l + \frac{\partial f_6}{\partial b_1} m + \frac{\partial f_6}{\partial b_2} n + \frac{\partial f_6}{\partial b_3} p = - f_6 \qquad \text{(F-21)}$$

The above set contains six simultaneous linear equations and six unknown (h,k,l,m,n,p). If the Jacobian of the above system of equation is nonzero, the system of equations has a unique solution. So, we get the Jacobian of above system, J.

$$J = \begin{vmatrix} \frac{\partial f_1}{\partial a_1} & \frac{\partial f_1}{\partial a_2} & \frac{\partial f_1}{\partial a_3} & \frac{\partial f_1}{\partial b_1} & \frac{\partial f_1}{\partial b_2} & \frac{\partial f_1}{\partial b_3} \\ \frac{\partial f_2}{\partial a_1} & \frac{\partial f_2}{\partial a_2} & \frac{\partial f_2}{\partial a_3} & \frac{\partial f_2}{\partial b_1} & \frac{\partial f_2}{\partial b_2} & \frac{\partial f_2}{\partial b_3} \\ \frac{\partial f_3}{\partial a_1} & \frac{\partial f_3}{\partial a_2} & \frac{\partial f_3}{\partial a_3} & \frac{\partial f_3}{\partial b_1} & \frac{\partial f_3}{\partial b_2} & \frac{\partial f_3}{\partial b_3} \\ \frac{\partial f_4}{\partial a_1} & \frac{\partial f_4}{\partial a_2} & \frac{\partial f_4}{\partial a_3} & \frac{\partial f_4}{\partial b_1} & \frac{\partial f_4}{\partial b_2} & \frac{\partial f_4}{\partial b_3} \\ \frac{\partial f_5}{\partial a_1} & \frac{\partial f_5}{\partial a_2} & \frac{\partial f_5}{\partial a_3} & \frac{\partial f_5}{\partial b_1} & \frac{\partial f_5}{\partial b_2} & \frac{\partial f_5}{\partial b_3} \\ \frac{\partial f_6}{\partial a_1} & \frac{\partial f_6}{\partial a_2} & \frac{\partial f_6}{\partial a_3} & \frac{\partial f_6}{\partial b_1} & \frac{\partial f_6}{\partial b_2} & \frac{\partial f_6}{\partial b_3} \end{vmatrix}$$

If $J \neq 0$, k,h,l,m,n and p are obtained by following equations.

$$h = \frac{1}{J} \begin{vmatrix} -f_1 & \frac{\partial f_1}{\partial a_2} & \frac{\partial f_1}{\partial a_3} & \frac{\partial f_1}{\partial b_1} & \frac{\partial f_1}{\partial b_2} & \frac{\partial f_1}{\partial b_3} \\ -f_2 & \frac{\partial f_2}{\partial a_2} & \frac{\partial f_2}{\partial a_3} & \frac{\partial f_2}{\partial b_1} & \frac{\partial f_2}{\partial b_2} & \frac{\partial f_2}{\partial b_3} \\ -f_3 & \frac{\partial f_3}{\partial a_2} & \frac{\partial f_3}{\partial a_3} & \frac{\partial f_3}{\partial b_1} & \frac{\partial f_3}{\partial b_2} & \frac{\partial f_3}{\partial b_3} \\ -f_4 & \frac{\partial f_4}{\partial a_2} & \frac{\partial f_4}{\partial a_3} & \frac{\partial f_4}{\partial b_1} & \frac{\partial f_4}{\partial b_2} & \frac{\partial f_4}{\partial b_3} \\ -f_5 & \frac{\partial f_5}{\partial a_2} & \frac{\partial f_5}{\partial a_3} & \frac{\partial f_5}{\partial b_1} & \frac{\partial f_5}{\partial b_2} & \frac{\partial f_5}{\partial b_3} \\ -f_6 & \frac{\partial f_6}{\partial a_2} & \frac{\partial f_6}{\partial a_3} & \frac{\partial f_6}{\partial b_1} & \frac{\partial f_6}{\partial b_2} & \frac{\partial f_6}{\partial b_3} \end{vmatrix}$$

$$k = \frac{1}{J}$$

$$\begin{vmatrix}
\frac{\partial f_1}{\partial a_1} & -f_1 & \frac{\partial f_1}{\partial a_3} & \frac{\partial f_1}{\partial b_1} & \frac{\partial f_1}{\partial b_2} & \frac{\partial f_1}{\partial b_3} \\
\frac{\partial f_2}{\partial a_1} & -f_2 & \frac{\partial f_2}{\partial a_3} & \frac{\partial f_2}{\partial b_1} & \frac{\partial f_2}{\partial b_2} & \frac{\partial f_2}{\partial b_3} \\
\frac{\partial f_3}{\partial a_1} & -f_3 & \frac{\partial f_3}{\partial a_3} & \frac{\partial f_3}{\partial b_1} & \frac{\partial f_3}{\partial b_2} & \frac{\partial f_3}{\partial b_3} \\
\frac{\partial f_4}{\partial a_1} & -f_4 & \frac{\partial f_4}{\partial a_3} & \frac{\partial f_4}{\partial b_1} & \frac{\partial f_4}{\partial b_2} & \frac{\partial f_4}{\partial b_3} \\
\frac{\partial f_5}{\partial a_1} & -f_5 & \frac{\partial f_5}{\partial a_3} & \frac{\partial f_5}{\partial b_1} & \frac{\partial f_5}{\partial b_2} & \frac{\partial f_5}{\partial b_3} \\
\frac{\partial f_6}{\partial a_1} & -f_6 & \frac{\partial f_6}{\partial a_3} & \frac{\partial f_6}{\partial b_1} & \frac{\partial f_6}{\partial b_2} & \frac{\partial f_6}{\partial b_3}
\end{vmatrix}$$

$$l = \frac{1}{j}$$

$$\begin{vmatrix}
\frac{\partial f_1}{\partial a_1} & \frac{\partial f_1}{\partial a_2} & -f_1 & \frac{\partial f_1}{\partial b_1} & \frac{\partial f_1}{\partial b_2} & \frac{\partial f_1}{\partial b_3} \\
\frac{\partial f_2}{\partial a_1} & \frac{\partial f_2}{\partial a_2} & -f_2 & \frac{\partial f_2}{\partial b_1} & \frac{\partial f_2}{\partial b_2} & \frac{\partial f_2}{\partial b_3} \\
\frac{\partial f_3}{\partial a_1} & \frac{\partial f_3}{\partial a_2} & -f_3 & \frac{\partial f_3}{\partial b_1} & \frac{\partial f_3}{\partial b_2} & \frac{\partial f_3}{\partial b_3} \\
\frac{\partial f_4}{\partial a_1} & \frac{\partial f_4}{\partial a_2} & -f_4 & \frac{\partial f_4}{\partial b_1} & \frac{\partial f_4}{\partial b_2} & \frac{\partial f_4}{\partial b_3} \\
\frac{\partial f_5}{\partial a_1} & \frac{\partial f_5}{\partial a_2} & -f_5 & \frac{\partial f_5}{\partial b_1} & \frac{\partial f_5}{\partial b_2} & \frac{\partial f_5}{\partial b_3} \\
\frac{\partial f_6}{\partial a_1} & \frac{\partial f_6}{\partial a_2} & -f_6 & \frac{\partial f_6}{\partial b_1} & \frac{\partial f_6}{\partial b_2} & \frac{\partial f_6}{\partial b_3}
\end{vmatrix}$$

$$m = \frac{1}{j}\begin{vmatrix} \frac{\partial f_1}{\partial a_1} & \frac{\partial f_1}{\partial a_2} & \frac{\partial f_1}{\partial a_3} & -f_1 & \frac{\partial f_1}{\partial b_2} & \frac{\partial f_1}{\partial b_3} \\ \frac{\partial f_2}{\partial a_1} & \frac{\partial f_2}{\partial a_2} & \frac{\partial f_2}{\partial a_3} & -f_2 & \frac{\partial f_2}{\partial b_2} & \frac{\partial f_2}{\partial b_3} \\ \frac{\partial f_3}{\partial a_1} & \frac{\partial f_3}{\partial a_2} & \frac{\partial f_3}{\partial a_3} & -f_3 & \frac{\partial f_3}{\partial b_2} & \frac{\partial f_3}{\partial b_3} \\ \frac{\partial f_4}{\partial a_1} & \frac{\partial f_4}{\partial a_2} & \frac{\partial f_4}{\partial a_3} & -f_4 & \frac{\partial f_4}{\partial b_2} & \frac{\partial f_4}{\partial b_3} \\ \frac{\partial f_5}{\partial a_1} & \frac{\partial f_5}{\partial a_2} & \frac{\partial f_5}{\partial a_3} & -f_5 & \frac{\partial f_5}{\partial b_2} & \frac{\partial f_5}{\partial b_3} \\ \frac{\partial f_6}{\partial a_1} & \frac{\partial f_6}{\partial a_2} & \frac{\partial f_6}{\partial a_3} & -f_6 & \frac{\partial f_6}{\partial b_2} & \frac{\partial f_6}{\partial b_3} \end{vmatrix}$$

$$n = \frac{1}{j}\begin{vmatrix} \frac{\partial f_1}{\partial a_1} & \frac{\partial f_1}{\partial a_2} & \frac{\partial f_1}{\partial a_3} & \frac{\partial f_1}{\partial b_1} & -f_1 & \frac{\partial f_1}{\partial b_3} \\ \frac{\partial f_2}{\partial a_1} & \frac{\partial f_2}{\partial a_2} & \frac{\partial f_2}{\partial a_3} & \frac{\partial f_2}{\partial b_1} & -f_2 & \frac{\partial f_2}{\partial b_3} \\ \frac{\partial f_3}{\partial a_1} & \frac{\partial f_3}{\partial a_2} & \frac{\partial f_3}{\partial a_3} & \frac{\partial f_3}{\partial b_1} & -f_3 & \frac{\partial f_3}{\partial b_3} \\ \frac{\partial f_4}{\partial a_1} & \frac{\partial f_4}{\partial a_2} & \frac{\partial f_4}{\partial a_3} & \frac{\partial f_4}{\partial b_1} & -f_4 & \frac{\partial f_4}{\partial b_3} \\ \frac{\partial f_5}{\partial a_1} & \frac{\partial f_5}{\partial a_2} & \frac{\partial f_5}{\partial a_3} & \frac{\partial f_5}{\partial b_1} & -f_5 & \frac{\partial f_5}{\partial b_3} \\ \frac{\partial f_6}{\partial a_1} & \frac{\partial f_6}{\partial a_1} & \frac{\partial f_6}{\partial a_3} & \frac{\partial f_6}{\partial b_1} & -f_6 & \frac{\partial f_6}{\partial b_3} \end{vmatrix}$$

$$P = \frac{1}{J} \begin{vmatrix} \frac{\partial f_1}{\partial a_1} & \frac{\partial f_1}{\partial a_2} & \frac{\partial f_1}{\partial a_3} & \frac{\partial f_1}{\partial b_1} & \frac{\partial f_1}{\partial b_2} & -f_1 \\ \frac{\partial f_2}{\partial a_1} & \frac{\partial f_2}{\partial a_2} & \frac{\partial f_2}{\partial a_3} & \frac{\partial f_2}{\partial b_1} & \frac{\partial f_2}{\partial b_2} & -f_2 \\ \frac{\partial f_3}{\partial a_1} & \frac{\partial f_3}{\partial a_2} & \frac{\partial f_3}{\partial a_3} & \frac{\partial f_3}{\partial b_1} & \frac{\partial f_3}{\partial b_2} & -f_3 \\ \frac{\partial f_4}{\partial a_1} & \frac{\partial f_4}{\partial a_2} & \frac{\partial f_4}{\partial a_3} & \frac{\partial f_4}{\partial b_1} & \frac{\partial f_4}{\partial b_2} & -f_4 \\ \frac{\partial f_5}{\partial a_1} & \frac{\partial f_5}{\partial a_2} & \frac{\partial f_5}{\partial a_3} & \frac{\partial f_5}{\partial b_1} & \frac{\partial f_5}{\partial b_2} & -f_5 \\ \frac{\partial f_6}{\partial a_1} & \frac{\partial f_6}{\partial a_2} & \frac{\partial f_6}{\partial a_3} & \frac{\partial f_6}{\partial b_1} & \frac{\partial f_6}{\partial b_2} & -f_6 \end{vmatrix}$$

Having found h,k,l,m,n, and p, we then use

$$a_1^{i+1} = a_1^i + h \qquad \text{(F-22)}$$

$$a_2^{i+1} = a_2^i + k \qquad \text{(F-23)}$$

$$a_3^{i+1} = a_3^i + l \qquad \text{(F-24)}$$

$$b_1^{i+1} = b_1^i + m \qquad \text{(F-25)}$$

$$b_2^{i+1} = b_2^i + n \qquad \text{(F-26)}$$

$$b_3^{i+1} = b_3^i + P \qquad \text{(F-27)}$$

and by an iterative method, the best approximation for a_1, a_2, a_3, b_1, b_2 and b_3 are obtained. As seen for 6 simultanous equations and six unknown we must find 36 partial differentials.

Solution of the Equations by Modified Newton-Raphson's Method

The system of equations can be solved by using modified Newton-Raphson method. Assume some initial values for a_1, a_2, a_3, b_1, b_2, and b_3 as a_1^1, a_2^1, a_3^1, b_1^1, b_2^1, and b_3^1, respectively. Then by using the following equation the new values for the prometers are obtained:

$$a_1^2 = a_1^1 - \frac{f_1(a_1^1, a_2^1, a_3^1, b_1^1, b_2^1, b_3^1)}{f_1(a_1^1, a_2^1, a_3^1, b_1^1, b_2^1, b_3^1)} \qquad \text{(F-28)}$$

$$a_2^2 = a_2^1 - \frac{f_2(a_1^2, a_2^1, a_3^1, b_1^1, b_2^1, b_3^1)}{f_2(a_1^2, a_2^1, a_3^1, b_1^1, b_2^1, b_3^1)} \qquad \text{(F-29)}$$

$$a_3^2 = a_3^1 - \frac{f_3(a_1^2, a_2^2, a_3^1, b_1^1, b_2^1, b_3^1)}{f_3(a_1^2, a_2^2, a_3^1, b_1^1, b_2^1, b_3^1)} \qquad \text{(F-30)}$$

$$b_1^2 = b_1^1 - \frac{f_4(a_1^2, a_2^2, a_3^2, b_1^1, b_2^1, b_3^1)}{f_4(a_1^2, a_2^2, a_3^2, b_1^1, b_2^1, b_3^1)} \qquad \text{(F-31)}$$

$$b_2^2 = b_2^1 - \frac{f_5(a_1^2, a_2^2, a_3^2, b_1^2, b_2^1, b_3^1)}{f_5(a_1^2, a_2^2, a_3^2, b_1^2, b_2^1, b_3^1)} \qquad \text{(F-32)}$$

$$b_3^2 = b_3^1 - \frac{f_6(a_1^2, a_2^2, a_3^2, b_1^2, b_2^2, b_3^1)}{f_6(a_1^2, a_2^2, b_3^2, b_1^2, b_2^2, b_3^1)} \qquad \text{(F-33)}$$

From the above relations, new values, a_1^2, a_2^2, a_3^2, b_1^2, b_2^2,b_3^2 are obtained. Then by repeating the procedure, the best approximate values for a_1, a_2, a_3, b_1, b_2, b_3, are obtained. Choices of f_1, f_2, f_3, f_4, f_5, and f_6 for a_1, a_2, a_3, b_1, b_2 and b_3, respectively, are not aribtirary. One choice causes the solution to diverge, and another causes the solution to converge (46). For six functions in six unknowns there are 6! ways of choosing 6 functions to find 6 unknowns, and often one of these will converge (46).

APPENDIX G

WATID Code

```
C  ********************************    AATI    ********************************
C
C
C
C     CREATED BY S.O. ROWE    9/1/76
C
C      TITLE = TITLE PRINTE AS HEADING
C      NWD= # WORDS IN SPECTRUM
C      ITAG=TAGWORD
C      NCENT= # CENTROIDS DESIRED FOUND AND USED
C      ICENT(JJ)= CENTROIDS USED
C      LW= # CHANNELS IN PEAK TO LEFT OF CENTROID
C      IRW= # CHANNELS IN PEAK TO RIGHT OF CENTROID
C     ITYPE = 0 --FRACTION
C             1 --CONCENTRATION
C             2 --CALCULATE AREA OF PEAK ONLY
C        IPNCH= 0 DONOT PUNCH OUT AREAS
C             = 1 PUNCH OUT KEEP AREAS AND ST. DEV.  (F10.3)
C
C
C        THLF AND THE TIMES MUST BE IN THE SAME UNITS(I.E. SEC,MIN.,ETC.)
C        EFF IS IN PER CENT
C        K = F(FROM CITTON OUTPUT) * 4.0E12
C
C      THIS PROGRAM IS A SUPPLEMENT TO IDENT. IT WILL READ IN NSPEC FILES AT A
C          TIME AND CALCULATE THE AREA OF THE DESIGNATED PEAKS.  IT THEN
C          USES THESE AREAS AS DESIGNATED BY ITYPE
C
C
C
      DIMENSION FACT(4),ICENT(50), DELT(50),TOTAL(500),YAR(50),YPR(50)
      DIMENSION TITLE(17),IARRAY(4096),JARRAY(4096),ITAG(5)
      REAL IARRAY
      DATA FACT/.383333,.341667,.026533,.013757/
C
C   READ IN PEAK INFO AND PEAK
C
      READ(5,1) INPC,NREC,IPNCH
 1000 READ(5,1,END=53) NSPEC,(ITAG(JJ),JJ=1,NSPEC)
      REWIND 11
      CALL READIN(INPC,NREC,NSPEC,ITAG)
      DO 100 ITG=1,NSPEC
      READ(5,3) (TITLE(J),J=1,17)
      READ(5,1) NCENT,(ICENT(JD),JD=1,NCENT)
      READ(5,1) LW,IRW,ITYPE
      IF(LW.EQ.0) GO TO 52
      ITAG=ITYPE
      NPTS=LW+IRW+1
      REWIND 11
      DO 18 LLL=1,NSPEC
      READ(11)IWED,(JARRAY(JZ),JZ=1,IWED)
      IF(IWED .EQ. ITAG(ITG)) GO TO 21
  18  CONTINUE
      GO TO 53
  21  WRITE(6,502)
      IF(ITYPE.NE.1) GO TO 4
C
C   GO IN INFO FOR CONCENTRATION CALCULATION
```

```
C
      READ(5,19)TIAR,TL,TD,FMASS,FF
      READ(5,20)R,THLF,EFF
      FLAM=.693147D/THLF
      TA=1.0-EXP(-FLAM*TIAR)
      TB =EXP(-FLAM*TD)
      TC=1.0-EXP(-FLAM*TL)
      TT=TA*TB*TC
      RR=R
C
C  ***************************************************************************
C    CALC. AREAS BY SUMMATION,K AND KP , AND GREGORY'S
C         (EXPLANATION OF K AND KP METHOD IS IN WRITE UP OF IDENT)
C   MIN AND MAX ARE LOWER AND UPPER BOUNDS OF PEAK WITH CENTROID ICENT(LC)
C
   9   DO 999 LC=1,NCENT
       INC=ICENT(LC)
C ****
C    INSURE LOCATION OF PEAK MAXIMUM
       AXMAX=0.0
       LEFT=INC-7
       JRITE=INC+7
       DO 1111 JXP=LEFT,JRITE
       IF(JARRAY(JXP) .LE. AXMAX) GO TO 1111
       AXMAX=JARRAY(JXP)
       IPOINT=JXP
 1111  CONTINUE
       ICENT(LC)=IPOINT
       INC=IPOINT
C *****
       ITOO= 9*(LC-1) + 1
       MIN=INC-LW
       MAX=INC+IRW
C
C    CALC BACKGROUND EQUATION--AVERAGE 4 PTS EITHER SIDE  OF PEAK LIMITS
C       FOR GREGORY'S AND SUMMATION METHODS
C
       BKL=0.0
       BKR=0.0
       DO 12 LY=1,4
       JL=MIN-LY+1
       JR=MAX+LY-1
       BKL=BKL+JARRAY(JL)
   12  BKR=BKR+JARRAY(JR)
       Y=BKL/4.0
       YY=BKR/4.0
       XX=MAX+2.5
       X=MIN-2.5
       RATIO=(Y+YY)/(2.0*JARRAY(INC))
       BCKG=Y+YY
       ITOP=0
       BM=(YY-Y)/(XX-X)
       BB=YY-BM*XX
C
C  SUBTRACT BCKGND PTS FROM DATA PTS TO GET TRUE PEAK BEFORE SMOOTHING
       DO 14 JA=MIN,MAX
       ARR=JARRAY(JA)
       XX=JA
```

```
      IARRAY(JA)=AVG - SM*XA - SB
      IF(IARRAY(JA) .LT. 0.0) IARRAY(JA)=0.0
   14 CONTINUE
C
C
C     SPECIAL METHOD
C
   10 SUMS=0.0
      SUM=0.0
      NPTS=MAX-MIN+1
      IP=INC-3
      IG=INC+2
      NGROUP=(NPTS-1)/3 +1
      LAST=0
      NVAL=(NGROUP-1)*3
      IF((NPTS-NVAL) .GE. 2) GO TO 13
      NGROUP=NGROUP-1
      LAST=1
   13 CONTINUE
      SUMGT=0.0
C
C
      DO 155 LG=1,NGROUP
      SUMG=0.0
      MNZ=(LG-1)*3 +MIN
      MXZ=MNZ+3
      IF(MXZ .GT. MAX ) MXZ=MAX
      NPZ=MXZ-MNZ+1
      NP2=NPZ-2
      NP1=NPZ-1
      DO 25 LL=MNZ,MXZ
      IX=LL-MNZ+1
   25 DELT(IX)=IARRAY(LL)
      DO 100 JJ=MNZ,MXZ
C
C
      PTS=IARRAY(JJ)
      IF((JJ.EQ.MNZ) .OR. (JJ.EQ.MXZ)) PTS=PTS/2.0
      SUMG=SUMG+PTS
  100 CONTINUE
      IF(NP2.GT.0) NP2=0
      DO 130 JB=1,NP2
      DO 125 JP=1,NP1
  125 DELT(JP)=DELT(JP)-DELT(JP+1)
      SIGN=(-1.0)**JB
      SUMG=SUMG-FACTR(JB)*(DELT(NP1)+SIGN*DELT(1))
      NP1=NP1-1
  130 CONTINUE
      SUMGT=SUMGT+SUMG
  155 CONTINUE
      SUMG=SUMGT
      IF(LAST.EQ.1) SUMG=SUMG+IARRAY(MAX)
      GPTS=MAX-MIN+1
      SIMPS=SUMG+SGN*GPTS*(1.0+GPTS/2.0)/2.0
C
C
C  ****STRAIGHT SUM
C
```

```
      DO 300 KE=MIN,MAX
  300 SUM=SUM+IARRAY(KE)
      SGPKSM=SUM +BCKG*BPTS*((1.0+BPTS/2.))/2.)
C
C     **********
C   K AND K-PRIME METHOD
C     DETERMINES ITS OWN BACKGROUND POINTS
C     **********
C
      SUMS=0.0
      IF(ITER .EQ.1) GO TO 312
      KP=0
      KL=0
      MINLO=MIN-10
      MAXLO=MAX+10
      DO 305 IJZ=MINLO,MAXLO
      KJZ=IJZ-MINLO+1
  305 YAR(KJZ)=JARRAY(IJZ)
      KNPTS=MAXLO-MINLO+1
      IDIST=KNPTS/2
      KINC=LM+II
      CALL SMOOTH(YAR,YPR,KNPTS)
      DO 309  LM=2,IDIST
      XJR1=YPR(KINC-LM)
      XJR2=YPR(KINC-LM-1)
      XJR3=YPR(KINC+LM)
      XJR4=YPR(KINC+LM+1)
      IF((KL.NE.0) .AND. (KP.NE.0)) GO TO 311
      IF(KL.NE.0) GO TO 308
      IF((KINC-LM).LT. 1) GO TO 309
      SIGYP=(.25*XJR1 + .125*YAR(KINC-LM))**.50
      TERM1=XJR1- SIGYP
      IF(TERM1 .LE. XJR2) KL=LM
  308 IF(KP.NE. 0) GO TO 309
      SIGYPR=(.25*XJR3 + .125*YAR(KINC+LM))**.50
      TERM2=XJR3 - SIGYPR
      IF(TERM2 .LE. XJR4) KP=LM
  309 CONTINUE
      IF(KP.EQ. 0) KP=7
      IF(KL .EQ. 0) KL=7
  310 SUMS=0.0
      LF=INC-KL
      INT=INC+KP
      DO 311 JXL=LF,INT
  311 SUMS=SUMS + JARRAY(JXL)
      SUMSKP=SUMS
C
C   DETERMINE # OF PTS IN BCKGND.  AVERAGE 4 PTS UNLESS PT IS NOT SUCH THAT
C        PT(N)-SQRT(PT(N)) < PT(I)-SQRT(PT(I))
C
      IRGHT=1
      ILCNT=1
      ILFLG=0
      IRFLG=0
      BACKL=JARRAY(LF)
      BACKR=JARRAY(IRT)
      TRML=BACKL+SQRT(BACKL)
      TRMR =BACKR+SQRT(BACKR)
```

```
      BCKL=BACKL
      BCKR=BACKR
      DO 316 JOP=1,3
      IF((LF-JOP-1) .LT. 1) GO TO 314
      ARRM1 =JARRAY(LF-JOP  )
      ARRML=JARRAY(LF-JOP-1)
      ARRP  =JARRAY(IRT+JOP)
      ARRP1=JARRAY(IRT+JOP+1)
      BKLPT=ARRM-SQRT(ARRM)
      BKLPT1=ARRM1-SQRT(ARRM1)
      IF((BKLPT .GT. TRML) .AND. (BKLPT1 .GT. TRML)) ILFLG=1
      IF(ILFLG .EQ. 1) GO TO 314
      ILCNT=ILCNT+1
      BCKL=BCKL+BKLPT
  314 IF(IRT+JOP+1 .GT. IRPO) GO TO 316
      BKRPT=ARRP-SQRT(ARRP)
      BKRPT1=ARRP1-SQRT(ARRP1)
      IF((BKRPT .GT. TRMR) .AND. (BKRPT1 .GT. TRMR)) IRFLG=1
      IF(IRFLG .EQ. 1) GO TO 316
      IRCNT=IRCNT+1
      BCKR=BCKR+BKRPT
  316 CONTINUE
      BCK=BCKL/ILCNT + BCKR/IRCNT
      XPTS=KL+KR+1
      SUMS=SUMS + BCK*XPTS/2.0
      SIGMS=SUMSKR+BCK*XPTS*XPTS/4.0)
C     ******
  312 SMCR=SUM
      SUMCR=SUMG
C
C  ***********************************************************************
C
      IF(ITYPE.EQ.1) GO TO 200
      IF(ITYPE.EQ.2) GO TO 215
C
C     STORE IN ARRAY FOR PRINTOUT AT END      (ITYPE=0)
C
      ITER=ITER+1
      IF(ITER.EQ.2) GO TO 90
      SMSKR=SUMS
      SKR=SMCR
      SGSMKR=SGRKSM
      SMGKR=SUMGR
      SIGGKR=SIGRKG
      MIN=IL
      MAX=IC
      GO TO 10
   90 RATIO=SUMGR/SMGKR
      RATIO1=SMCR/SKR
      TOTAL(ITOG)=SKR
      TOTAL(ITOG+1)=SMCR
      TOTAL(ITOG+2)=SQRT(SGSMKR)
      TOTAL(ITOG+3)=SMSKR
      TOTAL(ITOG+4)=SQRT(SIGRKS)
      TOTAL(ITOG+5)=SMGKR
      TOTAL(ITOG+6)=SUMCR
      TOTAL(ITOG+7)=SQRT(SIGSKR)
      TOTAL(ITOG+8)=RATIO
```

```
      GO TO 215
C
C     PERFORM  CON. CALC.
C
  200 IF(SUMCR.GT.0.0) GO TO 210
      SUMCR=SUMCR+BKG
      WRITE(6,6) SUMCR
  210 PPM=PM*SUMCR*FLAM**2.0/(EE*TT*EFF*PMASS)
      PPMS=PS*SUMS*FLAM**2.0/(EE*TT*EFF*PMASS)
      SIGPPM=PPM*SQRT(SIGPKG)/SUMCR
      SIGPPS=PPMS*SQRT(SIGPKS)/SUMS
C
C  OUTPUT DIFFERENT FORMS DEPENDING ON ITYPE
C
  215 WRITE(6,502)
      WRITE(6,11) (TITLE(J),J=1,17)
      IF(ITYPE.EQ.1) WRITE(6,4) TIKR,EE,TI,TT,TD,FLAM,PMASS,EFF
      IF(ITYPE .EQ. 2) WRITE(6,504) ICENT(LC)
      MIN=INC-LW
      MAX=INC+IRM
      IMN=MIN-4
      IMX=MAX+4
      WRITE(6,507) INC,IMN,IMX,INED
      WRITE(6,17)(JARRAY(JE),JE=IMN,IMX)
      WRITE(6,502)
      WRITE(6,2) Y ,YY
      WRITE(6,7) BM,FO
      WRITE(6,505) XL,KP
      WRITE(6,506) ILCNT,IRCNT
      IF(ITYPE.EQ.0) GO TO 999
      WRITE(6,8) SUMCR
      IF(ITYPE.EQ.1) WRITE(6,5) PPM,SIGPPM
      IF(ITYPE.EQ.1) WRITE(6,5) PPMS,SIGPPS
  999 CONTINUE
C
C
C  OUTPUT FRACTION TABLE
C
   52  IF(ITKP .EQ.1) GO TO 1500
       IF(ITKP.EQ.2) GO TO 1500
       WRITE(6,499)
       WRITE(6,501)
       WRITE(6,503)
       WRITE(6,502)
       DO 55 NN=1,NCENT
       MM= 9*NN
       NN=(MM-1)* 5 +1
   55  WRITE(6,500) ICENT(NN),(ITOTAL(JJ),JJ=NN,MM)
       IF(IPNCH .NE. 1) GO TO 1500
       NJD=NCENT*10
       WRITE(7,1) IHED
       WRITE(7,15) (ITOTAL(J +5),J=1,NJD,10)
       WRITE(7,15) (ITOTAL(J +4),J=1,NJD,10)
 1500 CONTINUE
       GO TO 1000
   53  WRITE(6,2000)
       STOP
C
```

```
  1   FORMAT(10I5)
  2   FORMAT(/2X,'BCKGND PTS ARE',2(5X,F10.4))
  3   FORMAT(17A4)
  4   FORMAT(/T40,'INTR.TIME= ',F10.4,T5),'FLUX=',E11.4,/T40,
     +'COUNT TIME=',F10.4,T80,'TT= ',E11.4,/T40,'DECAY TIME=',E11.4,
     +T40,'LAMBDA=',E11.4,/T40 ,'MASS = ',F10.4,T80,'EFF = ',E11.4)
  5   FORMAT(//20X,'CONCENTRATION =',E11.4,' PPM (NO/O2 ',E11.4,' PPM')
  6   FORMAT(/,T30,'TRUE AREA =',F10.3)
  7   FORMAT(/T3,'Y=',F10.3,' X +',F10.3)
  8   FORMAT(/T50,'AREA = ',E11.4)
 11   FORMAT(T30,17A4)
 15   FORMAT(8F10.3)
 16   FORMAT(5X,10F10.2)
 17   FORMAT(5X,10I7)
 19   FORMAT(4F10.3,E10.3)
 20   FORMAT(E10.3,2F10.3)
499   FORMAT(/////,20X,'SUMM ',33X,'KSKP ',27X,'GUESS ',14X,'RATIO',
     1' BCK/PEAKMAX',///)
500   FORMAT(1X,I6,5X,F9.1,5X,F9.1,3X,F9.1,4X,F9.1,3X,F9.1,4X,F9.1,3X,
     +F9.1,5X,F9.1,10X,F5.4)
501   FORMAT(2X,'CENT',8X,'AREA',7X,'6 PT.',5X,' +/-',12X,'AREA',6X,
     +' +/-',9X,'AREA',5X,'6 PT.',3X,'+/- ')
502   FORMAT(////)
503   FORMAT(3X,110('-'))
504   FORMAT(//40X,'CENTROID=',I6)
505   FORMAT(1X,/,10X,'KL=     ',I5,5X,'KP=     ',I5)
506   FORMAT(11X,'NBKPTL=',I5,5X,'NBKPTR=',I5)
507   FORMAT(/5X,'CENTROID= ',I6,10X,'CHANNELS ',I5,' TO ',I5,T30,
     +'TAGWORD= ',I5,/)
2000  FORMAT(///40X,'NORMAL  END OF JOB')
      END
```

```
      SUBROUTINE READIN(WORDS, NRECRD,NSPEC,ITAG)
      DIMENSION Y(50033),ITAG(50)
      INTEGER IARRAY(4096), HEADER, WORDS, HEAD(4)
      LOGICAL*1 JARRAY(16384)
      EQUIVALENCE (IARRAY(1),JARRAY(1))
C
C  *  THIS SUBROUTINE READS  NSPEC FILES OF SIZE WORDS WITH NRECRD PER
C  *    OF A MAGNETIC TAPE WHICH CONTAINS FILES OF TAGWORDS  AND WRITTEN
C  *    BY THE NORTHERN SCIENTIFIC ANALYZER--7 TRACK TAPE
C
      REWIND 3
  615 IHEDKP=7777
      ICNT=0
      IFLAG=0
      IFLCT=0
C
      ICNT=NSPEC
C
C
C     READ SPECTRUM OFF OF TAPE
C
   11 CONTINUE
      IFLCT=IFLCT+1
C  *
C  ***************************************************************************
      IF(WORDS.EQ.0) GO TO 22
      LAST=4*WORDS
      DO 10 II=1,4096
   10 IARRAY (II)=0
C   55555   READ A SPECTRUM
   34 READ(3,89,END=670) (JARRAY(L),L=2,4)
      HEADER=IARRAY(1)/4096
      IF(HEADER.GT.4095)GOTO12
      HEAD(4)=MOD(HEADER,8)
      DO 300 II=2,4
      HEADER=HEADER/8
  300 HEAD(5-II)=MOD(HEADER,8)
      IHED=1000*HEAD(1) +100*HEAD(2) +10*HEAD(3) + HEAD(4)
      IF (NPRCPO) 211,211,212
  211 READ(3,87)((JARRAY(I+J),J=1,3),I=1,LAST,4)
      GO TO 210
  212 READ(3,87) ((JARRAY(I+J),J=1,3),I=1,4096,4)
      IF (WORDS.LE.1024) GO TO 210
      READ(3,88) (JARRAY(L),L=16382,16384)
      READ(3,87) ((JARRAY(I+J),J=1,3),I=4093,8192,4)
      IF (WORDS.LE.2048) GO TO 210
      READ(3,88) (JARRAY(L),L=16382,16384)
      READ(3,87) ((JARRAY(I+J),J=1,3),I=8189,12288,4)
      IF (WORDS.LE.3072) GO TO 210
      READ(3,88) (JARRAY(L),L=16382,16384)
      READ(3,87) ((JARRAY(I+J),J=1,3),I=12285,16384,4)
C
C
C
  210 IF(IHED.EQ.IHEDKP)GO TO 11
      DO 602 JP=1,ICNT
      IF(IHED.EQ. ITAG(JP)) GO TO 655
  602 CONTINUE
```

```
      GO TO 11
  655 IFLAG=IFLAG+1
      IHEOKP=IHED
      WRITE(11) IHED,(IARRAY(JJ),JJ=1,WORDS)
  659 IF(IFLAG.EQ.NSPEC) GO TO 604
      GO TO 11
   22 WRITE(6,501)
      GO TO 199
   12 WRITE(6,200)
      GO TO 199
  604 WRITE(*,605)
      GO TO 199
  670 WRITE(6,675) IFILCT,IHED
   57 FORMAT(12A(12A1))
   58 FORMAT(3A1)
  200 FORMAT('1  NORMAL END - TAPE NUMBER ???? ENCOUNTERED')
  501 FORMAT('1   WORDS  EQUAL  ZERO ---CHECK FIRST CARD IN DATA SET')
  605 FORMAT('1   NORMAL END --- ALL DESIRED FILES FOUND')
  675 FORMAT(/10X,' END OF DATA  TAPE - - #FILES =',I5,' LAST TA=',I5/)
  199 RETURN
      END
```

```
      SUBROUTINE SMOOTH(Y,YP,NPTS)
      DIMENSION Y(50),YP(50)
      IMAX=NPTS-1
      YI=Y(1)
      DO 10 J=1,IMAX
      YP(J)=(YI +2.*Y(J) + Y(J+1))/4.
      YI=Y(J)
   10 CONTINUE
      YP(NPTS)=(YI + 3.*Y(NPTS))/4.0
      RETURN
      END
```

APPENDIX H

Properties of the Functions K(u) and F(u)

We want to show that the real parts of functions $F(\mu)$ and $K(\mu)$, which first appear in Eq. (2.3-12), Section 2, ($F_c(\mu)$ and $K_c(\mu)$) are even with respect to the variable μ, while the imaginary parts are odd with respect to variable μ.

Equation (2.3-7) is the starting point.

$$F(\mu) = [1/(2\pi)^{1/2}] \int_o^{x_o} \{[f^*(x) + f^*(-x)]\cos\mu x + i[f^*(x) - f^*(-x)]\sin\mu x\}dx. \tag{H-1}$$

The real and imaginary part of $F(\mu)$ are termed as $F_c(\mu)$ and $F_s(\mu)$, respectively:

$$F(\mu) = F_c(\mu) + iF_s(\mu) \tag{H-2}$$

Hence,

$$F_c(\mu) = \frac{1}{\sqrt{2\pi}} \int_o^{x_o} [f^*(x) + f^*(-x)] \cos\mu x \, dx \tag{H-3}$$

$$F_s(\mu) = \frac{1}{\sqrt{2\pi}} \int_o^{x_o} [f^*(x) - f^*(-x)] \sin\mu x \, dx \tag{H-4}$$

The following relations are true

$$F_c(\mu) = F_c(-\mu) \tag{H-5}$$

$$F_s(\mu) = -F_s(-\mu) \tag{H-6}$$

$K(\mu)$ is also composed of real and imaginary parts K_c and K_s.

$$K(\mu) = \frac{1}{\sqrt{2\pi}} \int_{-\infty}^{+\infty} \exp(-e^s)\, e^s \exp(i\mu s)\, ds$$

$$= \frac{1}{\sqrt{2\pi}} \int_{-\infty}^{+\infty} \exp(-e^s) e^s \cos(\mu s)\, ds + \frac{i}{\sqrt{2\pi}} \int_{-\infty}^{+\infty} \exp(-e^s) e^s \sin(\mu s)\, ds \qquad \text{(H-7)}$$

$$K(\mu) = K_c(\mu) + iK_s(\mu) \qquad \text{(H-8)}$$

Hence

$$K_c(\mu) = \frac{1}{\sqrt{2\pi}} \int_{-\infty}^{+\infty} \exp(-e^s) e^s \cos(\mu s)\, ds \qquad \text{(H-9)}$$

$$K_s(\mu) = \frac{1}{\sqrt{2\pi}} \int_{-\infty}^{+\infty} \exp(-e^s) e^s \sin(\mu s)\, ds \qquad \text{(H-10)}$$

Also,

$$K_c(\mu) = K_c(-\mu) \qquad \text{(H-11)}$$

$$K_s(\mu) = -K_s(-\mu) \qquad \text{(H-12)}$$

APPENDIX I

Gamma Function and Method of Computation

The gamma function for real and complex arguments plays a great role in both pure and applied mathematics. The gamma function for real arguments has been of great importance in analysis and statistics (48). The complex gamma function has been used for computations in atomic and nuclear physics (48).

The gamma function has several well-known definitions and relationships. One of the most interesting, as well as useful forms, is the infinite product due to F. W. Newman, ascribed also to Schlömilch, and taken by Weierstrass as the definition of $\Gamma(z)$ (48), namely,

$$\frac{1}{\Gamma(z)} = ze^{\gamma z} \prod_{n=1}^{\infty} \{(1 + \frac{z}{n}) e^{-z/n}\} \qquad \text{(I-1)}$$

where γ is Euler's constant ($\gamma \cong 0.577215664901533$). Another definition of $\Gamma(z)$ is given by Gauss's infinite product (also known as Euler's product):

$$\Gamma(z) = \lim_{n\to\infty} \{1.2.3 \ldots (n-1)n^2\} / z(z+1)(z+2) \ldots (z+n-1). \qquad \text{(I-2)}$$

The most familiar definition of $\Gamma(z)$, which is due to Euler, is

$$\Gamma(z) = \int_0^{\infty} e^{-t} t^{z-1} dt; \qquad \text{(I-3)}$$

This holds only for real parts, $R(z)>0$. In Fig. (I-1) a gamma function is shown. The three most important functional relations

are contained in Eqs. (I-4,5 and 6).

$$\Gamma(z+1) = z\Gamma(z) \qquad \text{(I-4)}$$

$$\Gamma(z)\Gamma(1-z) = \pi/\sin\pi z \qquad \text{(I-5)}$$

$$\Gamma(z)\Gamma(z+\tfrac{1}{n})\Gamma(z+\tfrac{2}{n}) \ \ldots\ \Gamma(z+\tfrac{n-1}{n}) = (2\pi)^{\frac{1}{2}(n-1)}\ n^{\frac{1}{2}-nz}\ \Gamma(nz). \qquad \text{(I-6)}$$

For actual computation of $\Gamma(z)$, the most useful formula is the asymptotic expansion due to J. Stirling (48). Actually, A. deMoivre developed the expansion, but Stirling completed the formula by determining the outside constant multiplier. Equations (I-7) and (I-8) are both divergent series, which nevertheless, furnish excellent approximations to $\Gamma(z)$ and $\ln\Gamma(z)$:

$$(z) \cong e^{-z} z^{(z-1/2)}\ (2\pi)^{1/2}\ \{1 + \frac{1}{12z} + \frac{1}{288z^2} - \frac{139}{51840z^3} - \frac{571}{2488320z^4}$$

$$+ \frac{163879}{209018880z^5} + \frac{5246819}{75246796800z^6} - \frac{534703531}{902961561600z^7} + O(\frac{1}{z^8})\}, \qquad \text{(I-7)}$$

$$\ln\ (z) \cong (z-\tfrac{1}{2})\ln z - z + 1/2(\ \ln 2\pi) + \sum_{m=1}^{\infty} \frac{[(-1)^{m-1}]B_m}{2m(2m-1)z^{2m-1}}, \qquad \text{(I-8)}$$

Where B_m denotes the Bernoulli numbers (38,47), i.e.,

$$B_1 = \frac{1}{6},\ B_2 = \frac{1}{30},\ B_3 = \frac{1}{42},\ B_4 = \frac{1}{30},\ B_5 = \frac{5}{66},\ \ldots.$$

The explicit expression for Eq. (I-8) is given by

$$\ln\Gamma(z)\cong(z-\tfrac{1}{2})\ln z-z+\frac{1}{2}\ln(2\pi)+\frac{1}{12z}-\frac{1}{360z^3}+\frac{1}{1260z^5}-\frac{1}{1680z^7}+\frac{1}{1188z^9}$$

$$-\frac{691}{360360z^{11}}+\frac{1}{156z^{13}}-\frac{3617}{122400z^{15}}+\ldots. \qquad \text{(I-9)}$$

Every power of z^{-1} occurs in Eq. (I-7), whereas only odd powers of z^{-1} are involved in Eq. (I-5), so that the asympotitc expansion for $\ln\Gamma(z)$ is usually preferable to that for $\Gamma(z)$, even though the latter series is obtainable from the former merely by the formal operation of taking the exponential. A number of other expansions for $\ln\Gamma(z)$, due to A. R. Forsyth, K. Pearson, E. E. Kummer, A. M. Legendre, and L. Bourguet are given in (49). More discussion for the gamma function, as well as general applications, may be obtained from (50,51,52).

By using the function "CGAMMA" (Appendix D), for x = 1 the function $\ln\Gamma(1+i\mu)$ was calculated from the logarithmic form of Eq. (I-4), namely

$$\ln\Gamma(z) = \ln\Gamma(z+1) - \ln(z). \qquad \text{(I-10)}$$

If $F(\mu)$ (Eq. 2.3-2) is determined for an equidistant set of μ's ranging from 0 to μ_o in steps of $\Delta\mu=0.1$, it is then convenient to use tabulated values of the gamma functions (Table I-1) (48).

In Table (I-1), $\ln\Gamma(1+i\mu)$ values are tabulated instead of $\Gamma(1+i\mu)$ values, thus mathematical expressions are deduced by having the real and imaginary parts of $\ln\Gamma(1+i\mu)$. Thus, the real and imaginary parts of $\Gamma(1+i\mu)$ may be calculated. Consider the complex function $\Gamma(z)$ having the form a+ib where a and b are real and imaginary parts.

$$z = x + iy \tag{I-11}$$

$$\Gamma(z) = \Gamma(x + iy) = a + ib \tag{I-12}$$

Writing complex function $\Gamma(z)$ in polar form yields

$$\Gamma(z) = |\Gamma(z)|e^{i\theta} \tag{I-13}$$

Where $|\Gamma(z)|$ and θ are modulus and argument of complex function $\Gamma(z)$, respectively.

so $$\tan\theta = \frac{b}{a} \tag{I-14}$$

by taking logarithm of both sides of Eq. (I-13), we obtain

$$\ln\Gamma(z) = \ln|\Gamma(z)| + i\theta \tag{I-15}$$

Let $$U \equiv \ln|\Gamma(z)| \tag{I-16}$$

$$V \equiv \theta \tag{I-17}$$

where U and V are the real and imaginary parts of $\ln\Gamma(z)$, respectively (tabulated values in Table I-1).

Hence,

$$\tan V = \tan\theta \tag{I-18}$$

Substituting of Eq. (I-18) in Eq. (I-14) yields

$$b = a \tan V \tag{I-19}$$

but $$|\Gamma(z)| = (a^2 + b^2)^{1/2} \tag{I-20}$$

Hence $$\ln|\Gamma(z)| = \ln(a^2 + b^2)^{1/2} \tag{I-21}$$

substituting Eq. (I-21) in Eq. (I-16) yields

$$U = \ln(a^2 + b^2)^{\frac{1}{2}} = [\ln(a^2 + b^2)]/2 \tag{I-22}$$

so

$$e^{2U} = a^2 + b^2 \tag{I-23}$$

Substituting b from Eq. (I-19) into Eq. (I-23) yields

$$e^{2U} = a^2 + a^2 \tan^2 V = a^2(1 + \tan^2 V) \tag{I-24}$$

or

$$a^2 = \frac{e^{2U}}{1 + \tan^2 V} \tag{I-25}$$

or

$$a = \pm \frac{e^{U}}{(1 + \tan^2 V)^{1/2}} \qquad \text{(I-26)}$$

Thus, substituting a from Eq. (I-26) into Eq. (I-19) yields

$$b = \pm \frac{e^{U} \tan V}{\sqrt{1 + \tan^2 V}} \qquad \text{(I-27)}$$

The signs for a and b are chosen according to the values of V(V=θ), as follows:

V = θ	a	b
$(0, \frac{\pi}{2})$	+	+
$(\frac{\pi}{2}, \pi)$	-	+
$(\pi, \frac{3\pi}{2})$	-	-
$(\frac{3\pi}{2}, 2\pi)$	+	-

Table I-1

Values of $\ln(1+iy)=U+iV$

y	U	V
0.0	0.00000 00000 00	0.00000 00000 00
0.1	- 0.00819 77805 65	- 0.05732 29404 17
0.2	- 0.03247 62923 18	- 0.11230 22226 44
0.3	- 0.07194 62509 00	- 0.16282 06721 68
0.4	- 0.12528 93748 21	- 0.20715 58263 16
0.5	- 0.19094 54991 87	- 0.24405 82989 05
0.6	- 0.26729 00602 14	- 0.27274 38104 91
0.7	- 0.35276 86908 60	- 0.29282 63511 87
0.8	- 0.44597 87835 49	- 0.30422 56029 76
0.9	- 0.54570 51286 05	- 0.30707 43756 42
1.0	- 0.65092 31993 02	- 0.30164 03204 68
1.1	- 0.76078 39588 41	- 0.28826 66142 39
1.2	- 0.87459 04638 95	- 0.26733 05805 81
1.3	- 0.99177 27669 59	- 0.23921 67844 65
1.4	- 1.11186 45664 26	- 0.20430 07241 49
1.5	- 1.23448 30515 47	- 0.16293 97694 80
1.6	- 1.35931 22484 65	- 0.11546 87935 89
1.7	- 1.48608 96127 57	- 0.06219 86983 29
1.8	- 1.61459 53960 00	- 0.00341 66314 77
1.9	- 1.74464 42761 74	+ 0.06061 28742 95
2.0	- 1.87607 87864 31	+ 0.12964 63163 10
2.1	- 2.00876 41504 71	+ 0.20345 94738 33
2.2	- 2.14258 42092 96	+ 0.28184 56584 26
2.3	- 2.27743 81922 04	+ 0.36461 40489 50
2.4	- 2.41323 81411 84	+ 0.45158 81524 41
2.5	- 2.54990 68424 95	+ 0.54260 44058 52
2.6	- 2.68737 61537 50	+ 0.63751 09190 46
2.7	- 2.82558 56411 91	+ 0.73616 63516 79
2.8	- 2.96448 14617 89	+ 0.83843 89130 96
2.9	- 3.10401 54399 01	- 0.94420 54730 39
3.0	- 3.24414 42995 90	+ 1.05335 07710 69
3.1	- 3.38482 90223 77	+ 1.16576 67132 86
3.2	- 3.52603 43067 09	+ 1.28135 17459 32
3.3	- 3.66772 81104 88	+ 1.40001 02965 76
3.4	- 3.80988 12618 23	+ 1.52165 22746 73
3.5	- 3.95246 71261 89	+ 1.64619 26242 69
3.6	- 4.09546 13204 51	+ 1.77355 09225 91
3.7	- 4.23884 14660 71	+ 1.90365 10190 19
3.8	- 4.38258 69752 28	+ 2.03642 07096 93
3.9	- 4.52667 88647 16	+ 2.17179 14436 05
4.0	- 4.67109 95934 09	+ 2.30969 80565 73
4.1	- 4.81583 29197 96	+ 2.45007 85299 47
4.2	- 4.96086 37766 87	+ 2.59287 37713 19
4.3	- 5.10617 81606 63	+ 2.73802 74148 20
4.4	- 5.25176 30342 30	+ 2.88548 56389 27
4.5	- 5.39760 62389 84	+ 3.03519 69949 22
4.6	- 5.54369 64183 04	+ 3.18711 22793 89
4.7	- 5.69002 29483 73	+ 3.34118 43443 27
4.8	- 5.83657 58764 54	+ 3.49736 80186 15
4.9	- 5.98334 58655 32	+ 3.65561 99647 12
5.0	- 6.13032 41445 53	+ 3.81589 85746 15

y	U	V
5.0	- 6.13032 41445 53	+ 3.81589 85746 15
5.1	- 6.27750 24635 84	+ 3.97816 38691 80
5.2	- 6.42487 30533 35	+ 4.14237 74050 86
5.3	- 6.57242 85885 29	+ 4.30850 21885 83
5.4	- 6.72016 21547 03	+ 4.47650 25956 68
5.5	- 6.86806 72180 48	+ 4.64634 42978 70
5.6	- 7.01613 75979 76	+ 4.81799 41933 05
5.7	- 7.16436 74421 06	+ 4.99142 03424 89
5.8	- 7.31275 12034 30	+ 5.16659 19085 37
5.9	- 7.46128 36194 29	+ 5.34347 91013 53
6.0	- 7.60995 96929 51	+ 5.52205 31255 15
6.1	- 7.75877 46746 55	+ 5.70228 61315 35
6.2	- 7.90772 40468 98	+ 5.88415 11702 39
6.3	- 8.05680 35089 04	+ 6.06762 21530 13
6.4	- 8.20600 89631 03	+ 6.25267 37967 05
6.5	- 8.35533 65025 11	+ 6.43928 16159 76
6.6	- 8.50478 23991 25	+ 6.62742 18579 12
6.7	- 8.65434 30931 23	+ 6.81707 14837 44
6.8	- 8.80401 51829 10	+ 7.00820 81345 02
6.9	- 8.95379 54158 79	+ 7.20081 01014 93
7.0	- 9.10368 06798 32	+ 7.39485 62984 36
7.1	- 9.25366 79950 15	+ 7.59032 62351 84
7.2	- 9.40375 45067 08	+ 7.78719 99928 77
7.3	- 9.55393 74783 21	+ 7.98545 82004 68
7.4	- 9.70421 42849 72	+ 8.18508 20125 03
7.5	- 9.85458 24074 86	+ 8.38605 30880 89
7.6	-10.00503 94267 90	+ 8.58835 35709 62
7.7	-10.15558 30186 86	+ 8.79196 60705 87
7.8	-10.30621 09489 48	+ 8.99687 36442 29
7.9	-10.45692 10687 39	+ 9.20305 97799 25
8.0	-10.60771 13103 15	+ 9.41050 83803 12
8.1	-10.75857 96829 95	+ 9.61920 37472 42
8.2	-10.90952 42693 78	+ 9.82913 05671 62
8.3	-11.06054 32217 92	+10.04027 38971 80
8.4	-11.21163 47589 48	+10.25261 91518 09
8.5	-11.36279 71628 04	+10.46615 20903 24
8.6	-11.51402 87756 02	+10.68085 88047 12
8.7	-11.66532 79970 81	+10.89672 57081 77
8.8	-11.81669 32818 48	+11.11373 95241 57
8.9	-11.96812 31369 01	+11.33188 72758 53
9.0	-12.11961 61192 31	+11.55115 62762 02
9.1	-12.27117 08338 67	+11.77153 41103 09
9.2	-12.42278 59312 81	+11.99300 86662 85
9.3	-12.57446 01059 08	+12.21556 80464 79
9.4	-12.72619 20940 29	+12.43920 06390 90
9.5	-12.87798 06720 44	+12.66389 50701 28
9.6	-13.02982 46547 39	+12.88964 02037 08
9.7	-13.18172 28939 51	+13.11642 51346 66
9.8	-13.33367 42765 47	+13.34423 91814 77
9.9	-13.48567 77234 95	+13.57307 18794 55
10.0	-13.63773 21082 47	+13.80291 29742 30

From (48).

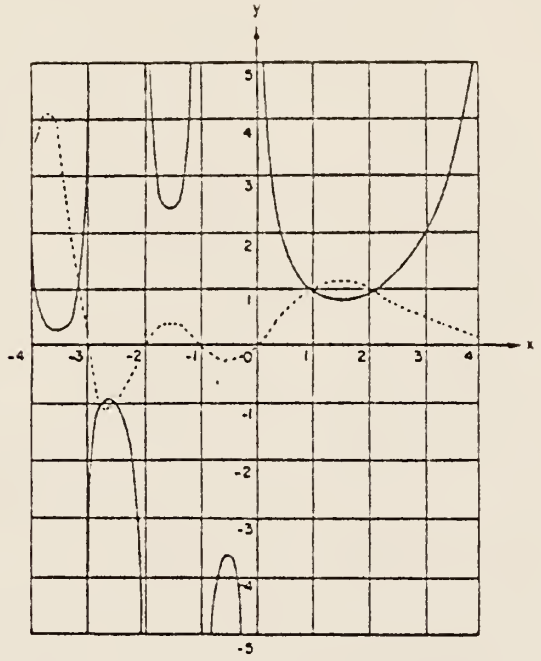

Fig. (I-1). Gamma function.
———, $y=\Gamma(x)$, ----, $y=1\Gamma(x)$ (47).

APPENDIX J

Fourier Decay Analysis Code
(Trapezoidal integration routine)

```
      REAL MUEND,KREAL,KIMAG,IMAG,ML,LAM,LAMF,LAMS,LAC,KR,KI,KIMA
      DIMENSION X(200),MU(200),WX(200),WMU(200),EXP(200),EXN(200)
      DIMENSION XABCIS(49),FCRDIN(49),XN(7),FN(7),CF(10),AF(10)
      DIMENSION LAM(250),G(250),LAC(250)
      DIMENSION FR(200),FI(200),KR(200),KI(200)
      COMPLEX*16  ZZ,CCEXP,CGAMMA
      REAL*8   PASS,CREAL,CIMAG
C**** ..... FORMATS FOR INPUT AND OUTPUT STATEMENTS .....
    1 FORMAT(F10.0,I5)
    2 FORMAT(F10.0,I5)
    3 FORMAT(2I5)
    4 FORMAT(2F10.0)
    5 FORMAT(2E15.8)
    6 FORMAT(4E15.8)
    7 FORMAT(8F10.0)
    8 FORMAT(2F10.3)
    9 FORMAT(//,5X,'NLAM=',I5,5X,'LAMS=',F10.3,5X,'LAMF=',F10.5,//,5X,'T
     1END=',F10.3,5X,'NXPTS=',I5,5X,'MUEND=',F10.3,//,5X,'MUPTS=',I5,5X,
     2'IMAXTP=',I5,5X,'NPTSTP=',I3)
   55 FORMAT(I5,2F10.0)
  310 FORMAT(14X ,9HG(LAMBDA),16X,6HLAMBDA)
  350 FORMAT(12X ,E15.8,10X,E15.8)
      READ(5,3)MODE
C**** ..... READ INPUT PARAMETERS .....
      READ(5,55)NLAM,LAMS,LAMF
      READ(5,1) TEND,NXPTS
      READ(5,2) MUEND,MUPTS
      READ(5,3) IMAXTP,NPTSTP
      WRITE(6,9) NLAM,LAMS,LAMF,TEND,NXPTS,MUEND,MUPTS,IMAXTP,NPTSTP
C**** ..... READ INPUT DATA .....
      READ(5,4) ((XABCIS(I),FCRDIN(I)),I=1,IMAXTP)
      WRITE(6,8)((XABCIS(I),FCRDIN(I)),I=1,IMAXTP)
      IF(MODE.EQ.0)GO TO 150
      READ(5,3)NUMB
      READ(5,7)(CF(I),I=1,NUMB)
      READ(5,7)(AF(I),I=1,NUMB)
      DO 151 J=1,IMAXTP
      FCRDIN(J)=0.0
      DO 151 I=1,NUMB
  151 FCRDIN(J)=FCRDIN(J)+AF(I)*EXP(-CF(I)*XABCIS(J))
  150 DO 3456 I=1,IMAXTP
 3456 FCRDIN(I)=ALOG(FCRDIN(I))
      XPI=3.1415926
      E=(6.2831852)**0.5
      XEND=ALOG(TEND)
      DELX=XEND/FLOAT(NXPTS)
      DELMU=MUEND/FLOAT(MUPTS)
      NUPTS=MUPTS+1
      MXPTS=NXPTS+1
      SUMMU=-DELMU
      SUMX=-DELX
   95 DO 100 L=1,MXPTS
      X(L)=SUMX+DELX
      T1=EXP(X(L))
      T2=1./T1
      CALL INTERP(IMAXTP,XABCIS,FCRDIN,NPTSTP,T1,FX1)
      CALL INTERP(IMAXTP,XABCIS,FCRDIN,NPTSTP,T2,FX2)
      FX1=EXP(FX1)
```

```
      FX2=EXP(FX2)
      EXP(L)=T1*FX1
      EXN(L)=T2*FX2
  100 SUMX=X(L)
      DO 88 I=2,NXPTS
   88 WX(I)=(X(MXPTS)-X(1))/(FLOAT(NXPTS))
      WX(MXPTS)=(X(MXPTS)-X(1))/(FLOAT(NXPTS)*2.)
      WX(1)=WX(MXPTS)
      DO 125 I=1,NUPTS
      MU(I)=SUMMU+DELMU
C**** ..... CALCULATE THE REAL AND IMAGINARY PARTS OF GAMMA .....
      PASS=MU(I)
      ZZ=CDEXP(CGAMMA(1.D0,PASS))/E
      KR(I)=DREAL(ZZ)
      KI(I)=DIMAG(ZZ)
C**** ..... CALCULATE FS AND FC BY NUMERICAL INTEGRATION .....
      FREAL=0.
      FIMAG=0.
      DO 810 K=1,NXPTS
      FREAL=FREAL+(EXP(K)+EXN(K))*DCOS(MU(I)*X(K))*WX(K)
  810 FIMAG=FIMAG+(EXP(K)-EXN(K))*SIN(MU(I)*X(K))*WX(K)
      FR(I)=FREAL*DELX/E
      FI(I)=FIMAG*DELX/E
  125 SUMMU=MU(I)
      DO 888 I=2,NUPTS
  888 WMU(I)=(MU(NUPTS)-MU(1))/(FLOAT(NUPTS))
      WMU(NUPTS)=(MU(NUPTS)-MU(1))/(FLOAT(NUPTS)*2.)
      WMU(1)=WMU(NUPTS)
      LAM(1) = LAMS
      DELX = ALOG((LAMF/LAMS)**(1./(FLOAT(NLAM-1))))
      DO 1211 I=2,NLAM
 1211 LAM(I) = LAMS*EXP(FLOAT(I-1)*DELX)
      WRITE(6,310)
      DO 1000 J=1,NLAM
      GLAM=0.
      LAD(J) = ALOG(1./LAM(J))
      DO 900 I=1,NUPTS
      GLAM = GLAM+((FR(I)*KR(I)+FI(I)*KI(I))*DCOS(LAD(J)*MU(I))+(FI(I)
     1*KR(I)-FR(I)*KI(I))*SIN(LAD(J)*MU(I)))*WMU(I)/((KR(I)**2 +
     2KI(I)**2 ))
  900 CONTINUE
      G(J)=(GLAM/XPI)*DELMU
C**** ..... PRINT OUTPUT .....
 1000 WRITE(6,350) G(J),LAM(J)
      CALL SEMILG(LAM,G,200)
      CALL EXIT
      END
```

```
      SUBROUTINE INTERP(IMAXTP,XABCIS,FORDIN,NPTSTP,TVX,TVF)
      DIMENSION XABCIS(101),FORDIN(101),XN(8),FN(8)
  800 IF(IMAXTP-1) 810,820,830
  810 TVF=0.
      GO TO 1000
  820 TVF=FORDIN(1)
      GO TO 1000
  830 IF(NPTSTP-IMAXTP) 850,840,840
  840 NPTSTP=IMAXTP-1
  850 XOTP=1.E25
      DO 890 INTP=1,IMAXTP
      ATP=TVX-XABCIS(INTP)
      IF(ATP)860,870,870
  860 ATP=-ATP
  870 IF(ATP-XOTP)880,890,890
  880 ITP=INTP
      XOTP=ATP
  890 CONTINUE
      IF(IMAXTP-ITP-1) 892,892,885
  885 IF(ITP-1) 892,892,891
  891 IF(ABS(TVX-XABCIS(ITP+1))-ABS(TVX-XABCIS(ITP-1))) 892,892,893
  892 INNTP=1
      GO TO 894
  893 INNTP=-1
  894 NPTSTP=NPTSTP+1
      DO 970 INTP=1,NPTSTP
      XN(INTP)=XABCIS(ITP)
      FN(INTP)=FORDIN(ITP)
      IF(INNTP) 900,900,910
  900 IGTP=ITP-INTP
      GO TO 940
  910 IGTP=ITP+INTP
  920 IF(IMAXTP-IGTP) 930,940,940
  930 ITP=ITP-1
      GO TO 970
  940 IF(IGTP) 950,950,960
  950 ITP=ITP+1
      GO TO 970
  960 ITP=IGTP
      INNTP=-INNTP
  970 CONTINUE
      NPTSTP=NPTSTP-1
      TVF=0.
      FAC =1.
      DO 990 JNTP=1,NPTSTP
      TVF=TVF+FAC *FN(1)
      DO 980 INTP=JNTP,NPTSTP
      IGTP=INTP-JNTP+1
  980 FN(IGTP)=(FN(IGTP+1)-FN(IGTP))/(XN(INTP+1)-XN(IGTP))
  990 FAC =FAC *(TVX-XN(JNTP))
 1000 RETURN
      END
```

```
SUBROUTINE SEMILG(A,B,NPTS)
DIMENSION IBUF(4000),A(250),B(250)
CALL LIMITS(48.,11.,25.,6.5)
CALL PLOTS(IBUF,4000)
CALL PLOT(0.,-11.,23)
CALL SCALOG(A,5.0,NPTS,1)
CALL SCALE (B,10.,NPTS,1)
CALL PLOT(1.,.5,23)
CALL AXIS(0.,0.,'Y',+1,10.,90.,B(NPTS+1),B(NPTS+2))
R=-B(NPTS+1)/B(NPTS+2)
CALL LGAXIS(0.,R,'X',-1,5.0,0.,A(NPTS+1),A(NPTS+2))
CALL LGLINE(A,B,NPTS,1,0,1,-1)
CALL PLOT(12.,0.,999)
RETURN
END
```

```
      FUNCTION CGAMMA(R,XIMAG)
C
C        THIS FUNCTION CALCULATES THE GAMMA FUNCTION OF A COMPLEX
C     ARGUMENT AND RETURNS IT IN A COMPLEX*8 VARIABLE.....
C
      COMPLEX*16 CGAMMA,Z,SUBT,CCMPLX,CDLCG
      REAL*8 D,TPI,R,XIMAG,SIGN,DLCG
      DIMENSION C(8)
      DATA D/12.000,360.000,1260.000,1680.000,1188.000,0.000,156.000,0.0
     100/
      DATA TPI/6.283185306/
      D(8)=122400./3617.
      C(6)=360360./691.
      Z=DCMPLX(R,XIMAG)
      SUBT=(0.,0.)
      IF(R.GE.9) GO TO 1
      SUBT=CDLCG(Z)
      Z=Z+1.
1     CGAMMA=(Z-5.0-1)*CDLCG(Z)-Z+5.0-1*CLOG(TPI)
      KT=1
      DO 2 I=1,15,2
      SIGN=(-1)**(KT+1)
      CGAMMA=CGAMMA+SIGN/(D(KT)*Z**I)
2     KT=KT+1
      CGAMMA=CGAMMA-SUBT
      RETURN
      END
```

```
      FUNCTION CIMAG(X)
      COMPLEX*16  X,Y
      REAL*8 CIMAG
      Y=(0.,-1.0)
      CIMAG=Y*X
      RETURN
      END
```

```
      FUNCTION DREAL(X)
      COMPLEX*16 X,Y
      REAL*8 DREAL
      Y=(1.,0.)
      DREAL=Y*X
      RETURN
      END
```

APPENDIX K

Fourier Decay Analysis Code
(Simpson's integration routine)

```
      REAL MUEND,KREAL,KIMAG,IMAG,ML,LAM,LAMF,LAMS,LAD,KR,KI,KIMA
      DIMENSION X(200),MU(200),WX(200),WMU(200),EXP(200),EXN(200)
      DIMENSION XABCIS(49),FCRDIN(49),XN(7),FN(7),CF(10),AF(10)
      DIMENSION LAM(250),G(250),LAD(250)
      DIMENSION FR(200),FI(200),KR(200),KI(200)
      COMPLEX*16  ZZ,CDEXP,CGAMMA
      REAL*8   PASS,CREAL,CIMAG
C**** ..... FORMATS FOR INPUT AND OUTPUT STATEMENTS .....
    1 FORMAT(F10.0,I5)
    2 FORMAT(F10.0,I5)
    3 FORMAT(2I5)
    4 FORMAT(2F10.0)
    5 FORMAT(2E15.8)
    6 FORMAT(4E15.8)
    7 FORMAT(8F10.0)
    8 FORMAT(2F10.3)
    9 FORMAT(//,5X,'NLAM=',I5,5X,'LAMS=',F10.3,5X,'LAMF=',F10.5,//,5X,'T
     1END=',F10.3,5X,'NXPTS=',I5,5X,'MUEND=',F10.3,//,5X,'MUPTS=',I5,5X,
     2'IMAXTP=',I5,5X,'NPTSTP=',I3)
   55 FORMAT(I5,2F10.0)
  310 FORMAT(14X ,9HG(LAMBDA),16X,6HLAMBDA)
  350 FORMAT(12X ,E15.8,10X,E15.8)
      READ(5,3)MODE
C**** ..... READ INPUT PARAMETERS .....
      READ(5,55)NLAM,LAMS,LAMF
      READ(5,1) TEND,NXPTS
      READ(5,2) MUEND,MUPTS
      READ(5,3) IMAXTP,NPTSTP
      WRITE(6,9) NLAM,LAMS,LAMF,TEND,NXPTS,MUEND,MUPTS,IMAXTP,NPTSTP
C**** ..... READ INPUT DATA .....
      READ(5,4) ((XABCIS(I),FCRDIN(I)),I=1,IMAXTP)
      IF(MODE.EQ.0)GO TO 150
      READ(5,3)NUMB
      READ(5,7)(CF(I),I=1,NUMB)
      READ(5,7)(AF(I),I=1,NUMB)
      DO 151 J=1,IMAXTP
      FCRDIN(J)=0.0
      DO 151 I=1,NUMB
  151 FCRDIN(J)=FCRDIN(J)+AF(I)*EXP(-CF(I)*XABCIS(J))
      WRITE(6,8)((XABCIS(I),FCRDIN(I)),I=1,IMAXTP)
  150 DO 3456 I=1,IMAXTP
 3456 FCRDIN(I)=ALOG(FCRDIN(I))
      XPI=3.1415926
      E=(6.2831852)**0.5
      XEND=ALOG(TEND)
      DELX=XEND/FLOAT(NXPTS)
      DELMU=MUEND/FLOAT(MUPTS)
      SUMMU=0.
      SUMX=0.
```

```
      DO 100 L=1,NXPTS
      X(L)=SUMX+DELX
      T1=EXP(X(L))
      T2=1./T1
      CALL INTERP(IMAXTP,XABCIS,FORDIN,NPTSTP,T1,FX1)
      CALL INTERP(IMAXTP,XABCIS,FORDIN,NPTSTP,T2,FX2)
      FX1=EXP(FX1)
      FX2=EXP(FX2)
      FXP(L)=T1*FX1
      FXN(L)=T2*FX2
  100 SUMX=X(L)
      CALL RATES (1,NXPTS,X,WX)
      DO 125 I=1,MUPTS
      MU(I)=SUMMU+DELMU
C**** ..... CALCULATE THE REAL AND IMAGINARY PARTS OF GAMMA .....
      PASS=MU(I)
      ZZ=CDEXP(CGAMMA(1.D0,PASS))/E
      KR(I)=DREAL(ZZ)
      KI(I)=DIMAG(ZZ)
C**** ..... CALCULATE FS AND FC BY NUMERICAL INTEGRATION .....
      FREAL=0.
      FIMAG=0.
      DO 810 K=1,NXPTS
      FREAL=FREAL+(FXP(K)+FXN(K))*COS(MU(I)*X(K))*WX(K)
  810 FIMAG=FIMAG+(FXP(K)-FXN(K))*SIN(MU(I)*X(K))*WX(K)
      FR(I)=FREAL*DELX/E
      FI(I)=FIMAG*DELX/E
  125 SUMMU=MU(I)
      CALL RATES (1,MUPTS,WL,WMU)
      LAM(1) = LAMS
      DELX = ALOG((LAMF/LAMS)**(1./(FLOAT(NLAM-1))))
      DO 1211 I=2,NLAM
 1211 LAM(I) = LAMS*EXP(FLOAT(I-1)*DELX)
      WRITE(6,310)
      DO 1000 J=1,NLAM
      GLAM=0.
      LAD(J) = ALOG(1./LAM(J))
      DO 900 I=1,MUPTS
      GLAM = GLAM+((FR(I)*KR(I)+FI(I)*KI(I))*COS(LAD(J)*MU(I))+(FI(I)
     1*KR(I)-FR(I)*KI(I))*SIN(LAD(J)*MU(I)))*WMU(I)/((KR(I)**2 +
     2KI(I)**2 ))
  900 CONTINUE
      G(J)=(GLAM/XPI)*DELMU
C**** ..... PRINT OUTPUT .....
 1000 WRITE(6,350) G(J),LAM(J)
      CALL SEMILG(LAM,G,200)
      CALL EXIT
      END
```

```
      SUBROUTINE INTERP(IMAXTP,XABCIS,FORDIN,NPTSTP,TVX,TVF)
      DIMENSION XABCIS(101),FORDIN(101),XN(8),FN(8)
  800 IF(IMAXTP-1) 810,820,830
  810 TVF=0.
      GO TO 1000
  820 TVF=FORDIN(1)
      GO TO 1000
  830 IF(NPTSTP-IMAXTP) 850,840,840
  840 NPTSTP=IMAXTP-1
  850 XDTP=1.E25
      DO 890 INTP=1,IMAXTP
      ATP=TVX-XABCIS(INTP)
      IF(ATP)860,870,870
  860 ATP=-ATP
  870 IF(ATP-XDTP)880,890,890
  880 ITP=INTP
      XDTP=ATP
  890 CONTINUE
      IF(IMAXTP-ITP-1) 892,892,895
  889 IF(ITP-1) 892,892,891
  891 IF(ABS(TVX-XABCIS(ITP+1))-ABS(TVX-XABCIS(ITP-1))) 892,892,893
  892 INNTP=1
      GO TO 894
  893 INNTP=-1
  894 NPTSTP=NPTSTP+1
      DO 970 INTP=1,NPTSTP
      XN(INTP)=XABCIS(ITP)
      FN(INTP)=FORDIN(ITP)
      IF(INNTP) 900,900,910
  900 IGTP=ITP-INTP
      GO TO 940
  910 IGTP=ITP+INTP
  920 IF(IMAXTP-IGTP) 930,940,940
  930 ITP=ITP-1
      GO TO 970
  940 IF(IGTP) 950,950,960
  950 ITP=ITP+1
      GO TO 970
  960 ITP=IGTP
      INNTP=-INNTP
  970 CONTINUE
      NPTSTP=NPTSTP-1
      TVF=0.
      FAC =1.
      DO 990 JNTP=1,NPTSTP
      TVF=TVF+FAC *FN(1)
      DO 980 INTP=JNTP,NPTSTP
      IGTP=INTP-JNTP+1
  980 FN(IGTP)=(FN(IGTP+1)-FN(IGTP))/(XN(INTP+1)-XN(IGTP))
  990 FAC =FAC *(TVX-XN(JNTP))
 1000 RETURN
      END
```

```
      SUBROUTINE RATES(IWT,NWT,WTAB,WATES)
      DIMENSION WTAB(100),WATES(100)
  819 WTA=NWT
      IF(NWT-2.GE.0) GO TO 39
   19 WATES(1)=0.
      GO TO 259
   39 IF(IWT-2.GE.0) GO TO 79
   59 WTDEL=(WTAB(1)-WTAB(NWT))/(WTA-1.)
      GO TO 99
   79 WTDEL=ALOG(WTAB(1)/WTAB(NWT))/(WTA-1.)
   99 IF(WTDEL.GE.0.) GO TO 990
  119 WTDEL=-WTDEL
  990 IF(NWT-2) 259,1190,139
 1190 WATES(1)= .5*WTDEL
      WATES(2)=WATES(1)
      GO TO 199
  139 NWTA=(WTA/2.+.1)
      NWTB=(WTA/2.-.1)
      NWTC=(WTA/4.+.1)
      NWTC=(WTA/4.-.1)
      WATES(1)=WTDEL/3.
      WTC=WATES(1)
      WATES(NWT)=WATES(1)
      DO 159 I=1,NWTP
      WATES(I+1)=WTDEL+WTC
      INDX=NWT-I
      WATES(INDX)=WTDEL+WTC
  159 WTC=-WTC
      WTD=1./24.
      IF(NWTC-NWTC.LE.0) GO TO 1790
 1590 WTC=-WTD
 1790 IF(NWTA-NWTB.LE.0) GO TO 199
  179 WATES(NWTB)=WATES(NWTB)-WTD*WTDEL
      WATES(NWTB+1)=WATES(NWTB+1)+5.*WTD*WTDEL
      WATES(NWTB+3)=WATES(NWTB)
      WATES(NWTB+2)=WATES(NWTB+1)
  199 IF(IWT-2.LT.0) GO TO 259
  219 DO 239 I=1,NWT
  239 WATES(I)=WATES(I)*WTAB(I)
  259 RETURN
      END
```

```
      FUNCTION CGAMMA(R,XIMAG)
C
C        THIS FUNCTION CALCULATES THE GAMMA FUNCTION OF A COMPLEX
C     ARGUMENT AND RETURNS IT IN A COMPLEX*8 VARIABLE.....
C
      COMPLEX*16 CGAMMA,Z,SUBT,CMPLX,CDLOG
      REAL*8 D,TPI,R,XIMAG,SIGN,DLOG
      DIMENSION C(8)
      DATA C/12.D00,360.D00,1260.D00,1680.D00,1188.D00,0.D00,156.D00,0.D
     1D0/
      DATA TPI/6.28318530D/
      C(8)=122400./3617.
      C(6)=3E0360./691.
      Z=CMPLX(R,XIMAG)
      SUBT=(0.,0.)
      IF(R.GE.9) GO TO 1
      SUBT=CDLOG(Z)
      Z=Z+1.
1     CGAMMA=(Z-5.D-1)*CDLOG(Z)-Z+5.D-1*DLOG(TPI)
      KT=1
      DO 2 I=1,15,2
      SIGN=(-1)**(KT+1)
      CGAMMA=CGAMMA+SIGN/(C(KT)*Z**I)
2     KT=KT+1
      CGAMMA=CGAMMA-SUBT
      RETURN
      END
```

```
      FUNCTION DIMAG(X)
      COMPLEX*16  X,Y
      REAL*8 DIMAG
      Y=(0.,-1.0)
      DIMAG=Y*X
      RETURN
      END
```

```
      FUNCTION DREAL(X)
      COMPLEX*16 X,Y
      REAL*8 DREAL
      Y=(1.,0.)
      DREAL=Y*X
      RETURN
      END
```

```
SUBROUTINE SEMILG(A,B,NPTS)
DIMENSION IBUF(4000),A(250),B(250)
CALL LIMITS(48.,11.,25.6,5)
CALL PLOTS(IBUF,4000)
CALL PLOT(0.,-11.,23)
CALL SCALOG(A,5.0,NPTS,1)
CALL SCALE (B,10.,NPTS,1)
CALL PLOT(1.,5,23)
CALL AXIS(0.,0.,'Y',+1,10.,90.,B(NPTS+1),B(NPTS+2))
R=-B(NPTS+1)/B(NPTS+2)
CALL LGAXIS(0.,R,'X',-1,5.0,0.,A(NPTS+1),A(NPTS+2))
CALL LGLINE(A,B,NPTS,1,0.1,-1)
CALL PLOT(12.,0.,999)
RETURN
END
```

APPENDIX L

Parameter Data for the Figures Obtained by FDA in Section 6.

Table L-1. Parameter Data for the Figures Obtained by FDA in Section 6.

Fig. No.	NLAM	LAMS	LAMF	TEND	NXPTS	MUEND	MUPTS	IMAXTP	NPTSTP
6.5	200	0.001	10.	40.16	100	2.0	100	8	6
6.6	200	0.001	10.	40.16	100	4.0	100	8	6
6.8	200	0.001	10.	156.700	100	1.0	100	23	6
6.9	200	0.001	10.	156.700	100	3.0	100	23	6
6.10	200	0.001	10.	29.350	100	2.0	100	7	6
6.11	200	0.001	10.	29.350	100	4.0	100	7	6
6.12	200	0.001	10.	28.22	100	1.0	100	7	6
6.13	200	0.001	10.	28.22	100	3.0	100	7	6
6.15	200	0.001	10.	124.250	100	1.0	100	25	6
6.16	200	0.001	10.	124.250	100	3.0	100	25	6
6.17	200	0.001	10.	24.300	100	1.0	100	6	6
6.18	200	0.001	10.	24.300	100	3.0	100	6	6
6.19	200	0.001	10.	25.500	100	1.0	100	5	6
6.20	200	0.001	10.	25.500	100	3.0	100	5	6

APPENDIX M

Iterative Method Code

```
      IMPLICIT REAL*8(A-H,O-Z)
      REAL*4 EPS
      COMMON/DATA1/N
      COMMON/DATA2/X(40),Y(40)
      COMMON/DATA3/W(40)
      EXTERNAL FCT
      N=12
      READ(5,222)  (X(I),Y(I),I=1,N)
  222 FORMAT(2F10.0)
      IEND=50
      EPS=1.E-3
      XRI=-1.D0
      XLI=-0.D0
      CALL DRTMI(B,F,FCT,XLI,XRI,EPS,IEND,IER,KT)
      IF(IER.EQ.0)GO TO 77
      PRINT 76,IEND
   76 FORMAT(//1X,'NO CONVERGENT B COULD BE FOUND WITH ',I2,' ITERATIONS
     1')
   77 PRINT 54
   54 FORMAT(//1X,'THE PARAMETERS FOR FITTING Y = A*(EXP(B*X))')
      PRINT 55,B
   55 FORMAT(2X,'B=',F10.5//)
      PRINT 56,KT
   56 FORMAT(1X,'TOTAL NUMBER OF ITERATIONS = ',I2)
      STOP
      END
```

```
      REAL FUNCTION FCT*8(B)
      IMPLICIT REAL*8(A-H,O-Z)
      COMMON/DATA1/N
      COMMON/DATA2/X(40),Y(40)
      COMMON/DATA3/W(40)
      FB1=0.D0
      FB2=0.D0
      FB3=0.D0
      FB4=0.D0
      DO 11 I=1,N
      W(I)=1./Y(I)
      FB1=FB1+W(I)*X(I)*Y(I)*DEXP(B*X(I))
      FB2=FB2+W(I)*((DEXP(B*X(I)))**2)
      FB3=FB3+W(I)*Y(I)*(DEXP(B*X(I)))
      FB4=FB4+W(I)*X(I)*((DEXP(B*X(I)))**2)
   11 CONTINUE
      FCT=FB1*FB2-FB3*FB4
      RETURN
      END
```

```
C                                                                       ORTM  10
C     ...................................................................ORTM  20
C                                                                       ORTM  30
C        SUBROUTINE ORTMI                                               ORTM  40
C                                                                       ORTM  50
C        PURPOSE                                                        ORTM  60
C           TO SOLVE GENERAL NONLINEAR EQUATIONS OF THE FORM FCT(X)=0   ORTM  70
C           BY MEANS OF MUELLER-S ITERATION METHOD.                     ORTM  80
C                                                                       ORTM  90
C        USAGE                                                          ORTM 100
C           CALL ORTMI (X,F,FCT,XLI,XRI,EPS,IEND,IER)                   ORTM 110
C           PARAMETER FCT REQUIRES AN EXTERNAL STATEMENT.               ORTM 120
C                                                                       ORTM 130
C        DESCRIPTION OF PARAMETERS                                      ORTM 140
C           X      - DOUBLE PRECISION RESULTANT ROOT OF EQUATION        ORTM 150
C                    FCT(X)=0.                                          ORTM 160
C           F      - DOUBLE PRECISION RESULTANT FUNCTION VALUE          ORTM 170
C                    AT ROOT X.                                         ORTM 180
C           FCT    - NAME OF THE EXTERNAL DOUBLE PRECISION FUNCTION     ORTM 190
C                    SUBPROGRAM USED.                                   ORTM 200
C           XLI    - DOUBLE PRECISION INPUT VALUE WHICH SPECIFIES THE   ORTM 210
C                    INITIAL LEFT BOUND OF THE ROOT X.                  ORTM 220
C           XRI    - DOUBLE PRECISION INPUT VALUE WHICH SPECIFIES THE   ORTM 230
C                    INITIAL RIGHT BOUND OF THE ROOT X.                 ORTM 240
C           EPS    - SINGLE PRECISION INPUT VALUE WHICH SPECIFIES THE   ORTM 250
C                    UPPER BOUND OF THE ERROR OF RESULT X.              ORTM 260
C           I      - I-TH ITERATION
C           IEND   - MAXIMUM NUMBER OF ITERATION STEPS SPECIFIED.       ORTM 270
C           IER    - RESULTANT ERROR PARAMETER CODED AS FOLLOWS         ORTM 280
C                      IER=0 - NO ERROR,                                ORTM 290
C                      IER=1 - NO CONVERGENCE AFTER IEND ITERATION STEPS ORTM 300
C                              FOLLOWED BY IEND SUCCESSIVE STEPS OF     ORTM 310
C                              BISECTION,                               ORTM 320
C                      IER=2 - BASIC ASSUMPTION FCT(XLI)*FCT(XRI) LESS  ORTM 330
C                              THAN OR EQUAL TO ZERO IS NOT SATISFIED.  ORTM 340
C                                                                       ORTM 350
C        REMARKS                                                        ORTM 360
C           THE PROCEDURE ASSUMES THAT FUNCTION VALUES AT INITIAL       ORTM 370
C           BOUNDS XLI AND XRI HAVE NOT THE SAME SIGN. IF THIS BASIC    ORTM 380
C           ASSUMPTION IS NOT SATISFIED BY INPUT VALUES XLI AND XRI, THEORTM 390
C           PROCEDURE IS BYPASSED AND GIVES THE ERROR MESSAGE IER=2.    ORTM 400
C                                                                       ORTM 410
C        SUBROUTINES AND FUNCTION SUBPROGRAMS REQUIRED                  ORTM 420
C           THE EXTERNAL DOUBLE PRECISION FUNCTION SUBPROGRAM FCT(X)    ORTM 430
C           MUST BE FURNISHED BY THE USER.                              ORTM 440
C                                                                       ORTM 450
C        METHOD                                                         ORTM 460
C           SOLUTION OF EQUATION FCT(X)=0 IS DONE BY MEANS OF MUELLER-S ORTM 470
C           ITERATION METHOD OF SUCCESSIVE BISECTIONS AND INVERSE       ORTM 480
C           PARABOLIC INTERPOLATION, WHICH STARTS AT THE INITIAL BOUNDS ORTM 490
C           XLI AND XRI. CONVERGENCE IS QUADRATIC IF THE DERIVATIVE OF  ORTM 500
C           FCT(X) AT ROOT X IS NOT EQUAL TO ZERO. ONE ITERATION STEP   ORTM 510
C           REQUIRES TWO EVALUATIONS OF FCT(X). FOR TEST ON SATISFACTORYORTM 520
C           ACCURACY SEE FORMULAE (3,4) OF MATHEMATICAL DESCRIPTION.    ORTM 530
C           FOR REFERENCE, SEE G. K. KRISTIANSEN, ZERO OF ARBITRARY     ORTM 540
C           FUNCTION, BIT, VOL. 3 (1963), PP.205-206.                   ORTM 550
C                                                                       ORTM 560
C     ...................................................................ORTM 570
```

```
C                                                                       DRTM 580
      SUBROUTINE DRTMI(X,F,FCT,XLI,XRI,EPS,IEND,IER,I)
C                                                                       DRTM 600
C                                                                       DRTM 610
      DOUBLE PRECISION X,F,FCT,XLI,XRI,XL,XR,FL,FR,TOL,TOLF,A,DX,XM,FM  DRTM 620
C                                                                       DRTM 630
C     PREPARE ITERATION                                                 DRTM 640
      IER=0                                                             DRTM 650
      XL=XLI                                                            DRTM 660
      XR=XRI                                                            DRTM 670
      X=XL                                                              DRTM 680
      TOL=X                                                             DRTM 690
      F=FCT(TOL)                                                        DRTM 700
      IF(F)1,16,1                                                       DRTM 710
    1 FL=F                                                              DRTM 720
      X=XR                                                              DRTM 730
      TOL=X                                                             DRTM 740
      F=FCT(TOL)                                                        DRTM 750
      IF(F)2,16,2                                                       DRTM 760
    2 FR=F                                                              DRTM 770
      IF(DSIGN(1.D0,FL)+DSIGN(1.D0,FR))25,3,25                          DRTM 780
C                                                                       DRTM 790
C     BASIC ASSUMPTION FL*FR LESS THAN 0 IS SATISFIED.                  DRTM 800
C     GENERATE TOLERANCE FOR FUNCTION VALUES.                           DRTM 810
    3 I=0                                                               DRTM 820
      TOLF=100.*EPS                                                     DRTM 830
C                                                                       DRTM 840
C                                                                       DRTM 850
C     START ITERATION LOOP                                              DRTM 860
    4 I=I+1                                                             DRTM 870
C                                                                       DRTM 880
C     START BISECTION LOOP                                              DRTM 890
      DO 13 KT=1,IEND                                                   
      X=.5D0*(XL+XR)                                                    DRTM 910
      TOL=X                                                             DRTM 920
      F=FCT(TOL)                                                        DRTM 930
      IF(F)5,16,5                                                       DRTM 940
    5 IF(DSIGN(1.D0,F)+DSIGN(1.D0,FR))7,6,7                             DRTM 950
C                                                                       DRTM 960
C     INTERCHANGE XL AND XR IN ORDER TO GET THE SAME SIGN IN F AND FR   DRTM 970
    6 TOL=XL                                                            DRTM 980
      XL=XR                                                             DRTM 990
      XR=TOL                                                            DRTM1000
      TOL=FL                                                            DRTM1010
      FL=FR                                                             DRTM1020
      FR=TOL                                                            DRTM1030
    7 TOL=F-FL                                                          DRTM1040
      A=F*TOL                                                           DRTM1050
      A=A+A                                                             DRTM1060
      IF(A-FR*(FR-FL))8,9,9                                             DRTM1070
    8 IF(I-IEND)17,17,9                                                 DRTM1080
    9 XR=X                                                              DRTM1090
      FR=F                                                              DRTM1100
C                                                                       DRTM1110
C     TEST ON SATISFACTORY ACCURACY IN BISECTION LOOP                   DRTM1120
      TOL=EPS                                                           DRTM1130
      A=DABS(XR)                                                        DRTM1140
      IF(A-1.D0)11,11,10                                                DRTM1150
```

```
   10 TOL=TOL*A                                                          DRTM1160
   11 IF(DABS(XR-XL)-TOL)12,12,13                                        DRTM1170
   12 IF(DABS(FR-FL)-TOLF)14,14,13                                       DRTM1180
   13 CONTINUE                                                           DRTM1190
C     END OF BISECTION LOOP                                             DRTM1200
C                                                                       DRTM1210
C     NO CONVERGENCE AFTER IEND ITERATION STEPS FOLLOWED BY IEND        DRTM1220
C     SUCCESSIVE STEPS OF BISECTION OR STEADILY INCREASING FUNCTION     DRTM1230
C     VALUES AT RIGHT BOUNDS. ERROR RETURN.                             DRTM1240
      IER=1                                                             DRTM1250
   14 IF(DABS(FR)-DABS(FL))16,16,15                                     DRTM1260
   15 X=XL                                                              DRTM1270
      F=FL                                                              DRTM1280
   16 RETURN                                                            DRTM1290
C                                                                       DRTM1300
C     COMPUTATION OF ITERATED X-VALUE BY INVERSE PARABOLIC INTERPOLATIONDRTM1310
   17 A=FR-F                                                            DRTM1320
      DX=(X-XL)*FL*(1.D0+F*(A-TOL)/(A*(FR-FL)))/TOL                     DRTM1330
      XM=X                                                              DRTM1340
      FM=F                                                              DRTM1350
      X=XL-DX                                                           DRTM1360
      TOL=X                                                             DRTM1370
      F=FCT(TOL)                                                        DRTM1380
      IF(F)18,16,18                                                     DRTM1390
C                                                                       DRTM1400
C     TEST ON SATISFACTORY ACCURACY IN ITERATION LOOP                   DRTM1410
   18 TOL=EPS                                                           DRTM1420
      A=DABS(X)                                                         DRTM1430
      IF(A-1.D0)20,20,19                                                DRTM1440
   19 TOL=TOL*A                                                         DRTM1450
   20 IF(DABS(DX)-TOL)21,21,22                                          DRTM1460
   21 IF(DABS(F)-TOLF)16,16,22                                          DRTM1470
C                                                                       DRTM1480
C     PREPARATION OF NEXT BISECTION LOOP                                DRTM1490
   22 IF(DSIGN(1.D0,F)+DSIGN(1.D0,FL))24,23,24                          DRTM1500
   23 XR=X                                                              DRTM1510
      FR=F                                                              DRTM1520
      PRINT 49
   49 FORMAT(///1X,'ITERATION',5X,'ROOT OF FCT')
      PRINT 50,I,XR
   50 FORMAT(6X,I2,9X,F8.4)
      GO TO 4                                                           DRTM1530
   24 XL=X                                                              DRTM1540
      FL=F                                                              DRTM1550
      XR=XM                                                             DRTM1560
      FR=FM                                                             DRTM1570
      PRINT 51
   51 FORMAT(///1X,'ITERATION',5X,'ROOT OF FCT')
      PRINT 52,I,XL
   52 FORMAT(6X,I2,9X,F8.4)
      GO TO 4                                                           DRTM1580
C     END OF ITERATION LOOP                                             DRTM1590
C                                                                       DRTM1600
C                                                                       DRTM1610
C     ERROR RETURN IN CASE OF WRONG INPUT DATA                          DRTM1620
   25 IER=2                                                             DRTM1630
      RETURN                                                            DRTM1640
      END                                                               DRTM1650
```

RESOLUTION OF COMPOSITE RADIOACTIVE DECAY CURVES BY FOURIER DECAY ANALYSIS

by

ALI JOWZANI-MOGHADDAM

B. S., National University of Iran, 1975

AN ABSTRACT OF
A MASTER'S THESIS

submitted in partial fulfillment of the

requirements for the degree

MASTER OF SCIENCE

Department of Nuclear Engineering

KANSAS STATE UNIVERSITY
Manhattan, Kansas

1978

ABSTRACT

The purpose of this work was to investigate the Fourier Decay analysis (FDA) method for the analysis of multicomponent decay curves for finding coefficients and exponents. A computer code was developed in order to make the analysis possible. This code consists of two numerical integrations, an interpolation routine, and gamma function calculation routine. This code is applicable to any set of composed of independent exponentials data. The analysis results are in the form of a plot as well as numbers. First for testing the FDA method, data were constructed. All the problems involved in the FDA method, such as, numerical integration, cutoff error, interpolation effect, and data scatter were investigated.

The FDA method was used for determination of half-life of ^{13}N. The data were obtained by fast neutron irradiation of the samples of NH_4NO_3 and wheat in the KSU TRIGA Mark II nuclear reactor. The annihiliation radiation gamma rays were detected by a Ge(Li) detector. For each sample the data were accumulated and were analyzed by the FDA method, an iterative least squares method and a transform (by logarithm) least squares method. The results obtained by FDA were much better than those obtained by the other methods. The average half life of ^{13}N (from NH_4NO_3) by the FDA method was 9.93 m compared to that for the iterative method, 11.54 m, and the TLS method, 12.93 m. For wheat, the average half life of ^{13}N was 10.12 m, 16.08 m, and 16.18 m from the FDA, the iterative and the TLS methods, respectively. The average ^{13}N half life reported in published literature is 10 m.